2. Accelerator Physics

Overview of Proposed Projects on Accelerator R&D

The linear collider is an ambitious project. The center of mass energy will be a factor of 5 to 10 larger than that achieved at the SLC, and the required luminosity is four orders of magnitude larger than the SLC luminosity. The reliability required for performing high energy physics places difficult demands on the accelerating structures and their associated RF systems. The need for high luminosity places extreme demands on all of the accelerator systems due to the need to produce and maintain a very low emittance beams with very large bunch energy and beam power.

Two technological solutions have been extensively developed. One uses an innovative RF source at X Band with a normal-conducting structure design (NLC/GLC), and the other uses a more conventional RF source at L band with a superconducting RF structure design. It is the superconducting option which will undergo further development. Most of the research and development work has been done at the large laboratories, which have the engineering resources for large-scale prototyping (of, for example, accelerating structures, modulators, klystrons, and RF distribution systems) and the resources to build large test facilities (*e.g.*, FFTB, NCLTA and ASSET at SLAC, ATF at KEK, and TTF at DESY).

These test facilities have partly demonstrated that the concept of a Linear Collider may be feasible in reality. However, considerable additional work is required before a 0.5 to 1.0 TeV cms linear collider can be successfully constructed and operated. Challenges exist in beam dynamics, source technology, RF technology, magnet and kicker technology, ground motion characterization, vibration suppression and compensation, instrumentation and electronics, and control systems.

Summary of R&D Covered by the Proposal

The sub-proposals presented here represent an initial overlap of what university groups can do and what the lab groups have suggested is needed. Since linear collider construction is expected to be underway in less than about ten years, these sub-proposals are expected to bear fruit on a commensurate time scale.

Although these sub-proposals represent an early step in the development process, they span a rather significant part of the work that needs to be done. We present below a brief summary, organized by major topic, of the how the sub-proposals meet the R&D needs of the Linear Collider program.

Among the topics still needing attention are ultra precise (~1 nanometer) beam size monitors for the interaction point, cryogenic sensors (for superconducting final doublet vibration control), and superconducting quadrupole vibration system tests.

Beam simulations and calculations

The linear collider must produce and maintain a beam with unprecedented low emittance, with low jitter, low losses, and few halo particles. It must also preserve the polarization

of the electrons (and possibly positrons). Beam dynamics simulations and calculations are needed to learn to control the effects that cause emittance growth, jitter, particle and polarization loss, and halo production. The beam in the injector system, comprising source, damping rings and bunch compressors, is susceptible to space charge effects; dynamic aperture limitations from damping wigglers and chromaticity correction; emittance growth from misalignments and intrabeam scattering; instabilities from electron clouds, ions, and wake fields; and coherent synchrotron radiation. In the main linac the emittance must be preserved in the presence of wake fields and alignment errors. The transport and collimation of the beam halo is a serious concern for detector backgrounds. Each of these areas requires substantial additional calculational work before a linear collider can be successfully built and operated.

Electron and positron source technology

Positron sources for the linear collider could be of the conventional type, with several operating in parallel to avoid fracturing targets, or could be based on undulator radiation striking a thin target. The latter idea has advantages including the possibility of producing polarized positrons, but suitable undulator prototypes must be produced, and a beam test of the principle is desirable. Other work includes studies of photocathodes.

RF Technology

The gradient performance of superconducting cavities is limited by the *Q* of the cavities. Understanding the limitations of superconducting cavities and extending their performance will allow for an enhanced energy goal for the TESLA main linacs, reduced cost, or both.

Kicker and Magnet Technologies

One of the novel and controversial features of the TESLA design is its large damping rings which require fast kickers to inject and eject bunches one at a time. The circumference (and presumably the cost) could be reduced if faster kickers were available.

Permanent magnet technology is attractive for many parts of any linear collider complex. These include the fixed energy damping rings, beam transport lines, and the X-band main linacs. This technology offers the possibility of eliminating costs associated with electromagnets which require power supply systems, and may require cooling water systems. The performance capabilities of magnets based on permanent magnet materials (especially their radiation resistance) must be understood before considering them for reducing the costs of several subsystems throughout linear colliders.

Ground Motion, Vibration, and Mechanical Support Systems

The choice of a site for a linear collider will include consideration of the vibrations inherent at the site. The characterization of ground vibrations as a function of depth will help determine the depth at which a linear collider will have to be located.

The rf structures and magnets in the NLC main linacs will have to be accurately moved and, due to their great number, the development of an inexpensive system to do this will reduce costs. The final focus magnets in NLC and TESLA also require movers with even greater accuracy but their number is smaller.

Instrumentation and electronics

The very small vertical and longitudinal emittances of a linear collider beam are near or beyond present beam size resolution limits. The linear collider will require the development of monitors surpassing the performance of present designs. Sensitive monitors for transverse-longitudinal beam "tilt" would improve the ability to minimize emittance growth. Control of the beam halo requires a monitor which can detect low intensity halo despite the presence of a high intensity beam core.

The linear collider will have special requirements for electronics: radiation hardness, speed and depth of data acquisition, and reliability.

Control Systems

The international nature of the linear collider collaboration lends itself to the possibility of a truly global accelerator network for controlling the machine. Exploration of the capabilities of such a network and its basic unit (the virtual control room) will help demonstrate the feasibility of this technique.

Non-e^+e^- collisions

A major facility like the Linear Collider should enable a broad spectrum of physics programs. In addition to the high energy e^+e^- operation, other possible programs include *Z*-pole studies at a separate collision region, e^-e^- or $\gamma\gamma$ at the high energy region, or Compton backscattered photons from the spent beams. In the latter case, there is a novel program with polarized photons on fixed target, and also a platform for prototyping the laser-beam issues for $\gamma\gamma$ without disrupting the initial high energy e^+e^- program.

We now present the accelerator R&D sub-proposals.

Contents

2. Accelerator Physics: 28

2.2: Beam Test Proposal of an Optical Diffraction Radiation Beam Size Monitor at the SLAC FFTB

(progress report)

Accelerator Physics

Contact person
Yasuo Fukui
fukui@slac.stanford.edu
(650) 926-2146

Institution(s)
UCLA
KEK
SLAC
Tokyo Metropolitan
Tomsk Polytechnic

Funds awarded (DOE)
FY04 award: 40,000
FY05 award: 45,000
FY06 award: 50,000

Progress Report on FY04 activity

Project name Beam Test Proposal of an Optical Diffraction Radiation Beam Size Monitor at the SLAC FFTB

Classification Accelerator

Contact Person Yasuo Fukui
fukui@slac.stanford.edu (650) 926-2146

Institutions and Personnel

University of California at Los Angeles, Department of Physics and Astronomy :
David B. Cline, Yasuo Fukui, Feng Zhou

Stanford Linear Accelerator Center :
Marc Ross, Paul Bolton

KEK, High Energy Accelerator Research Organization, Japan :
Junji Urakawa, Makoto Tobiyama, Toshiya Muto, Pavel V. Karataev, Alexander S. Aryshev

Tokyo Metropolitan University, Physics Department:
Ryosuke Hamatsu

Tomsk Polytechnic University, Russia:
Alexander P. Potylitsyn, Gennady A. Naumenko, A. Sharafutdinov

FY04 Activity Overview

This proposal was awarded $40K in FY03, and $40K in FY04 by DoE. In FY2003, progress has been made in the theoretical and simulation work which has been mostly done by the collaborators at the Tomsk Polytechnic University. A part of the approved budget in FY2003 was carried over to FY2004 on works on making the target slit and the alignment system of the target, a vacuum chamber modification, recycling a gamma calorimeter, a part of the optics and laser alignment system. A paper was published on the design of this experiment and submitted to the PAC2003. [Pub. 1]

In FY04, we have completed our calculation and simulation of the ODR beam size monitor for the beam test at the SLAC FFTB through two collaboration meetings, one at KEK in March 2004 and another at SLAC in August 2004. Because of the higher beam energy at the SLAC FFTB(28.5 GeV), compared with that at KEK ATF(1.3 GeV), we need modification of the target and utilizing a lens optics system in order to overcome the difficulty due to the larger g factor and the pre-wave zone effect, and the beam divergence effect. At KEK ATF, we have started testing the idea of using the dis-phased conductive slit target and the lens system in a pre-wave zone as supporting beam test for this proposal, by making changes in the existing ODR beam size monitoring system for the 1.3 GeV electron beam. [Pub. 2]

FY2004 Project Activities

Two collaboration meetings were held in FY2004. The first meeting was held on March 19th at KEK ATF. The agenda at the KEK meeting was:

1) Overview plan (15 min) Yasuo Fukui
2) Baseline theory and calculation and the ATF proposal (60 min) Gennady Naumenko
3) Development of the ODR beam size monitor at KEK-ATF (30 min) Pavel V. Karataev
4a) Diffraction radiation of 30-GeV electrons in the VUV and soft X-ray region. (15 min) Alexander P. Potylitsin
4b) Diffraction radiation interferometry and bunch length determination. (15 min) Alexander P. Potylitsin
5) Discussion on the Letter of Intent (30 min) All members

Talk files are posted at: http://www.physics.ucla.edu/hep/ODR_FFTB/Meeting/March19_KEK/talk_files/. Basic experiment plans have been developed and the ODR photon yield was calculated.

The second meeting was held on August 10th at SLAC. The agenda at the SLAC meeting was:

1) Overview of the FFTB beam test proposal of the ODR beam size monitor 30 min Yasuo Fukui
2) Review of the ODR beam size monitor experiment at KEK ATF 60 min Toshiya Muto
3) Beam size measurement and the ODR photon yield at FFTB 90 min Gennady Naumenko
4) Comments on the Beam size measurement at FFTB 30 min Alexander Potylitsin
5) Discussion on the Experiment plan 60 min. All members

Talk files are posted at: http://www.physics.ucla.edu/hep/ODR_FFTB/Meeting/Aug10_SLAC/.

Step by step plans were discussed in this collaboration meeting, in order to solve problems due to large $\gamma\lambda$ (sensitivity/measurability issue of the beam size), due to $\gamma^2\lambda$ (pre-wave zone effect), and due to small $1/\gamma$ (beam divergence issue).

ODR transverse beam size measurement with the electron beam energy at 28.5 GeV at the SLAC FFTB is completely different from that at 1.3 GeV at the KEK ATF or at the lower energy electron beam experiment. The advantages and disadvantages (and solutions for those) of the ODR beam size measurement at the SLAC FFTB are the following:

Advantage 1) Because of the larger $\gamma\lambda$, the slit opening can be much larger, which reduces the beam halo background.

Disadvantage 1) Because of the larger $\gamma\lambda$, conventional method of measuring the ratio of ODR photons in the valley and that in the peak with a simple slit opening does not work. Because the ratio is too small to measure. (Solution: This can be solved by using the dis-phased target.)

Disadvantage 2) Because the $\gamma^2\lambda$ is much larger than the distance of the detector from the target, so-called near field effect distorts the ODR photon yield as a function of the opening angle.

(Solution: This can be solved by using an lens optics system which restores the relation of the photon emitting angle to the offset at the detector.)

Disadvantage 3) Because the 1/γ, the typical peak opening angle of the ODR photon, is comparative to the beam divergence at the SLAC FFTB, the opening angle distribution of the ODR photons is distorted/smeared.
(Solution: This can be solved by using the curved slit target surface and make the ODR emitting angle larger than the beam divergence.)

These solutions are under the beam test at the KEK ATF by using the existing set-up of the ODR transverse beam size measurement experiment.

Manufacturing test samples of the dis-phased flat conductive target has been initiated at Tomsk, Russia. Figure 1 shows samples of the dis-phased target which are used in the supporting ODR experiment at the KEK ATF. The target configuration in the Figure 1 is to measure the vertical beam size.

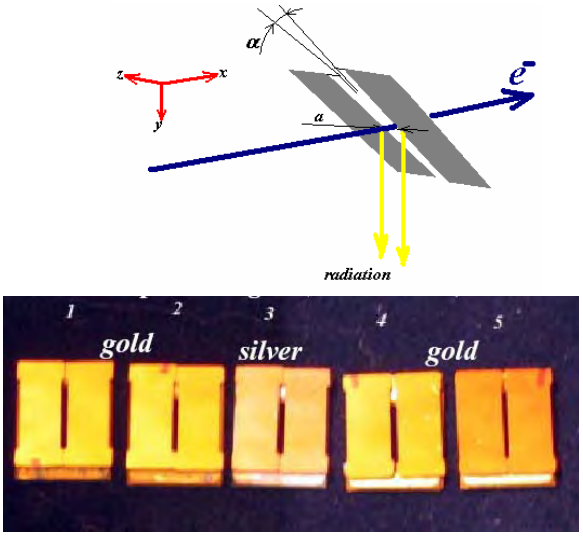

Figure 1 Dis-phased targets

Because there exists an ODR beam size measurement set-up and the beam time is available at the KEK ATF, supporting R&D experiments have been initiated at the KEK ATF to demonstrate the effectiveness of planned solutions for the ODR transverse beam size measurement, by using only non-US funding. The experimental set-up at the KEK ATF is shown in Figure 2. Figure 3 shows the preliminary ODR photon yield measurement data as a function of the beam offset position at the KEK ATF. Two-dimensional interference picture was measured with the dis-phased target at the KEK ATF which agrees well with the calculation.

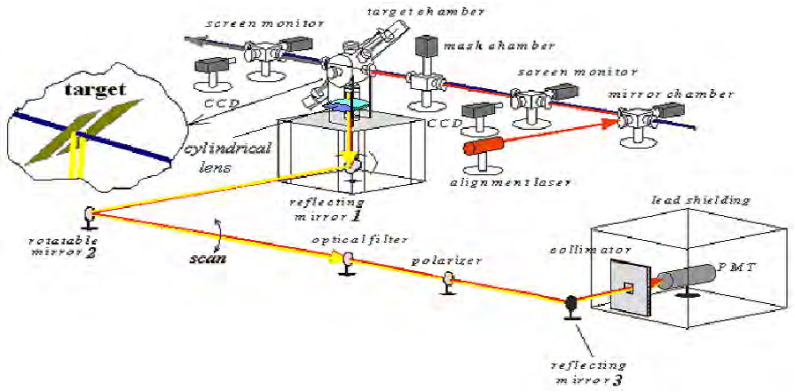

Figure 2 Beam test set-up at the KEK ATF

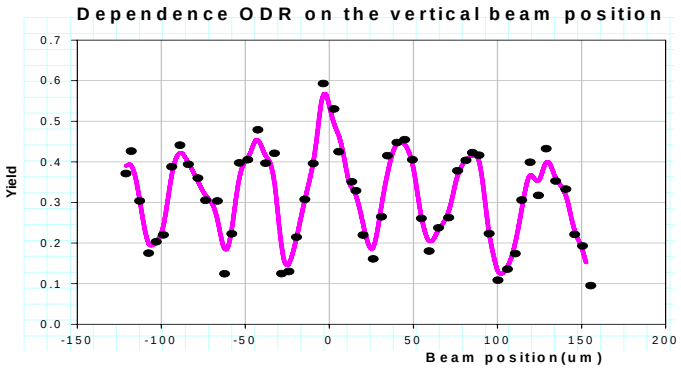

Figure 3 Preliminary ODR yield as a function of the beam position

Figure 4 shows the curved dis-phased slit target which makes the opening angle of the ODR photons induced on the conductive target larger than the beam divergence. At the SLAC FFTB, beam divergence is comparative to the $1/\gamma$, the typical opening angle of the ODR photons at the peak.

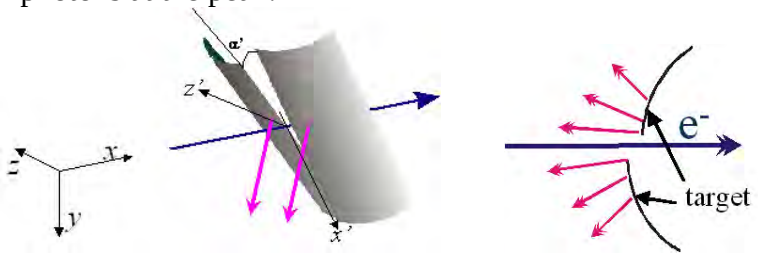

Figure 4 a dis-phased conductive slit target with curved surface

Figure 5 shows the lens optics system which can restore the relation of the ODR photon opening angle at the target to the offset at the detector, for the curved disphased target. Figure 6 shows the min/max ratio of the ODR photon yield as a function of the transverse beam size with this target and the lens optics system.

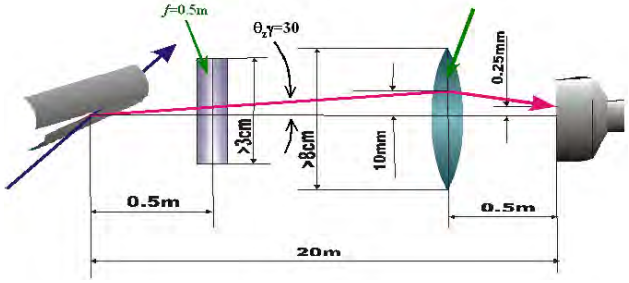

Figure 5 Lens Optics system for a dis-phased conductive slit target with curved surface

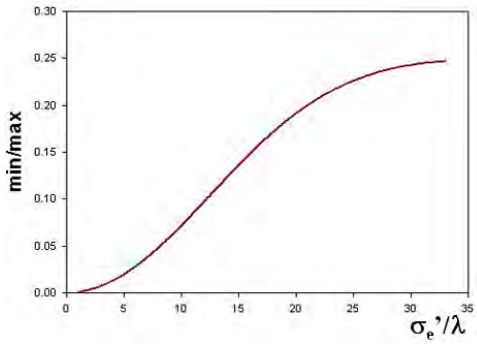

Figure 6 min/max ODR photon yield ratio as a function of the transverse beam size with the curved dis-phased target

The SLAC FFTB beam line is scheduled to be converted to an injection beam line for the LCLS project in the calendar year 2006. The SLAC beam has been off due to the stand-down since the end of 2004, but it will resume the FFTB operation in May 2005. Currently three experiment groups at the FFTB, STTS, E166 and E167, are scheduled to use the beam time. And the procedure is going on to obtain the beam time for this ODR beam size monitor test experiment before the shutdown of the FFTB beam line. This experiment requires much shorter beam time than those three beam experiments, and beam time can be easily assigned, once the approval procedure is completed. Figure 7 shows the drawings and a picture of the moving system of the target and the wires for the auxiliary transverse beam size measurement at the same z location. The transverse size of the dis-phased slit target can be as large as 60 mm. The slit opening width are 1 mm and 2.5 mm which gives the ratio of ODR intensity to OTR one as 0.98 and 0.9, respectively.

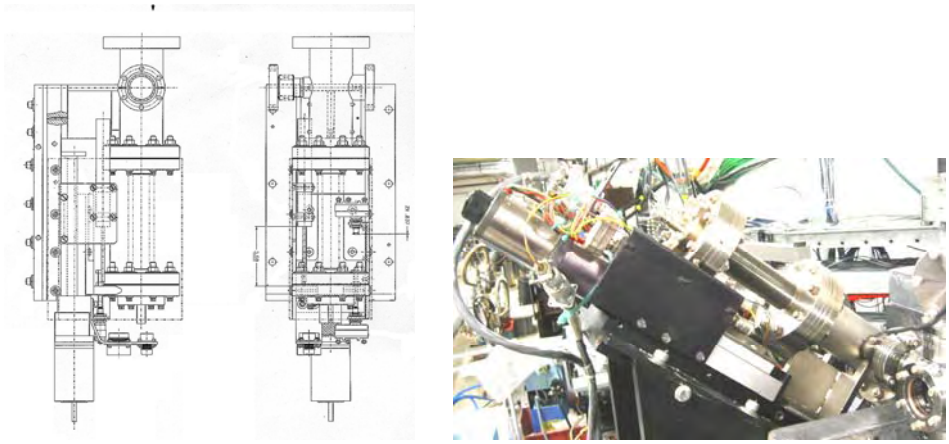

Figure 7 target moving system

We studied the recoil effect of the beam bunch due to the beam's passing through conductive slit target and generating/inducing diffraction radiation, and we concluded that the recoil effect was negligible and it was too small to measure in the ODR beam size monitoring at the SLAC FFTB. [Pub. 3]

As stated in the FY04 Activity Report, UCLA has supported the travel cost of Tomsk collaborators to give talks in the August 2004 SLAC collaboration meeting. The purchase is underway to obtain the dis-phased conductive slit targets which are manufactured in a company in Tomsk, Russia. The ODR beam size measurement will be initiated with a photo tube and a lens optics system by using multi bunches of the beam. For the single bunch measurement of the transverse beam size, a triggerable CCD camera will be used which will be covered by the FY05 funding.

Budget

Institution	Item	FY2003	FY2004	FY2005	FY2006	FY2007	FY Total
UCLA	Salaries and Wages	$ 16,000	$ 21,200	$ 21,000	$ 22,000	$ 25,000	$ 115,200
	Vacuum chamber modification	$ 5,000	$ 0	$ 0	$ 0		$ 5,000
	Slit Target	$ 3,000	$ 5,000	$ 5,000	$ 5,000	$ 5,000	$ 23,000
	CCD Camera System/Filter	$ 0	$ 0	$ 20,000	$ 4,000	$ 2,000	$ 26 ,000
	Phototubes/γ calori.	$ 2,000	$ 1,000	$ 1,000	$ 0	$ 0	$ 4,000
	Optics/Calib. System	$ 7,000	$ 1,000	$ 2,000	$ 2,000	$ 2,000	$ 14,000
	DAQ system		$ 0	$ 1,000	$ 6,000	$ 5,000	$ 12,000
	Computing tools			$ 1,000	$ 4,000	$ 4,000	$ 9,000
	Indirect costs	$ 4,000	$ 5,500	$ 10,000	$ 9,000	$ 9,000	$ 37,500
UCLA Sub-Total		$ 37,000	$ 33,700	$ 61,000	$ 54,000	$ 52,000	$ 237,700
SLAC	Experi. set-up Data taking/analysis SLAC	$ 0	$ 0	$ 1,000	$ 2,000	$ 2,000	$ 5,000
KEK	Experi. set-up Data taking/analysis KEK	$ 0	$ 0	$ 1,000	$ 6,000	$ 6,000	$ 13,000
Tokyo Met. Univ.	Experi. set-up Data taking/analysis Tokyo M. U.	$ 0	$ 0	$ 1,000	$ 2,000	$ 2,000	$ 5,000
Tomsk Poly. Univ.	Experi. set-up Data taking/analysis Tomsk Pol. U.	$ 3,000	$ 6,300	$ 6,000	$ 6,000	$ 8,000	$ 29,300
Total Other Inst. Support by UCLA		$ 3,000	$ 6,300	$ 9,000	$ 16,000	$ 18,000	$ 52,300
UCLA Grand Total		$ 40,000	$ 40,000	$ 70,000	$ 70,000	$ 70,000	$ 290,000

Publications

1. Y. Fukui, et al., “Design of an Optical Diffraction Radiation Beam Size Monitor at SLAC FFTB”, a contr. paper to the PAC2003 Conference, 2003, Portland, Oregon.
2. G. Naumenko, “Some features of diffraction and transition radiation at the distance less than $\gamma^2\lambda$.”, Nucl. Inst. and Meth., B227(2005)87-94
3. Potylitsyn, et al., “Coherent Radiation Recoil Effect for the Optical Diffraction Radiation Beam Size Monitor at SLAC FFTB”, Nucl. Inst. and Meth., B227(2005)170-174

2.3: Design and Fabrication of a Radiation-Hard 500-MHz Digitizer Using Deep Submicron Technology

(progress report)

Accelerator Physics

Contact person
K.K. Gan
gan@mps.ohio-state.edu
(614) 292-4124

Institution(s)
Ohio State
SLAC

Funds awarded (DOE)
FY04 award: 60,000
FY05 award: 135,000
FY06 award: 135,000

Design and Fabrication of a Radiation-Hard 500-MHz Digitizer Using Deep Submicron Technology

K.K. Gan*, M.O. Johnson, R.D. Kass, J. Moore, C. Rush
Department of Physics, The Ohio State University

S. Smith
Stanford Linear Accelerator Center

Project Summary

The proposed International Linear Collider (ILC) will use tens of thousands of beam position monitors (BPMs) for precise beam alignment. The signal from each BPM is digitized and processed for feedback control. The demand on the digitizers depends on their location at the accelerator complex. The two large damping rings require the fastest high-precision and high-bandwidth digitizers. We propose to continue the development of the digitizers that were originally designed for the warm linear collider. The specification of the digitizers for the ILC is not yet finalized but we expect similar digitizers are needed[1].

We propose to continue the design of an 11-bit (effective) digitizer with 500 MHz bandwidth and 2 G samples/s. The digitizer is somewhat beyond the state-of-the-art and hence not commercially available. Moreover we plan to design the digitizer chip using the deep-submicron technology that has proven to be very radiation hard (up to at least 60 Mrad). We use enclosed layout transistors and guard rings developed for high-energy physics applications to increase the radiation hardness. This mitigates the need for costly shielding and long cable runs while providing ready access to the electronics for testing and maintenance. Once a digitizer chip has been successfully developed via several prototype runs, an engineering run at a cost of ~$150,000 will produce all the chips necessary for the ILC, including those BPMs that require less demanding digitizers. We have extensive experience in chip design using Cadence[2]. This proposal was reviewed by the Holtkamp Committee in 2002 and 2003 and awarded, for both years, a rank of 2 on the scale of 1 to 4 with 1 having the highest ranking. This proposal was funded by DOE in FY03 and has been reviewed for three more years, FY04-6. Most of the circuit blocks in the chip have been designed and simulated and we plan to submit the first prototype chip for some of the circuit blocks soon. We request continue funding for FY05 and FY06 to continue the design work and submit more prototype chips to evaluate and improve the design.

Project Plans

The digitizer chip is very challenging: large bandwidth (500 MHz), high precision (11 bits), and fast sampling speed (2 G samples/s). We capitalize on the experience of our engineering staff that, over the last ten years, has designed radiation hard chips for ATLAS, CLEO III, and CMS. Our most recent design of the DORIC and VDC chips for the ATLAS pixel detector uses the IBM deep submicron technology with feature size of 0.25 μm to achieve radiation hardness[3]. In addition, we have extensive experience designing fast analog electronics systems such as those used in high-resolution drift chambers.

We propose a 12-bit pipelined digitizer as shown in Fig. 1. In this scheme the input is crudely digitized in the first stage (3-bit cell). The digitized value is then subtracted from the sampled input value, amplified by eight and presented to the second stage. This identical process is repeated for each of the four stages. A one-bit comparator follows the last stage so the final result can be rounded to 12 bits.

The 12-bit digitizer is somewhat beyond the state-of-the-art. However, there is one characteristic of the BPM that may ease the design requirements. The input from each bunch to this system is a sequence of doublets. We currently design the digitizer for a bunch spacing of 1.4 ns. The bunch spacing is expected to be somewhat larger for the dumping rings of the ILC and this will improve the feasibility of the project. Only one parameter is needed to completely specify a doublet. Thus the requirements could be met with a digitizer sampling at the bunch frequency (1/1.4ns or 714 MHz). By interleaving three digitizers, we can have a chip with 2 G samples/s to provide more redundancy. In the following, we first discuss the required precision of some of the circuits in the digitizer and then the control of the errors in order to achieve the desired precision.

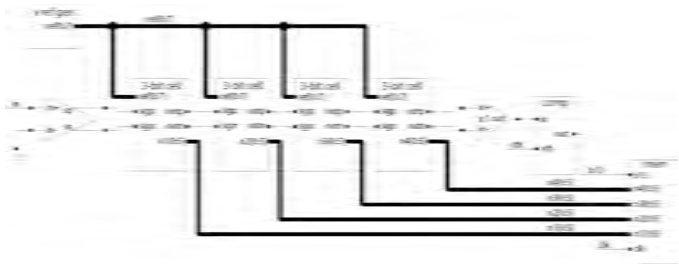

Figure 1. Schematic of a 12-bit pipelined digitizer.

Precision

Submicron CMOS does not allow large power supply voltages, 2.5 V is common. This limits the internal signal swing. We can estimate the necessary precision by assuming that a 3 V full scale range can be achieved for the differential internal signals. This means the LSB is 3 V/4096 or 732 μV. Thus comparator thresholds must be stable and accurate to one half the LSB or 366 μV. Amplifier and sample/hold gains must be stable and accurate to about the same precision, 0.01% (~ 0.5/4096) of full scale. Charge injection errors in the sample/hold circuits must also be controlled to the same level of precision.

* Contact: K.K. Gan, 614-292-4124, gan@mps.ohio-state.edu

Error Control

There are three types of errors in the digitizer:
1. Offset errors: uncertainties in the comparator thresholds, fixed charge injection from the sample/hold, and amplifier offset.
2. Gain errors: uncertainties in the gain stages and sample/hold gain.
3. Dynamic errors: uncertainties in the timing and amplifier and sample/hold settling times.

Offset and Gain errors will be measured as part of the qualification test on raw chips. These errors do not have to be measured individually. For example the offset error from the comparator, the charge injection offset and amplifier offset will be measured as a single number. These values will be loaded into an on-chip memory. The raw digitized numbers will be used only as indices to tables of "correct values", which will be used to calculate the true input value. The maximum number of these calibration values is estimated to be 72. With this scheme, we only require stability in the design and process. Based on experience, this level of stability should be achievable over a modest temperature range. In addition these devices can be recalibrated in the field.

Dynamic errors will be controlled by careful design. By means of simulation and prototyping we will design each of the internal functions to have sufficient bandwidth to settle in the required time.

Process

The proposed digitizer requires several amplifiers with a gain of eight. Let us assume that we allow half the bunch period (0.7 ns) to sample and the other half to hold. To settle to 12 bits with a precision of one half the LSB requires nine time constants ($e^{-9} \sim 0.5/2^{12}$) or a rise time of 171 ps (2.2τ with τ = 700 ps/9). To accomplish this the fabrication process must provide a product of gain (8) and bandwidth ($1/2\pi\tau$) of 16.4 GHz. The IBM process SiGe BiCMOS 6HP/6DM is available through MOSIS and features 40 GHz NPN bipolar transistors along with 0.25 μm CMOS.

Progress Report

We continue on the design and simulation of the 3-bit cell, which is the heart of the digitizer. The internal structure of the 3-bit cell is shown in Fig. 2. The status of the design is as fellow:

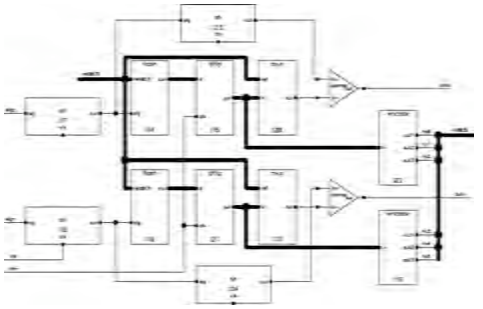

Figure 2. Schematic of a 3-bit cell.

Sample/Hold Circuit:

The sample/hold circuit is the most critical component of the 3-bit cell. The latest design of the sample/hold is shown in Fig 3. We use AC coupled stages internally since the waveforms to be digitized have no DC component. This allows for a very simple sample/hold circuit with gain that is set by a capacitor ratio, C1/C2. The DC operating point of the circuit is maintained by a slow feedback loop. The output of the feedback amplifier is driven by MOS transistors biased in the sub-threshold region. This results in very high output impedance.

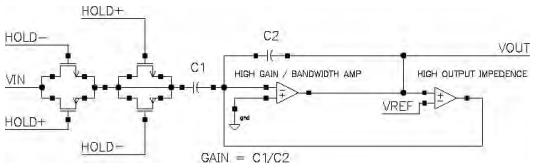

Figure 3. Schematic of a sample/hold circuit.

The switch on resistance is proved to be small enough to allow 9 time constants of charging in 700 ps. A second, half-size dummy sampling switch has been added to cancel the injected charge from the first switch. However, the injected charge depends on the input signal size. We are investigating more complex topologies with switches on the input plus switches in the feedback loop of the amplifier in order to reduce the injected charge to an acceptable level to achieve the desired precision.

We have designed an AC amplifier to be the heart of the sample/hold circuit. The sampling circuits need an amplifier with a gain of one for buffering and gain of eight for error amplification. The amplifier is stable and has a smooth closed-loop frequency response. The amplifiers settle to the desired voltage within the hold time. The unity gain

amplifier has fast rise time but the amplifier with a gain of eight still requires some improvements. The gain-bandwidth still needs another factor of two improvements.

Simulations of the sample/hold circuit indicate that we have achieved a precision of about 10 bits with a fully differential circuit. With the problems/solutions identified above, we hope to improve the design to achieve the desired precision.

Comparator Circuit:

We have improved the design of the comparator that uses fully differential BiCMOS, including the output latching circuits. The design uses bipolar transistors for the actual comparisons and FET's for current control and active loads. The circuitry is fast and hence adequate for 714 MHz operation.

MUX Circuit:

The multiplexer circuit has been improved. The digital logic portion works at full speed and the analog part is also fast but somewhat noisy. Some more improvements are desirable.

Op-amp Circuit:

The op-amp subtracts the digitized value from the sampled input value to produce the residual for the next stage. The circuit has been designed but has not yet achieved the desired precision.

Encoder Circuit:

The encoder circuit has been designed and performs satisfactorily.

In FY04 we were supposed to submit for fabrication a prototype chip for the 3-bit cell. However, the approved total budget of $60K was not sufficient for the cost of $54K for a prototype run via MOSIS given that some funds need to be allocated for engineering design. We therefore concentrate on improving the design of the 3-bit cell. We are currently laying out a three-bit cell to test the major blocks (sample/hold switches and amplifier, and comparators with latches). On our last chip design project we were able to use component libraries and Cadence rules files developed at LBNL, CERN, and Rutherford, but this is not available for the BiCMOS process we have chosen for this ADC. We are in the process of converting or creating PCELLS (resizable transistor layouts) for the radiation-resistant enclosed transistors. We have converted some of the transistor layouts to the new semiconductor process, but must then add to or rewrite the Cadence rules files for layout, extraction and design rule checks. We will simulate the chip from the extracted layout including parasitic capacitance to verify the design before the submission. The chip will allow us to test the accuracy of the simulations and provides feedback on the needed improvements.

Goals for the Year 2004–5

We will evaluate the 3-bit cell chip from the first prototype run to test the accuracy of the simulations. This will provide the much-needed feedback for further improvements. We plan to irradiate the chip to test the radiation hardness. We know from previous experience that the CMOS part of this process is rad-hard but the radiation hardness of the SiGe NPN transistors is unknown.

The design and development activities will include:

1. Continued improvement of a prototype 12-bit digitizer
2. Testing of a 3-bit cell, including radiation hardness tests
3. Layout, submission and testing of a prototype 12-bit prototype

We plan to have one submission in this funding cycle.

Goals for the Year 2005-6

The design and development activities will include:

1. Continued improvement of a prototype 12-bit digitizer
2. Layout, submission and testing of a prototype 12-bit prototype
3. Continued system design of the full 12-bit digitizer

We plan to have two submissions in this funding cycle.

Budget Description

The design work is performed by an electrical engineer paid for by the Department of Physics of The Ohio State University. He is assisted by a technician paid for by this project. The technician has a Bachelor degree in electronic engineering technology from DeVry University and is currently studying part time for a Bachelor degree in electrical engineering at The Ohio State University. He has worked on the optical electronics for the pixel detector of the ATLAS experiment over the last few years. The travel budget allows the designers to make one trip per year to SLAC to discuss the design with our SLAC collaborator. The MOSIS cost for the prototype digitizer using the IBM 0.25 Micron SiGe BiCMOS 6HP/6DM process is now $54,000. This is about $9,000 more than what was in the three-year proposal. Given that the actual funding is below the proposed budget, we have to split the cost of the four submissions over three years.

Budget

Inst.	Item	FY03	FY04	FY05	FY06
OSU	Engineering Time	25,695	25,695	25, 695	21,681
OSU	Travel	1,259	1, 259	1, 259	1, 259
OSU	Digitizer	0	20,000	95,000	101,000
OSU	Indirect costs	13,046	13,046	13,046	11,060
SLAC		0	0	0	0
	Grand total	$40,000	$60,000	$135,000	$135,000

Bibliography

1. Marc Ross, private communication.

2. www.cadence.com

3. K.K. Gan *et al.*, "Radiation-Hard ASICs for Optical Data Transmission in the ATLAS Pixel Detector", Nucl. Phys. B (Proc. Suppl.) 125, 282 (2003).

2.4: RF Beam Position Monitors for Measuring Beam Position and Tilt

(progress report)

Accelerator Physics

Contact person
Yury Kolomensky
yury@physics.berkeley.edu
(510)642-9619

Institution(s)
UC Berkeley
Notre Dame
SLAC

Funds awarded (DOE)
FY04 award: 40,000
FY05 award: 34,600
FY06 award: 34,600

Precision RF Beam Position Monitors for Measuring Beam Position and Tilt Progress Report

UC Berkeley Senior Personnel
Yury G. Kolomensky

Collaborating Institutions
Stanford Linear Accelerator Center: Marc Ross, Steve Smith, Joseph Frisch, Michael Woods
University of Notre Dame: Michael D. Hildreth

Contact Person:
Yury G. Kolomensky
yury@physics.berkeley.edu
(510)642-9619

1. Objectives

Controlling beam emittance is important for future linear colliders as well as high-brightness light sources. Transverse wakefields (from beam-to-RF-structure misalignments) and dispersion (from beam-to-quadrupole misalignments) in the linac could lead to an emittance dilution that is correlated along the bunch length (*i.e.*, the tail of the bunch is deflected relative to the head). The ability to detect beam pitch is important in order to identify the primary sources of emittance dilution. For single beam bunches at the ILC, $2-15$ mrad beam tilt would correspond to 10% emittance growth.[1]

In addition to measurements of the transverse beam offsets along the linac, measurements of the beam position and energy near the interaction point are of great importance for the physics program of the future linear collider. Energy spectrometers at the interaction point aim at measuring the energy of the colliding beams with the precision of 10^{-4} or better.[2] Such precision will require a measurement of the beam position before and after the spectrometer magnets with the resolution of $\mathcal{O}(50\ \mathrm{nm})$, and comparable stability.

Resonant RF cavity beam position monitors[3] can be used to measure the average position of the bunch train with high precision, as well as determine the bunch-to-bunch variations. In a single-bunch mode, *i.e.* in the mode where the time interval between the bunches is larger than the fill time of of the cavity, the same cavities can be also used to measure the head-to-tail position differences, or bunch tilts. The cavity BPMs are a good match for the precision beam diagnostics at the ILC due to their narrow bandwidth and clean separation between resonant modes. In the following, we will briefly describe the RF beam position monitors, report our R&D activities last year, and outline plans for the cavity system.

2. Beam Position Monitors

A typical beam position monitor consists of three copper cavities, two (X and Y) cavities for monitoring the horizontal and vertical displacements of the beam, a Q cavity to provide an *in-situ* measurement of beam charge and phase. The position cavities are typically tuned to the dipole TM_{210} mode while the Q cavity

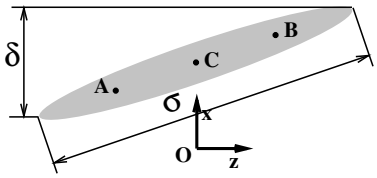

Fig. 1. Tilt of the bunch relative to the **z** axis of the cavity.

uses the monopole TM_{110} mode. The BPMs constructed at SLAC in 1960s[3] use three independent cavities which are easy to manufacture and tune. On the other hand, new C- and X-band monitors constructed at KEK and BINP as a prototype for the NLC use a more compact single-cavity design.[4]

The resonance frequency of the cavities is typically a multiple of the carrier RF frequency. To achieve good position resolution and stability, the cavities are tuned to a high value of $Q > 1000$ which increases the resonant pickup. Custom RF electronics with I/Q demodulation[5] provides information on both amplitude and phase of the beam-induced signals. Measuring both amplitude and phase of the RF signals reduces systematic effects and increases position sensitivity.

3. Beam Tilt Measurement

One of the main objectives of this proposal is to demonstrate that the RF cavities can be used for measuring small tilts of individual beam bunches. This can be done my measuring the imaginary part of the beam-induced RF pulse, or a phase difference between the RF signals from a dipole and Q cavities.

A short beam bunch of charge q centered the distance x_0 from the electrical center O of the cavity (point O in Fig. 1) induces an RF pulse with voltage

$$V(t) = Cqx_0 \exp(j\omega t) \tag{1}$$

where C is some calibration constant, ω is the resonant frequency of the cavity, and time t is computed from the time the center of the pulse passed through the cavity. If the bunch is pitched by amount δ from head to tail, the RF voltage is instead

$$V(t) = Cq \exp(j\omega t) \left[x_0 - j\frac{\delta\sigma\omega}{16c} \right] \tag{2}$$

The beam tilt introduces a phase shift

$$\Delta\phi = \frac{\Delta x}{x_0} = -\frac{\delta\sigma\omega}{16cx_0} \tag{3}$$

equivalent to an offset of $\Delta x \approx 10$ nm for a typical ILC beam size of $\sigma = 300$ μm and a tilt of $\delta = 2$ μm. For small offsets of $x_0 \sim 1$ μm, the phase shifts of $\approx 0.7^o$ should be measurable. It is clear that for this measurement the phase information is vital: it would be hard to extract the small offset from the amplitude signal alone (*e.g.* by measuring the RF power). For the phase measurement, the challenge is to be able to keep the beam centered at the cavity with high accuracy, and to be able to maintain the phase stability. The former requires being able to position the electrical center of the cavity near the beam axis (by either moving the beam or the cavity), and the latter requires precise temperature and environment control, as well as good cancellation of the dominant monopole mode in the dipole X cavity.[5]

4. Scope of the Project

A set of high-resolution C-band beam position monitors have been constructed at BINP and is currently being tested at the Accelerator Test Facility (ATF) at KEK by the NanoBPM Collaboration.[6] The monitors

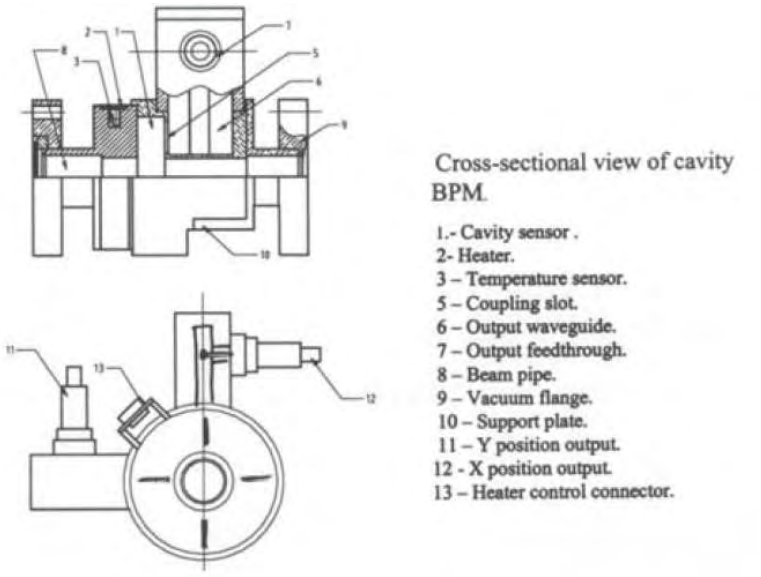

Fig. 2. C-band position monitor constructed at BINP for the NanoBPM collaboration.

use a single-cavity circular design, with transverse coupling slots for the position-sensitive X- and Y-dipole modes (see Fig. 2. The demodulation scheme employed by the SLAC group involves down-mixing the RF pulse to an intermediate frequency of 15-20 MHz and digitizing the IF signals with a 100 MHz sampling ADC. Information on the amplitude and phase of the RF pulse is then obtained in the offline analysis of the IF data, shown in Fig. 3.

We are taking part in the NanoBPM project, and are responsible for the online monitoring and offline analysis of the data. The main objective of the work at KEK is to gain operational experience with the precision BPM hardware and demonstrate nanometer-scale position resolution and sensitivity of the beam-induced RF signals in the position cavities to beam tilt.

Application of the precision RF BPMs to measuring beam parameters (*e.g.*, beam energy) near the interaction point of the linear collider requires high position resolution and high stability, possibly in the presence of synchrotron radiation from the spectrometer dipoles and other adverse environmental effects. These aspects of the precision monitor operation will be tested in the test experiments being developed at SLAC.[9] Berkeley group is part of the experiment T-474[10] which aims to develop a working prototype of the energy spectrometer with resolution and stability suitable for achieving a 100 part per million measurement of beam energy at the ILC. We are also contributing to the design and optimization of the BPM hardware and electronics for the beam tests being planned in FY06-07.

5. Progress Report and Future Schedule

This project is part of the national Linear Collider R&D program which is described in detail in *"A University Program of Accelerator and Detector Research for the Linear Collider"*[7] by the US Linear Collider Research and Development Group.[8] The project received funding from DOE for FY03 and FY04-06 under DOE contract DE-FG02-03ER41279.

In the first two years of the project (2004-2005), we are working in collaboration with groups at SLAC, LLNL, and KEK in developing the prototype of the nanometer precision beam position monitor. The NanoBPM Collaboration[6] has completed several beam tests at the ATF facility at KEK with the precision C-band cavities constructed at BINP. The present structure consists of a reference (charge-sensitive)

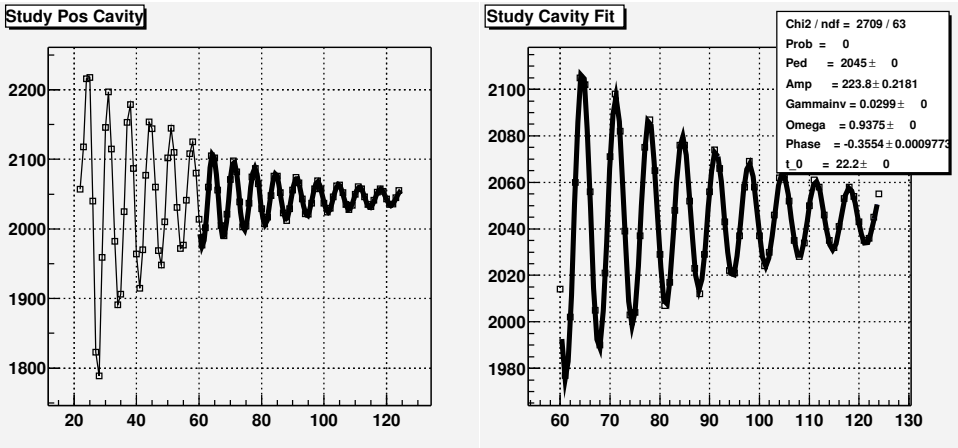

Fig. 3. Intermediate frequency signals produced by a single beam bunch at the ATF from BINP position cavities. A fit to the data produces information about the amplitude and phase of the beam-induced signals.

cavity and three pairs of (X, Y) BPMs[4] mounted on precision movers, and allows for the measurement of the position and tilt resolution. The best resolution from the latest run in December 2004 was found to be in the range of $20 - 30$ nm

The position and tilt sensitivity of each cavity was calibrated against known mover offsets, as shown in Fig. 4. After calibration, the position error for the middle cavity is computed for each pulse as

$$\Delta y_2 = y_1 \cdot \left(\frac{z_3 - z_2}{z_3 - z_1}\right) + y_3 \cdot \left(\frac{z_2 - z_1}{z_3 - z_1}\right) - y_2 \tag{4}$$

where $z_{1,2,3}$ are z locations of electrical centers of the BPMs, and $y_{1,2,3}$ are BPM measurements. The RMS of the distribution in Eq. (4) measures the BPM resolution, while the mean of the distribution is a measure of relative misalignments and electronic and mechanical stability.

Fig. 5 shows the measured resolution as a function of time in during a two-hour run. The top plot shows the resolution computed form Eq. (4), and it ranges typically between 50 and 100 nm. The raw resolution is limited by the cross-talk between X and Y dipole modes in the cavities. Linear regression against tilt signals and X positions improves the resolution in Y direction to $20 - 40$ nm (bottom plot in Fig. 5), although occasional outliers, possibly due to changes in beam conditions, are visible.

More beam tests are scheduled for 2005 at the ATF. In addition to the existing NanoBPM structure, three more position monitors have been installed approximately 5 meters downstream. Build by the KEK group, these cavities employ a completely different mechanical support system and electronics, and as such present an independent option for precision beam monitoring. More importantly however, demonstrating stability of electrical and mechanical offsets between the two systems would go a long way towards achieving stringent requirements for the energy spectrometry at the linear collider.

The milestones for the future KEK tests include

- Demonstrating sensitivity of the BPMs to beam tilts in 10 mrad range.
- Demonstrating the stability of the BPM position measurements of below 50 nm over several hours.
- Demonstrating the stability of the relative offset between the SLAC-LLNL and KEK structures.

A related project of demonstrating the performance of BPM-based energy spectrometer in the presence of large beam-induced backgrounds and other systematic effects has been proposed at End Station A (ESA)

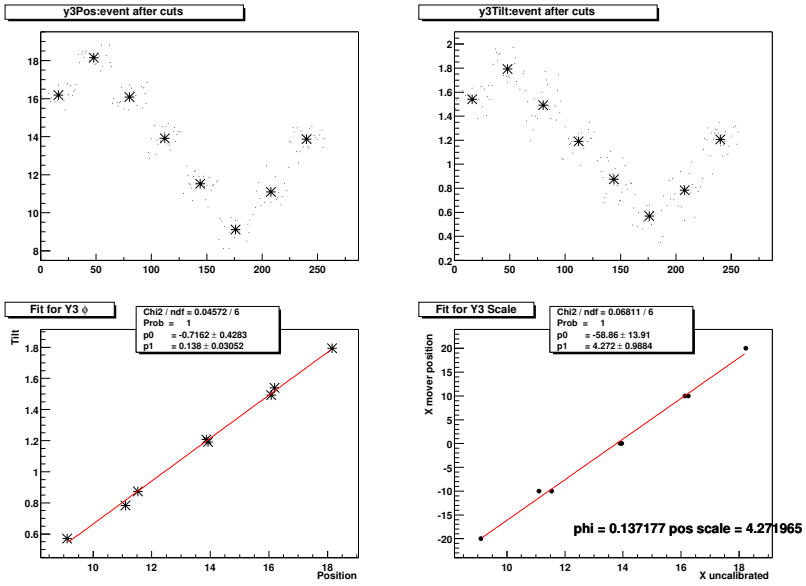

Fig. 4. Calibration of cavity Y3 against known mover offsets. The cavity was moved vertically from -20 to $+20$ μm relative to the nominal position in 10 μm steps. The top plots show the raw data for the position and tilt signals as a function of time, where dots represent individual pulses and stars show the average BPM measurement for each mover position. The slope of the plot in the lower left determines the relative phase shift of the position signal relative to the reference cavity, and the slope of the plot in lower right determines the position calibration constant.

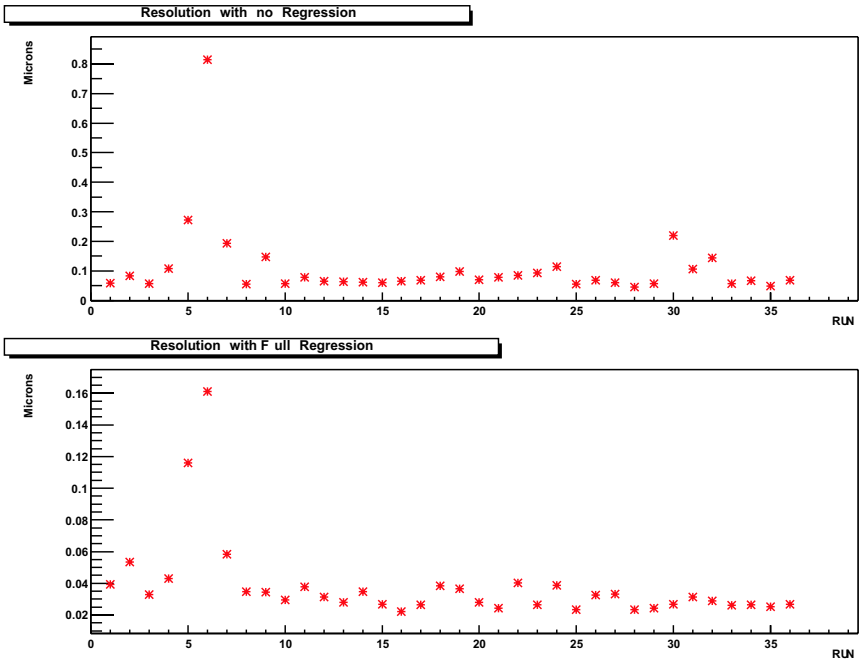

Fig. 5. Beam position resolution in Y direction (μm) as a function of time. Each data point corresponds to approximately one minute of beam data. Top plot shows the raw position resolution, and the bottom plot shows the resolution after linear regression against beam positions in X and beam tilts in X and Y directions.

at SLAC for FY05 and beyond.[9,10] We will be involved in assembling a set of precision cavities with associated RF processing electronics for beam tests in 2005-2006. The resolution and stability requirements for the energy spectrometer are similar to what is aimed at by the NanoBPM project. However, the beam and environmental properties in End Station A, in particular RF interference, beam-induced backgrounds, beam spot size and beam energy, are more closely matched to the ILC design. In addition, we plan to use rectangular S-band cavities,[3] which suppress X/Y coupling. Thus, ESA tests are complementary to the NanoBPM program at the ATF. Ultimately, the two beam test programs will converge on the common design of the beam position monitors suitable for precision linac beam diagnostics and for the energy spectrometer.

References

1. P. Tenenbaum *et al.*, preprint SLAC-PUB-9265 (2002).
2. M. Hildreth, *"A Demonstration of the Electronic and Mechanical Stability of a BPM-Based Energy Spectrometer for an e+e- Linear Collider*, in Ref. [7].
3. Z. D. Farkas *et al.*, preprint SLAC-PUB-1823 (1976).
4. M. Ross *et al.*, preprint SLAC-PUB-9887 (2003).
5. D. H. Whittum, Yu. G. Kolomensky, *Rev. Sci. Instrum.* **70**, 2300 (1999).
6. NanoBPM Collaboration, `http://www-project.slac.stanford.edu/lc/local/nanoBPM/nanoBPM.htm`.
7. University Consortium for Linear Collider R&D and Linear Collider Research and Development Working Group: *"A University Program of Accelerator and Detector Research for the Linear Collider"*, `http://www.hep.uiuc.edu/LCRD/pdf_docs/LCRD_UCLC_Big_Doc/` (2003).
8. Linear Collider Research and Development Working Group, `http://www.hep.uiuc.edu/LCRD/` (2002).
9. Yu. Kolomensky *et al.*, *"Beam Instrumentation Tests for the Linear Collider using the SLAC A-Line and End Station A"*, SLAC-LOI-2003.2 (2003).
10. M. Hildreth *et al.*, SLAC Test Beam Request T-474, *"Linear Collider - BPM-based energy spectrometer 2"* (2004).

2.5: Non-intercepting electron beam diagnosis using diffraction radiation

(renewal)

Accelerator Physics

Contact person
Bibo Feng
bibo.feng@vanderbilt.edu
(615) 343-6446

Institution(s)
Vanderbilt

Funds awarded (NSF)
FY04 award: 9,040

New funds requested
FY05 request: 60,600
FY06 request: 62,700
FY07 request: 0

Non-intercepting electron beam diagnostics using diffraction radiation

Personnel and Institution(s) requesting funding

B. Feng, W. E. Gabella, W. M. Keck Foundation Free-Electron Laser Center, and S. Csorna, Department of Physics and Astronomy, Vanderbilt University

Project Leader

Bibo Feng
bibo.feng@vanderbilt.edu
(615)-343-6446

Project Overview

The Linear Collider presents new challenges for beam instrumentation. Some of the beam dimensions are of the order of a few nm (at the i.p.), and to be able to reach these small sizes, the beams have to be tightly controlled and understood from their very inception onward. A number of different techniques are available in the arsenal of beam size and beam emittance measurements (e.g. transition radiation, metal wire, laser wire, laser interferometry, cavity BPM). Experiments of electron bunch profile measurements have been conducted using coherent synchrotron radiation (CSR), coherent transition radiation (CTR), as well as coherent diffraction radiation (CDR) [1, 2, 3, 7]. Because the CDR perturbs the electron beam less than CTR, it is a better choice for monitoring the electron beam bunch shape. The use of diffraction radiation (DR) for measuring the transverse beam dimension is a new non-invasive technique, only partially investigated at the present time [4, 5]; for example transverse beam size and emittance measurements have not been performed even though it is apparently possible to make precision measurements of bunch length, emittance at low energies, and the transverse size. (A recent experiment at KEK, by a Japan-Russia collaboration, has presented vertical beam size measurements using optical diffraction radiation[9].

This collaborative effort involving physicists and facilities from Cornell and Vanderbilt is aimed toward a comprehensive investigation of the potential use of DR over the broad spectrum of energies to be found at the Linear Collider. A graduate student, Tamas Sashalmi, at Vanderbilt University has started on this project. He does his doctoral dissertation on this topic and we anticipated he will be done in about two years.

Diffraction radiation is emitted from relativistic electron bunches passing through an aperture in a metal screen. The simplest aperture is a circular hole or a slit. The DR, like the transition radiation, is in the forward direction along the electron path, and in the backward direction along the direction of specular reflection from the the metal screen. The DR intensity is proportional to the square of γ, and it is distributed in angle as $1/\gamma$, where γ is the electron energy factor ($E_{beam}/m_e c^2$); thus, both the intensity and the angular distribution can be used to deduce the beam energy [6]. The DR technique can be developed as a low cost, compact, and non-intercepting monitor which can be very useful for each element of the Linear Collider, starting with the injection linac, the damping rings and the main linac. DR has the potential capability to diagnose multiple beam parameters such as longitudinal and transverse beam sizes, energy, position, divergence and emittance. The DR technique also can be developed as a single shot measurement. As the DR technique measures the spectrum and angular distribution in the frequency domain, it has very high spatial and time resolution, and it is easy to satisfy the requirements of the Linear Collider facility. The goal in spatial resolution

in this proposal is less than 1 μm in the longitudinal and transverse beam size measurement. From the analysis of measured data, the error on bunch length is estimated to be of the order of about 20%.

The coherent properties are included in the DR spectrum in which the radiation wavelength is nearly equal to the beam bunch length. In the case of the LC, 100 μm bunch lengths would produce radiation in the 0.1 mm wavelength region. The CDR has a fixed phase relative to the electron bunches, and the measurement of the coherent radiation gives the longitudinal bunch form factor $f(\omega)$ and hence provides information about the longitudinal bunch distribution function $S(z)$. Therefore, the electron distribution in a bunch can be obtained from the inverse Fourier transformation of the form factor. In addition, the angular distribution of the DR from an electron passing through a slit in a metal foil has polarization properties because of the interference effects between the two half-planes of the radiator. The electron beam transverse dimension can be measured through the analysis of the angular distribution of the diffraction radiation [4, 5].

Broader Impact

The budget for this project is mostly for a graduate student and two summers of undergraduate help. The graduate student has been invaluable in motivating experiments and data analysis. He is also being trained as an accelerator physicist with talents needed by many existing and planned particle beam machines. Vanderbilt University has a joint physics and astronomy training program with Fisk University, an historically black college. It is part of the plan to be more active in this collaboration and hire undergraduates from Fisk for summer work.

Results of Prior Research

The UCLC collaboration and NSF have kindly supported this effort over the last two years. First with seed money and most recently with a year of salary for a shared graduate student in the study of coherent diffraction radiation electron diagnostics. This and other linear collider efforts receive broad support from the FEL Center director Dr. David Piston, in the form of support staff, vacuum hardware, and other materials and supplies.

Seed Money for Non-Intercepting Electron Beam Diagnostics
Award: NSF PHY-0303702
Award period: September 15, 2003 to August 31, 2004
Award amount: $11,020

This was awarded by the NSF for UCLC work and is administered as a sub-contract with Cornell University. The money was used to purchase a Golay cell detector(QMC Instru. Ltd, Model OAD-7). The detector was received in July 2004 and is planned to measure the coherent diffraction radiation in the Center. The grant also paid for the very valuable trips to the 2004 Beam Instrumentation Workshop and the 2004 Free Electron Lasers Conference, where we published our initial experiment results [7]. It was very helpful to see the state of the international research.

Non-Intercepting Electron Beam Diagnostics
Award: NSF PHY-0355182
Award period: September 1, 2004 to August 31, 2005
Award amount: $9,040

This is also an award by the NSF for UCLC work and is administered as a sub-contract with Cornell University. The money is being used to pay a graduate student. He is shared with Dr. W.E. Gabella and is working on electro-optic and diffraction radiation diagnostics.

Recently, we have accomplished several of our research tasks. We designed and built a DR radiator, modified a Martin-Puplett type interferometer, and carried out preliminary electron bunch length measurements using coherent diffraction radiation from a slit. As an application, we investigated the effects of changing linear accelerator parameters such as phase and cathode heating on the electron bunch length. The research results were published on the 26th International Free Electron Laser Conference [7].

The CDR experiments were carried out at the Vanderbilt FEL Center on a Mark III type linear accelerator. The electron beam energy is variable between 25 and 45 MeV. The electron beam macropulse duration is about 8μs, and the average beam current is about 150 mA. The pulse contains 23,000 bunches, each with approximately 50 pC and a bunch length of approximately 1 ps.

The diffraction radiator is mounted at an angle of 45° to the electron beam. The diffraction radiator consists of two separated screens and a stepping motor to adjust the width of slit. The resolution of the stepping motor is 5 μm per step. We select a polished silicon wafer as the screen because of its flatness. The thickness of screen is about 500 μm and its size is about $75 \times 50 mm^2$. One of the silicon screens is mounted on an adjustable frame, so the reflection angle can be changed in order to keep both screens coplanar. The gap of the radiator is adjustable, when closed it operates as a transition radiator. DR or TR is emitted as the electron beam passes through the radiator. This radiation passes through a quartz window and is reflected by a parabolic mirror and a couple of flat mirrors into an interferometer to measure the radiation spectrum. The experimental system was aligned using a HeNe laser injected upstream into the beam line.

The interferometer is a wire grid Martin-Puplett type. The incident light is split onto orthogonal polarization components by a 45° tilted polarizing grid splitter. One component is reflected and focused onto a reference detector; the other is incident onto another vertical polarizing grid where the light is split into two beams, reflected by the roof mirrors, and finally recombined and focused onto a pyroelectric detector(P4-45, Molectron Inc.). A second Golay cell detector (ODA-7, QMC Instrument ltd) was purchased but is not currently functioning; it will be repaired and tested. The frequency limitation of the interferometer is determined by the diffraction losses, the finite aperture of the detector and the grating constant of the wire grid. The frequency range is estimated between 2 cm^{-1} and 50 cm^{-1} (wavelengths of 5 mm to 200 μm).

A typical CDR interferogram is shown in Fig. 1. The electron beam had an energy of 25 MeV and an average macropulse current of 135 mA. It was focused and centered between the edges of the two screens. The transverse beam size was about 2.5 mm and the slit width was set to 5 mm. The CDR spectrum is obtained by Fourier transformation of the interferogram as shown in Fig. 2. We observed relative strong power peak at the frequency of 0.13 THz (wavelength of 2.3 mm). The low frequency part of the spectrum is suppressed by the detector and the interferometer.

A simpler technique to extract the electron beam bunch length from the CDR interference spectrum was introduced in reference [8]. Assuming a Gaussian longitudinal electron distribution of pulse length σ and the low frequency suppressed by the interferometer at cut-off frequency $1/\xi$, the time domain interferogram of the coherent radiation is described as

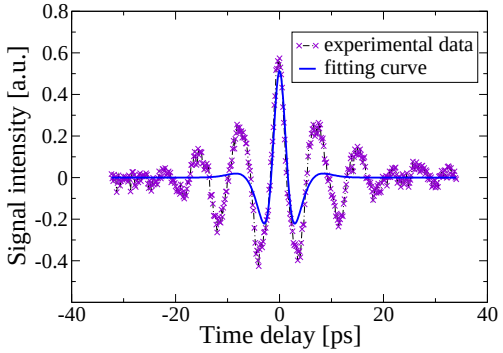

Figure 1: Typical CDR interferogram and time domain fit.

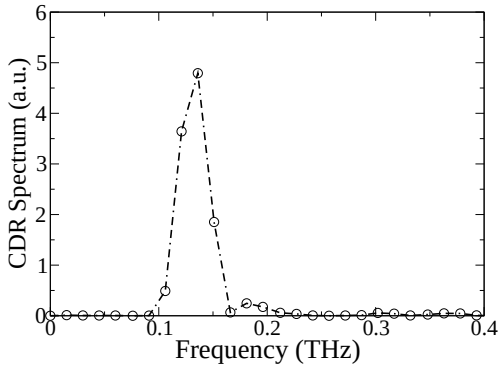

Figure 2: CDR spectrum corresponding to interferogram in Fig. 1.

$$S(t) = e^{-\frac{t^2}{4\sigma^2}} - \frac{2\sigma e^{-\frac{t^2}{4(\sigma^2+\xi^2)}}}{\sqrt{\sigma^2+\xi^2}} + \frac{\sigma e^{-\frac{t^2}{4(\sigma^2+2\xi^2)}}}{\sqrt{\sigma^2+2\xi^2}}. \quad (1)$$

The bunch length σ can be obtained by fitting this two parameter formula to the time-domain interferogram. For example, a fit is shown in Fig. 1,which gives the electron bunch length $\sigma \simeq 0.87$ ps.

Facilities, Equipment and Other Resources

We propose the measurement of the coherent DR spectrum from a slit in a metal foil. The longitudinal profile will be evaluated from the fast Fourier transform of the autocorrelation function and the use of the minimal phase approximation. The results will be compared to that of intercepting CTR (Coherent Transition Radiation) and non-intercepting electro-optic measurement experiments conducted in the same environment.

In addition, we propose to measure the electron beam transverse dimension through the analysis of the angular distribution of DR. A simple CCD camera can measure the angular polarization of DR. The total intensity of angular distribution has a minimum value when the beam passes through the center of slit. In practice, this property can be used to center the electron beam in the slit, and it may be a useful tool with which a cavity BPM can be centered on the beam.

It should be noted that much more accurate angular information of DR can be obtained by

placing two slits. We also propose to measure interference from the forward radiation off one slit as it interferes coherently with the backward radiation from the other. Analyzing the whole angular distribution in the normal plane and fitting it to the theoretical prediction allows us to determine the transverse dimension of electron beams, beam energy and emittance.

The bulk of the design and construction of the apparatus will be done at the Vanderbilt FEL Center, where there are available experienced scientists, mechanical and design engineers and where, importantly, a minimum of eight hours of beam time per week will be made available to this project. The undergraduate and graduate students at Vanderbilt University will also join to accomplish this project.

FY2005 Project Activities and Deliverables

In the first year, We will design and build a radiator as well as its housing chamber for the experiments. The two pieces of thin metal foils or aluminum coated silicon plates can be used as the radiator. The slit of the radiator should be moved to intercept the electron beam by an actuator. The slit width will be adjusted by moving the two half foils in the same plane. It emits transition radiation when the slit is closed, thereby allowing us to directly compare the results from DR and TR techniques.

We will also measure the DR angular distribution from the radiator to yield the beam transverse dimension according to the angular distribution theoretical calculation. We will measure the interference image from two DR screens with slits to obtain more detail information of the angular distribution of DR, and derive the electron beam properties such as beam transverse size, beam energy and beam angular spread.

The first year deliverables will be a DR radiator,a technical report describing the coherent DR and incoherent DR experimental results at Vanderbilt.

FY2006 Project Activities and Deliverables

During in the second year, we will carry out the beam property experiments using coherent DR and incoherent DR at the Cornell accelerator facility with higher electron beam energy. The device for measuring the angular distribution will be designed and built for accommodating different wavelengths and radiation bandwidths corresponding to different beam energy and slit width of the radiator.

The third year deliverables will be a technical report describing the coherent DR and incoherent DR experimental results at Cornell accelerator facility.

Budget justification

We expect that this year will be primarily devoted to studying the properties of the DR under varying beam conditions at Vanderbilt. The graduate student will have the primary responsibility for scheduling runs, acquiring data and doing a significant portion of the data analysis.

We expect that the second year will be primarily devoted to studying the properties of the DR under varying beam conditions at Cornell and Vanderbilt. Low energy running (50 MeV) can be efficiently performed at Vanderbilt, high energy running will be at Cornell (CESR). The graduate student will have the primary responsibility for scheduling runs, acquiring data and doing a significant portion of the data analysis.

A minimal amount of travel funds is included to cover collaboration meetings. We expect that on the basis of what we learn during this year, we will need to buy additional specialized equipment and electronics.

Two-year budget, in then-year K$

Institution: Vanderbilt University (Indirect costs are calculated at 52% rate for the first year and at 53% rate for the second year on total salaries, fringe benefits,travel, and materials and suplies)

Item	FY2005	FY2006	Total
Other Professionals	0	0	0
Graduate Students	20.5	21.2	41.7
Undergraduate Students	2.6	2.7	5.3
Total Salaries and Wages	23.1	23.9	47
Fringe Benefits	1.6	1.6	3.2
Total Salaries, Wages and Fringe Benefits	24.7	25.5	50.2
Optics Calib. System	8	0	8
CCD Camera System	0	7	7
Total Equipment	8	7	15
Tuition	6	6	12
Travel	4	4	8
Materials and Supplies	2	3	5
Other direct costs	0	0	0
Total direct costs	44.7	45.5	90.2
Indirect costs	15.9	17.2	33.2
Total direct and indirect costs	60.6	62.7	123.4

References

[1] A.H. Lumpkin, N.S. Sereno, D.W. Rule,"First measurements of subpicosecond electron beam structure by autocorrelation of coherent diffraction radiation", Nucl. Inst. and Meth. A 475 (2001) 470-475;

[2] B. Feng, M. Oyamada, F. Hinode, S. Sato, Y. Kondo, Y. Shibata and M. Ikezawa,"Electron bunch shape measurement using coherent diffraction radiation", Nucl. Inst. and Meth.A 475(2001),492-497;

[3] R.B. Fiorito, D.W. Rule, "Diffraction radiation diagnostics for moderate to high energy charged particle beams", Nucl. Inst. and Meth. B 173 (2001) 67-82;

[4] M. Castellano, "A new non-intercepting beam size diagnostics using diffraction radiation from a slit", Nucl. Inst and Meth. A 394(1997)275-280;

[5] M. Castellano, V.A. Verzilov, L. Catani, A. Cianchi, G. Orlandi and M. Geitz, "Measurements of coherent diffraction radiation and its application for bunch length diagnostics in particle accelerators", Phys. Rev. E, 63(2001) 056501-8;

[6] T. I. Smith,"Instrumentation and diagnostics for free electron lasers", AIP Conference Proceeding No.252, p124, 1992.

[7] B. Feng, W.E. Gabella, T.R. Sashalmi, S.E. Csorna, "Electron Beam Diagnostics Using Diffraction Radiation", Proc. of Int. FEL Conf. 2004, Trieste, Italy, TUPOS58,2004;

[8] A. Murokh, J.B. Rosenzweig,M. Hogan, H. Suk, G. Travish, U. Happek, "Bunch length measurement of picosecond electron beams from a photoinjector using coherent transition radiation", Nucl. Inst and Meth. A 410(1998) 452-460.

[9] P. Karataev, S. Araki, R. Hamatsu, H. Hayano, T. Muto, G. Naumenko, A. Potylitsyn, N. Terunuma, and J. Urakawa, "Beam-size measurement with optical diffraction radiation at KEK accelerator test facility", Phys. Rev. Lett., 3(2004)44802.

2.6: Electro-optic measurement of picosecond bunches in a bunch train

(renewal)

Accelerator Physics

Contact person
Bill Gabella
b.gabella@vanderbilt.edu
(615) 343-2713

Institution(s)
Vanderbilt

Funds awarded (NSF)
FY04 award: 18,083

New funds requested
FY05 request: 46,400
FY06 request: 50,300
FY07 request: 0

Electro-optic measurement of picosecond bunches in a bunch train

Classification (subsystem)

Accelerator Instrumentation: non-destructive electron bunch length measurement, broadly applicable

Personnel and Institution(s) requesting funding

William E. Gabella, Bibo Feng, John Kozub, Tamas Sashalmi, W. M. Keck Free-electron Laser Center, Vanderbilt University, Nashville, TN 37235

Collaborators

Court Bohn, Department of Physics, Northern Illinois University

Project Leader

William E. Gabella
b.gabella@vanderbilt.edu
615-343-2713, (F) 615-343-1103

Project Overview

In next linear collider designs, the effort to create and maintain short electron/positron bunches requires a robust technique to measure bunch lengths. Superconducting technology, next generation linear collider (ILC) designs have bunch lengths as short as 300 μm, or 1 ps, and a desirable goal is to measure the length to 10% or better. Short bunches have the advantage of avoiding the "bow-tie" degradation of the luminosity from the depth of focus while using strong focusing and small spots at the interaction region. The bunch length also needs to be short compared to the RF wavelength in the linac to avoid nonlinear effects from the accelerating gradient. Control of the bunch length in the magnetic bunch compressor after the damping rings requires accurate measurement of the length. The variation of length with position in the bunch train is also important to create uniform luminosity over the collision time and to correct any "long-range" wakefield or other effects on the bunch train which could lead to worsening of the effective emittance of the train. In the superconducting linear collider designs, the bunch train can be very long with 2800 to 4900 bunches spaced every 340 ns to 180 ns. Measurement and control of the bunch train becomes all the more important and difficult with so many bunches spaced over the relatively long time of 1 ms. Measurement and control of the bunch train quality is important to free-electron lasers which, for example, generate a laser pulse in an oscillator with bunch 1, amplify it with bunch 60, and bunch 120, all the way to bunch 18000, say. The bunches need quite a tight tolerance to have effective amplification and saturated energy.

Currently measuring electron bunch lengths with coherent transition radiation (or coherent diffraction radiation, or coherent synchrotron radiation), requires scanning a mm-wave interferometer and thus acquires signal over many electron pulses[1]-[2]. A technique using the perturbing effects of the passing electron bunch's electric field on a crystal (electro-optic, or EO, effect) measured by a fast Ti:sapphire laser has been demonstrated at the free-electron laser center (FELIX) in the Netherlands[3]-[6]. A non-destructive, single shot measurement of a 1.7 ps long electron beam is performed with an estimated accuracy of 0.37 ps. The wakefields behind the electron beam are also measured with this technique. The SLAC SPPS facility has demonstrated the generation and measurement of very short electron bunch lengths of 50 to 80 fs for single bunches.

The goal of this proposal is to perform EO measurements of the length of the electron bunches in the Vanderbilt free-electron laser (FEL). A short pulse Ti:sapphire laser, approximately 15 fs will be used

as the probe laser. This should yield an error of less than 240 fs on a single-shot measurement of a 1 ps electron beam (assuming a chirped pulse length of about 4 ps for good signal to noise); chirped for a shorter electron pulse of 0.3 ps (assuming a chirp of 1.2 ps) this would result in a resolution of less than 130 fs. Ref. [6] gives the minimum intrinsic resolution as $\Delta t = \sqrt{t_0 t_c}$, where t_0 is the unchirped pulse length and t_c is the chirped pulse length.

A Ti:sapphire oscillator will be installed at the Vanderbilt Free-electron Laser Center. It will be synchronized with the electron beam (and FEL laser beam). A laser with a 15 fs pulse length and approximately sub-100 fs synchronization is available. This should happen before the end of the calendar year. The EO crystal holder and the laser beamline to the electron beamline will be designed and built. There is currently operating a diagnostics chamber on the FEL that measures coherent transition radiation and coherent diffraction radiation from the FEL electron bunches[2]. With the electro-optic measurement in the same chamber, this will give three complementary bunch length diagnostics.

For linac physics reasons, as well as for free-electron laser physics reasons, it is interesting to measure the evolution/change of the electron bunch through the bunch train. As mentioned above, FEL's need good quality bunch trains: the electron bunches throughout the train need to be evenly spaced and of equivalent length. The bunch train is affected by the RF fill time in the linac, the quality of the RF pulse, the long range wakefields, and any variation in the electron source.

Single-shot EO measurements will be compared to coherent transition radiation measurements of the bunch length, as well as sampling measurementswith the EO technique (using an unchirped pulse and stepping through the electron bunch) . The electron beam at the FEL has a single pulse charge of 50 pC, however the Compton xray machine at the Center has single bunch charges of 1-5 nC in 8 ps and is available for experiments.

The Vanderbilt FEL Center has the needed expertise for these experiments. The Center routinely runs a 45 MeV electron linac with high average power as a driver for the FEL. The Center also runs a tunable, back-scattered xray source that uses a high-charge, 45 MeV electron bunch and a Ti:sapphire driven glass laser capable of 20 TW in 8 ps. The electron bunch and the laser are synchronized on the picosecond level. An optical parametric generator system capable of tunable light from UV to mid-IR is also run by Center personnel. That system is based on a Ti:sapphire oscillator and amplifiers driving nonlinear interactions in crystals to generate tunable wavelength light.

Broader Impact

The budget for this project is mostly for a graduate student and two summers of undergraduate help. The graduate student has been invaluable in motivating experiments and data analysis. He is also being trained as an accelerator physicist with talents needed by many existing and planned particle beam machines. Vanderbilt University has a joint physics and astronomy training program with Fisk University, an historically black college. It is part of the plan to be more active in this collaboration and hire undergraduates from Fisk for summer work.

Results of Prior Research

The UCLC collaboration and NSF have kindly supported this effort over the last two years. First with seed money and most recently with a year of salary for a shared graduate student with Dr. Bibo Feng's efforts in the study of coherent diffraction radiation electron diagnostics. This and other linear collider efforts receive broad support from the FEL Center director Dr. David Piston, in the form of support staff, vacuum hardware, and other materials and supplies.

Seed Money for Electro-optic bunch length measurements
Award: NSF PHY-0303702
Award period: September 15, 2003 to February 28, 2005
Award amount: $11,209

This was awarded by the NSF for UCLC work and is administered as a sub-contract with Cornell University. The money was used to purchase a pulse-picker to reduce the 80 MHz Ti:sapphire output to the 30 Hz needed for the probe laser. This will reduce the background on the spectrometer or other detection device. The pulse-picker was received in December 2004 and is being tested with another 80 MHz Ti:sapphire laser in the Center. The grant also paid for a very valuable trip to the Victoria Linear Collider Workshop in July 2004. It was very helpful to see the state of the international research. The remaining portion is being used to purchase electro-optic crystals.

Single-shot, electro-optic bunch length measurement of a picosecond electron bunch length
Award: NSF PHY-0355182
Award period: September 1, 2004 to August 31, 2006
Award amount: $18,082

This is also an award by the NSF for UCLC work and is administered as a sub-contract with Cornell University. The money is being used to pay a graduate student. He is shared with Dr. Bibo Feng and is working on electro-optic and diffraction radiation diagnostics. The diffraction radiation experiment is currently taking data[2].

Facilities, Equipment and Other Resources

The FEL Center is a world-class free-electron laser facility at Vanderbilt University. Within the Center there are ten staff engineers, scientists and technicians. Their specialties include mechanical engineering and mechanical design, high-vacuum engineering, operation and maintenance of high power pulsed lasers, RF/microwave engineering, data acquisition, electronics and pulsed power, data analysis, and more. The Center houses the FEL which is based on a 45 MeV, a Compton backscattered xray source which uses a photocathode RF gun and a 20 J, 8 ps laser, and an optical parametric amplifier laser system. Center staff operate, maintain, and upgrade these machines.

Vanderbilt University has very good talent and equipment in the scientific machine shop which the Center routinely uses and has subsidized access to.

FY2005 Project Activities and Deliverables

This year the fast Ti:sapphire laser will be installed. There will be a variety testing and diagnostics performed. The detector for the electro-optic measurement will be rehabilitated and tested. It is an older, but high quality CCD spectrometer.

First bunch length measurement could occur on the Compton xray machine due to easy accessibility. It is a self-shielded linear accelerator, with staff working around the machine while it is pulsing. This gives easy access to optics near the beamline.

The design and start of construction for the laser beamline from the second floor to the first floor (FEL vault) will occur. This is a longer run and will involve several remote controlled mirrors. It has the added difficulty of maintaining the fast laser pulse, and large bandwidth which is easily disturbed even by passage through air.

These activities will be reported on at the linear collider and collaboration workshops. Students will be collaborating on all linear collider experiments with analysis work on the coherent diffraction radiation and coherent transition radiation measurements.

Graduate students will attend the U. S. Particle Accelerator School.

FY2006 Project Activities and Deliverables

The electro-optic measurements of bunch length of the FEL electron beam will be carried out. Multi-pulse measurement, stepping through the electron bunch train will be performed. With other electron bunch length monitoring, and FEL laser bunch length monitoring, there will exist a plethora of measurements to compare.

These activities will be published in appropriate journals and reported on by the students at conferences and workshops. Students will attend the U. S. Particle Accelerator School.

Budget justification: Vanderbilt University

The budget is dominated by support for a graduate student and for summer students. This will train new accelerator physicists at a time when there appears a current and future need. The summer students will be introduced to a research intensive environment and to linear collider and laser activities. Currently, there exists a joint scientific training grant between Fisk University, an historically black college, and Vanderbilt University. This relationship is being explored for possible summer students and collaborators.

The new graduate student will need a computer for data analysis.

At the FEL Center travel budgets are small, so for the students and this author to report on activities, two to three trips are budgeted. The graduate student should attend the U. S. Particle Accelerator school each year. This is not only instructive, but it allows her to make connections and to appreciate the breadth and depth of accelerator physics and beam dynamics.

The materials and supplies envisioned are for fast laser optics, *i.e.* lenses, mirrors, vacuum windows, all must have very small dispersion.

Three-year budget, in then-year K$

Institution: Vanderbilt University, Nashville, TN

Item	FY2005	FY2006	Total
Graduate Students	13.7	21.2	34.9
Undergraduate Students	2.6	2.7	5.3
Total Salaries and Wages	16.3	23.9	40.2
Fringe Benefits, Health Insurance	1.6	1.6	3.2
Tuition Share (no overhead)	4	0.6	4.6
Total Salaries, Wages and Fringe Benefits	21.9	26.1	48
Computer	2	0	2
Travel	4	4	8
Materials and Supplies	4	3	7
Total direct costs	31.9	33.1	65
Indirect costs(1)	14.5	17.2	31.7
Total direct and indirect costs	46.4	50.3	96.7
(1) Vanderbilt University has 52% rate FY05 and 53% FY06.			

References

[1] R. Lai, U. Happek, and A. J. Sievers, "Measurement of the longitudinal asymmetry of a charged particle beam from the coherent synchrotron or transition radiation spectrum," Phys. Rev. **E 50**, R4294 (1994).

[2] B. Feng, W. E. Gabella, and T. R. Sashalmi, "Electron Beam Diagnostics using Diffraction Radiation," in the *Proceedings of the 2004 International Free-electron Laser Conference, August 29-September 3, 2004, Trieste, Italy.*

[3] I. Wilke, A. M. MacLeod, W. A. Gillespie, G. Berden, G. M. H. Knippels, and A. F. G. van der Meer, "Single-shot electron-bunch length measurement," Phys. Rev. Lett. **88**, 124801-1 (2002).

[4] X. Yan, A. M. MacLeod, W. A. Gillespie, G. M. H. Knippels, D. Oepts and A. F. G. van der Meer, "Application of electro-optic sampling in FEL diagnostics," Nucl. Inst. and Meth. **A 475**, 504 (2001).

[5] X. Yan, A. M. MacLeod, W. A. Gillespie, G. M. H. Knippels, D. Oepts and A. F. G. van der Meer, "Subpicosecond electro-optic measurement of relativistic electron pulses," Phys. Rev. Lett. **85**, 3404 (2000).

[6] Z Jiang and X. C. Zhang, "Measurement of spatio-temporal terahertz field distribution by using chirped pulse technology," IEEE Jour. Quant. Elect. **36**, 1214 (2000).

[7] M. J. Fitch, A. C. Melissinos, P. L. Colestock, J.-P. Carneiro, H. T. Edwards and W. H. Hartung, "Electro-optic measurement of the wake fields of a relativistic electron beam," Phys. Rev. Lett. **87**, 034801-1 (2001).

[8] M. J. Fitch, A. C. Melissinos and P. L. Colestock, "Picosecond electron bunch length measurement by electro-optic detection of the wakefield," published in the Proc. of the Particle Accelerator Conference 1999.

2.7: Design for a Fast Synchrotron Radiation Imaging System for Beam Size Monitoring

(renewal)

Accelerator Physics

Contact person
Jim Alexander
jima@lns.cornell.edu
(607) 255-5259

Institution(s)
Albany
Cornell

Funds awarded (NSF)
FY04 award: 21,082

New funds requested
FY05 request: 23,503
FY06 request: 0
FY07 request: 0

Design for a Fast Synchrotron Radiation Imaging System for Beam Size Monitoring

Classification (accelerator/detector: subsystem) Accelerator: Beam Monitoring.

Personnel and Institution(s) requesting funding

Jim Alexander, Mark Palmer, Cornell University
Jesse Ernst, State University of New York, Albany

Project Leader Jim Alexander
email: jima@lns.cornell.edu
phone: 607-255-5259

Overview of Project

With the high intensity, low emittance beams needed to reach the luminosity goals of the linear collider, beam size monitoring will play an important role in machine operation. In the damping rings synchrotron radiation (SR) emitted by the bunch can provide a means of measuring transverse bunch size and shape. With suitable imaging and high speed detection of the SR, bunch size, shape, and position may be determined with single bunch discrimination and minimal disturbance to the passing beam. A system fast enough to capture such a "snapshot" of a single beam bunch would be a useful addition to the Linear Collider diagnostics package and also be a valuable contribution to general accelerator physics and technology.

We propose to develop imaging and detection techniques that could be used to directly image the synchrotron radiation.

Although the details of the damping ring of the future ILC are not known yet, the older NLC and TESLA designs indicate a range of possibilities. In the NLC(TESLA) damping ring designs, the vertical bunch size at the midpoint of the dipole magnets is $\sim 5(7)\mu m$ and the horizontal size is $\sim 35(45)\mu m$. Beam energy is $\sim 2(5)$ GeV and the critical energy is about $3\gamma^3\hbar c/\rho = 8(6)$ keV. Synchrotron radiation is cast forward in a narrow cone of opening angle $1/\gamma$. An imaging system working in the optical region would be diffraction limited and incapable of resolving the small vertical size of the beam, but wavelengths below 1nm (ie X-rays above $\sim$1keV) will provide sufficient resolution. An optimal choice for the working energy is thus constrained from below by diffraction, from above by critical energy, and must be chosen to permit maximal transmission by the optical components yet maximal absorption by the detector.

Imaging and detecting these photons poses interesting technical challenges. A system suitable for damping ring use requires three principal components:

1. A point-to-point imaging optical system suitable for $\sim 1 - 10$ keV X-rays. Several technologies exist, including grazing angle mirror systems, diffracting aluminum or beryllium lenses, and Fresnel zone plates. Each has advantages and disadvantages. Grazing angle systems are inherently achromatic, but require high precision control of the surface figure. Diffracting lenses and zone plates are wavelength specific and would require a monochromator upstream, but are mechanically less demanding. (A monochromator has the useful side-effect of reducing flux and therefore minimizing thermal load on the dimensionally sensitive optical elements.) Diffracting systems also introduce absorption which must be kept low by suitable choice of material.
2. A low-noise, high speed, high resolution two-dimensional detector with sufficiently fast response to cleanly separate the closely spaced bunches that one will encounter in a Linear Collider damping ring (1.4 ns for NLC, 20ns for TESLA). Solid state pixel detectors are a plausible detector choice, offering 2-dimensional imaging and high granularity, as well as a low capacitance, low noise source adaptable to the needs of high speed readout. Careful study of the signal transmission

characteristics, starting from the absorption processes, through the drift, diffusion, and charge collection in the detector, and the subsequent transport, switching, amplification, and measurement of the signal charge must be undertaken to fully understand the factors that determine achievable bunch resolution time. 1ns resolution may be achievable in silicon, but subnanosecond resolution likely demands higher mobility materials such as GaAs. (Commercial photodiode receivers for 10GBit/sec ethernet systems exhibit 30ps rise and fall times.) Initial calculations indicate that radiation hardness is also likely to be a significant factor. The intrinsic spatial resolution of the detector and the magnification of the optical system must be optimized together to achieve best resolution.

3. A high speed data acquisition system to extract signals from the detector, perform signal processing and pass results to accelerator control systems in real time. Appropriate software would be required to render the results in a form easily interpreted by an operator.

A well developed literature exists for X-ray optics of the varieties mentioned above [see for instance Handbook of Optics, Vol III, Michael Bass, Ed. and references therein]. Applications are typically related to focussing X-rays to maximize intensity, and high speed time-resolved detection of an imaged low emittance beam will require additional development. Conventional detection systems use flourescent screens to convert X-rays to optical photons which are then detected by a standard CCD camera, offering no useful time resolution.

A system that would offer 10ns resolution could usefully image single TESLA bunches, and is within the range of today's technology but not actually available. A system that would offer 1ns resolution could image single NLC bunches, but may require some technological development. A system that would offer 10ps resolution could permit intrabunch resolution, i.e., bunch tomography, but will demand both technological advance and a deep understanding of the physical processes of the detection mechanism.

We propose to investigate a range of technologies applicable to Xray imaging in the appropriate energy range, and to the development of a high speed bunch imaging device. We will explore in detail the fundamental physical processes that determine its ultimate time resolution.

We build on our ten year's experience with silicon detectors and high speed data acquisition technology. We also have ready access to appropriate facilities, including the Cornell Nanofabrication Facility (CNF), the X-ray lines at the Cornell High Energy Synchrotron Source (CHESS), and of course the CESR storage ring itself, whose energy and beam size parameters, and bunch spacings are relevant to the existing LC damping ring designs. Readily available simulation tools include PISCES (for signal development and transport in solid state detectors), SPICE (for general electronics design), and SHADOW (for xray optics design). We will use these, or others as necessary, and develop our own Monte Carlo simulation of the entire chain from the point of radiation to the final step of detection. We also have available an extensive stock of small prototype silicon detectors and a well equipped detector development laboratory (including probe station, wire bonder, etc.) which can be used to empirically study general properties of signal development in silicon detectors and cross check the simulations and calculations.

Results from Prior Support

Prior research in this area has been supported as part of the current grant NSF PHY-0355182, entitled "University-based Accelerator R&D for a Linear Collider", in the amount $128,315, covering the period 9/1/04-8/31/06. Under this grant, the specific activity entitled "Design for a Fast Synchrotron Radiation Imaging System for Beam Size Monitoring" is supported at the level of $21,082. Results of this prior research are described below.

In the past year we have developed simulation and calculational tools for studying key issues and optimizing design features of a high-speed xray camera and associated xray optics. In particular we have investigated the impact of xray energy choice, which in our design is a tunable parameter to be determined by a monochromator, on signal size, S/N ratio, achievable precision in beam size, shape, and centroid parameters, and radiation damage. A serious issue emerging from this study is that of radiation damage, and we have mapped out the ratio of signal size to radiation dose as a function of

xray energy to find optimal conditions. As a function of energy, both the xray flux and the absorption characteristics are changing, and a problem for radiation dose arises as xray energies decrease and the energy deposition in the semiconductor, though smaller per photon, is nevertheless more and more concentrated in smaller and smaller volumes of material and leads to serious dose rate issues. For silicon the signal/dose ratio is maximized just below the K-shell edge at 1.836 keV, but in absolute terms the dose rate remains very high. In GaAs the situation is similiar but the absolute dose rate is even more severe. We are now developing concepts for a mechanical shutter system to limit the duty cycle of exposure since the natural signal acquisition duty cycle in a damping ring application will be low and radiation impinging on the detector outside the signal acquisition times contributes only to damage. In the proposed activities for FY05 (see below) we will deploy a real detector in CESR and among other things be able to explore the radiation damage issues.

Broader Impact

We are involving graduate students in this project – including a theory student working on his thesis in general relativity – and intend to bring in undergraduates starting in the summer. Commissioning the device and analyzing the data are excellent projects for students, and overall this enterprise is like an entire HEP experiment in miniature, comprising signal detection, signal processing and data acquisition, calibration, data quality control and monitoring, data analysis, quantitative results – and a publication at the end. In these days when HEP experiments are multi-decade endeavours, this kind of project offers excellent short term training opportunity.

FY05 Project Activities and Deliverables

We propose a one year program to build and install a prototype beam size monitor in the CESR accelerator to acquire hands-on experience with this kind of system.

Because the timing constraints in CESR are relatively relaxed (14ns between bunches) we can use existing silicon strip detectors for the front end. We need to build readout electronics for the detectors, and for this purpose we have designed and submitted for fabrication a circuit board which will hold the detectors and the frontend preamplifiers, and we will build a backend digitization and data acquisition system which is cloned directly from existing designs that currently are used to process bunch-by-bunch signals from fast BPMs and other beam monitoring devices in CESR. The silicon strip detectors are 6.4mm $\times$ 6.4mm prototypes left over from old CLEO III detector development projects. Their size and response characteristics are well matched to the CESR parameters. We have designed and are building a new analog front end preamp to match the detector output to the 72MHz digitization system. In this initial prototype study we will use simple pinhole optics for imaging the synchrotron radiation on the detector and will deploy the apparatus in an existing CHESS xray beamline. As this system is built primarily from existing designs and existing hardware where-ever feasible, the costs are well understood and have been kept as low as possible. The details are laid out in the budget justification below.

Budget justification

We ask for funding for the following electronics components needed for a 32-channel readout system.

preamp board	$1200
analog boards (4)	$3200
timing board	$600
I/O board	$450
digital board	$1400
power supply	$1000
timing pickup module	$300
cables, connectors and misc.	$500
xray pinhole structures (3)	$2400
xray filters	$750
beryllium vacuum window	$400
miscellaneous expenses	$800
mechanical shutter system:	
control board	$1350
pulsed power supply	$950
monitor and feedback	$300
materials	$1000
Total	$16,600

In addition, we request travel funds for Jesse Ernst who will travel to Ithaca 6 times at an average cost of $350 per trip, and funds for other miscellaneous expenses incurred at SUNY Albany in the execution of the project.

Budget tables: all figures in K$.

Institution: Cornell University

Item heightOther Professionals	0
Graduate Students	0
Undergraduate Students	0
Total Salaries and Wages	0
Fringe Benefits	0
Total Salaries, Wages and Fringe Benefits	0
Equipment	14.8
Travel	0
Materials and Supplies	1.8
Other direct costs	0
Albany subcontract	4.65
Total direct costs	21.25
Indirect costs (58%)	2.253
Total direct and indirect costs	23.503

Institution: State University of New York, Albany

Item heightOther Professionals	0
Graduate Students	0
Undergraduate Students	0
Total Salaries and Wages	0
Fringe Benefits	0
Total Salaries, Wages and Fringe Benefits	0
Equipment	0
Travel	2.1
Materials and Supplies	1.0
Other direct costs	0
Total direct costs	3.1
Indirect costs(50%)	1.550
Total direct and indirect costs	4.65

2.9: Radiation damage studies of materials and electronic devices using hadrons

(progress report)

Accelerator Physics

Contact person
David Pellett
pellett@physics.ucdavis.edu
(530) 752-1783

Institution(s)
UC Davis
Fermilab
SLAC

Funds awarded (DOE)
FY04 award: 33,059
FY05 award: 38,000
FY06 award: 38,000

Project Name

Radiation Damage Studies of Materials and Electronic Devices Using Hadrons

Classification (Accelerator)

LCRD 2.9

Personnel and Institution

University of California, Davis, Department of Physics:
Maxwell Chertok, David E. Pellett (professors)

Collaborators

Stanford Linear Accelerator Center:
James E. Spencer, Zachary R. Wolf (staff scientists)

Fermi National Accelerator Center:
James T. Volk (staff scientist)

Project Leader

David E. Pellett
email pellett@physics.ucdavis.edu
phone (530) 752-1783

Project Overview Radiation effects are an important but understudied area that are seldom part of the basic design process for many reasons. Notwithstanding, many materials and electronic devices should be tested for their ability to survive in the radiation environment expected at any future linear collider (LC). Radiation-sensitive components of the accelerator and detectors will be subjected to large fluences of hadrons as well as electrons and gammas during the lifetime of the accelerator. Examples are NdFeB permanent magnets which have many potential uses in the damping rings, injection and extraction lines and final focus, even though the linacs will be superconducting; electronic and electro-optical devices which will be utilized in the detector readout, possible gamma channels and accelerator control systems; and CCDs which will be required for the vertex detector.

UC Davis has two major facilities (see description below) which can be used to provide needed information on hadron radiation damage, the McClellan Nuclear Reactor Center (MNRC), located in Sacramento (approximately 50 mi. round trip from the Davis campus), and the UC Davis Crocker Nuclear Laboratory (CNL) cyclotron (on campus). This project is in the second year of a three year program funded by the US Department of Energy under LCRD contract DE-FG02-03ER41280. It is described more fully in the 2004 LCRD Accelerator Proposal, Sec. 2.9. The initial study in this program concerns radiation damage from fast neutrons in samples of NdFeB permanent magnet materials from different vendors using the MNRC facilities.

Permanent magnet beam optical elements have been in use in the SLAC damping rings and their injection and extraction lines since 1985. They are also candidates for use in final focus quads, damping rings, wigglers and possibly elsewhere in the LC. It appears advantageous to use NdFeB for such magnets due to its lower cost and its higher energy product, $(BH)_{\max}$,

relative to SmCo. However, because its Curie temperature, T_C, is much lower than that of SmCo, one needs to better understand and characterize the degradation of its magnetic properties due to radiation damage.

Neutrons from photonuclear reactions are expected to be an important source of radiation damage to most materials in the beam tunnels and damping ring enclosures. The radiation doses have been estimated in the NLC beam tunnel using a simulation based on electron losses [1]. These losses create showers of secondary particles dominated by electrons, positrons, photons and neutrons. The neutron energy spectrum is broad but peaked near 1 MeV. In a region under a magnet, approximately 25 cm below the beam line, the equivalent fluence of 1 MeV neutrons (normalized to radiation damage in silicon) was estimated to be 1.9×10^{14} cm^{-2} for 10 years of operation. The magnets themselves are likely to see much higher neutron fluences, especially in other locations, such as the damping rings. Brown and Cost [2] have shown that the remanence of NdFeB permanent magnets may be reduced significantly for neutron fluences of this order of magnitude and higher when irradiated at an elevated temperature (350 K). We know that the rate of reduction with fluence depends on the type of magnet, its operating point during irradiation, the intrinsic coercivity of the material and the manufacturer of the material [3]. Thus, it is necessary to characterize the radiation damage of candidate materials for LC NdFeB permanent magnets using neutron fluences to determine the useful life of any proposed devices based on using such materials. Our measurements appear to be unique in their ranges of loading or operating points and they complement the measurements of Ito, et al. using 200 MeV protons [4]. As Ito et al. make clear, there are discrepancies between available measurements with protons and the damage mechanisms which are not understood. Further, there also appear to be inconsistencies between the available neutron damage studies and the proton measurements so that this work is needed if NdFeB magnets are to be considered for the baseline LC design. Clearly, the measurements will be useful for other applications.

Of course, high doses of gammas and electrons are also present in these areas but the associated radiation damage is expected to be much less than from the neutrons [3]. SLAC is in a good position to verify this with bremsstrahlung on candidate materials. Samples of NdFeB and SmCo have been tested at SLAC (with Lockheed Martin) together with many other materials using Co^{60} gammas with no observable effects up to 1 MGy – as expected [5].

Existing measurements of the radiation environment in the SLAC damping rings should provide an estimate of the neutron fluences in the LC damping ring magnets. The existence of significant neutron fluences have been demonstrated along the beam line in the SLC electron damping ring and their sources have been studied [6]. Fermilab is also estimating beam loss distributions and particle fluxes for LC collimation systems which will help specify the requirements elsewhere.

The considerations above led us to begin our study with the effects of 1 MeV-equivalent neutrons on NdFeB samples with different values of coercivity and from different manufacturers. The presence of B^{10} in the material with its very large thermal neutron capture cross section greatly increases the radiation dose delivered for a given thermal neutron fluence relative to fast neutrons, so measuring the effect of thermal neutrons is also important since this effect leads to irreparable damage in contrast to Co^{59} conversion to Co^{60} or the possible use of Gd as a substitution dopant for Nd.

We did not propose to test SmCo samples in this program. There is already a proof of

principle for the use of SmCo in the SLC and evidence from Ito et al. [4] that the material is considerably more radiation-hard than NdFeB. Further, SmCo presents a more difficult handling and disposal problem due to the copious production of the long-lived radioactive isotopes Sm^{153} and Co^{60} by thermal neutrons. We also note that SmCo damage has been studied in the SLAC damping rings by the SLAC people in this proposal [6].

The latter part of this project will involve testing electronic and electro-optical devices and materials for LC accelerator and detector applications [7] using neutrons at MNRC or at CNL or 63 MeV protons in the CNL radiation test beam. While we have done a total of six irradiations so far on PM materials we will begin our first fiber optic materials with the next PM irradiation run.

Current Research Progress

As mentioned earlier, this project is in the second year of a three year program funded by the US Department of Energy under LCRD contract DE-FG02-03ER41280. We briefly summarize the progress in this section. More detailed information has been presented at conferences and is available on the web [3][8]. Latest results of current work will be given at PAC2005 [9].

Test assemblies of NdFeB magnet blocks with iron flux returns have been fabricated that fit into the MNRC reactor test chambers and provide a broad variation in operating points over the different constituent blocks. A conceptual diagram showing how the magnet is constructed from NdFeB magnet blocks and iron flux returns is shown in Fig. 1. The assemblies that have been tested so far have considerably thinner flux returns than indicated in the diagram or than were simulated in order to fit into the existing vessel as well as to reduce radiation levels and insure uniform dose distributions. The basic configuration is an asymmetric quadrupole magnet with simple two-pole geometry and a gap which can be varied through the choice of the flux return pieces. Typical block dimensions are in the range 6-9 mm. The gap has thus been chosen in the range 2-7 mm. In the case shown, the load-line of the lowest block is far into the first B-H quadrant (from the field of the adjacent, larger block and circuit) and is nearly the same throughout the block while its matching partner at the top has material that is clearly in the second quadrant as does the larger block. As the gap is decreased, the difference increases - making the upper one more susceptible to damage. The magnetizations of individual blocks were measured using a Helmholtz coil facility in the SLAC Magnetic Measurements Group. Also, field scans were made using a special Hall probe fixture. Details of the design of the magnet test assemblies and results of field measurements are given in the report by Spencer and Volk [3].

An initial irradiation of a magnet assembly was performed directly downstream of a hydrogen target in a SLAC beam line, achieving a dose of 10 kGy of gammas and 1 kGy of 1 MeV equivalent neutrons (stated as tissue equivalent dose to simplify comparisons). The two most significant radioactive isotopes were Be^7 and Cr^{51} from the B and Fe with the latter 20 times stronger but still less than one μCi. The next strongest after these was down another factor of 4 from the Be^7. Half lives are of order one to two weeks. There was no evidence of radiation from the Nd derived isotopes nor from any substitution elements such as Dy, Pr or Tb.

Magnet structures using blocks manufactured by Sumitomo and isolated (open circuit) Shin-Etsu blocks of N50M and N34Z were used, among others, for irradiation at MNRC as they provide a wide variation in magnetization characteristics. They have been subjected to a continuing series of irradiations using 1 MeV-equivalent neutrons in the NIF facility at the MNRC reactor.

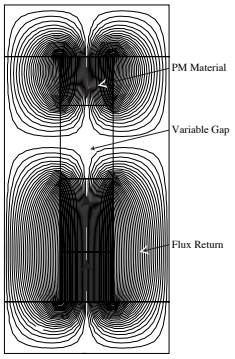

Figure 1: Schematic diagram of magnet test structure showing magnetization vectors.

The irradiation takes place inside the reactor vessel but outside the core inside a shielded container which provides attenuation of thermal neutrons and significantly reduces gamma ray exposure. Magnets are attached to a hexagonal structure inside the container. The container is rotated during irradiation to insure uniform neutron doses between samples. Various forms of dosimetry were provided. The irradiations have been relatively short (46 minutes) to allow safe handling of the irradiation vessel by reactor personnel and to avoid long delays for the induced radioactivity to decay prior to shipping to SLAC for measurement. Gamma ray spectroscopy was performed on samples after irradiation to characterize the radiation and to evaluate the effect of doping the material by the manufacturer with other rare earth substitutions [8]. As described above, such measurements are important but seldom made.

The results of the irradiation at SLAC and the initial series of irradiations at MNRC were presented at EPAC04 [8]. The results of the first three MNRC runs are shown in Table 1. Details of the blocks and the numbering scheme are given in [3]. The larger blocks are now at top (#7) and bottom (#5). Easy axis strength errors are small and repeatable even for the small blocks. Fig. 2 shows the magnetization loss of the blocks vs. run number. Run 1 corresponds to no radiation (corresponding to Table 1). Run 2 was the irradiation in End Station A at SLAC. The remaining runs were at MNRC with 9.7×10^{12} n/cm^2 for Run 3 and 1.9×10^{13} n/cm^2 each for Runs 4 and 5. The total 1 MeV-Si equivalent neutron dose delivered at MNRC was 35 Gy.

Table 1: Initial magnetizations for irradiated blocks and damage rate

Block	M_x (G)	M_y (T) $\pm$ (G)	M_z (G)	$\delta M_y/\delta D$ (G/Gy)
#7 (top)	167	1.0904± 7	483	-1.6
#3 (mid)	-414	1.0950± 5	343	-1.2
#5 (bot)	-444	1.0727± 7	283	-0.7
N34Z1	-382	1.1102 ±2	-382	-0.4
N50M1	-144	1.3717± 1	-2.8	-1.4

The results are consistent with fast neutron damage being proportional to dose, but depending as well on the disposition of the effective load lines relative to the nonlinear part of the hysteresis curve. The two larger blocks bracket the smaller one and the variation of the damage with dose is roughly twice as great for #7 as for #5. We have also investigated

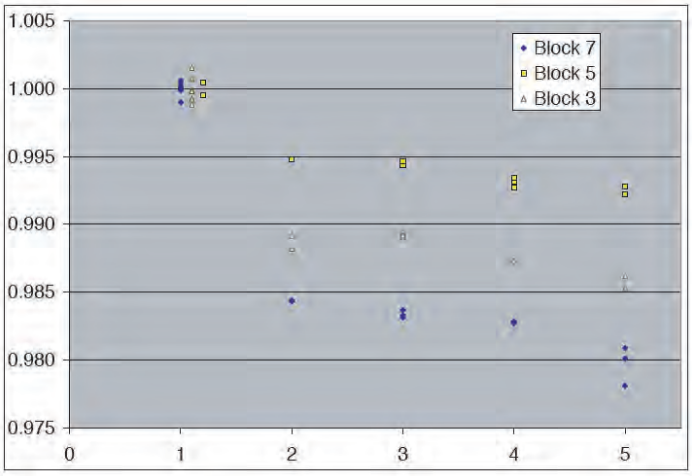

Figure 2: Magnetization loss vs. radiation run number.

the effects on magnet radiation resistance and induced radioactivity due to the presence of additional rare-earth components such as Tb (as revealed by the gamma spectra) [8].

In the last year, we had encountered some delays in this program due to changes in personnel at MNRC and the shutdown at SLAC but our irradiations at MNRC are now progressing well. We have constructed a portable magnet measuring stand which uses stepping motor micropositioners controlled by a laptop computer running LabVIEW to automate the Hall probe measurements. New magnet blocks using materials from Hitachi (HS36, HS48) and a new magnet structure with three more blocks in a higher field configuration have been added to the series of tests. Results from the current work will be presented at PAC05 in Knoxville in May [9].

Table 2 gives results for three different types of blocks from our first 43 min run in NIF taken before shipping and magnetic measurements to obtain trace elements as well as sources and levels of radioactivity. While "Ref" refers to a 3-block magnet (#3, 5 & 7 in Table 1) with a thin iron return yoke, the overall volumes of material and their geometries in the 3 samples were comparable to obtain uniformity of dose throughout their volumes. Similarly, all blocks were Ni plated. For completeness, we note that Fe has 4 stable isotopes ranging from A=54-58 with ${}_{26}Fe^{56}$(91.7%) while Ni has 5 ranging from A=58-64 with ${}_{28}Ni^{58}$(67.9%).

Essentially all of the observed lines have been identified but a number were not tabulated to save space e.g. some Tb^{160} levels with higher rates than Co^{60} were left out because they don't affect our conclusions. The sources of most lines are clear e.g. n-capture on Fe^{58}, Nd^{146} or the substitution element Tb^{159}. Neutron knockout (n,2n) on Nd^{148} also has a cross section comparable to capture leading to Nd^{147} while (n,p)-exchange reactions on Fe^{54}, Ni^{60} or trace contaminants esp. from the rare earths are also seen. Pm^{151} results from $Nd^{150}(n,\gamma)Nd^{151}$ followed by β^- decay. It follows from Table 2 that N50Z has about 55% as much Tb as N34Z. Based on known capture cross sections for Fe^{58} and Tb^{159} and relative abundances one infers a large substitution in N34Z that greatly improves its RR.

Table 3 compares a newer block (HS36) from Hitachi with a block having comparable characteristics to Shin-Etsu's N34Z. Clearly, they are doped differently i.e. the Hitachi block uses Pr^{141} as well as Dy which has 8 stable isotopes as compared to Tb^{159} which also has only a

Table 2: Radioactive species by count rate.

Element $_Z\mathrm{X}^A$	Decay Prob.[a]	Energy [keV]	Block Type[b]		
			N34Z	N50M	Ref
$_{65}\mathrm{Tb}^{160}$	0.270	298.6	47.6	26.5	-
$_{65}\mathrm{Tb}^{160}$	0.168	879.3	28.4	15.6	-
$_{65}\mathrm{Tb}^{160}$	0.127	966.1	22.3	12.4	-
$_{65}\mathrm{Tb}^{160}$	0.130	1177.9	11.9	6.5	-
$_{27}\mathrm{Co}^{60}$	1.000	1173.2	2.8	2.4	2.4
$_{27}\mathrm{Co}^{60}$	1.000	1332.4	2.6	2.1	2.2
$_{61}\mathrm{Pm}^{151}$	0.229	340.1	2.6	3.1	2.4
$_{60}\mathrm{Nd}^{147}$	0.280	91.2	2.3	2.8	1.7
$_{60}\mathrm{Nd}^{147}$	0.131	531.0	2.1	2.6	2.0
$_{61}\mathrm{Pm}^{151}$	0.088	167.8	1.2	1.4	1.1
$_{61}\mathrm{Pm}^{151}$	0.072	275.3	1.0	1.3	1.0
$_{61}\mathrm{Pm}^{149}$	0.031	285.9	0.9	1.4	1.0
$_{25}\mathrm{Mn}^{54}$	1.000	834.8	0.3	0.3	1.0
$_{26}\mathrm{Fe}^{59}$	0.565	1099.2	0.3	0.1	0.3

[a]Taken from [10].

[b]Resized blocks from Sumitomo Metals, Ltd.

single isotope. The magnetic HH comparisons will appear in the PAC05 paper together with Hall probe scan distributions.

Facilities, Equipment and Other Resources

UC Davis has two major facilities which can be used to provide needed information on hadron radiation damage, the McClellan Nuclear Reactor Center (MNRC), located in Sacramento (approximately 50 mi. round trip from the Davis campus), and the UC Davis Crocker Nuclear Laboratory (CNL) cyclotron (on campus).

The MNRC reactor has a number of areas for irradiating samples with neutron fluxes up to 4.5×10^{13} n/cm^{2}s. A specialized area (NIF) allows irradiation with 1 MeV-equivalent neutrons in a flux of 4.2×10^{10} n/cm^{2}s while suppressing thermal neutrons and gammas by large factors. Other areas allow irradiating very large objects at lower fluxes.

The CNL radiation test beam consists of protons of up to 63.3 MeV kinetic energy spread over a rather uniform beam spot 7 cm in diameter. A typical central flux is 4.2×10^9 protons/cm^{2}s (0.56 kRad/s (Si)). A secondary emission monitor calibrated with a Faraday cup is used to measure the beam fluence to an accuracy of better than 5%. The beam profile has been established by a variety of means, showing the dose to have fallen by only 2% at a radius of 2 cm. The facility can also produce a neutron beam with a flat energy spectrum extending to 70 MeV kinetic energy. We have used the CNL proton facility for a wide variety of tests on electronic devices and detector components.

References

[1] S. Roesler et al., "Dose to Electronics in NLC Beam Tunnel," SLAC RP 99-15, Dec. 1999.

Table 3: Radioactive species by count rate.

Element ${}_Z\mathrm{X}^A$	Decay Prob.[a]	Energy [keV]	Block Type[b]		
			N34Z	N50M	HS36
${}_{65}\mathrm{Tb}^{160}$	0.270	298.6	47.6	28.4	-
${}_{65}\mathrm{Tb}^{160}$	0.168	879.3	28.4	15.6	-
${}_{65}\mathrm{Tb}^{160}$	0.127	966.1	22.3	12.4	-
${}_{65}\mathrm{Tb}^{160}$	0.130	1177.9	11.9	6.5	-
${}_{27}\mathrm{Co}^{60}$	1.000	1173.2	2.8	2.4	-
${}_{27}\mathrm{Co}^{60}$	1.000	1332.4	2.6	2.1	-
${}_{61}\mathrm{Pm}^{151}$	0.229	340.1	2.6	3.1	34.4
${}_{61}\mathrm{Pm}^{151}$	0.088	167.8	1.2	1.4	15.0
${}_{25}\mathrm{Mn}^{54}$	1.000	834.8	0.3	0.3	12.9
${}_{59}\mathrm{Pr}^{142}$	0.036	1575.6	-	-	12.9
${}_{61}\mathrm{Pm}^{151}$	0.072	275.3	1.0	1.3	11.8
${}_{61}\mathrm{Pm}^{149}$	0.031	285.9	0.9	1.4	3.7
${}_{66}\mathrm{Dy}^{165}$	0.15	94.8	-	-	2.8
${}_{60}\mathrm{Nd}^{147}$	0.280	91.2	2.3	2.8	2.0
${}_{60}\mathrm{Nd}^{147}$	0.131	531.0	2.1	2.6	1.9

[a]Taken from [10].

[b]N-series from Shin-Etsu, HS from Hitachi.

[2] R.D. Brown and J.R. Cost, "Radiation-Induced Changes in Magnetic Properties of Nd-Fe-B Permanent Magnets," *IEEE Trans. Magnetics Vol. 25*, 1989.

[3] James Spencer and James Volk, "Permanent Magnets for Radiation Damage Studies," presented at PAC03, SLAC-PUB 9876, 2003.
http://www.slac.stanford.edu/pubs/slacpubs/9750/slac-pub-9876.pdf

[4] Yoshifumi Ito et al., "Magnetic flux loss in rare-earth magnets irradiated with 200 MeV protons," *Nucl. Instr. and Meth. B 183*, 2001.

[5] H.B. Luna et al., "Bremsstrahlung Radiation Effects in Rare Earth PM's", *Nucl. Instr. and Meth. A285* (1989) 349.

[6] James Spencer, et al., "Further Experience with SLC Permanent Magnet (PM) Multipoles," presented at PAC03, SLAC-PUB 9884, 2003.
http://www.slac.stanford.edu/pubs/slacpubs/9750/slac-pub-9884.pdf

[7] E. Colby et al., "Gamma Radiation Studies on Optical Materials," *IEEE Trans. Nucl. Sci. 49* (2002) 2857-2869.

[8] J. Allen et al., "Radiation Damage Studies with Hadrons on Materials and Electronics," presented at EPAC04, SLAC-PUB 10500, 2004.
http://www.slac.stanford.edu/pubs/slacpubs/10500/slac-pub-10534.pdf

[9] J. Allen et al., "Fast Neutron Damage Studies on NdFeB Materials," abstract submitted to PAC2005.

[10] B. Shleien,Ed., *The Health Physics and Radiological Health Handbook*,Scinta, Inc., Silver Spring, Md., 1992.

2.10: BACKGAMMMON: A Scheme for Compton Backscattered Photoproduction at the International Linear Collider

(new proposal)

Accelerator Physics

Contact person
S. Mtingwa
mtingwa@ncat.edu
(336) 334-7423

Institution(s)
NCA&T

New funds requested
FY05 request: 160,200
FY06 request: 193,700
FY07 request: 207,000

BACKGAMMON: A Scheme for Compton Backscattered Photoproduction at the International Linear Collider

Classification (subsystem)

Accelerator: beyond the interaction point

Personnel and Institution(s) requesting funding

S. Danagoulian, Department of Physics, North Carolina A&T State University

Collaborators

S. Mtingwa, Department of Physics, North Carolina A&T State University
M. Strikman, Department of Physics, Pennsylvania State University
R. Pitthan, Stanford Linear Accelerator Center
Y. Kolomensky, University of California, Berkeley

Project Leader

S. Danagoulian
danagous@ncat.edu
(336) 334-7646

Project Overview

We propose to investigate the possibility of Compton backscattering low energy laser pulses off the spent electron and positron beams at the International Linear Collider. The hot backscattered photons would then scatter off fixed targets for a rich variety of physics studies in a scheme dubbed BACKGAMMON, for BACKscattered GAMMas On Nucleons. The first objective would be to operate a heavy quark factory, since the cross sections for charm and bottom quark production would be favorable for producing large numbers of these flavors. Secondly, if the incident laser pulses are circularly polarized, the backscattered photons would be circularly polarized as well, allowing the possibility of producing polarized τ pairs on fixed targets. Also, BACKGAMMON's polarized hot photons could scatter off polarized targets and play an important role in elucidating the spin structure of nucleons. Finally, there is the possibility of studying the photon structure function for the spent electron beam scattering off laser photons.

The original idea of using a next generation linear collider for producing Compton backscattered photon beams for operation of a heavy quark factory is described in Reference [1], which was before the advent of the current generation of B factories using electron-positron colliders. There it was shown that, if one had an electron beam of hundreds of GeV energy, then one could produce on the order of 10^9 B meson pairs per year for studies of CP violation in the B meson system. Such studies would complement nicely the current results from the SLAC/BaBar and KEK/Belle B Factories. Soon after the description of BACKGAMMON for heavy quark production, it became clear that this scheme could be used to operate a polarized τ factory as well. This and subsequent ideas are contained References [2-6].

Milburn [7] and independently Arutyunian and collaborators proposed the original idea of using Compton backscattering in accelerators [8-10]. The detailed theory of Compton backscattering, incorporating the accelerator lattice functions of the initial electron beam, was derived

in Reference [1]. The first practical application of Compton backscattering in a physics experiment was the measurement by Ballam et al. of γ p hadronic cross sections in a bubble chamber at SLAC [11]. Since that initial experiment, there have been a number of studies using Compton backscattered photons, including the Brookhaven National Laboratory's Laser Electron Gamma Source (LEGS) Facility [12,13] and applications of Compton backscattered photon beams to measure the polarization of electron beams [14-19]. Thus, Compton backscattering has enjoyed a rich history.

This project describes research that is unobtrusive to the baseline International Linear Collider (ILC) design. It should be viewed as an add-on experiment that is worthy of further study. Accordingly, in this project, three physics objectives initially would be pursued:

BACKGAMMON I

Unpolarized laser pulses would be incident on the spent electron beam to produce unpolarized hot photons for the photoproduction of heavy quark flavors to study a variety of phenomena, including CP violation in the neutral B meson system, high precision studies of bottom and charm decays, searching for rare and forbidden bottom and charm decays, QCD studies using heavy quark pair events, heavy quark spectroscopy, heavy quark baryons, and other checks on the Standard Model.

BACKGAMMON II

While BACKGAMMON I is using the spent electron beam, circularly polarized laser pulses would be incident on the spent positron beam to produce circularly polarized hot photons for the photoproduction of polarized τ pairs, to study a variety of phenomena, including improving the τ neutrino mass limits from such decays as $\tau^- \rightarrow K^- K^+ \pi^- \nu_\tau$, searching for CP violation in the lepton sector of the Standard Model, searching for rare and forbidden decays, studying the Lorentz structure of τ decays, and other checks of the Standard Model.

BACKGAMMON III

At the conclusion of BACKGAMMON II, the polarized hot backscattered photons would be incident on polarized nucleon targets to measure the gluon contribution to the nucleon spin. An excellent discussion of this point is contained in Reference [20]. The spin content of the nucleon still is not understood fully.

LASER REQUIREMENTS

In Reference [5], the laser requirements of BACKGAMMON are discussed briefly. There, it is emphasized that the laser requirements in this scheme are less stringent than those for a $\gamma - \gamma$ collider. For the $\gamma - \gamma$ collider, the aim is to convert each electron in the collider bunch into a hot photon, leading to the requirement of 1 Joule per laser flash with a 1 kHz repetition rate. In BACKGAMMON, for 10^9 electrons per bunch, only 1 mJ per laser pulse at 1kHz would produce the 10^9 B pairs per year; while for 10^{10} electrons per bunch, as called for in the ILC designs, 10^{10} B pairs per year would be produced. Moreover, if one could push the laser rep rate up to the 10 kHz called for in the ILC designs, then one could produce up to 10^{11} B pairs per year. These B meson pairs would be produced in a much cleaner background than that of the hadron machines, such as the 10^{11} B pairs per year proposed for the BTeV experiment at Fermilab.

A specific laser design and implementation at BACKGAMMON could lay the groundwork for the $\gamma - \gamma$ collider laser system, with the main difference being the lower laser power

requirements for BACKGAMMON. For the $\gamma - \gamma$ collider, it has been suggested that a diode pumped semiconductor laser is plausible [21]. However, for the high repetition rates needed in both these schemes, it may be necessary to time-multiplex a set of lasers. More R&D is needed to settle this issue.

Broader Impact This research will be performed with the assistance of two graduate students and two undergraduate students from North Carolina A&T State University (NCA&T). NCA&T has a Masters program in physics; thus, the graduate students working on this project would use their work to satisfy the thesis requirement. For the undergraduate students, the project would provide invaluable research opportunities so that they could appreciate firsthand the art of basic scientific research. For both the graduate and undergraduate students, the goal would be to encourage them to proceed to the doctorate in physics.

NCA&T is a public institution that is part of the University of North Carolina System. More importantly, it is one of the Historically Black Colleges and Universities, with both graduate and undergraduate enrollments containing in excess of ninety percent (90%) African-American students. Moreover, the physics program enrolls a number of women students, in some years comparable in number to the number of men students. Thus, this research project would proceed within a student environment that is composed of sizable numbers of underrepresented gender and ethnic groups.

NCA&T's partnership with Penn State, SLAC, and UC-Berkeley would be extremely advantageous for all involved. Not only would those institutions become better acquainted with the students' abilities, hopefully leading to future recruitment opportunities, but the students would gain a better appreciation of what is needed to perform at such institutions at the next level of their studies.

Hopefully, the research results from this project will be implemented at the ILC. In the meantime, the results will be presented at physics conferences and workshops and published in premier physics journals.

Results of Prior Research

We recently made substantial progress on linear collider research under two NSF grants: Planning Grant Award number PHY-0303702 (9/15/03 - 8/31/04) and the current Grant number PHY-0355182 (9/1/04 - 8/31/06). North Carolina A&T was a subcontractor with Cornell University, and the grants were for an accelerator project entitled, *Damping Ring Studies for the LC*. The goal was to derive more computationally friendly formulas for the phenomenon of intrabeam scattering (IBS). IBS involves multiple small-angle Coulomb scatterings of particles within a bunch. To compute emittance growth rates due to IBS, the theory involves a series of matrix inversions and computations of the determinants of matrices at each of the many lattice points in the damping ring. To compute emittance growth rates versus bunch charge, popular mathematical codes take many hours to give results. Thus, approximations to the theory are necessary to reduce greatly the time needed to compute emittance growth rates. We derived such computationally-friendly approximations and showed that they give excellent agreement with the full theory for damping rings corresponding to both warm and cold linear collider designs.

For the lower energy damping rings for the warm linear collider designs, IBS would be the most important impediment to achieving ultra low beam emittances. Now that the decision has been made to use cold linear collider technology, the damping ring energies are sufficiently

high that IBS does not seem to be a big problem, although in some designs it is not negligible and should always be checked.

The results of that work are now being revised for publication in Physical Review ST AB. Also, it has much broader applicability than to just the ILC. It can be applied readily to proton accelerators and other electron accelerators, such as synchrotron light sources.

Facilities, Equipment and Other Resources

This project will involve calculations to support the concept of a hot photon factory at the ILC. As such, the main resource will be the computational facilities available at North Carolina A&T. The university offers main frames and personal computers in computer labs across the campus, with sufficient computer assistance to satisfy student and faculty needs. Moreover, the Department of Physics has its own computer lab with local workstations that are available to students and faculty. However, the computer labs are sometimes oversubscribed; thus, annually we would like to purchase two (2) personal computers and computational software to assist with this project.

FY2005 Project Activities and Deliverables

During the first year, we will study the feasibility of using the disrupted beams after the electron-positron interaction point for Compton backscattering laser pulses. Initial work on this issue, as reported by Rainer Pitthan at the recent SLAC Workshop on Machine Detector Interface at the ILC looks promising. Pitthan's talk is posted at the workshop Website www-conf.slac.stanford.edu/mdi/talks/CrossingAngle/ILC_MDI05_Pitthan.pdf. We will study the backgrounds from the electron-positron interaction point to insure that they are manageable and design beamlines to bring the best quality electron and positron spent beams to the two interaction points with the lasers. On the theoretical side, we will understand the details of the angular dependences of the polarizations of the photoproduced τ pairs, and we will perform theoretical studies of the physics issues as outlined above. This would involve both analytic approaches and simulations of the phenomenology. The results of all the first year's activities will be written up in a detailed report.

FY2006 Project Activities and Deliverables

We will understand the requirements on the laser systems and decide how best to implement them for BACKGAMMON. For instance, should a system of lasers be time-multiplexed to match the 10 kHz repetition rate of the electron and positron bunches. We will undertake a detailed study that couples the entire system from the electron-positron interaction point to the electron and positron-laser interaction points to the backscattered photons on the fixed targets. Also, we will begin detailed simulations of the experiments that are being proposed. The results of all the second year's activities will be written up in a detailed report.

FY2007 Project Activities and Deliverables

In the third year, we will concentrate on the detector design and data acquisition. We will study the FOCUS experiment (Fermilab E831) and determine how to improve its detector system for BACKGAMMON I. One advantage of BACKGAMMON I is that the statistics will be several orders of magnitude higher so that a much higher data acquisition rate will have to be implemented. Also, we will propose appropriate detector systems for BACKGAMMONS II and III. By the end of the third year, we will produce a technical design report of the proposed experiments. Finally, we will investigate the possibility of using the spent electron beam to probe the photon structure function. For a review, see Reference [22].

Budget justification:

The entire project will consist mainly of computational and theoretical calculations, with heavy use of simulation codes. The first year's budget will provide research assistantships for two (2) graduate students and two (2) undergraduate students; travel for domestic and international conferences and the Principal Investigator, consultant, and collaborators to visit each other's institutions for the purpose of working on the project; materials and supplies in the form of two (2) personal computers, computer software and other miscellaneous materials; consultant services for S. Mtingwa at the rate of $524 per day for 41.1 days; and tuition support for two (2) graduate students. Note that individual items such as the PCs, which cost less than $5,000, are not considered equipment under NCA&T's regulations.

During the second year, we provide two (2) months summer salary for the PI and we include the same funds as requested the first year, increased mostly for inflation.

During the third year, we include the same funds as requested the second year, increased mostly for inflation.

Fringe benefits are 24% of faculty salaries and 7.65% of $6,000 graduate student summer salary. Other direct costs are tuition for two graduate students. Indirect costs are calculated at North Carolina A&T's 40% rate on modified total direct costs, which excludes tuition.

Three-year budget, in then-year K$

Institution: Institution 1

Item	FY2005	FY2006	FY2007	Total
Faculty (Summer)	0	13.0	13.6	26.6
Other Professionals	0	0	0	0
Graduate Students	30	32	34	96
Undergraduate Students	14	15	16	45
Total Salaries and Wages	44.0	60.0	63.6	167.6
Fringe Benefits	0.5	3.6	3.7	7.8
Total Salaries, Wages and Fringe Benefits	44.5	63.6	67.3	175.4
Equipment	0	0	0	0
Travel	15	16	18	49
Materials and Supplies	12	14	16	42
Consultant Services	21.5	22.6	23.7	67.8
Other direct costs	30	31	32	93
Total direct costs	123.0	147.2	157.0	427.2
Indirect costs	37.2	46.5	50.0	133.7
Total direct and indirect costs	160.2	193.7	207.0	560.9

References

[1] S. Mtingwa and M. Strikman, Phys. Rev. Lett. 64, (1990) 1522.

[2] S. Mtingwa and M. Strikman, in : D. Cline and A. Fridman (eds.), CP Violation and Beauty Factories and Related Issues in Physics, Ann. New York Acad. Sci. Vol. 619 (1991) 211.

[3] S. Mtingwa and M. Strikman, in: D. Cline (ed.), Rare and Exclusive B & K Decays and Novel Flavor Factories, Conference Proceedings, Vol. 261, American Institute of Physics Publication, AIP, New York, 1992, p. 236.

[4] S. Mtingwa and M. Strikman, in: D. Axen, D. Bryman, and M. Comyn (eds.), The Vancouver Meeting, Particles & Fields '91, World Scientific, Singapore, 1992, p. 1106.

[5] S. Mtingwa and M. Strikman, Nucl. Instr. And Meth. A 455 (2000) 50.

[6] S. Mtingwa and M. Strikman, Nucl. Instr. And Meth. A 472 (2001) 189.

[7] R. Milburn, Phys. Rev. Phy. Lett. 10 (1963) 75.

[8] F. Arutyunian and V. Tumanian, Phys. Lett. 4 (1963) 176.

[9] F. Arutyunian and V. Tumanian, Sov. Phys. Usp. 83 (1964) 339.

[10] F. R. Arutyunyan, I.I. Gol'dman, V.A. Tumanyan, Sov. Phys. JETP 18 (1964) 218.

[11] J. Ballam, et. al., Phys. Rev. Lett. 23 (1969) 498.

[12] A.M. Sandorfi, et al., IEEE Trans. Nucl. Sci. NS-30 (1983) 3083.

[13] C.E. Thorn, et al., Nucl. Instr. And Meth. A 285 (1989) 447.

[14] V.N. Baier and V.A. Khoze, Sov. J. Nucl. Phys. 9 (1969) 238.

[15] C. Prescott, SLAC Internal Report, SLAC-TN-73-1, 1973.

[16] D.B. Gustavson, et al., Nucl. Instr. and Meth. 165 (1979) 177.

[17] L. Knudsen, et al., Phys. Lett. B 270 (1991) 97.

[18] G. Bardin, et al., SACLAY Report, DAPNIA-SPhN-96-14, 1996.

[19] G. Bardin, C. Cavata, J.-P. Jorda, Compton polarimeter studies for TESLA, SACLAY Internal Report, 1997.

[20] S. Alekhin, et al., Eur. Phys. J. C 11 (1999) 301.

[21] TESLA Technical Design Report, Appendices, The Photon Collider at TESLA, DESY 2001-011 (2001).

[22] M. Krawczyk, M. Staszel, and A. Zmbrzuski, Phys. Rep. 345 (2001) 265.

2.11: Ground Motion studies at NuMI

(new proposal)

Accelerator Physics

Contact person
Mayda Velasco
mvelasco@lotus.phys.nwu.edu
(847) 467-7099

Institution(s)
Northwestern

New funds requested
FY05 request: 28,489
FY06 request: 0
FY07 request: 0

Proposal Name: Ground Motion studies at NuMI. [1]

Classification (subsystem)

Beamline, interaction region stability.

Personnel and Institution(s) requesting funding

Northwestern University, Department of Physics and Astronomy:
Mayda Velasco (Assistant Professor),
Michał Szleper (Research Associate),
Summer student.

Collaborators

FNAL: Shekhar Mishra, Vladimir Shiltsev.

Project Leader

Mayda Velasco
mvelasco@lotus.phys.northwestern.edu
847 467 7099

Project Overview

Ground motion can cause significant deterioration in the luminosity of a linear collider. Vibration of numerous focusing magnets causes continuous misalignments, which makes the beam emittance grow. For this reason, understanding the seismic vibration of all potential LC sites is essential and related efforts in many sites are ongoing.

The proposed studies were requested by the LC project leader at FNAL, Shekhar Mishra. They will be a continuation of the measurements carried out recently by the Northwestern group, which focused on how the ground motion effects vary with depth. Knowledge of depth dependence of the seismic activity is needed in order to decide how deep the LC tunnel should be at sites like Fermilab. The measurements will be made in the NuMI tunnel. We take advantage of the fact that from the beginning to the end of the tunnel there is a height difference of about 350 ft and that there are about five different types of dolomite layers.

The proposed study has two main goals. First, carrying extended and more systematic measurements which will check the stability of the vibration amplitudes at different depths over

[1] Item ID 55: R & D list for NLC available in `http://www-conf.slac.stanford.edu/lcprojectlist/asp/projectlistbyanything.asp`.

long periods of time. This will allow a better control and more efficient averaging out of the daytime variation effects and a better study of other time dependences, before the actual depth dependence can be descerned with more accuracy. New measurements should also clarify the relatively few poorly understood features of the existing results. The second objective will be making a measurement in the first 150 ft under ground, which the previous study did not cover, but results provided motivation to do so.

The proximity of Northwestern to Fermilab allows us to go to the tunnel frequently in order to change the location of the probes, exchange storage disks and batteries for the equipment (whatever needed) and program data taking for the next period of time.

Broader Impact

We plan to hire a summer student to work on this project. The student will be hired from the SROP (Summer Research Opportunity Program) NU-minority program. This project may be a good opportunity for a young student to learn a variety of issues in modern experimental high energy physics, including both NuMI and LC issues, and to acquire some basic hardware and software skills.

In the past, we have already worked with both an undergraduate physics student and a prospective graduate student on ground motion projects.

Results of Prior Research

First test measurements were made in 2003 in the Aurora Mine, 200 ft below ground level, where measurements using a different equipment had already been made before (V. Shiltsev).

In spring 2004, the equipment was installed in the NuMI tunnel. Measurements were made at three locations inside the tunnel: in the NuMI target hall (depth ∼150 ft), in the absorber hall (∼280 ft) and in the MINOS near detector hall (∼350 ft). Data taking lasted two weeks in total.

Measurements scanned effectively the frequency range of 0.1 - 50 Hz. From an offline data analysis, the following observations have been made:

- Vibrations below 1 Hz come mainly from natural sources. The vibration amplitudes vary slowly in time, but no regular pattern was observed within the timescale of the study.
- Dependence on depth of vibrations below 1 Hz seemed not be present, or could not be discerned outside the limits set by the natural time variations.
- Human activity is the main source of vibrations above 1 Hz. It presents significant day/night and weekday/holiday variations, amounting up to a factor of 3 in the total amplitude averaged over 30 minutes long intervals.
- Significant amount of vibrations above 1 Hz was due to local in-tunnel sources, many of them being strongly time dependent and irregular.

- Vibrations coming from surface sources were visible and their amplitudes depended on, besides depth itself, many details of the study location. These included, e.g., the distance to the nearest shaft or ventillation tunnel.
- Dependence on depth in the range of 150 - 350 ft below ground was found insignificant and possible to descern only after subtracting the vibrations from local sources. Since earlier studies revealed a drop by a factor of ∼2 of the vibration amplitudes between ground level and 150 ft underneath, this precisely turned out to be the range where most attenuation happens.
- Vibrations in the vertical and horizontal directions were found similar to each other.
- Overall, vibration amplitudes were inside the tolerance limits of a linear collider, confirming earlier results from the NuMI target hall (DESY group, W. Bialowons et al.), from data collected with a different equipment.

Preliminary results were shown at the ICAR meeting in Argonne, May 2004 (see `http://diablo.phys.northwestern.edu/~ michals/mszleper_icar.pdf`).

The final results were reported at the LC Workshop in Victoria, Canada, July 2004 (see `http://diablo.phys.northwestern.edu/~ michals/mszleper_victoria.pdf`).

This research was funded by a grant from the state of Illinois to do accelerator development, ICAR.

Facilities, Equipment and Other Resources

Northwestern has invested $25K in equipment toward this project using ICAR funds (see Table 1). Preparations, including learning the hardware, setting up the software, and organizational issues, involved altogether over a year of work. All of the equipment has been tested and its performance studied. We have been advised by people who had done similar ground motion studies at other sites in the past (in particular A. Seryi of SLAC). An offline Fourier analysis program has been adapted to work in a Linux environment and to input the required data format. Software has been developed to facilitate data analysis.

2	broadband seismometers	$6,500.00	$13,000.00
2	seismometer cables	$325.00	$650.00
1	DL-24 data recorder w/ 1 GB microdrive	$11,240.00	$11,240.00
1	12V 33 Ah battery	$175.00	$175.00
1	control interface	$700.00	$700.00
1	power supply	$160.00	$160.00
	handling charge		$5.00
	shipping and insurance		$160.00
total			$26,050.00

We foresee the same equipment and software resources could be used for the proposed study. A desirable upgrade would concern a pair of new removable data storage disks (2 × 8 Gb capacity), as explained below.

FY2005 Project Activities and Deliverables

All the equipment is presently stored at Northwestern University and needs be transported to Fermilab and installed in the NuMI tunnel.

A series of short test measurements will be made in order to check the proper operation of the hardware and online software. The quality of the data will be checked off-line.

Measurements must be made at a few different places in the tunnel, including the NuMI target hall, the absorber hall and the MINOS hall. Exact locations and times will depend on the accessibility of the relevant parts of the tunnel and must be negotiated with the NuMI management. Each measurement will be 3-4 weeks long. This will require several short accesses to the tunnel in order to replace the data storage disk and reprogram data taking for the next period of time. Offline data analysis will proceed in parallel.

These measurements will reveal the long-term variations of the seismic activity in different frequency ranges. The results will allow to determine the maximum size of natural variations of the vibration amplitudes below 1 Hz and provide more comparative input to test the stability of the results above 1 Hz. A longer data taking period will permit to separate the proper dependence on depth from daily and other accidental variations.

An additional measurement will be made in a selected location within the first 150 ft below ground. Depending on the accessibility, this measurement may take one or more days, or more than one measurement may be actually made. The results will determine how fast the noise attenuation occurs in this region.

FY2006 Project Activities and Deliverables

N/A

FY2007 Project Activities and Deliverables

N/A

Budget justification: Institution 1

The timescale to complete the project is defined mainly by the length and number of measurements and will be close to 3 months. As offline data analysis will run mostly in parallel, it will not change timescales significantly. Currently, we have no grant to cover a Research Associate position for LC related R&D. We therefore request funding for 3 months of salary for a Research Associate.

We request funding for travel that will cover the full expenses of the participation in international conferences or workshops, for the research associate and the PI. For exmaple, we will like to participate in the ILC SNOWMASS summer study this year. We anticipate that at

least two such participations in total will be worthwhile and reasonable. We also anticipate at least one visit for further discussions and consultation with ground motion experts in other labs within the US.

The proposed measurements will be made using essentially the same equipment and computing resources we have used in our previous study. However, as we want to extend our measurements to cover much larger periods of time (and for technical reasons, possibly increase the probing frequency), we will be collecting and storing much larger amounts of data. Consequently, for all practical purposes, having a more efficient system for data storage and transfer will be important. The simplest upgrade would consist of using a pair of removable data storage disks (2×8 Gb capacity). Large disk capacity will decrease the frequency of necessary human accesses to the equipment down to a manageable level, while using two disks will allow quick exchange of one with another without losing much data taking time.

Three-year budget, in then-year K$

$28,489

Institution: Northwestern University

Item	FY2005	FY2006	FY2007	Total
Other Professionals	$11,531	0	0	11,531
Graduate Students	0	0	0	0
Undergraduate Students	0	0	0	0
Total Salaries and Wages	$11,531	0	0	11,531
Fringe Benefits	2,579	0	0	2,579
Total Salaries, Wages and Fringe Benefits	$14,110	0	0	14,110
Equipment	$2,500	0	0	2,500
Travel	$6,000	0	0	6,000
Materials and Supplies	0	0	0	0
Other direct costs	0	0	0	0
Institution 2 subcontract	0	0	0	0
Total direct costs	$22,610	0	0	22,610
Indirect costs(1)	5,876	0	0	5,876
Total direct and indirect costs	$28,489	0	0	28,489

(1) Includes 25% of first $22,610 subcontract costs

2.15: Investigation of acoustic localization of rf cavity breakdown

(progress report)

Accelerator Physics

Contact person
George Gollin
g-gollin@uiuc.edu
(217) 333-4451

Institution(s)
Illinois
SLAC

Funds awarded (DOE)
FY04 award: 23,785
FY05 award: 35,000
FY06 award: 35,000

Project name

Investigation of acoustic localization of rf cavity breakdown (LCRD 2.15)

Classification (accelerator/detector:subsystem)

Accelerator

Institution(s) and personnel

University of Illinois at Urbana-Champaign, Department of Physics:
George D. Gollin (professor); Michael J. Haney (electrical engineer); Jeremy Williams (postdoc); Joseph Calvey, Michael Davidsaver, Justin Phillips (undergraduates).

University of Illinois at Urbana-Champaign, Department of Electrical and Computer Engineering:
William D. O'Brien (professor)

Stanford Linear Accelerator Center:
Marc Ross (staff scientist)

Contact person

George Gollin
g-gollin@uiuc.edu
(217) 333-4451

Project Overview

Electrical breakdown in accelerating structures and RF couplers produces electromagnetic and acoustic signals that may be used to localize (in a non-invasive fashion) the breakdown site inside a cavity. Other indications of breakdown (microwave, X-ray, and dark current measurements) have proven insufficient to elucidate the basic physics of breakdown. During tests of the ILC design it will be important to record information describing electrical breakdown in order to understand why cavities and couplers break down, and how cavity/coupler design and operating conditions influence accelerator reliability.

The goal of this project is to understand the acoustic properties of ILC RF couplers in order to relate the acoustic signatures of breakdown events to the underlying minor electromagnetic catastrophes taking place inside the structures. A wildly optimistic (and unlikely) outcome would be to develop a technique allowing derivation of an invertible acoustic Green's function for an individual structure. This Green's function could be used to predict the signals arriving at various sensors as functions of the acoustic excitation caused by a coupler breaking down. The inverse function, provided with data from a sufficiently large number of sensors, would yield information about the discharge. A more realistic outcome will be to determine how well acoustic information can be used to localize and classify different breakdown modes in ILC couplers.

Our first year of investigation has concentrated on building software tools and developing a small amount of laboratory infrastructure so that we can begin learning about the problems we are confronting. Since these effects are well described by classical mechanics, the research has proved ideal for participation by undergraduates. The students have been remarkably productive and insightful, and are continuing their involvement.

Results of Previously Supported Activities

Our work began in FY03 when a one-year Department of Energy grant supported it. (The present project is funded through a three-year grant.) Initially we worked with warm copper NLC main linac structures. However, much of what we have learned can be applied to studies of ILC couplers.

Since NLC structures are held at high temperature when they are assembled by brazing, the copper's grain size grows so that sound waves must propagate through a crystalline medium with irregularly shaped grains a few millimeters in size which are oriented randomly. The speed of sound in copper is about five millimeters per microsecond, so acoustic waves with frequencies in the MHz range (whose wavelengths are comparable to the grain size) are disrupted by scattering as they propagate.

In FY03 we had worked with two sets of copper dowels on loan from the Fermilab NLC structure factory. The copper stock was from a shipment of material used to construct actual NLC test structures; one set of dowels had been heat-annealed to bring up its grain size, while the other had not and, consequently, had microscopic grains.

We borrowed several 1.8MHz transducers (and associated signal conditioning electronics) from Bill O'Brien's lab as well as purchasing a pair of 500 kHz Panametrics transducers ourselves. A schematic diagram of our copper/transducer setup is shown in Figure 1. A variety of measurements for dowels of different lengths (including speed of sound, attenuation length, and beam spread) provided us with a nice set of experimental inputs with which to confront our acoustic models.

We developed a pair of three-dimensional models for the propagation and detection of acoustic waves in copper. Both described copper as a (possibly irregular) grid of mass points connected by springs. (We can vary the individual spring constants and the arrangement of interconnections to introduce irregularities representing grains into our simulated copper.) The models may seem naïve, but they are able to support a variety of complex phenomena and it is a simple matter to tune various physical properties (such as the speeds of sound for compression- and shear-acoustic waves) through adjustments of the models' parameters.

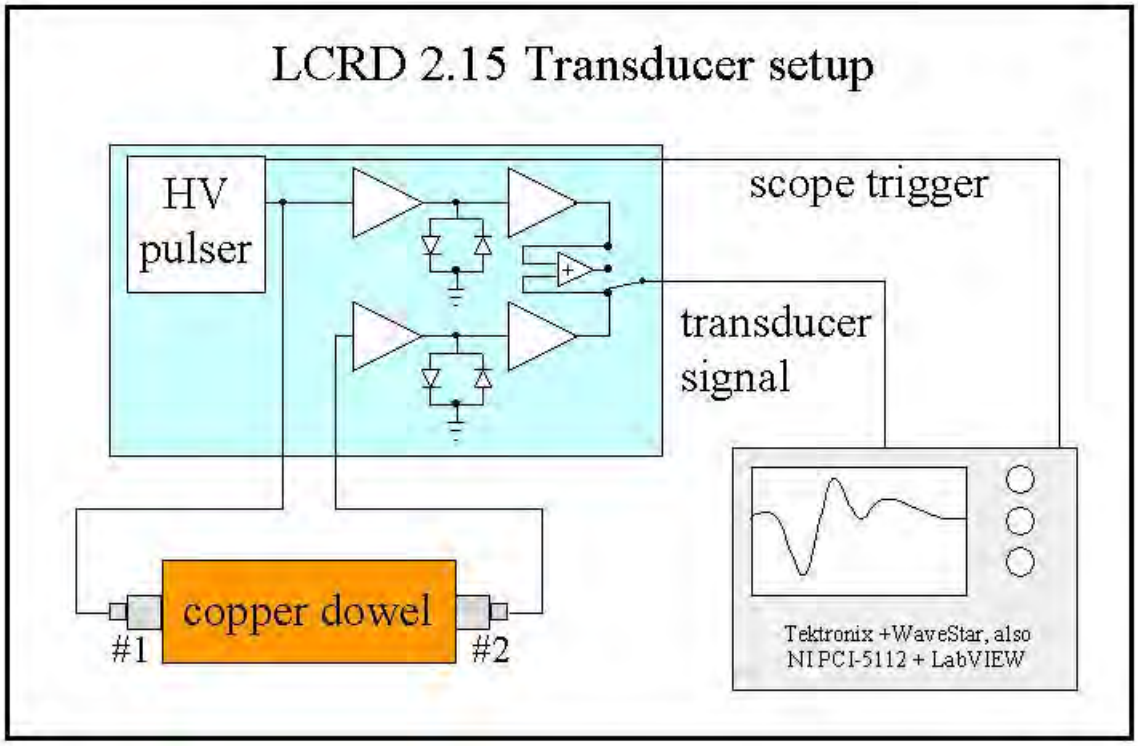

Figure 1. Copper/transducer laboratory setup. We can listen for echoes returning to the transducer which fires pings into the copper, or listen to the signal received by a second transducer, or the sum of signals from the two transducers.

One of the models uses *MatLab* as a computational engine, generating an analytic solution to the coupled equations describing the forces acting on each mass point. The other, written by two of the students, performs a fourth-order Runge-Kutta numerical integration to compute the response of mass points to acoustic perturbations. We have found it invaluable to be able to compare the detailed predictions of the models in order to verify their accuracy: scattering off grains produces very complicated effects and it is important to confirm that our calculations are accurate. Our numerical integration model is able to handle considerably larger systems than is possible with *MatLab*. However, when applied to smaller systems (with a few hundred mass points), both models agree to an accuracy consistent with integration step size and machine precision.

Some of our modeling involves two-dimensional grids of roughly 10^5 points. We "drive" signals into them using a transducer model in which the piezoelectric device is described as a damped oscillator excited by shocks of short duration. Because of reflections at the ends of the cable used to drive the real transducers, the actual drive signal is complicated; we find we can model it adequately as a series of four closely spaced impulses. Figure 2 shows a comparison of our simulation and measurements of the transducer signal for a pair of echoes in a copper dowel. We have used the first echo to guide our selection of drive parameters; the shape of the second echo is well reproduced.

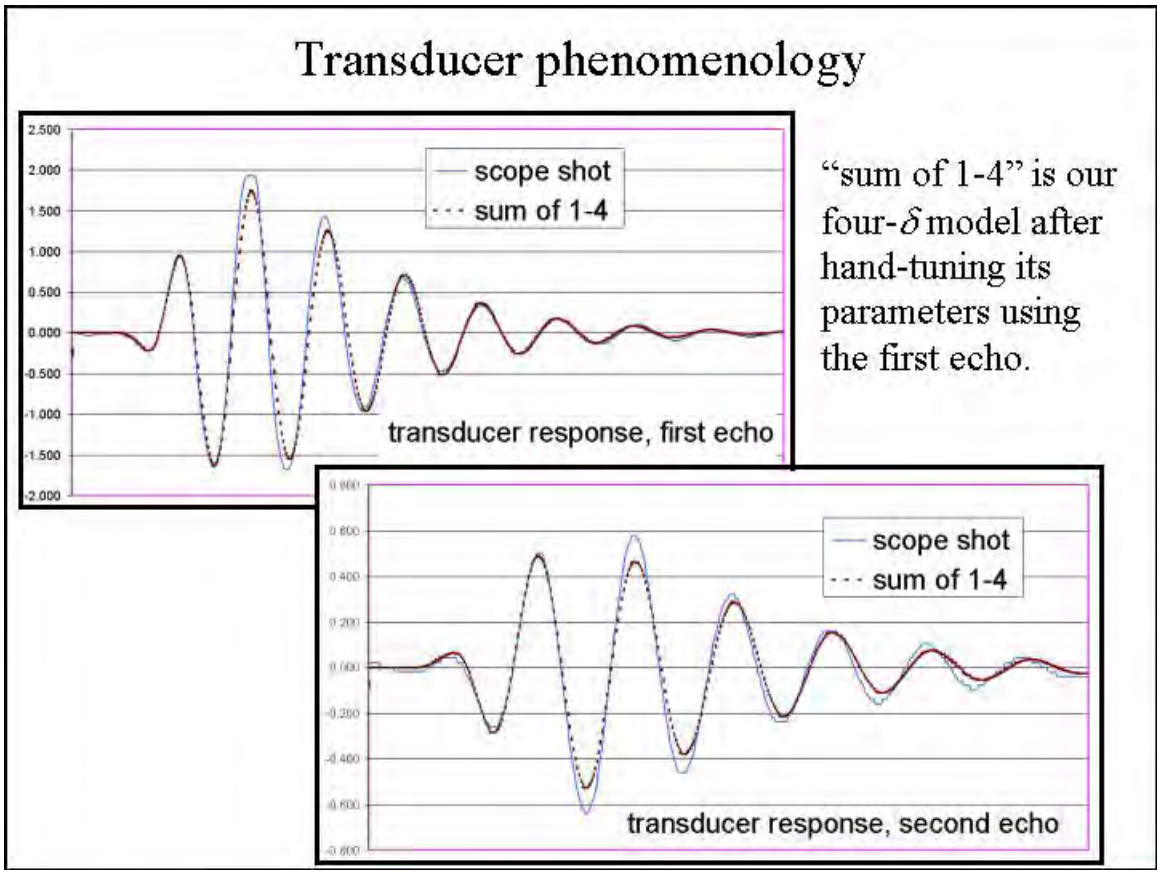

Figure 2. Modeling the excitation of a piezoelectric transducer.

Propagation of a simulated acoustic wave in a homogeneous 250×650 point grid is shown in Figure 3a. The lateral spread of the pulse is a consequence of the relatively small number of mass points receiving the initial excitation.

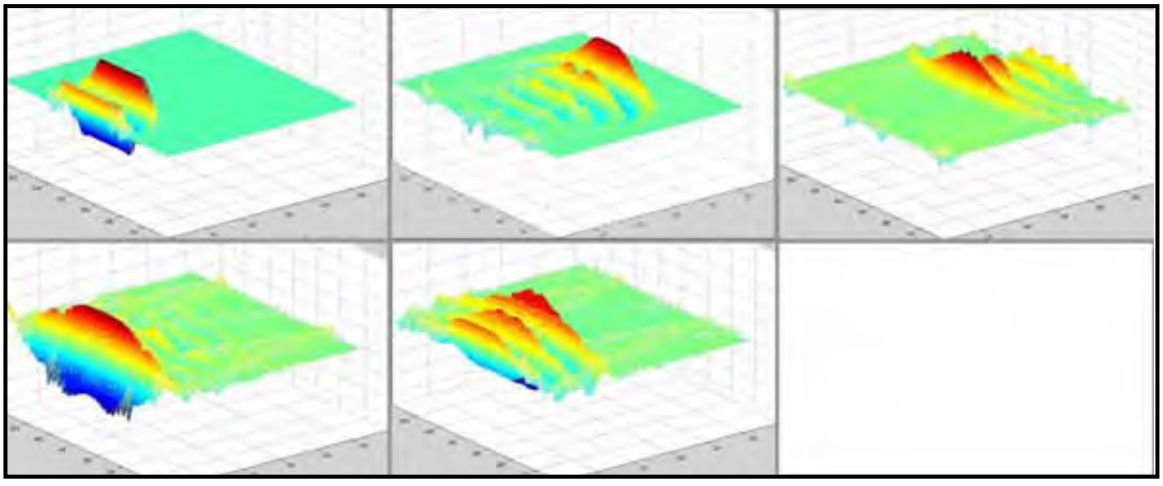

Figure 3a. Acoustic pulse propagating in a homogeneous 250×650 point grid.

We can simulate the transducer signal as a function of time by summing the amplitudes at the "face" of a transducer as it experiences the effects of the acoustic pulse. Results, shown in comparison with a real oscilloscope record of transducer signal vs. time are shown in Figure 3b. They are promising but need more refinement.

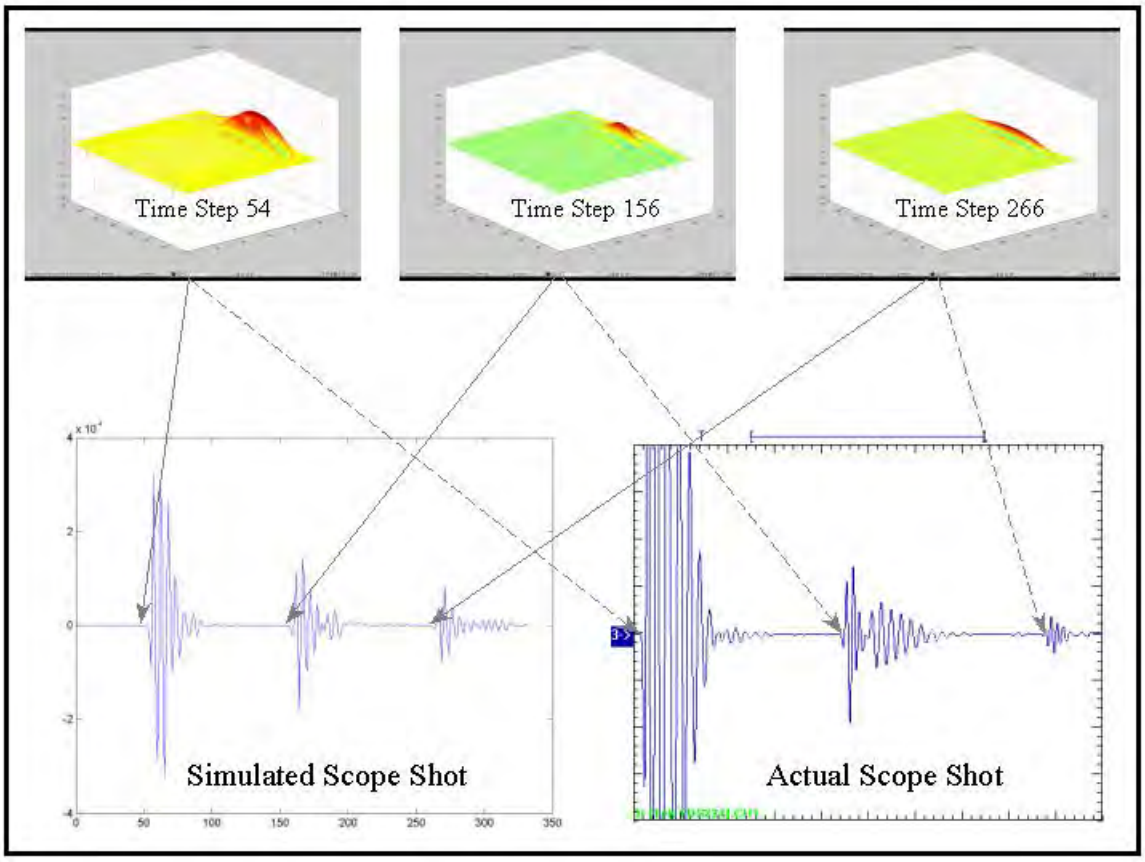

Figure 3b. Simulated transducer response to an acoustic pulse propagating in a homogeneous 250×650 point grid. The transducer is at the downstream edge of the array.

The effect of inhomogeneities on an acoustic wave is dramatic, as can be seen in Figure 4, below. Spring constants in the parallelogram-shaped region are half as large as those used elsewhere in the grid. The disruption suffered by the pulse dumps a significant amount of acoustic energy into the "bulk" of the copper. The version of the simulation shown in the figure does not include any damping. Even so, the echo returning to the transducer is badly disrupted.

Notice the acoustic "glow" which washes over the transducer site due to scattering off the discontinuities in material properties evident in Figure 4. We see this sort of effect in the (real) heat-treated dowels when driving them with our 1.8 MHz transducers, as can be seen in Figure 5, below.

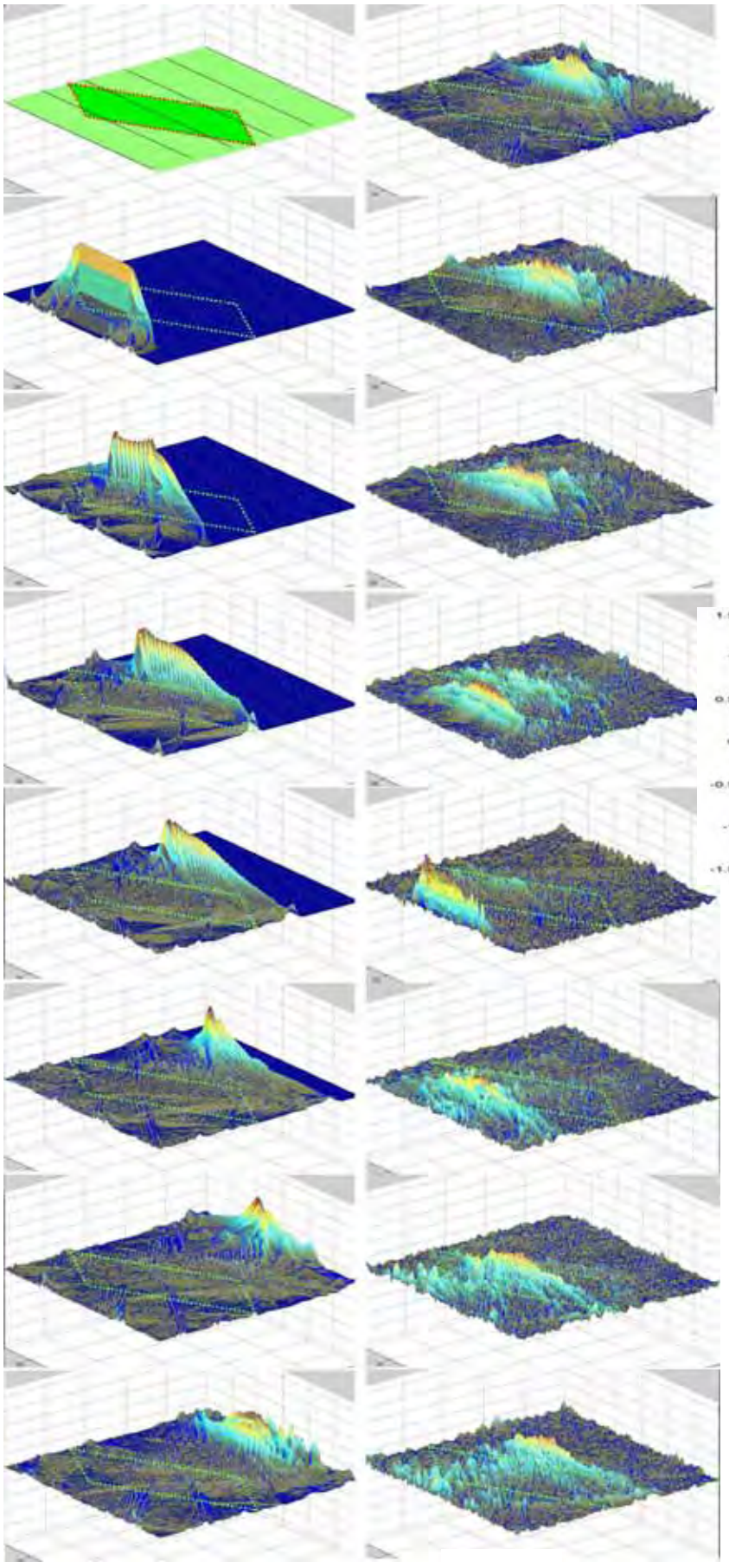

Figure 4. Propagation of an acoustic wave through an asymmetry in a two-dimensional grid. Spring constants inside the region indicated by the parallelogram are half as large as they are outside the parallelogram.

Simulated signal in the transducer (which generates the initial pulse and then measures subsequent acoustic activity) is shown in the small graph below.

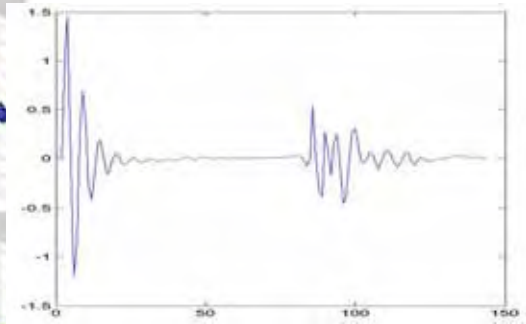

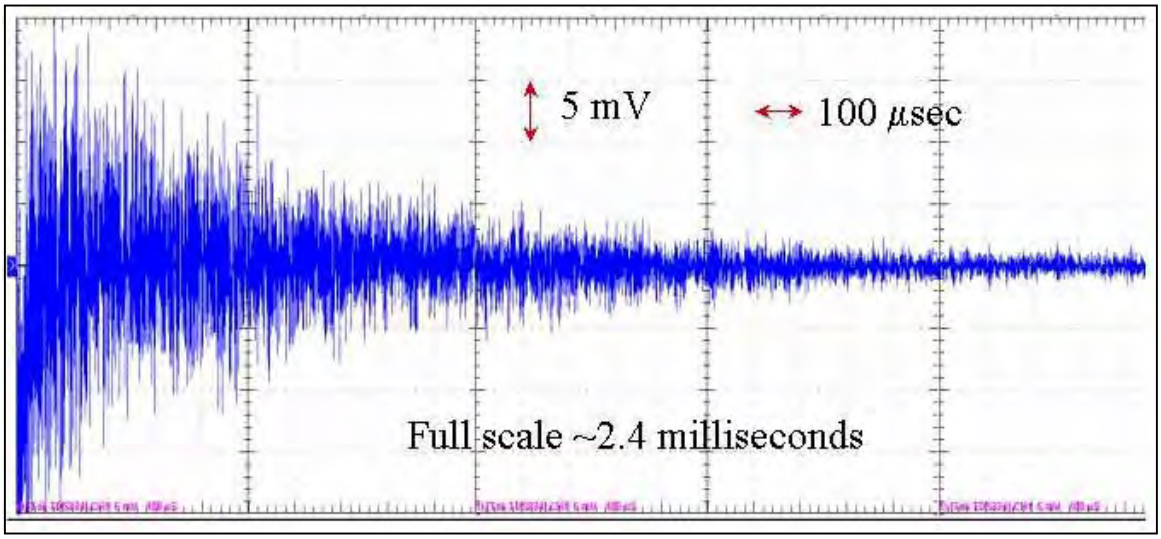

Figure 5. Acoustic glow at long times observed in a heat-treated (grainy) long copper dowel. Note that the scope trace is NOT showing noise: the fine structure is remarkably reproducible from shot to shot. Configuration uses a single transducer: ping, then listen to baseline signal as pulse travels into copper, pumping energy into acoustic baseline "glow." Scope scales are 5 mV and 100 μsec per division.

The amplitude of an acoustic pulse decreases because of attenuation as well as scattering of energy out of the pulse. Not surprisingly, a pulse bouncing back and forth in a heat-treated (grainy) dowel dies out more rapidly than does a pulse traveling in a dowel which hasn't been heat-treated. This is evident in Figure 6, which shows a comparison of the sizes of the first and second echoes for pulses traveling in short (2.5 cm length) copper dowels.

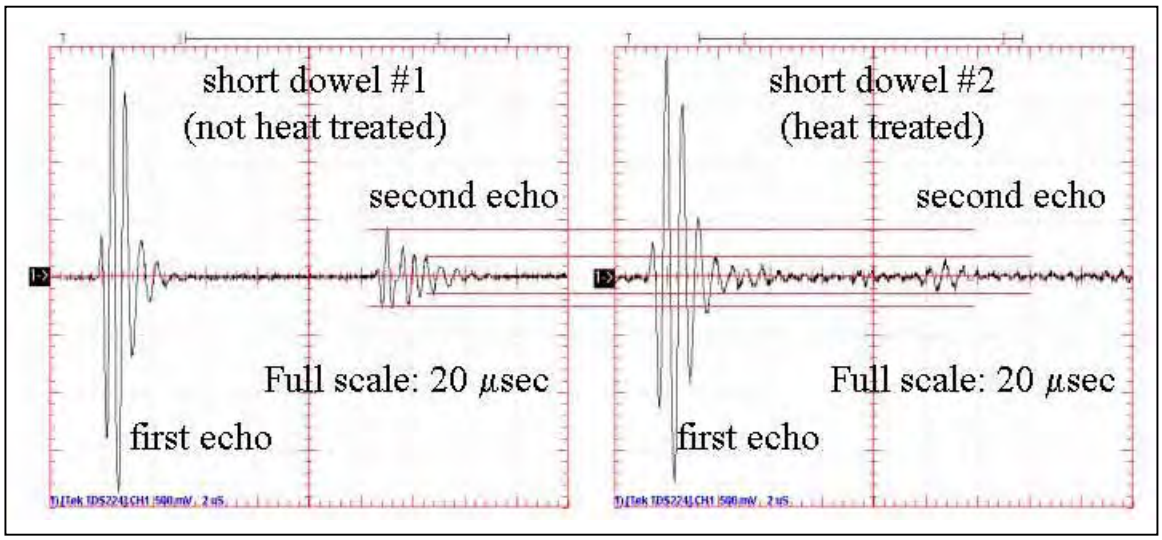

Figure 6. Pulses associated with the first and second echoes in short (2.5 cm) copper dowels. Note the relative sizes of the first and second echoes in each dowel; more energy is scattered out of the pulse traveling in the heat-annealed (grainy) copper. Horizontal and vertical scales are 2 μsec and 500 mV per division respectively.

Results of First Year Activities Supported by This Grant

Our work continued in FY04. We increased the sophistication of our model to incorporate arbitrary numbers of grains, and began studying our ability to reconstruct the source of an acoustic signal.

Figure 7 shows the propagation of an acoustic wave in a two-dimensional "copper" lattice containing roughly 600 grains. The initial wave front was excited as an even mix of shear and compression waves. The different propagation speeds of the (slower) shear wave and (faster) compression wave are clearly seen, even in the presence of the disruption caused by scattering off the grains.

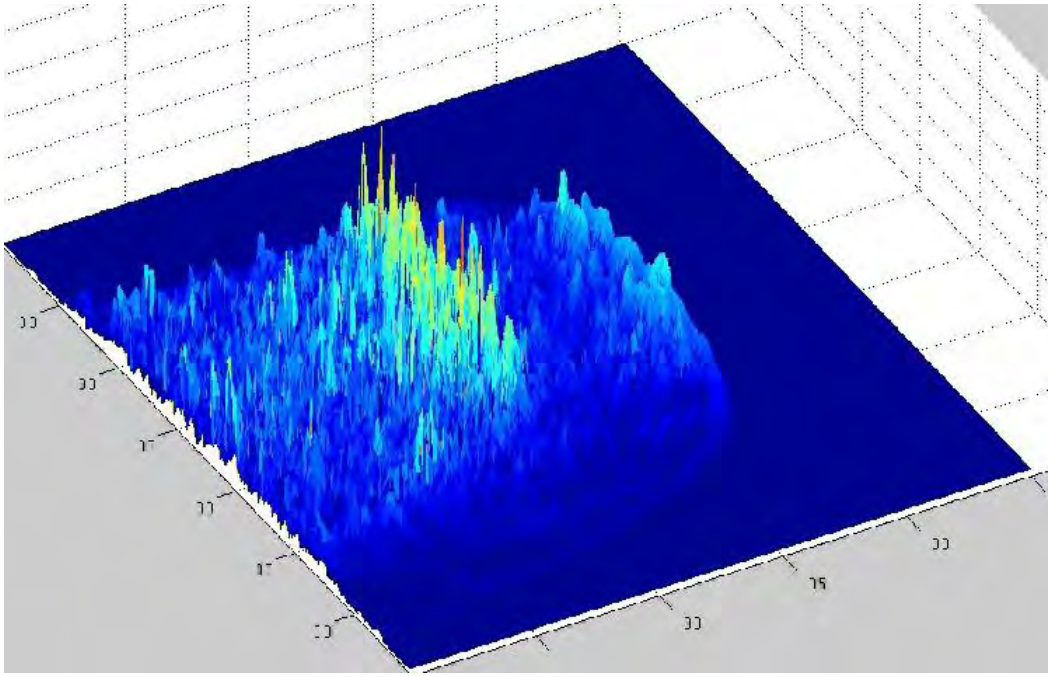

Figure 7. Propagation of a 50% shear-, 50% compression-mode pulse through a grainy "copper" grid.

We are still able to see reasonably clear signals in our (simulated) receiving transducer in spite of the grain-induced degradation in signal quality.

The primary issue to be resolved is whether or not we can reconstruct the location and extent of an electrical breakdown in a three-dimensional structure. To that effect, we have been working with the 5-cell NLC structure shown in Figure 8. Our model is an incomplete representation of the structure: it is a cylinder containing five cylindrical voids, as illustrated in Figure 9. We drive excitations into it from one point on the wall of the largest void and register the received transducer signals for the four transducer locations shown in the figure.

Figure 8. Five-cell NLC accelerating structure used in FY04 investigations.

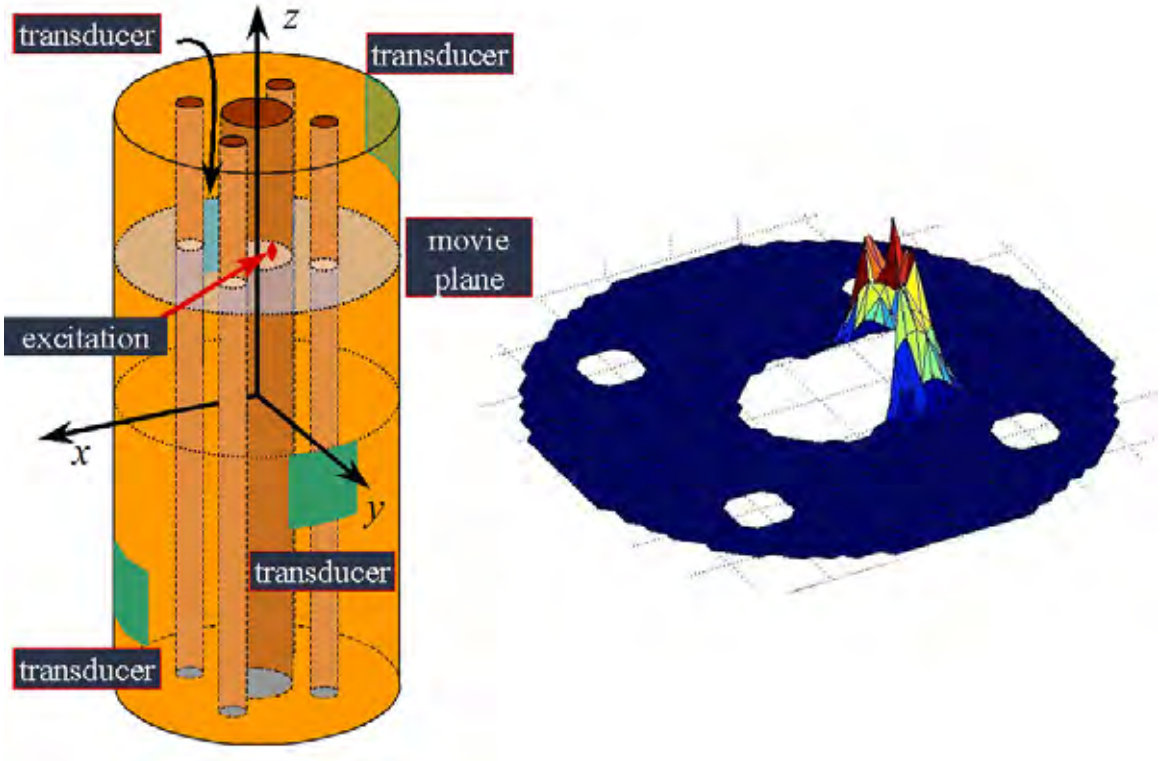

Figure 9. Simple three-dimensional model for NLC accelerating structure. Acoustic excitations are applied at the indicated point; the effects on mass points are shown for the plane containing the excitation.

We find that our ability to reconstruct the breakdown event depends on the amount of information available from the transducers. Even with only four ideal transducers, placed as shown in Figure 9, we are able to reconstruct the origin of the spark by playing the transducer signals backwards, using them to drive signals back into the copper as illustrated in Figure 10, and looking for the time of sharpest peak to be found in the data.

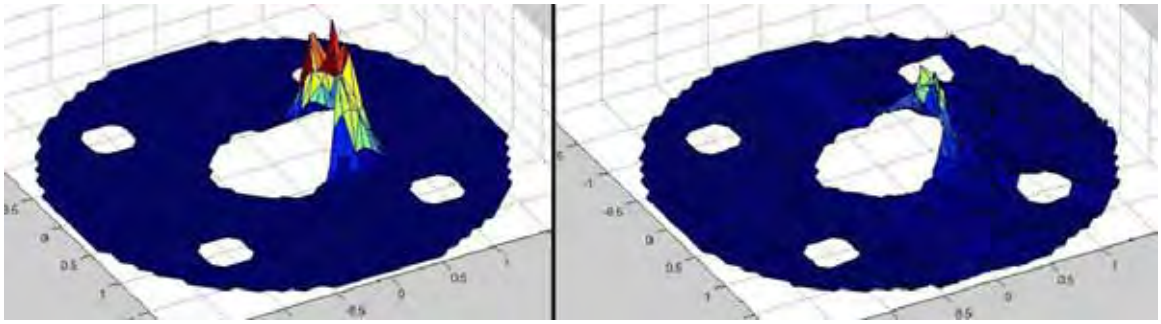

Figure 10. Simulations of generated (left) and reconstructed (right) acoustic excitation using four ideal transducers.

Transducers capable of providing this level of information, however, must be able to determine the motion of the copper surface in all three dimensions. Commercial devices of this sort are available, but their price is considerably higher than for simple compression wave sensors. We are currently studying algorithms that are appropriate for single-signal devices.

Since the technology recommendation last August, we have begun investigating the geometry of ILC RF couplers in order to begin modeling their acoustic properties in place of those of the NLC warm copper linac structures. We expect that the tools we have developed in the last two years will work well for simulating the coupler.

A Few Comments

Active participants in LCRD 2.15 are constrained by the academic calendar: Gollin teaches (although he had been relieved of teaching duties during the Spring and Fall 2004 terms in order to focus on Linear Collider work), while Calvey, Davidsaver, and Phillips are undergraduates with full course loads. Most of our progress occurs during the summer.

Calvey and Davidsaver will graduate in 2006, while Phillips will graduate in 2005. They have all expressed a great deal of interest in continuing on LCRD 2.15, and will be even more productive than they were last summer.

Our budget is simple, consisting primarily of salaries for three undergraduate students, the costs of additional instrumentation, and a small amount of travel money.

More detailed information about recent progress is available on the web in various talks linked to Gollin's home page http://www.hep.uiuc.edu/home/g-gollin/.

UIUC Budget for LCRD 2.15 (awarded by DOE)

Item	FY04	FY05	FY06
Summer + academic year salary, 3 undergraduates (assume 750 hours/year/student, $6.15/hr)	$13,845	$13,846	$13,846
Panametrics transducers (e.g. A133R-RM, $250)	$500	$2,000	$2,000
Signal conditioning circuitry for transducers	$500	$500	$500
National Instruments NI PXI-5112 digitizers	-	$10,000	$10,000
Travel (one trip to SLAC each year)	$1,047	$860	$860
Indirect costs	$7,893	$7,794	$7,794
Totals	$23,785	$35,000	$35,000

2.18: Control of Beam Loss in High-Repetition Rate High-Power PPM Klystrons

(progress report)

Accelerator Physics

Contact person
Chiping Chen
chenc@psfc.mit.edu
(617) 253-8506

Institution(s)
Mission Research Corp
MIT

Funds awarded (DOE)
FY04 award: 20,000
FY05 award: 30,000
FY06 award: 0

2.18: Control of Beam Loss in High-Repetition Rate High-Power Klystrons

(Progress Report)

Accelerator Physics

Contact person
Chiping Chen
chenc@psfc.mit.edu
617 253-8056

Institution(s)
Massachusetts Institute of Technology

Funds Awarded (DOE)
FY04 Award: $20,000
FY05 Award: $30,000
FY06 Award: $35,000

Progress Report
Research supported under a supplemental to DOE Grant No. DE-FG02-05ER40919

Control of Beam Loss in High-Repetition Rate High-Power Klystrons

Chiping Chen
Leader
Intense Beam Theoretical Research Group
Plasma Science and Fusion Center
Massachusetts Institute of Technology
Cambridge, Massachusetts 02139

A major thrust in the Linear Collider (LC) program is the development of high-power klystrons to power a TeV-class LC.

For the cold technology, the development includes L-Band Multi-Beam Klystrons (MBKs). The required specifications for the L-Band power source are: 10 MW power output, 3.0 ms pulse length, 10 Hz repetition rate, 60% efficiency, and several years of lifetime. Some progress has been made in the US and in the Europe on L-Band MBK. For example, Communication Power Industries (CPI), Inc. tested a 10MW MBK with 60 ms plus length (factor of 20 short of the specification) and observed rf breakdown at the rf output window. The LC community still needs to develop an L-Band klystron that meets the full specifications for LC.

For the warm technology, the development has been aimed at X-band periodic permanent magnet (PPM) focusing klystrons. The required specifications for X-band power source are: 75 MW power output, 1.6 ms pulse length, 120 Hz repetition rate, and 20,000 hour lifetime. After nearly a decade of intense research and development at SLAC, KEK and elsewhere, the SLAC group achieved, in June 2003, the operation of a 75 MW XP-3 klystron with a pulse length of 1.6 ms and a repetition rate of 120 Hz (SLAC Website http://www-group.slac.stanford.edu/kly/ppm_klystron/ppm_kly.html). However, the 20,000-hour lifetime remains to be fulfilled.

The goals of our research program are to develop a better understanding of beam losses in LC klystrons, and to do innovative research to improve klystrons. In particular, our efforts include:

(a) Determination of the current limit of a finite-size bunched beam and applied it to successfully establish the operating condition for Linear Collider (LC) klystrons (Hess and Chen, 2004);
(b) Innovative research on beam physics applicable to a L-Band multiple ribbon-beam klystrons (MRBK) with better reliability and better efficiency (Bhatt and Chen, 2005; Zhou, Bhatt and Chen, 2005);
(c) Exploration of the current limit in conventional multi-beam klystrons (MBK) which use cylindrical beams instead of our innovative elliptic beams.

We presented our results from efforts a) and b) at the Victoria Linear Collider Workshop, July 28 - 31, 2004.

Table 1 Parameters of Several LC PPM Klystrons (from Hess and Chen, 2004)

Parameter	50 MW XL-PPM (SLAC)	75 MW XP-1 (SLAC)	50 MW C-Band Toshiba/KEK	75 MW PPM-1 BINP/KEK	75 MW XP-3 (SLAC)
f (GHz)	11.4	11.4	5.7	11.4	11.4
I_b (A)	190	257	317	266	260
γ_b	1.83	1.96	1.67	1.94	2.00
B_{rms} (T)	0.20	0.16	0.17	0.14	0.21
a (cm)	0.48	0.54	0.90	0.55	0.54
a	0.75	0.77	0.79	0.79	0.74
$\sigma_{e,exp}$	0.19	0.28	0.25	0.20	0.16
$\sigma_e/\sigma_e(0,0)$	0.90	0.79	0.85	0.82	0.95
$\sigma_{e,exp}/\sigma_e(0,0)$	0.80	1.15	0.8	1.0	0.68
Beam Power Loss	0.8%	Significant but not measured	Small but not measured	30%	~ 1.0%

We have derived the current limits for LC PPM klystrons and compared them with experimental observations of beam losses. The results are summarized in Table 1 from Hess and Chen, 2004). Table 1 lists the key parameters for the five PPM klystrons (Sprehn, *et al*, 1998; Sprehn, *et al*, 2000; Matsumoto, *et al*, 2001; Chin, *et al*, 2001; SLAC Website http://www-group.slac.stanford.edu/kly/ppm_klystron/ppm_kly.html): operating frequency f, average beam current I_b, beam energy γ_b, the rms magnetic field strength B_{rms}, and the pipe radius a. Table I also shows the values for $a = 2\pi a/\gamma_b L$ and the experimental space charge (current) parameter $\sigma_{e,exp}$, which can be computed using the formulas $L = \beta_b c/f$ and $N_b = I_b/ef$. The theoretical limit is $\sigma_e/\sigma_e(0,0)$. If the experiment value $\sigma_{e,exp}/\sigma_e(0,0)$ is greater than $\sigma_e/\sigma_e(0,0)$ in a klystron, then substantial beam loss occurs. If the experimental value $\sigma_{e,exp}/\sigma_e(0,0)$ is less than $\sigma_e/\sigma_e(0,0)$ in a klystron, then small beam loss could still occurs due to beam halo formation (Chen and Pakter, 2000; Pakter and Chen, 2000). Our results show good agreement with the experimental observations.

To adapt the recommendation of the cold technology by the 12-member international panel in August, 2004, we are placing our emphasis on L-Band MBKs with our innovative elliptic beams (Bhatt and Chen 2005; Zhou, Bhatt and Chen, 2005) as well as with conventional cylindrical beams.

Multiple ribbon-beam klystrons (MRBKs) have the following advantages over the conventional multiple cylindrical-beam klystrons:

a) Higher efficiency (80% vs. 60%),
b) Few beams (4 vs. 6),
c) Lower magnetic field (1.6 kG rms vs. 5 kG rms),
d) Energy-free permanent magnet vs. energy-consuming pulsed magnet.

These advantages would reduce the construction and operating costs of LC and improve the reliability of rf power sources. These attractive features motivated us to accelerate the R&D on MRBKs.

To this end, we have invented a technique to focus a relativistic ellipse-shaped beam and discovered an exact paraxial equilibrium state for a high-intensity periodically twisted elliptic beam (Zhou, Bhatt and Chen, 2005). Such elliptic electron beam would be use to build an L-Band MRBK.

As an example, we have considered a relativistic ribbon beam with voltage $V_b = 114$ keV , current $I_b = 32.75$ A, aspect ratio $a/b = 5$, and non-axisymmetric periodic permanent magnet focusing with $B_0 = 2.2$ kG , $S = 2.2$ cm , and $k_{0y}/k_{0x} = 1.52$ (Zhou, Bhatt and Chen, 2005). We propose four such beams in a 10 MW L-Band multiple-ribbon-beam klystron (MRBK) for a linear collider (LC).

For such a system the matched solution of the generalized envelope equations is calculated numerically as shown in Figs. 1(a)-1(c) with the corresponding parameters: $k_{0x} = 1.56$ cm^{-1}, $k_{0y} = 2.39$ cm^{-1}, $\sqrt{k_{z0}} = 0.917$ cm^{-1}, and $K = 1.11 \cdot 10^{-2}$. The solution to the generalized envelope equations shows that the semiaxes of the elliptical beam remain roughly constant with small oscillations, that the orientation of the ellipse twists periodically with an amplitude of ten degrees, and that the normalized rotation flow velocities a_x and a_y oscillate with the magnet periodicity. Shown in Figs. 1(a) and 2(b), the dotted curves are the envelopes and angle of the beam ellipse obtained from the PFB2D simulation. It is worthwhile pointing out that the normalized velocities m_x, m_y, a_x and a_y vanish at $s = 0$ which makes it a natural matching point for a parallel-flow beam with negligibly small emittance (Bhatt and Chen, 2005).

The PFB2D simulation also shows that the transverse beam distribution preserves the equilibrium profile as it propagates. In Fig. 2, 10,000 particles (a sample of the $5 \cdot 10^5$ particles in the PFB2D simulation) are plotted in the (x, y) plane and $(x, dy/ds)$ plane for five snapshots within one period: $s/S = 9.0, 9.25, 9.5, 9.75$ and 10.0 for the same beam shown in Fig. 1. This also suggests that the beam equilibrium is stable, although we have not done a full stability analysis of the beam equilibrium.

We plan to generalize our non-relativistic elliptic diode theory (Bhatt and Chen, 2005) to the relativistic regime to facilitate the full design of relativistic elliptic beams in the L-Band MRBK. We also plan to carry out a design study of the L-Band MRBK and communicate our results to rf source development groups at SLAC, KEK and elsewhere.

Finally, we plan to determine the current limit in a conventional MBK with cylindrical electron beams. In contrast to the X-Band PPM klystrons, the MBK uses an immerse electron flow. The canonical angular momentum of the electron beam at the cathode is non-zero. Based on earlier work (Hess, 2002), we expect that such a non-zero canonical angular momentum will have an important effect on the current limit. We will compare the results with the experimental observations at CPI and elsewhere.

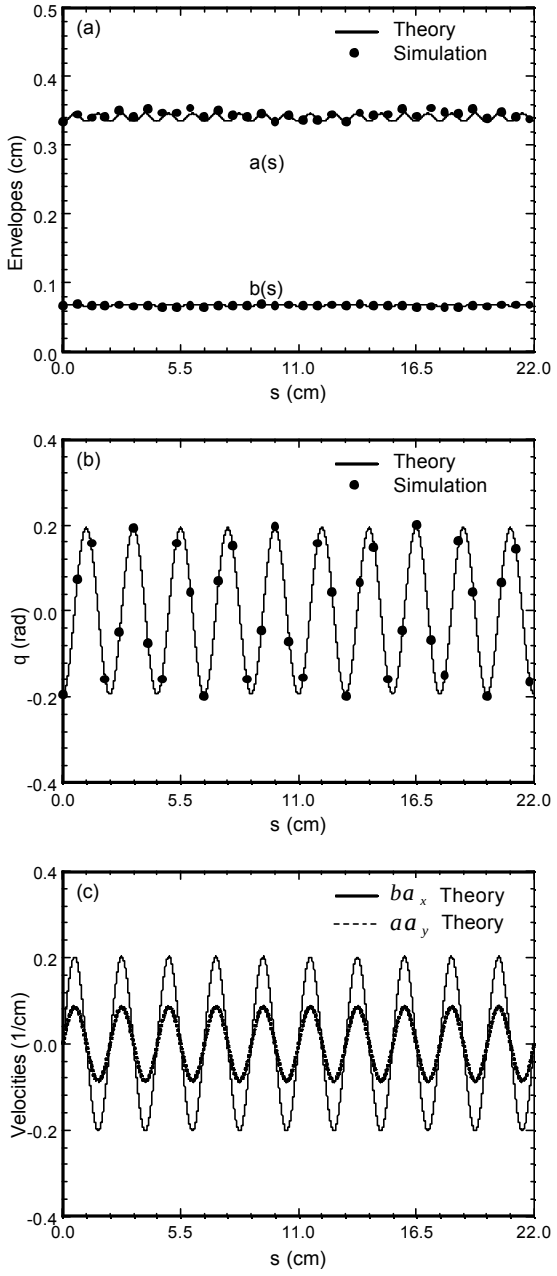

Fig. 1 Plots of (a) envelopes $a(s)$ and $b(s)$, (b) twist angle $q(s)$, and (c) normalized rotational velocities $b(s)a_x(s)$ and $a(s)a_y(s)$ versus the axial distance s for the relativistic twisted ellipse-shaped beam in Table 1. The solid and dashed curves are the generalized envelope solution, whereas the dotted curves are from the PFB2D simulation.

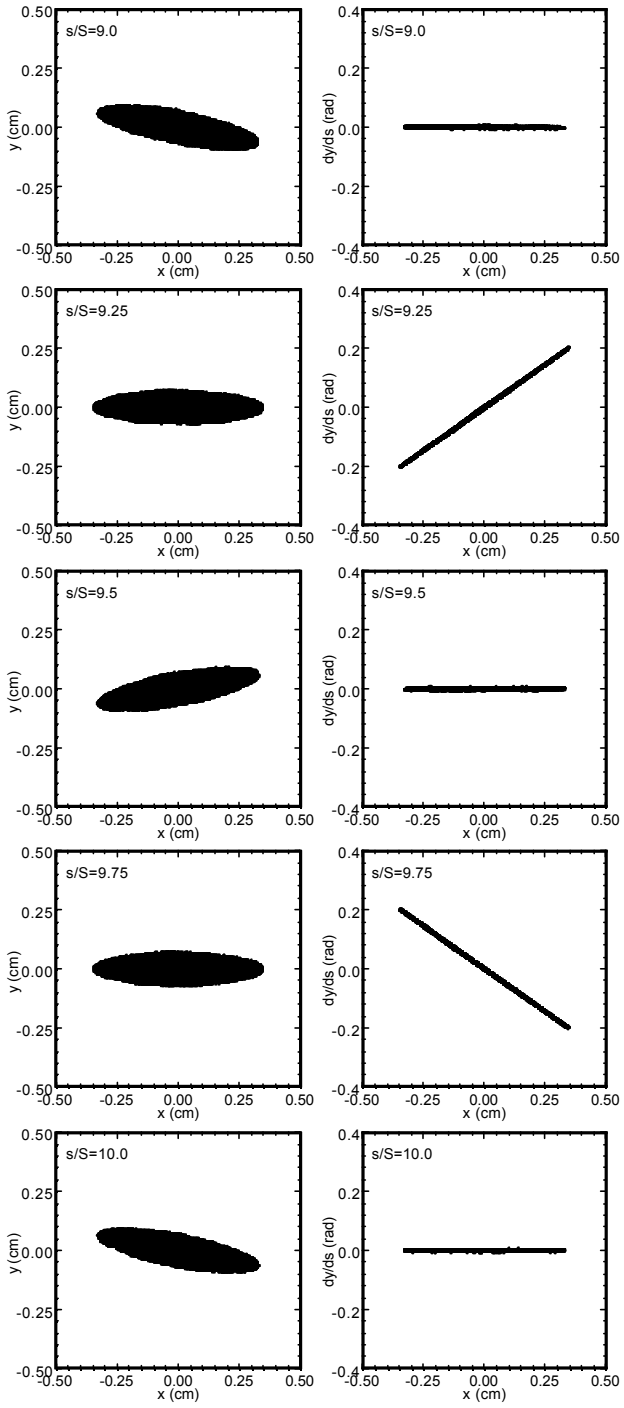

Fig. 2 Plots of 10,000 particles (a sample of the $5 \cdot 10^5$ particles in the PFB2D simulation) in the (x, y) plane and $(x, dy/ds)$ plane for five snapshots within one period: s/S = 9.0, 9.25, 9.5, 9.75 and 10.0 for the same beam shown in Fig. 1.

Funds of $30K and $35K are requested for FY2005 and FY2006, respectively, according to the award agreement and budget submitted in June, 2004. An approximate breakdown of that agreement is summarized in Table 2 for the 3-year period.

Table 2. Approximate breakdown of the budget in award agreement

Item	FY04	FY05	FY06	Total
Chiping Chen (PI)	$10,000	$11,400	$13,000	$34,400
2 Graduate Students	$7,800	$16,400	$19,800	$44,000
Travel	$2,200	$2,200	$2,200	$6,600
Total	$20,000	$30,000	$35,000	$85,000

This budget is modest for the proposed research efforts.

References

Bhatt, R., and C. Chen, 2005, Phys. Rev. ST-AB 8, 014201

Chen, C. and R. Pakter, 2000, Phys. Plasmas **5**, 2203.

Chin, Y.H. *et al*, 2001, in: Proceedings of the 2001 Particle Accelerator Conference, edited by P. W. Lucas and S. Webber, p. 3792.

Hess, M., 2002, Ph. D. Thesis, MIT.

Hess, M. and C. Chen, 2004, Phys. Rev. ST-AB **7**, 092002.

Matsumoto, H., *et al*, 2001, in: Proceedings of the 2001 Particle Accelerator Conference, edited by P. W. Lucas and S. Webber, p. 993.

Pakter, R., and C. Chen, 2000, IEEE Trans. Plasma Sci. **28**, 502.

Sprehn, D., *et al*, 1998, in: Proceedings of 19th International Linac Conference, Argonne National Laboratory Report ANL-98/28, p. 689.

Sprehn, D., *et al*, 2000, in: H.E. Brandt (Ed.), Intense Microwave Pulses VII, SPIE Proc. **4301**, p. 132.

Zhou, J., R. Bhatt, and C. Chen, 2005, "Exact paraxial cold-fluid equilibrium for a high-intensity periodically twisted ellipse-shaped charged-particle beam," Phys. Rev. Lett., submitted for publication.

2.22: Investigation of Novel Schemes for Injection/Extraction Kickers

(progress report)

Accelerator Physics

Contact person
George Gollin
g-gollin@uiuc.edu
(217) 333-4451

Institution(s)
Cornell
Fermilab
Illinois

Funds awarded (DOE)
FY04 award: 22,822
FY05 award: 16,822
FY06 award: 16,822

Project name

Investigation of Novel Schemes for Injection/Extraction Kickers (LCRD 2.22)

Classification (accelerator/detector:subsystem)

Accelerator

Institution(s) and personnel

University of Illinois at Urbana-Champaign, Department of Physics:
George D. Gollin, (professor); Michael J. Haney (electrical engineer); Jeremy Williams (postdoc); Guy Bresler, Joseph Calvey, Keri Dixon, Michael Davidsaver, Justin Phillips (undergraduates).

Fermi National Accelerator Laboratory:
David A. Finley (staff scientist), Chris Jensen (engineer), Vladimir Shiltsev (staff scientist)

Cornell University, Department of Physics:
Gerald F. Dugan (professor), David L. Rubin (professor)

Contact person

George Gollin
g-gollin@uiuc.edu
(217) 333-4451

Project Overview

The 2820 bunches of an ILC pulse would require an unacceptably large damping ring if the 337 ns linac bunch spacing were used in the damping ring. As a result, the TESLA 500 GeV design[1] called for 20 ns bunch separation in a 17 km circumference damping ring; a fast kicker would deflect individual bunches on injection or extraction, leaving the orbits of adjacent bunches in the damping ring undisturbed. A number of the kicker designs which had been considered involve the creation of individual magnetic field pulses of sufficiently short duration so that only one bunch is influenced by a pulse. The demands of short rise/fall times and pulse-to-pulse stability are challenging; a system capable of generating shorter pulses would allow the construction of a smaller damping ring.

It is interesting to consider a design in which the pulsed kicker is replaced by a low-*Q* RF device filled with a broadband signal whose amplitudes, frequencies, and phases correspond to the Fourier components of a periodic, narrow pulse. Instead of energizing the system only when a bunch was about to be injected (or extracted) to the damping ring, the device would run continuously. This might allow the frequencies, phases, and relative amplitudes of the impulse to be determined with great precision. With a properly

[1] *TESLA Technical Design Report*, http://tesla.desy.de/new_pages/TDR_CD/start.html (March, 2001).

chosen set of parameters, the system would kick every M^{th} bunch in a train, leaving undisturbed the train's other (M - 1) bunches. Injection (or extraction) of an entire bunch train would be completed by the end of the M^{th} orbit through the system. We are studying a kicker with M = 60, admitting the construction of a 6 km circumference damping ring.

We will assume that the damping ring beam is organized as a number of bunch trains with an inter-train gap between the tail of one bunch train and the head of the next. The kicker system would be installed in a bypass section of ring. During injection, a deflector system would route the beam through the bypass. Once injection was completed, each deflector would be turned off during the passage of a gap between bunch trains. The beam would then orbit in the damping ring, bypassing the kicker. At extraction, the deflectors would be energized again, routing the beam through the kicker for extraction.

Brief description of the Fourier series pulse compression kicker

A general discussion of a Fourier-series kicker system can be found on the web.[2] We will focus on a particular implementation in which an RF amplifier sends a broadband signal down a waveguide to a $Q \approx 25$ RF structure. Dispersion in the waveguide shifts the relative phases of the Fourier components of the signal so that it is compressed: RF power arrives at the RF structure in short, periodic bursts, filling it in order to eject the target bunch without disturbing adjacent bunches. The RF structure is able to store energy, so its maximum field strength is approximately 20 times greater than the maximum field strength in the downstream end of the waveguide.

A schematic representation of the kicker is shown in Figure 1. Our studies assume the values for the kicker's parameters shown in Table 1.

[2] George D. Gollin and Thomas R. Junk, *Speculations About a Fourier Series Kicker for the TESLA Damping Ring,* http://www.hep.uiuc.edu/home/g-gollin/Linear_collider/fourier_series_kicker.pdf (2002).

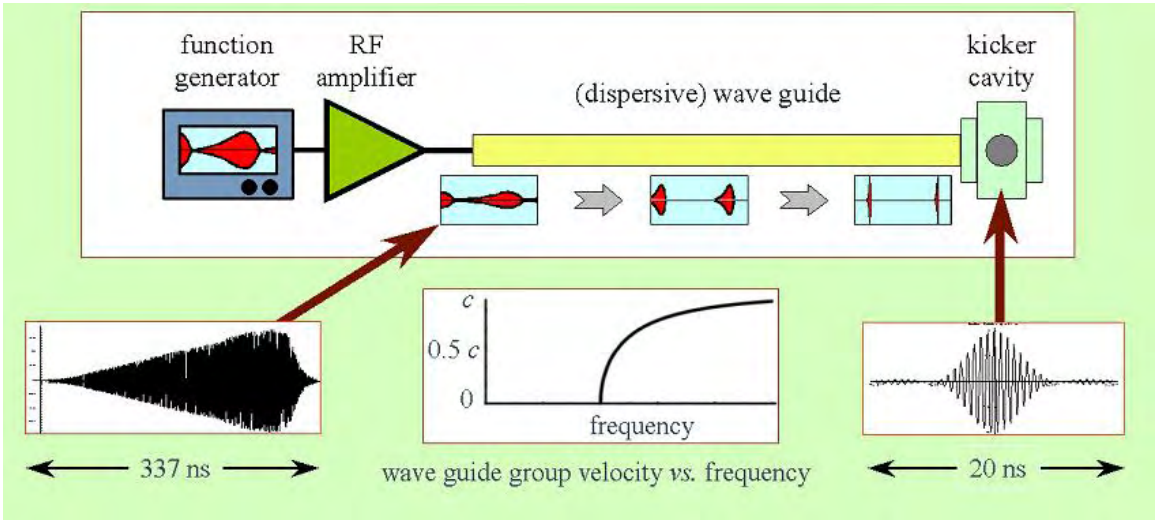

Figure 1: Schematic representation of a Fourier series pulse compression kicker.

Parameter	Symbol	Value
Main linac bunch frequency	f_L ($\omega_L \equiv 2\pi f_L$)	3 MHz
Damping ring bunch frequency	f_{DR} ($\omega_{DR} \equiv 2\pi f_{DR}$)	180 MHz
RF structure center frequency	f_{RF} ($\omega_{RF} \equiv 2\pi f_{RF}$)	1845 MHz
RF structure Q	Q	25
Waveguide cutoff frequency	f_{cutoff}	1300 MHz
On field integral	$A(0)$	(100 ± .07) Gauss-meters
Off field integral	$A(t)$	(0 ± .07) Gauss-meters
f_{DR} / f_L	N	60
f_{RF} / f_{DR}	Γ	10.25
f_{RF} / f_L	ΓN	615
Bunch length	δ_B or τ_B	±6 mm ~ ±20 ps
Karma	☺	Impeccable

Table 1: Fourier series pulse compression kicker parameters.

The kicker's field integral is a function of time, naturally. We use the term "major zero" to refer to the kicker's (zero-valued) field integral when an unkicked bunch passes through the device. Since the bunch spacing in a train is uniform, the time interval between major zeroes is the same as the interval between the kicking impulse and the first major zero.

Kicker impulse function

We have been studying an impulse function of the following form:

$$A(t) = \frac{1}{N^2}\frac{\sin^2\left(\frac{1}{2}\omega_{DR}t\right)}{\sin^2\left(\frac{1}{2}\omega_L t\right)}\cos\left(\omega_{RF}t\right) = \frac{1}{N^2}\frac{\sin^2\left(\frac{1}{2}N\omega_L t\right)}{\sin^2\left(\frac{1}{2}\omega_L t\right)}\cos\left(\Gamma N\omega_L t\right). \qquad (1)$$

The initial term, a normalized ratio of squares of sine functions, is shown in Figure 2 for an interval ±25 ns around the kicking peak. This envelope function sets the spacing between kicking peaks and major zeroes. The parameter N is the ratio of the bunch spacing in the main linac and damping ring.

Besides controlling the locations of the major zeroes, this envelope function also flattens the kicker's field integral $A(t)$ in the vicinity of the zeroes since the ratio of the squares of sine functions also has zero slope at major zeroes in $A(t)$. This way, the variation in field integral between the center and ends of an individual (unkicked) bunch is insignificant.

Frequency spectrum of envelope function

The frequency spectrum of the envelope function is shown in Figure 3. Because the kicker signal is periodic, the envelope function's spectrum is discrete, with individual Fourier components separated by the main linac bunch frequency f_L, 3 MHz in the present case. Note that the spectrum peaks at zero frequency, then descends linearly, becoming exactly zero at Nf_L = 180 MHz.

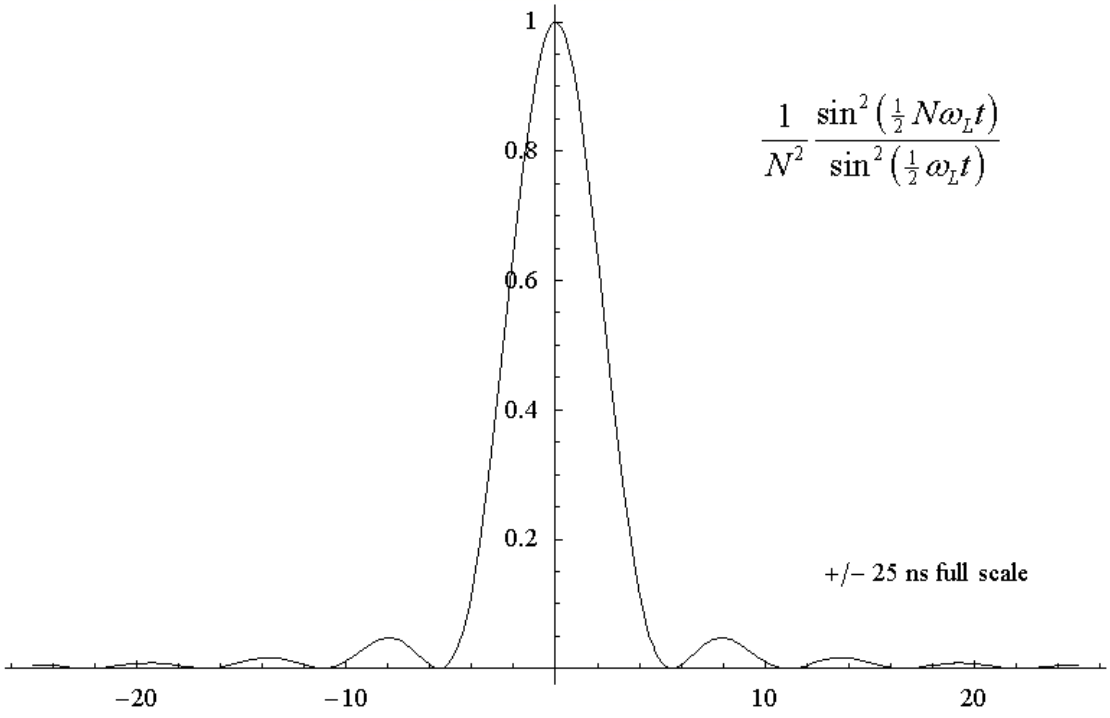

Figure 2: Envelope function ±25 ns around the kicking peak. Unkicked bunches pass through the kicker during zeroes in the field integral.

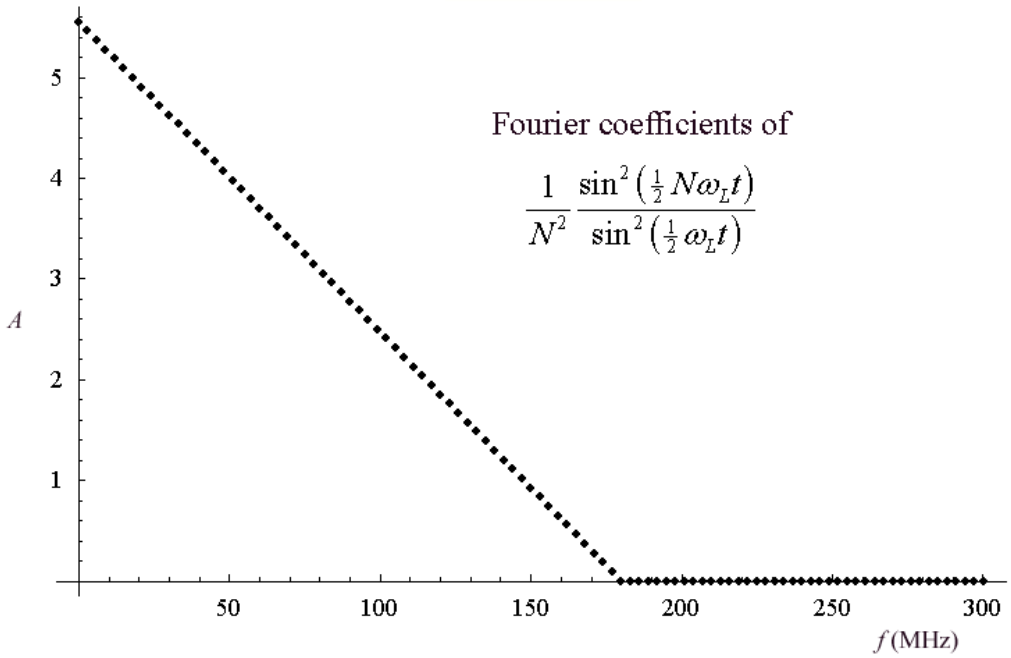

Figure 3: Fourier amplitudes of the envelope function; plot extends from 0 to 300 MHz. Note that there are 60 non-zero amplitudes and that the spacing between frequency components is f_L = 3 MHz.

Because $A(t)$ is an even function, its Fourier expansion consists entirely of cosines.

High frequency modulating function

We must choose the frequency of the modulating cosine so that $\cos(\Gamma N\omega_L t) = +1$ whenever a bunch is to be kicked, of course. But we can further flatten the field integral $A(t)$ at the major zeroes immediately before and after the kicking pick with an appropriate choice of f_{RF}. To do this we select a cavity center frequency f_{RF} that makes the modulating cosine zero as the first (or last) unkicked bunch traverses the kicker, when $t = \pm 1 / f_{DR}$. With a value of f_{RF} satisfying this requirement, we will have the modulating cosine run through the values of 0, -1, 0, +1, … at successive major zeroes. Note that the value of Γ must differ from an integer by 0.25 in order for the modulating cosine to be zero at the first major zero. In addition, N must be an integer multiple of 4 in order for the modulating cosine to assume the value +1 at all kicking peaks.

The resulting field integral (using f_{RF} = 1845 MHz) is shown in Figure 4 for an interval ±25 ns around the kicking peak.

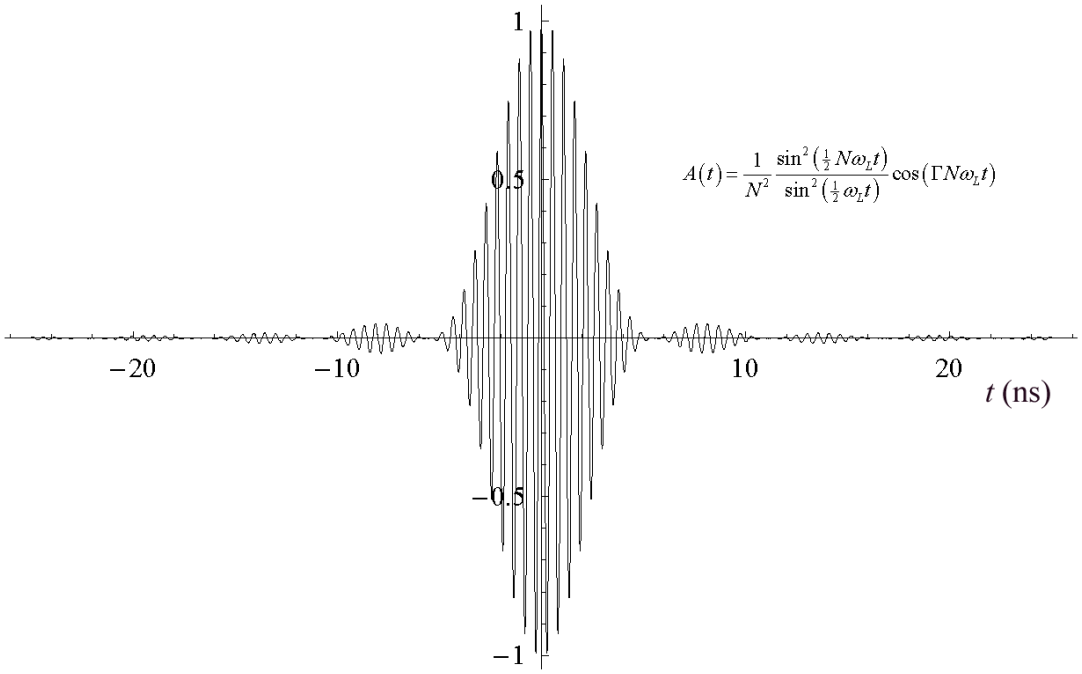

Figure 4: Kicker field integral $A(t)$ in an interval ±25 ns around the kicking peak.

Frequency spectrum of the impulse, including effects of the modulating function

The useful trigonometric identity $\cos(a)\cos(b) = \cos(a+b)/2 + \cos(a-b)/2$ lets us immediately write the Fourier expansion of $A(t)$ in terms of the Fourier series for the

envelope function described above. A graph of the Fourier amplitudes of $A(t)$ is shown in Figure 5. These amplitudes will yield a unit strength kicking pulse.

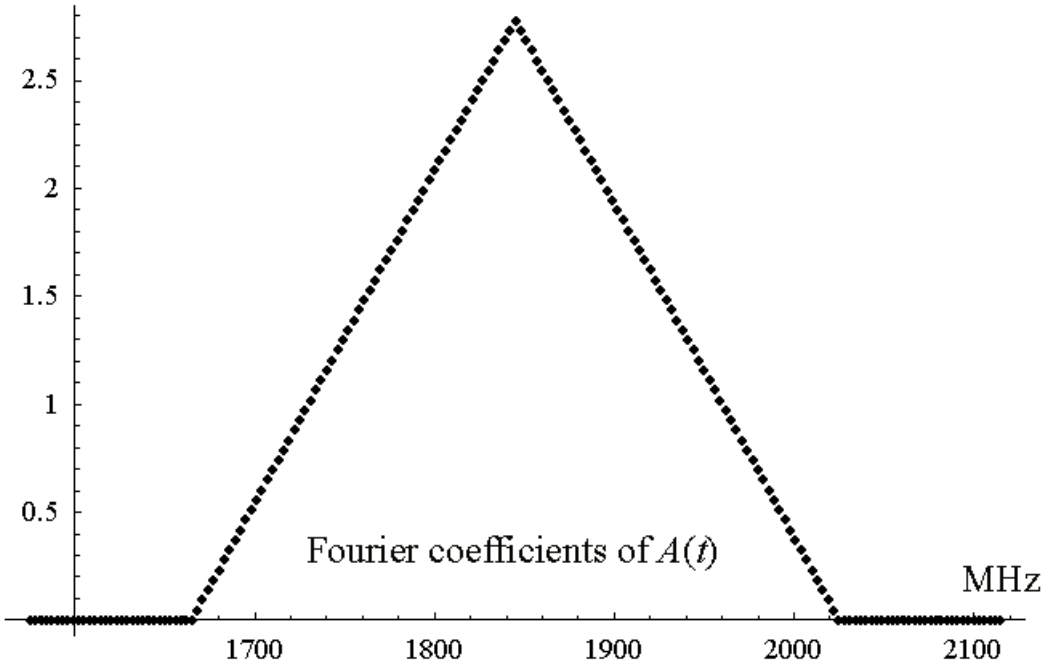

Figure 5: Fourier amplitudes of the field integral impulse $A(t)$. The peak is at frequency f_{RF} = 1845 MHz; the amplitudes become identically zero at f_{RF} ± 180 MHz. These amplitudes will yield a unit strength kicking pulse.

Details of the kicking peak

Figure 6 shows the kicking peak for the time interval (-50 ps, 50 ps). The shape is dominated by the high frequency modulation term $\cos(\Gamma N \omega_L t)$. The kick drops rapidly away from its maximum at $t = 0$. This raises two separate issues. Is the kicker's injection efficiency adequate? Are extracted bunches sufficiently free of kicker-induced distortion so that head-center-tail effects do not degrade the ILC's luminosity? Recall that the RMS width of a damping ring bunch is ±20 ps.

One promising strategy would be to install a corrector in the injection and extraction lines in order to compensate for the time dependence of the impulse delivered to a bunch. A single-frequency RF system running at f_{RF} could deliver an impulse of the opposite sign to bunches shortly before/after injection/extraction. The residual error in kick after a corrector, shown in Figure 7, is about a third as large as the required kicker precision of 0.07%.

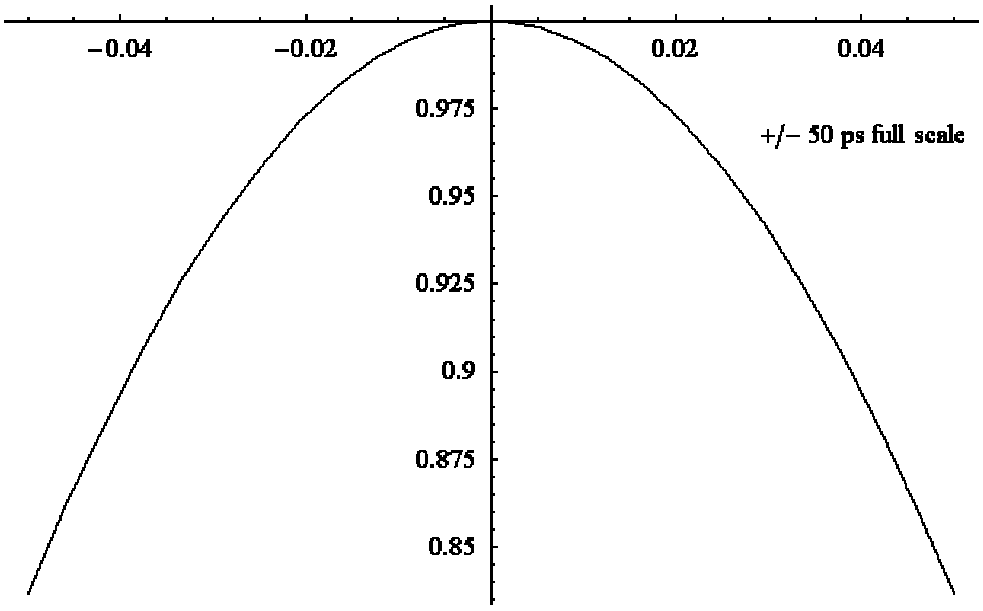

Figure 6: Kicking peak in a time interval ± 50 ps around $t = 0$. RMS bunch length is 20 ps.

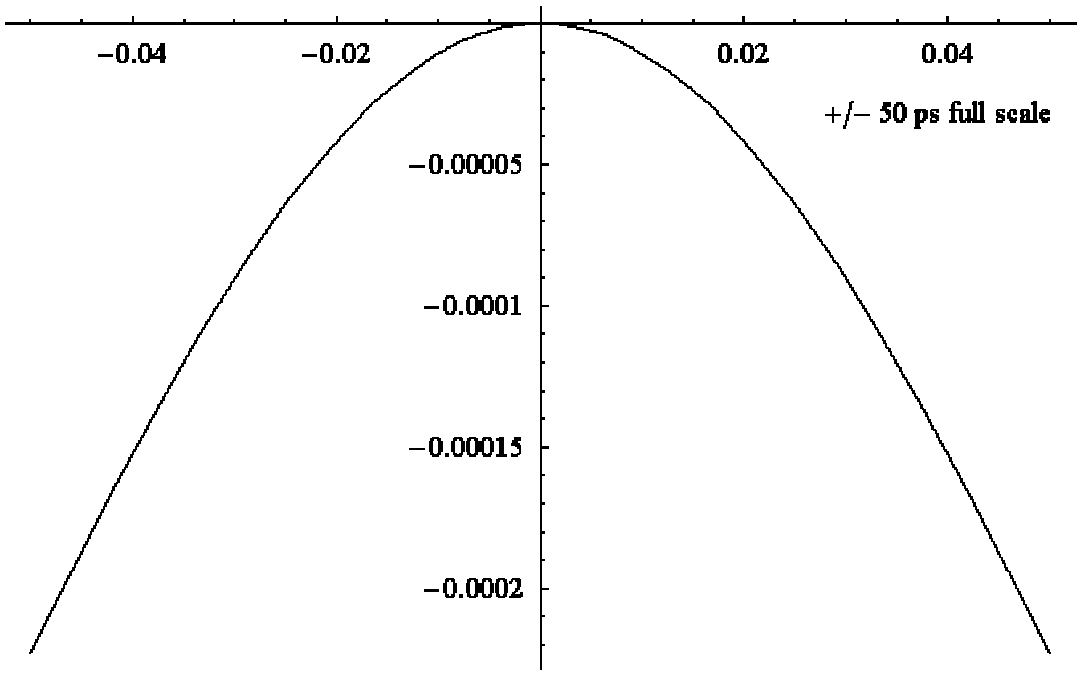

Figure 7: Fractional kick error, including an injection/extraction line corrector, in a time interval ± 50 ps around $t = 0$. Maximum allowable error is 0.0007, roughly three times the error at 50 ps.

Modifications to the kicker RF system intended to flatten the kicking peak will generally increase the required amplifier bandwidth, through introduction of a low frequency tail, higher frequency bands in the vicinity of harmonics of the cavity center frequency, or both.

Details of the major zeroes

Figures 8a, 8b, 8c, and 8d show the impulse function in ±50 ps intervals around the first four major zeroes. Note that the choice of modulation frequency makes the error in the vicinity of the zeroes cycle through four different shapes: descending cubic, downwards quadratic, ascending cubic, and upwards quadratic. This may have the virtue of canceling some of the accumulated errors for bunches which make multiple passes through the kicker before being extracted. As it stands, the kick error when a bunch transits the kicker during a single orbit is small compared to the maximum allowable error of 0.0007. Details of this will depend on the tune of the damping ring.

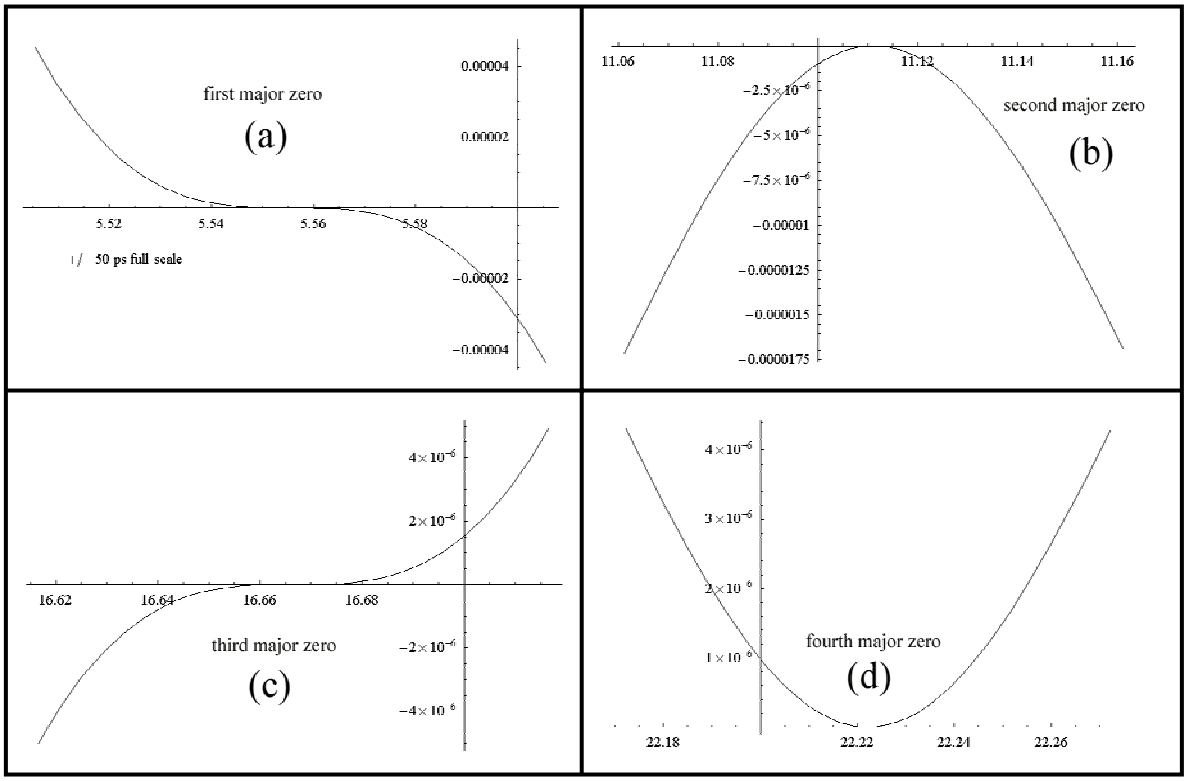

Figure 8: Impulse function in a time interval ± 50 ps around the first four major zeroes. Note that the maximum allowable deviation from zero is .0007, substantially larger than the simulated kicker error.

Low-*Q* cavity

The Fourier series kicker needs to apply a ±10% bandwidth impulse to kicked bunches. It is an interesting technical challenge to devise a method to sum the effects of the various frequency components. An early (naïve!) conception of the kicker[3] used one cavity for each frequency component, letting the beam sum the effects of the individual Fourier components. Another idea[4], originally described by Joe Rogers, uses a low-*Q* cavity that can support the range of frequencies comprising the kicking pulse.

Amplitude and phase lag of cavity response to driving signal

We have not modeled the required cavity in any detail. In our simulations we assume it has $Q = 25$, is linear, and produces fields of adequate quality. We ignore the effects of reflections at its input port and describe the cavity's response to a driving signal of frequency ω and amplitude S_{drive} this way:

$$A(t) = A_{cavity}\cos(\omega t - \varphi) = \frac{S_{drive}}{\sqrt{\left(\omega_0^2 - \omega^2\right)^2 + \left(\frac{2\omega_0\omega}{Q}\right)^2}}\cos(\omega t - \varphi)\ . \qquad (2)$$

Here ω_0 is the cavity's center frequency; the phase lag φ is defined as

$$\varphi \equiv \tan^{-1}\left(\frac{2\omega_0\omega}{Q\left(\omega_0^2 - \omega^2\right)}\right). \qquad (3)$$

The ratio $A(t)/S_{drive}$ over the required bandwidth is shown in Figure 9. The phase lag φ is shown in Figure 10. (These are the equations describing the response of a damped, driven harmonic oscillator.)

Fourier amplitudes and phases of driving signal arriving at the cavity

Since the cavity stores energy and its response is frequency dependent, dividing the Fourier amplitudes shown in Figure 5 by the response function $A(t)/S_{drive}$ generates the distribution of Fourier amplitudes that must be delivered by the amplifier to the downstream end of the waveguide to generate a unit-strength kicking pulse. This spectrum is shown in Figure 11. (Bear in mind that we have not yet modeled the frequency-dependent transfer efficiency of power from the waveguide into the cavity.)

The phase relationship between input and response changes considerably as the frequency crosses through resonance. Including the frequency-dependent phase of the

[3] Ibid.

[4] See, for example, George D. Gollin, *Studies of Alternative TESLA Damping Ring Designs*, http://www.hep.uiuc.edu/home/g-gollin/talks/AAC_damping_rings.pdf (2004).

cavity response allows us to plot the required field as a function of time at the downstream end of the waveguide. This is shown in Figure 12.

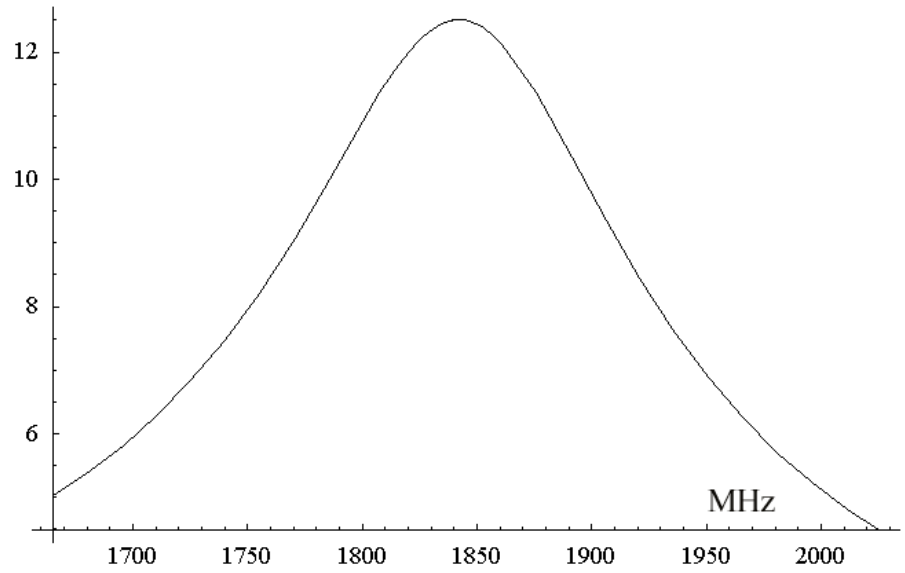

Figure 9: Cavity response to driving fields, assuming a $Q = 25$ cavity with center frequency 1845 MHz.

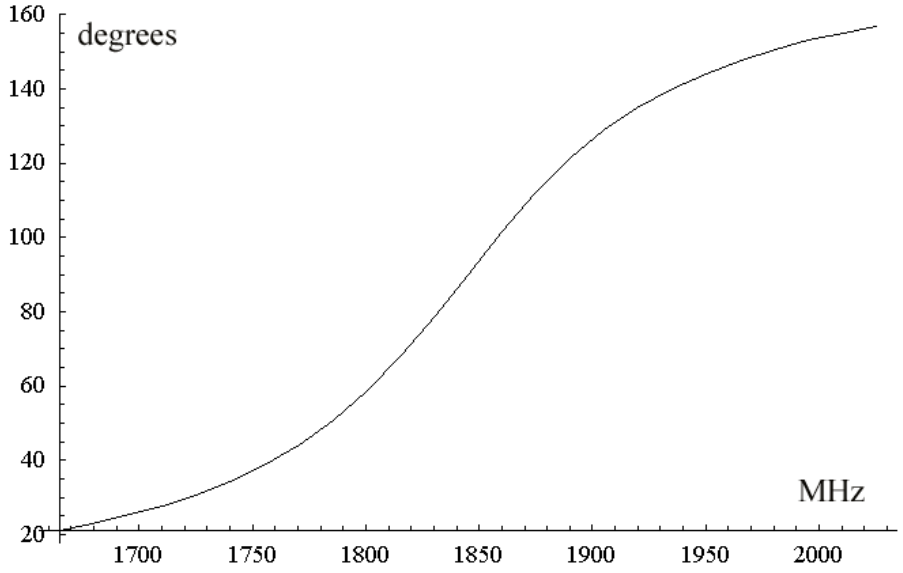

Figure 10: Phase lag between cavity response and driving fields.

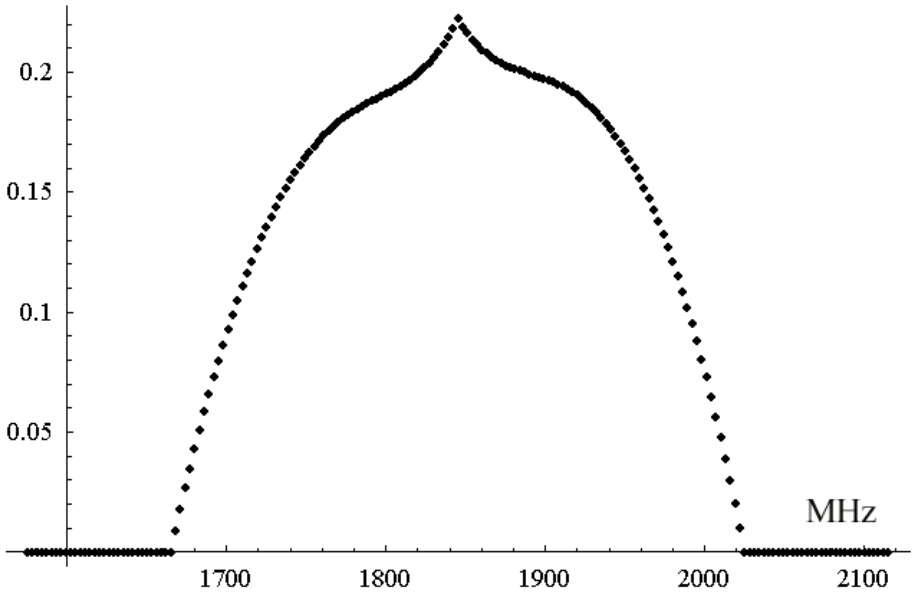

Figure 11: Fourier amplitudes required at the downstream end of the waveguide to generate a unit-strength kicking peak in the RF cavity. The amplitudes were derived by dividing the coefficients in Figure 5 by the cavity's frequency-dependent response.

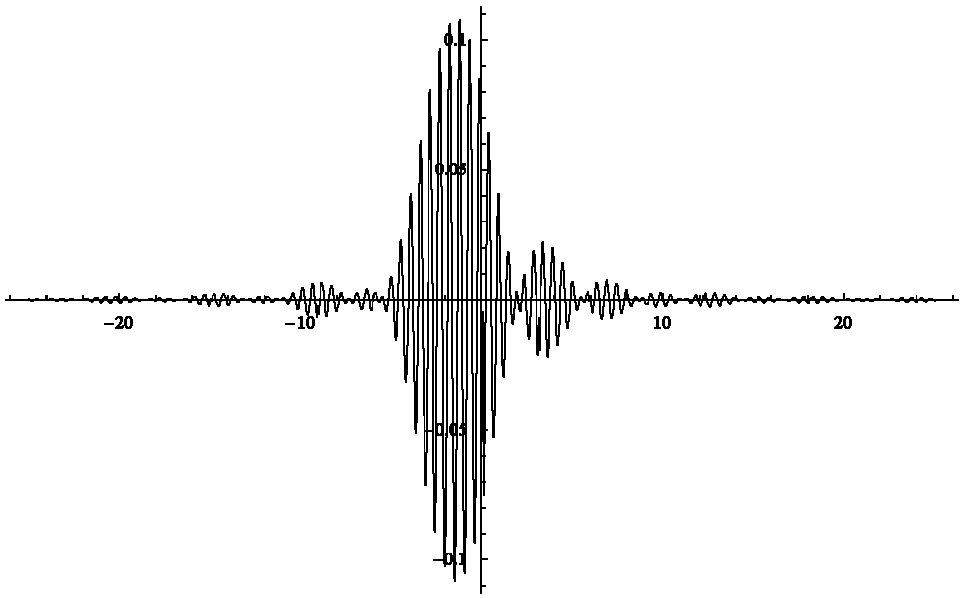

Figure 12: Field at the downstream end of the waveguide that will generate a unit-strength kicking peak in the RF cavity. Note the difference in the maximum amplitude in the waveguide in comparison with the cavity field, shown in Figure 4.

It is possible that the kicker system's sensitivity to errors might be reduced (at the expense of greater input power) if the cavity center frequency were chosen to be above or below the kicking pulse's frequency band. This is worth investigating in detail at a later time.

Waveguide

We consider a rectangular waveguide with cutoff frequency f_{cutoff} = 1300 MHz driven in its dominant mode[5]. The cutoff frequency depends on the waveguide's geometry, shown schematically in Figure 13. When $b > a$, we have $f_{cutoff} = c/(2b)$, where c is the speed of light in vacuum. Our 1300 MHz waveguide has $b \approx 11.5$ cm.

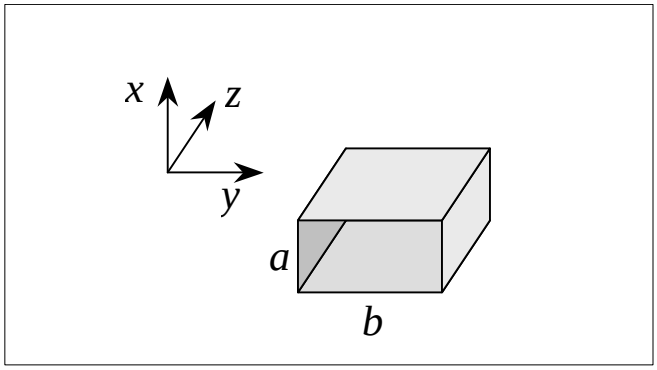

Figure 13: Waveguide geometry. Power propagates in the +z direction. For this waveguide, $f_{cutoff} = c/(2b)$ = 1300 MHz.

Group velocity

Besides providing a path between the amplifier and the RF structure, the waveguide serves as the dispersive transport that compresses the amplifier signal. The waveguide's group velocity as a function of frequency is

$$v_g = c\sqrt{1-\left(\frac{f_{cutoff}}{f}\right)^2} = c\sqrt{1-\left(\frac{\omega_{cutoff}}{\omega}\right)^2}\ . \qquad (4)$$

Figures 14 and 15 show plots of $v_g(f)$ in the frequency ranges 0 to 4000 MHz and 1665 to 2025 MHz.

[5] See, for example, Frank S. Crawford, Jr., *Waves, Berkeley Physics Course—Volume 3*, McGraw-Hill, New York (1968).

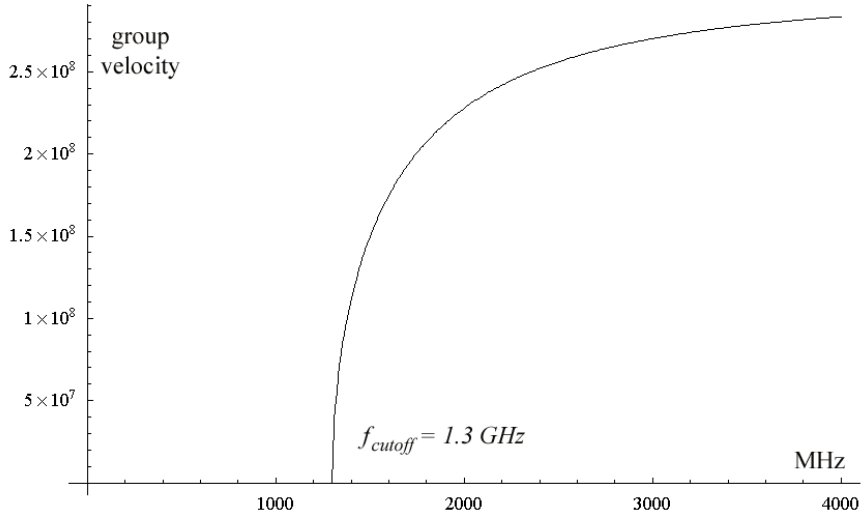

Figure 14: Waveguide group velocity as a function of frequency in the range 0 to 4000 MHz.

Energy pumped into the upstream end of the waveguide will propagate down the guide with speed equal to the group velocity. Because $v_g(f)$ is frequency dependent, the relative phases of various Fourier components will vary with position along the length of the waveguide in a way that allows the delivery of a compressed pulse to the cavity.

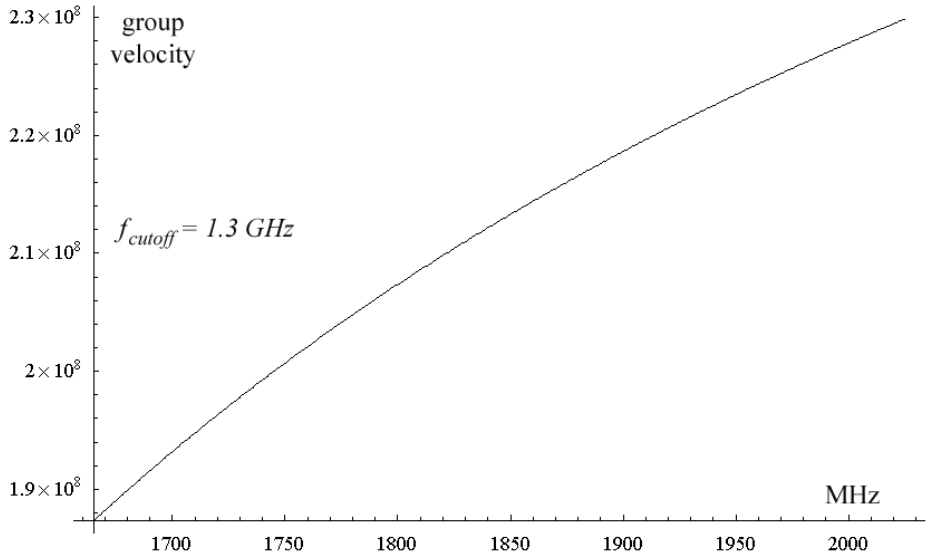

Figure 15: Waveguide group velocity in the kicker's frequency band, 1665 to 2025 MHz.

Phase lag as a function of frequency and position

Imagine that a single Fourier component with angular frequency ω is propagating in the *z* direction. We can write its amplitude at a fixed *z* position as $a\cos[\omega(t - t_{propagation})]$. The time delay $t_{propagation}$ because power flows down the waveguide at the (finite) group velocity: we expect $t_{propagation} = z/v_g$.

Since the group velocity is frequency dependent, the propagation times for different Fourier components flowing through a waveguide will vary so that their relative phases at the end of the waveguide will be different from their initial values at the entrance to the waveguide. We have

$$t_{propagation}(z,\omega) = \frac{z}{v_g(\omega)} = \frac{z}{c}\left[1-\left(\omega_{cutoff}/\omega\right)^2\right]^{-\frac{1}{2}}. \qquad (5)$$

The phase lag for a Fourier component of angular frequency ω relative to one of infinite frequency is, as a function of distance *z* along the waveguide,

$$\Delta\varphi(z,\omega) = \omega\left[t_{propagation}(z,\omega) - t_{propagation}(z,\infty)\right] = \omega z\left[\frac{1}{v_g(\omega)} - \frac{1}{c}\right]. \qquad (6)$$

The relative change in phase per meter of waveguide for adjacent Fourier components (separated in frequency by 3 MHz) is plotted in Figure 16. From the plot one can see, for example, that increasing the waveguide length by one meter will increase the phase lag of the 1800 MHz Fourier component by ~4° relative to that of the adjacent (1803 MHz) component.

Shown in Figure 17a are plots of the field amplitudes in the waveguide as functions of time at *z* positions increased in 5 meter intervals. We have adjusted the graphs' origins to keep the amplitude distributions near the center of each plot. The plots are presented in reverse time-order, with the compressed pulse at the downstream end of the waveguide appearing first. Figure 17b shows similar plots, but spaced at 20 meter intervals. Figure 17c is an enlarged version of the 80 meter plot from Figure 17b. Unusual features in the graphs are artifacts.

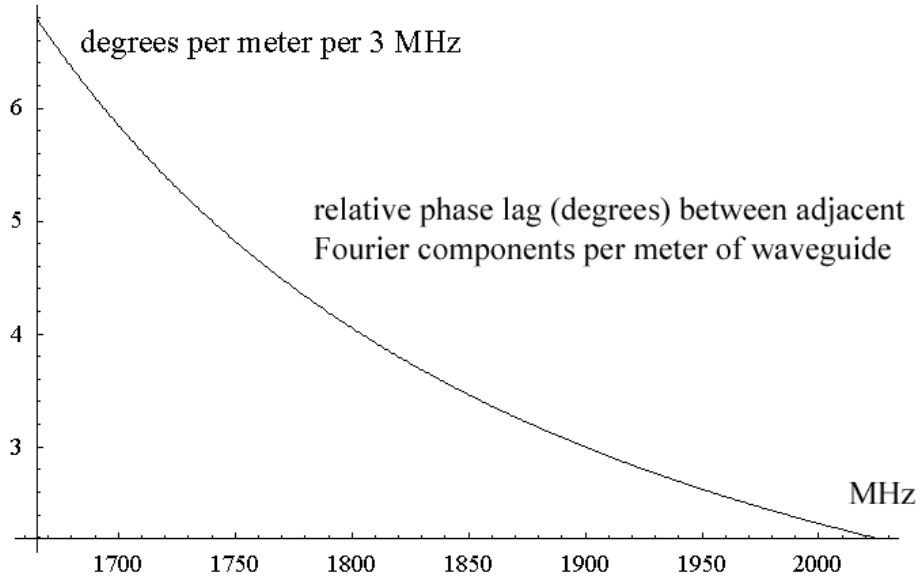

Figure 16: Relative phase lag (in degrees) of adjacent Fourier components induced per meter of waveguide.

Notice that the peak power required from an amplifier at the upstream end of an 80-meter waveguide is not particularly different from the amplifier's average power output. The field amplitude at the entrance to the waveguide is roughly one percent as large as the maximum field inside the RF kicking structure.

We have not yet optimized the length or cutoff frequency of the waveguide. Operating with a cutoff frequency closer to the cavity's center frequency would provide more dispersion per meter, allowing use of a shorter waveguide at the expense of greater sensitivity to inaccuracies in waveguide geometry.

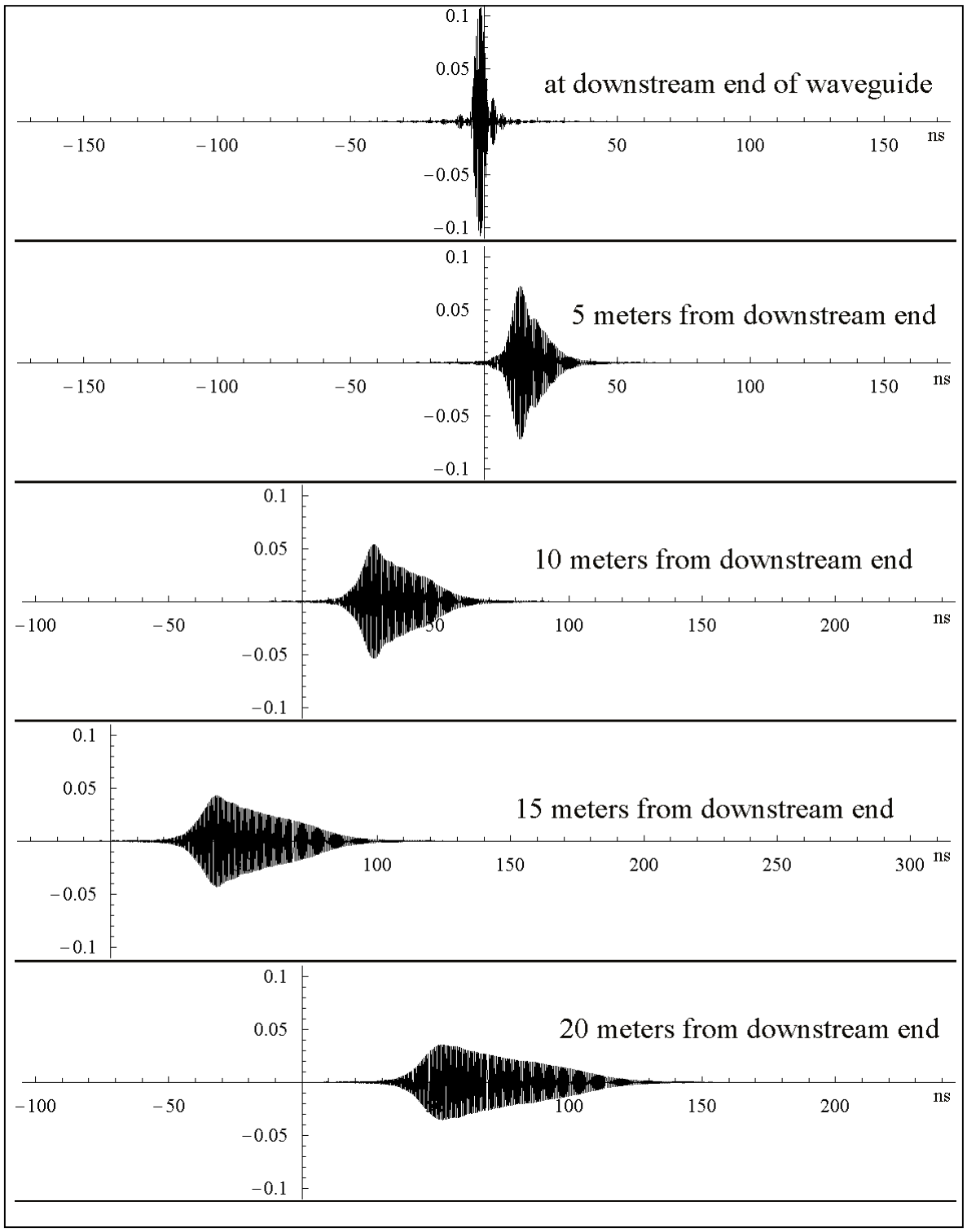

Figure 17a: Fields at different distances from the downstream end of the waveguide, shown as functions of time.

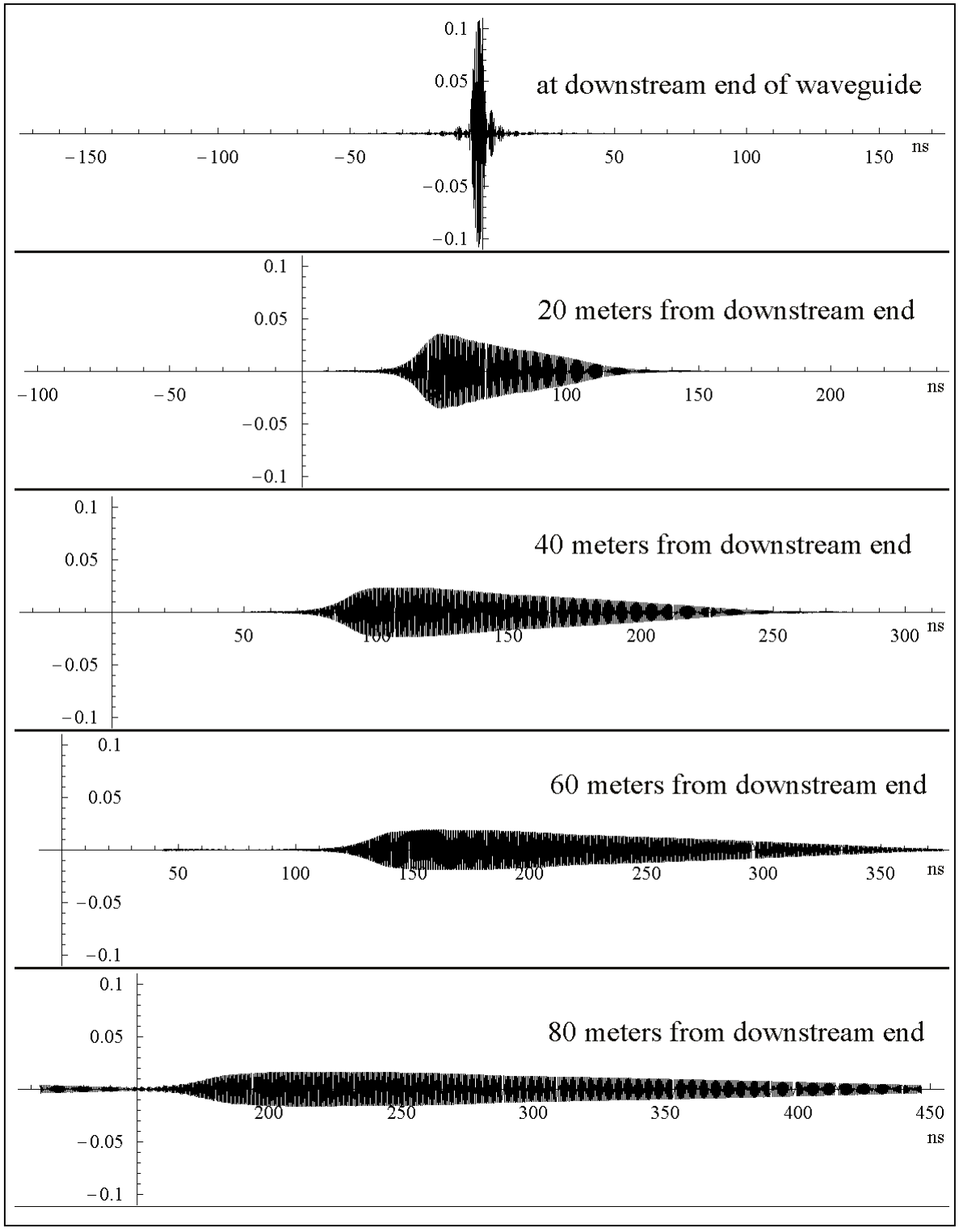

Figure 17b: Fields at different distances from the downstream end of the waveguide, shown as functions of time.

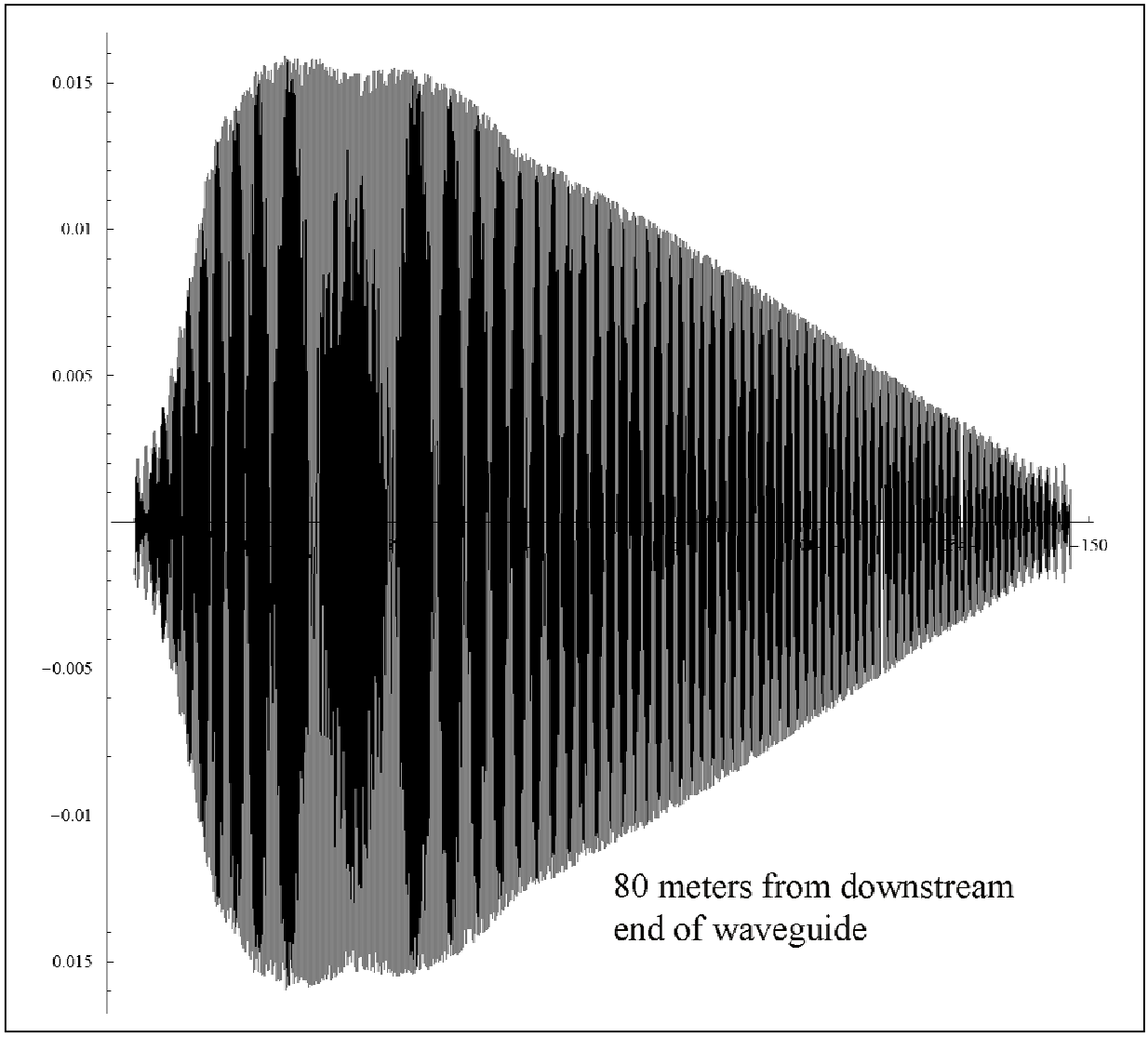

Figure 17c: Field 80 meters from the downstream end of the waveguide, shown as a function of time.

Power amplifier

We will assume that a 100 Gauss-meter impulse (3 MeV/c) is adequate. The kicking impulse under consideration requires an amplifier capable of generating signals in the frequency range (1800 ± 180) MHz.

Estimate of required amplifier power

Recall that the electric and magnetic fields in a resonant structure are 90° apart in phase. As a result, we can estimate the energy stored in the RF structure if we know its volume and the maximum electric or magnetic field it contains. Consider a generic RF device, shown schematically in Figure 18.

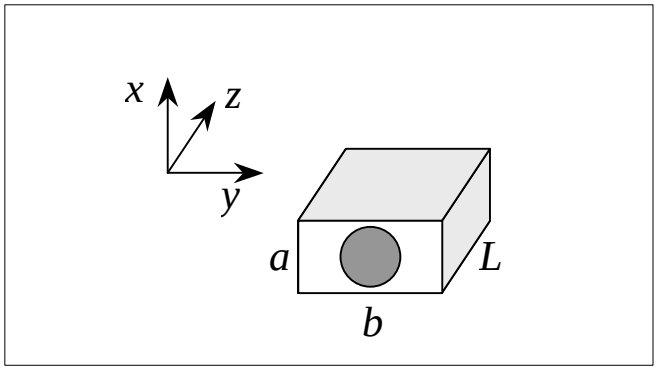

Figure 18: Generic RF kicking structure. Beam travels along +*z*.

The energy densities associated with electric and magnetic fields are $\varepsilon_0 E^2$ and B^2/μ_0 when E and B are expressed in units of V/m and T.

To inject or extract a bunch, the field strength in the kicker must satisfy

$$\langle E \rangle L \geq 3 \text{ MeV} \quad \text{or} \quad \langle B \rangle L \geq 0.01 \text{ T} \cdot \text{m} \tag{7}$$

Recall that the average values of $\sin(z)$ and $\sin^2(z)$ over the interval $(0,\pi)$ are $2/\pi$ and ½, respectively. If we assume the fields in the RF structure vary sinusoidally with z for a half wavelength along the structure's length, we will have

$$\frac{\langle E^2 \rangle}{\langle E \rangle^2} = \frac{\langle B^2 \rangle}{\langle B \rangle^2} \sim \frac{1/2}{2/\pi} = \frac{\pi}{4} \tag{8}$$

so that

$$\left\langle E^2 \right\rangle \sim \frac{\pi}{4}\left(\frac{3\ \text{MeV}}{\text{L}}\right)^2 \quad \text{and} \quad \left\langle B^2 \right\rangle \sim \frac{\pi}{4}\left(\frac{0.01\ \text{T}\cdot\text{m}}{\text{L}}\right)^2. \tag{9}$$

As a result, the energy stored in the RF device will be

$$U = abL\varepsilon_0 \left\langle E^2 \right\rangle = abL\left\langle B^2 \right\rangle / \mu_0 \sim \frac{ab\pi\varepsilon_0 \cdot 9\times 10^{12}}{4L} = \frac{ab\pi \cdot 10^{-4}}{4L\mu_0} = 62.5\frac{ab}{L}. \tag{10}$$

A device with $a = b = 5$ cm and $L = 10$ m will hold energy $U = .015625$ joules. Since the kicker is filled at 3 MHz, it requires 47 kW of RF power, neglecting losses and various coupling efficiencies. Note that the transverse electric field inside an RF structure of these dimensions is approximately 300 kV/m.

Amplifier technology

It appears that this power range, frequency and bandwidth suggest the use of a traveling wave tube amplifier (TWTA) rather than a klystron.[6] We have not yet made more than a cursory investigation of technical issues associated with the choice of amplifier.

Programmable function generator

We imagine driving the RF amplifier input with a programmable function generator. The device could be reprogrammed to compensate for drifts in the behavior of the amplifier, waveguide, and RF structure.

We have not yet selected a commercial device with suitable properties.

What is missing

We have not modeled the coupling efficiencies between amplifier and waveguide or waveguide and RF structure. It is possible that reflections at the coupler between the waveguide and the cavity will require a circulator to be installed in the waveguide. We have not studied the effects of losses in the waveguide, or of nonlinear behavior anywhere in the system. We have not yet simulated in detail the kicker's effect on bunches that pass through it a number of times before being extracted.

Sensitivity to errors

The TESLA Technical Design Report[7] describes the maximum allowable kicker error as 0.07 Gauss-meters, both for bunches that are to pass through the kicker undisturbed

[6] Ralph Pasquinelli, private communication.
[7] TESLA *Technical Design Report*, http://tesla.desy.de/new_pages/TDR_CD/ (2001).

(when its field integral is zero) and bunches that are to be extracted. Imperfections or drifts in amplifier performance, waveguide geometry, RF structure parameters, and bunch timing will all contribute to kicker performance errors. In this section we assume that injection and extraction line correctors are installed (as discussed previously) and describe the effects of various problems on kicker error.

RF structure Q error

The RF structure's response to driving fields depends on *Q*: both the frequency dependence and the overall magnitude of the cavity fields are affected by an error in *Q*. Shown in Figure 19 are plots of the fractional kick error as functions of deviation in *Q*. The three curves correspond to the center, head, and tail of a bunch, assuming the "head" and "tail" positions are $\pm 2.5\sigma$ (±50 ps) from the bunch center along the beam's direction of travel. Full scale deviation in *Q* shown in the plot is ±0.1%, giving rise to fractional kick errors of approximately ±0.0006, slightly smaller than the maximum tolerable kick error of ±0.0007 (0.07%).

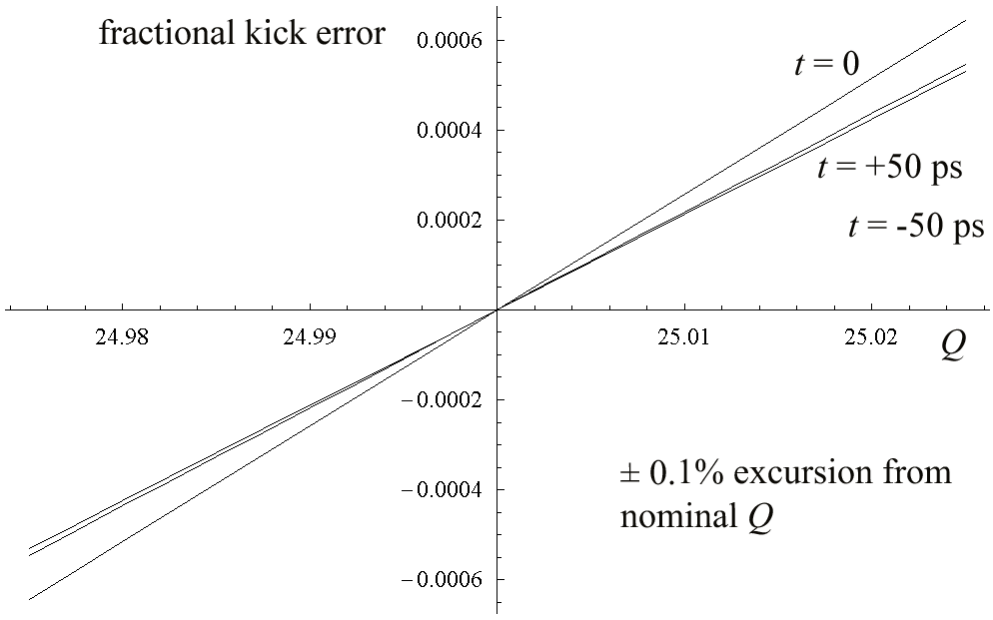

Figure 19. Fractional kick error caused by deviations in *Q* for the center (*t* = 0), head (*t* = -50 ps), and tail (*t* = +50 ps) of an extracted bunch.

The impulse error is smaller for unkicked bunches and is shown in Figure 20, in which comparisons of the effects on the kicked and first two unkicked bunches are plotted. The impulse error during an interval ±10 ns around the kicked bunch is shown in Figure 21.

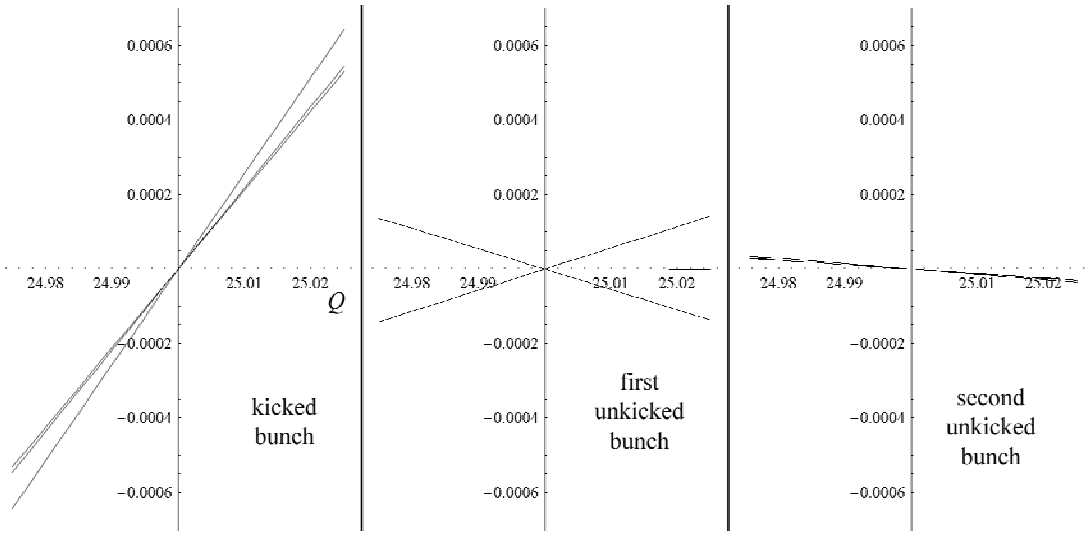

Figure 20. Kick error caused by deviations in *Q* for the center, head, and tail of the kicked and first two unkicked bunches. Full vertical scale corresponds to 0.07 Gauss-meters (2.1 keV/*c*).

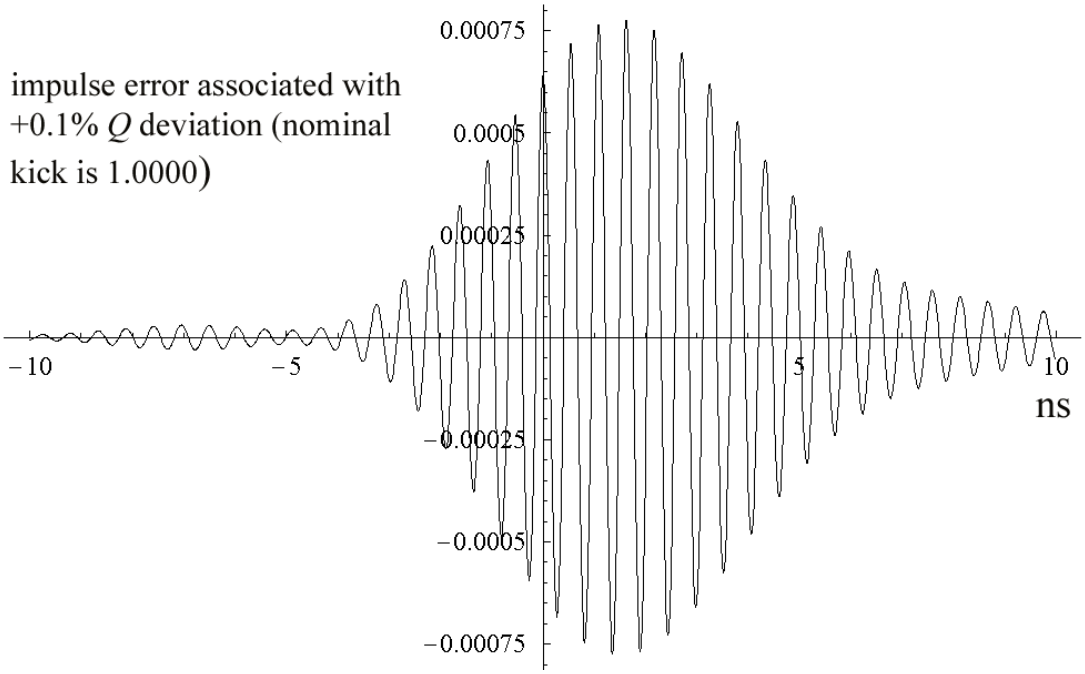

Figure 21. Kick error as a function of time caused by a +0.1% deviation in *Q*. Note that bunches are only in the kicker at integral multiples of the damping ring bunch spacing, 5.56 ns in our model.

RF structure center frequency error

The RF structure's response will be altered if its natural frequency deviates from the nominal value. The associated error in kicker impulse is shown in Figure 22 as a function of frequency deviation for the center, head, and tail of the kicked bunch.

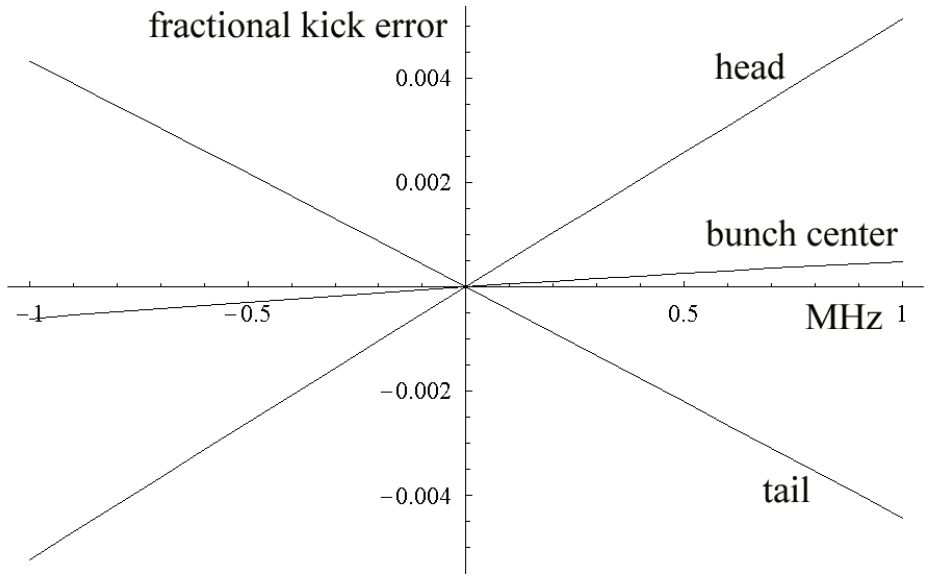

Figure 22. Kick error as a function of cavity center frequency error (MHz).

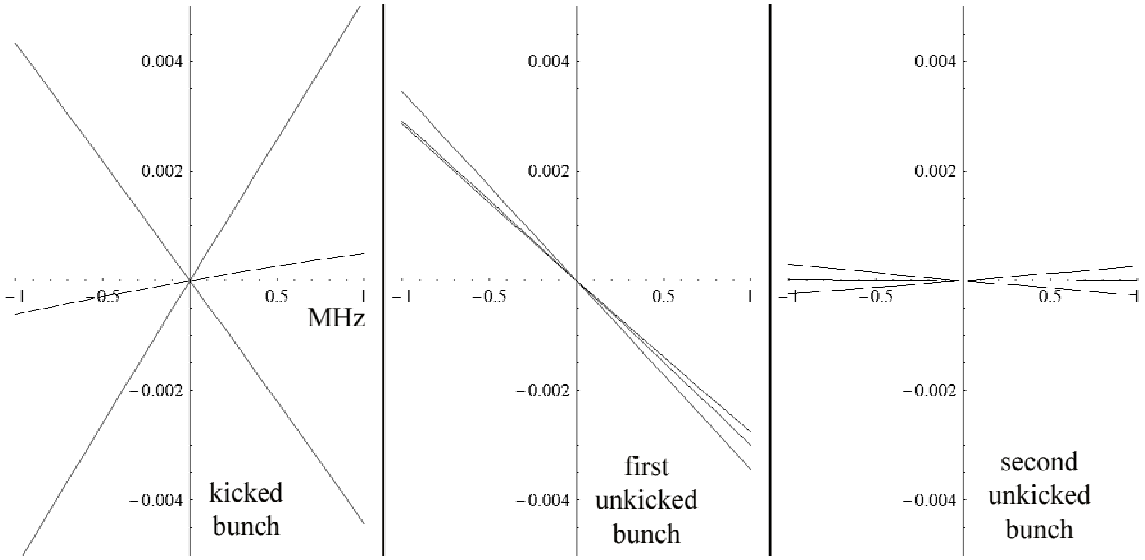

Figure 23. Kick error as a function of cavity center frequency error for kicked, first unkicked, and second unkicked bunches.

The effect is most significant for the head and tail of the kicked bunch; Figure 24 shows a graph of impulse error as a function of time for this bunch when the cavity center frequency is mistuned by 180 kHz (0.01%). Full horizontal scale in the plot is ±50 ps ($\pm 2.5\sigma$).

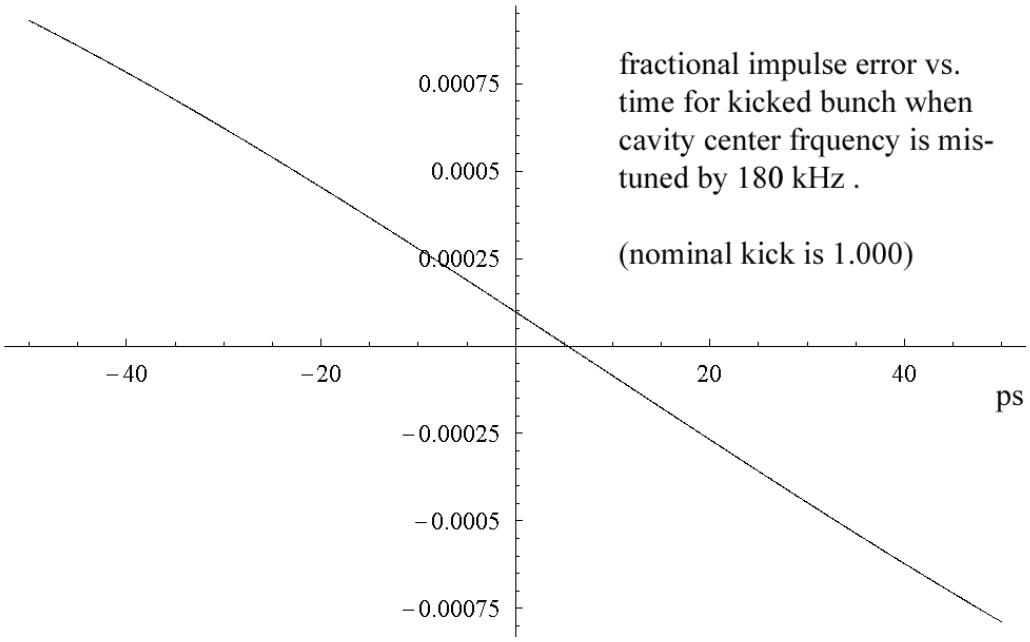

Figure 24. Kick error as a function of time when the cavity center frequency is mistuned by 180 kHz (shown for the kicked bunch only).

Cavity mistuning should be maintained below 0.01% during operation.

Waveguide length error

Changes in the length of the waveguide will shift the arrival time of the kicking pulse at the cavity relative to the arrival time of a bunch, as well as shifting the relative phases of the different frequency components contributing to the kick. Both of these effects change the arrival time of the kick with the same sign.

Figure 25 shows the effect of a 1 mm waveguide length error. The two curves represent the ideal and delivered impulses as functions of time; full scale in the plot is ±10 ps. Note the ~5 ps shift in the positions of the peaks. Since the waveguide's group velocity is ~2/3 *c* in the kicker's frequency band, we see that most of the shift in the location of the peak is caused by the overall increase in propagation distance, rather than the dispersion-induced shift in the relative phases of the Fourier components. This isn't surprising: the phase difference between adjacent Fourier components only changes by a few degrees per meter of waveguide: a one millimeter length error will only shift their relative phases by a few thousandths of a degree. Most of the change in the time structure of the kicking peak comes about through its delayed arrival at the RF cavity.

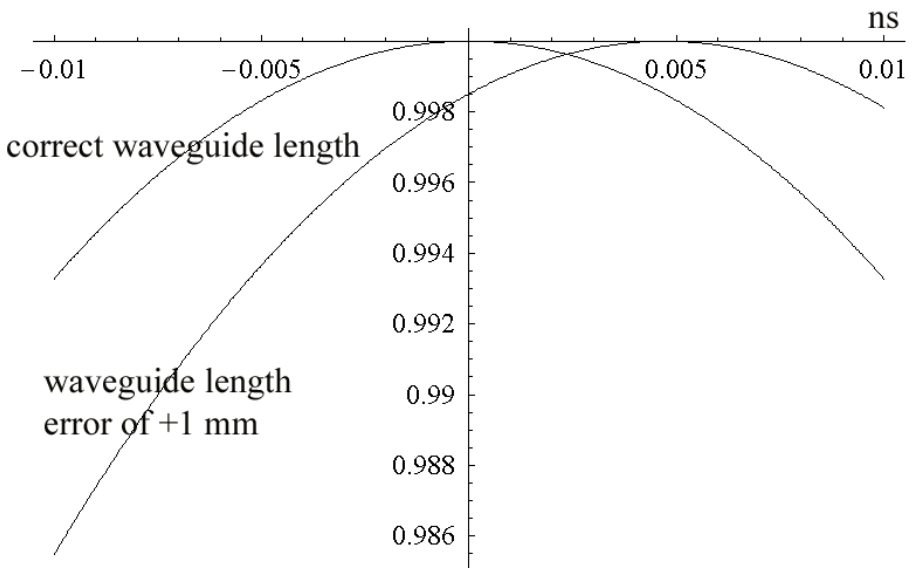

Figure 25. Effect of a 1 mm waveguide length error. The two curves represent the ideal and delivered impulses as functions of time; full scale in the plot is ±10 ps.

When the waveguide error is too large, the shape of the kicking peak will change so that the injection/extraction line correctors can no longer flatten the peak with sufficient accuracy. As a measure of this change in shape, we plot the difference between the delivered kick and an ideal impulse in Figure 26, in which the peaks of the delivered and ideal impulse curves have been aligned.

Most of the deviation from the ideal impulse evident in Figure 26 is due to the difference in size of the delivered kick. Rescaling the kicks to have the same magnitude as the ideal impulse yields the curves plotted in Figure 27. This is encouraging: it would be sensible to build the waveguide to an accuracy in length of a centimeter or better, but it is easy to compensate for errors (or thermally induced changes) in length by tuning the amplitude and timing of the amplifier signal injected into the waveguide.

The effect on unkicked bunches is also small, as can be seen in Figure 28. The effect on later unkicked bunches is even less than on the first unkicked bunch: as long as the waveguide length is controlled to an accuracy of a centimeter, adjusting the overall size and timing of the amplifier signal will compensate adequately for small changes in waveguide length.

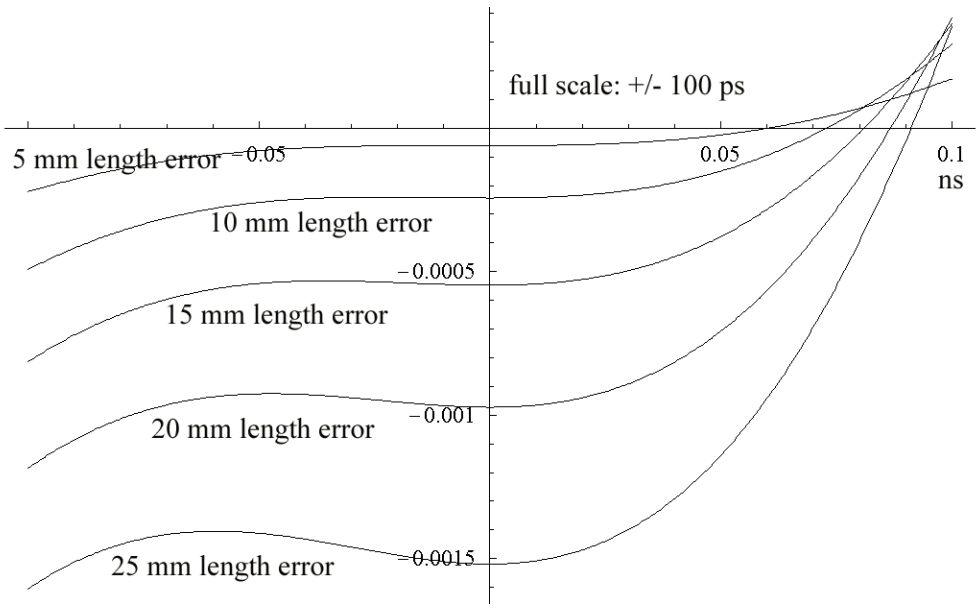

Figure 26. Effect of waveguide length error. Plotted are the differences between the delivered kicks and an ideal impulse for waveguides that are 5 mm, 10 mm, 15 mm, 20 mm, and 25 mm too long. The peaks in the delivered kicks have been shifted in time to align with the peak in the ideal impulse centered at $t = 0$.

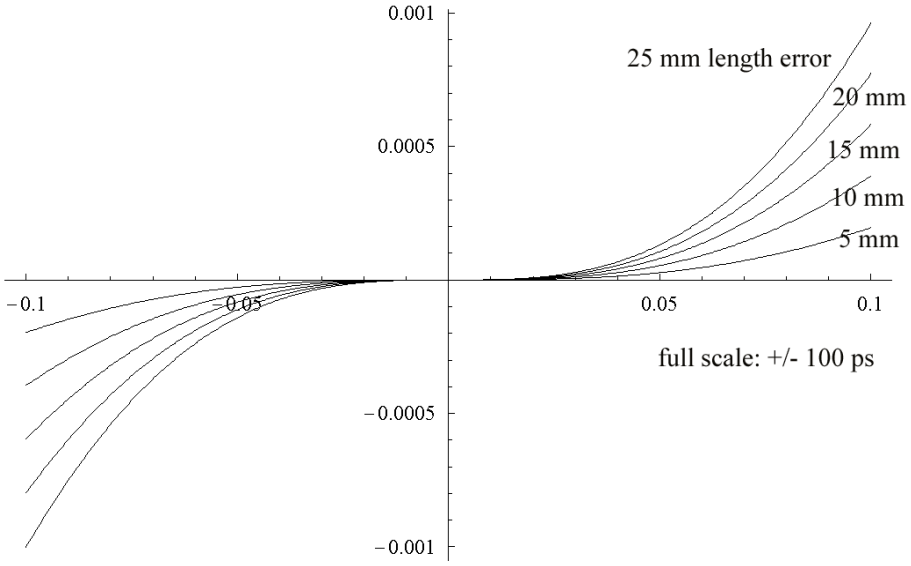

Figure 27. Differences between delivered kicks and an ideal impulse for waveguides that are 5 mm, 10 mm, 15 mm, 20 mm, and 25 mm too long. The peaks in the kicks have been shifted in time to align with the peak in the ideal impulse that is centered at $t = 0$. In addition, the delivered kicks have been rescaled to have the same magnitude as the ideal impulse.

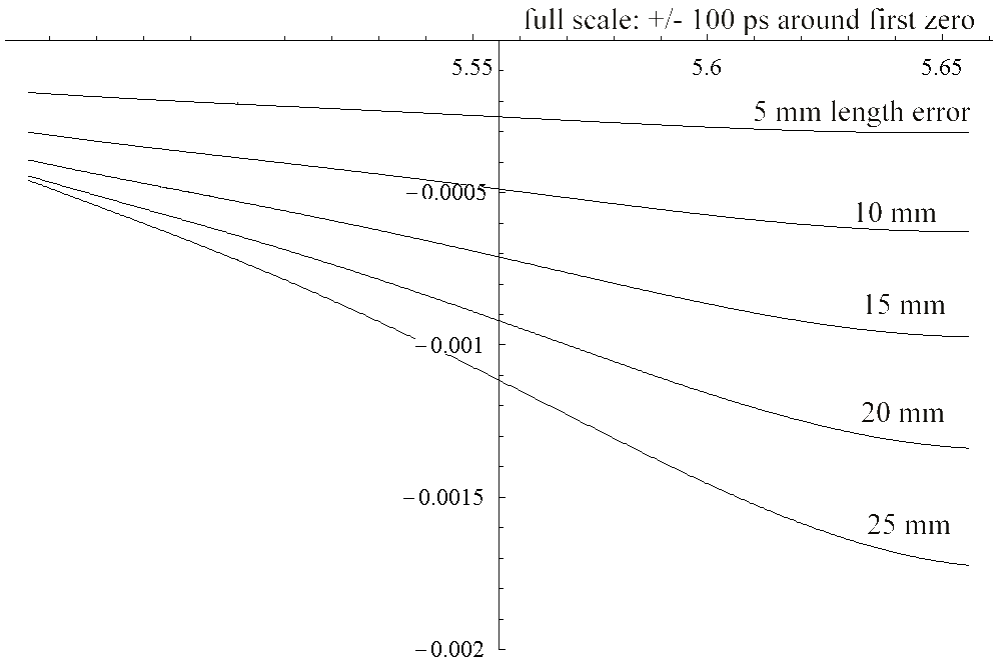

Figure 28. Differences between delivered kicks and an ideal impulse at the arrival time of the first unkicked bunch for waveguides that are 5 mm, 10 mm, 15 mm, 20 mm, and 25 mm too long. The peaks in the kicks have been shifted in time to align with the peak in the ideal impulse that is centered at $t = 0$. The time region in the plot is centered on the arrival time of the first unkicked bunch.

Waveguide cutoff frequency error

Recall that the cutoff frequency for the rectangular waveguide shown in Figure 13 is $f_{cutoff} = c/(2b)$, where b is the larger of the waveguide's transverse dimensions. Inaccuracies and thermal drifts in waveguide geometry will change the cutoff frequency, and therefore the frequency dependence of the group velocity. It should be possible to correct for this by reprogramming the function generator that drives the amplifier.

The problems arising from drifts in cutoff frequency will be seen in a number of ways. The average group velocity will change, so the propagation time between amplifier and cavity will shift. This causes mistiming between the kicking peak and the beam. In addition, the phase differences between the various Fourier components arriving at the cavity are changed, leading to an error in pulse shape.

How large an error in f_{cutoff} might be tolerable? We can use the sensitivity to waveguide length errors as a rough indicator. Figures 25 - 28 suggest that a centimeter length change does not distort the pulse shape by an unacceptable amount. The relative phases of adjacent Fourier components change by a few hundredths of a degree per centimeter of waveguide, so we can ask what change in cutoff frequency might have a similar effect on the phases. After traveling the full length of the waveguide, frequency components separated by 3 MHz are split in phase by typically 300 degrees. As a result, a fractional error in error in group velocity, and therefore in cutoff frequency, that is small compared

to a part in 10^4 ought to be tolerable. Since $\delta v_g/v_g \sim \delta b/b$, we will need the waveguide transverse dimension to be stable a few microns.

To some extent we should see the same kinds of effects arising due to errors in waveguide cutoff frequency as we do with errors in length: there will be an overall time displacement of the kicking peak and a reduction in its amplitude, as well as distortion in the shapes of the impulse function in the vicinity of the zeroes. Some correction through adjustment of the timing and overall amplitude of the signal coming out of the function generator can (partially) compensate for this.

The shift in arrival time of the kicking peak is shown in Figure 29 for a 100 kHz displacement in cutoff frequency away from the nominal value of 1.3 GHz. Note the ~30 ps displacement of the peak from $t = 0$.

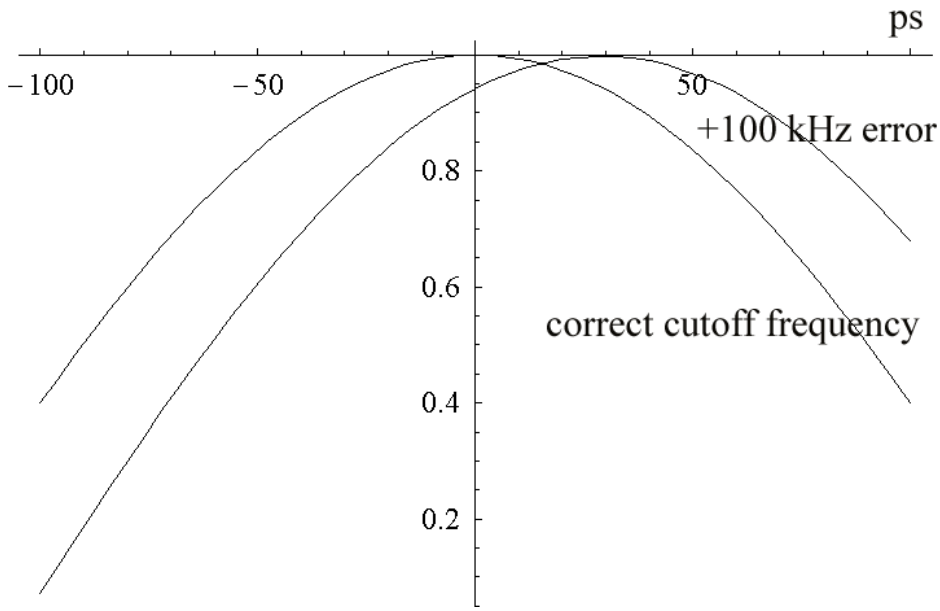

Figure 29. Effect of a 100 kHz cutoff frequency error. The two curves represent the ideal and delivered impulses as functions of time; full scale in the plot is ±100 ps. Nominal f_{cutoff} is 1.3 GHz.

The influence on the *shape* of the kicking peak is shown in Figure 30 in which we plot the difference between the delivered kick and an ideal impulse after the peaks of the delivered and ideal impulse curves have been aligned in time, and rescaled to have the same peak amplitude. The impact on the accuracy of the zero in impulse at the first unkicked bunch is shown in Figure 31. From these figures we see that it is harder to correct the impulse function at the first unkicked bunch than it is at the kicked bunch by rescaling and shifting in time: the impulse errors 50 ps away from the bunch centers are larger for the unkicked bunch. As it stands, this naïve correction scheme will be adequate for cutoff frequency errors smaller than about 20 kHz,

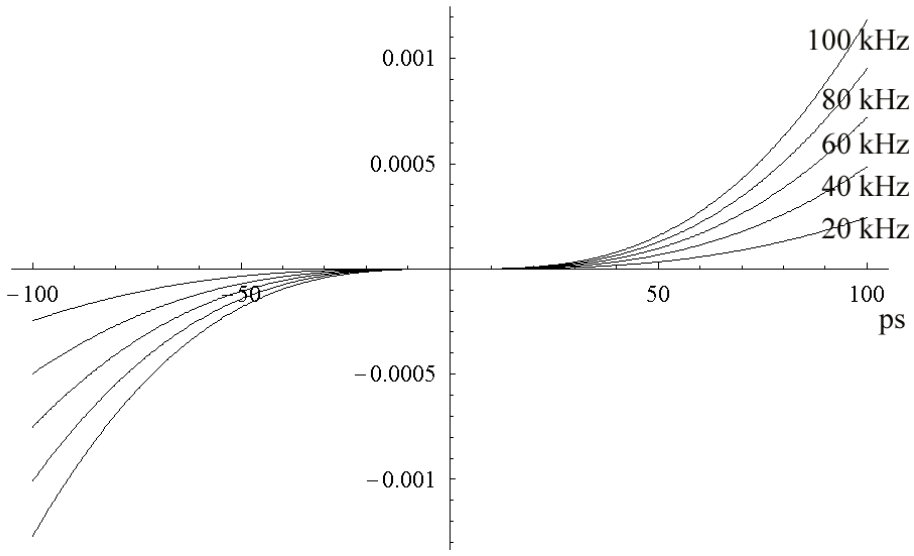

Figure 30. Effects of cutoff frequency errors. The curves represent the difference between delivered and ideal impulses as functions of time after aligning the time of the peaks and rescaling the peak amplitudes. Full scale in the plot is ±100 ps. Nominal f_{cutoff} is 1.3 GHz. Errors in cutoff frequency for individual curves are indicated on the plot.

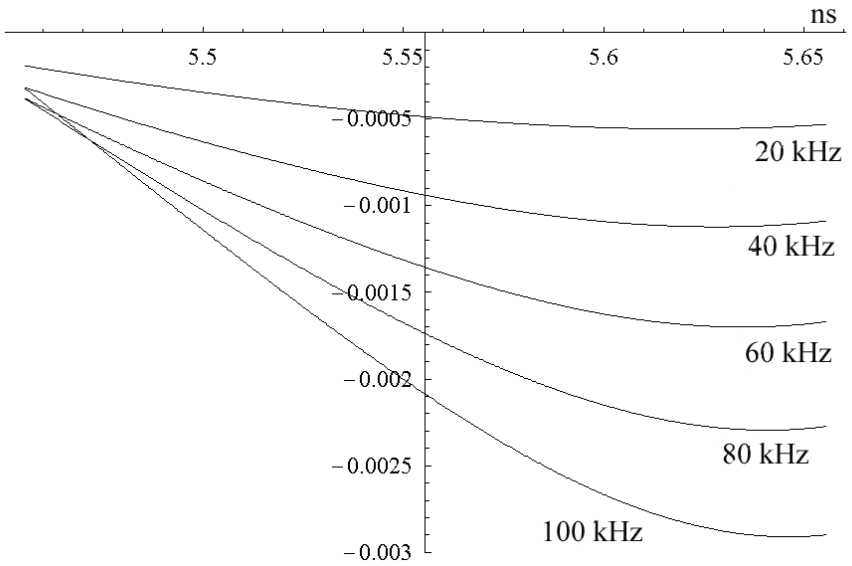

Figure 31. Effects of cutoff frequency errors. The curves represent the difference between delivered and ideal impulses as functions of time. The peaks in the kicks have been shifted in time to align with the peak in the ideal impulse that is centered at $t = 0$. The time region in the plot is centered on the arrival time of the first unkicked bunch.

Amplifier gain error: linear frequency dependence

Any effect that causes the delivery of an incorrect set of amplitudes and phases for the various Fourier components to the RF structure will generate impulse errors. To see how sensitive the impulse function is to amplifier gain errors we model these errors assuming a linear frequency dependence: $\Delta G = \alpha(f\text{-}f_{RF})$. Naturally, other forms of frequency dependence are possible! However, since we are working with a signal whose full bandwidth is only ±10% of its principal frequency, a linear model seems a sensible choice for the time being. How large can α become without overly distorting the impulse function?

Figures 32, 33, and 34 show the consequences for α values of 0.5% per 180 MHz, 1.0% per 180 MHz, 1.5% per 180 MHz, and 2.0% per 180 MHz. In the plots, the impulse functions have been rescaled to agree in amplitude at $t = 0$ with the nominal kick. Full (horizontal) scale in the figures is ±100 ps. Since the full bandwidth in the impulse function is ±180 MHz, the different curves correspond to maximum deviations from ideal gain of ±0.5%, ±1.0%, ±1.5%, and ±2.0%. As before, it is the first unkicked bunch that is most susceptible to problems: amplifier gain errors (for errors that increase linearly with distance from the center frequency) should be kept smaller than ±1% over the full ±180 MHz band.

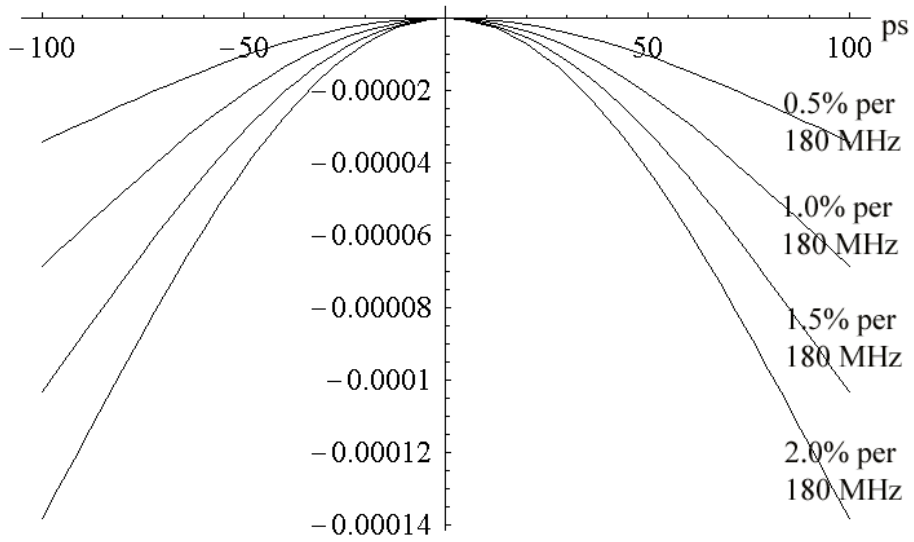

Figure 32. Effects of an amplifier gain error that grows linearly with frequency. The curves represent the difference between delivered and ideal impulses as functions of time. The time region in the plot is centered on the arrival time of the kicked bunch.

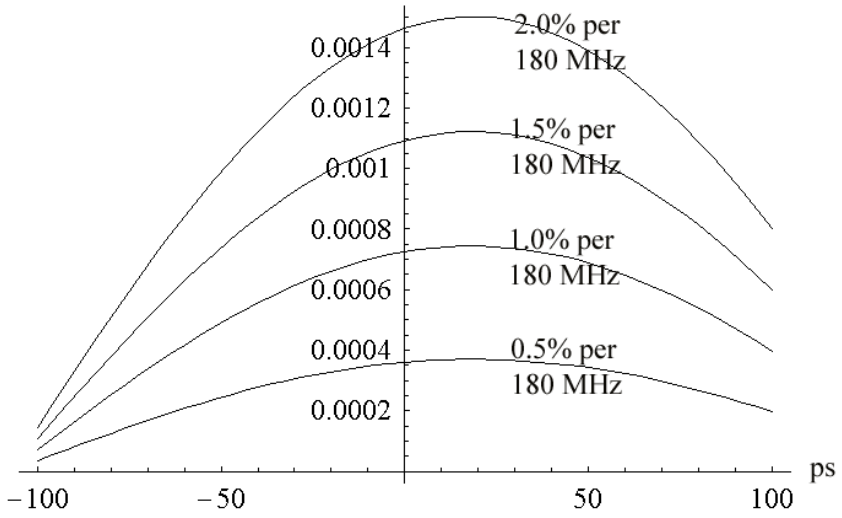

Figure 33. Effects of an amplifier gain error that grows linearly with frequency. The curves represent the difference between delivered and ideal impulses as functions of time. The time region in the plot is centered on the arrival time of the first unkicked bunch.

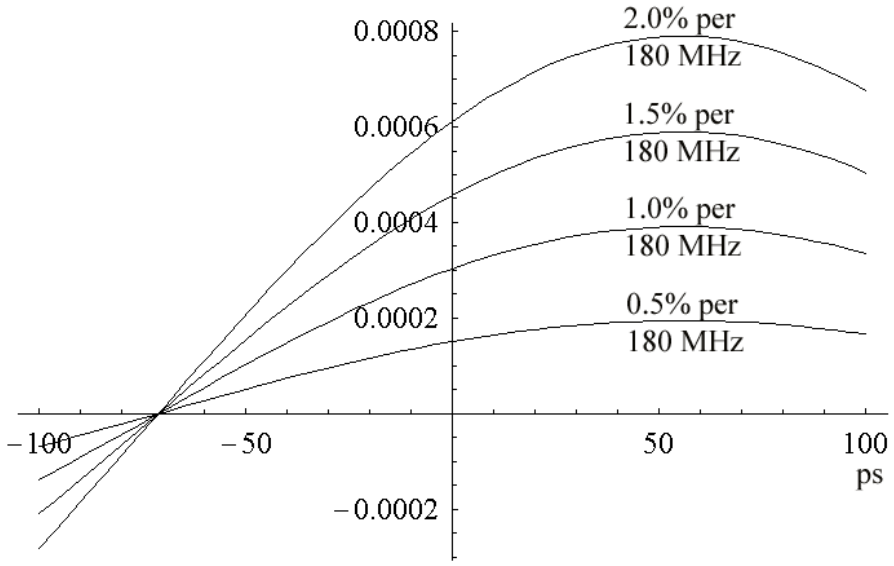

Figure 34. Effects of an amplifier gain error that grows linearly with frequency. The curves represent the difference between delivered and ideal impulses as functions of time. The time region in the plot is centered on the arrival time of the second unkicked bunch.

Amplifier phase error: linear frequency dependence

To study sensitivity to amplifier phase errors we again assume a linear frequency dependence: $\Delta\phi = \beta(f-f_{RF})$.

Figures 35, 36, and 37 show the consequences for β values of 0.2º per 180 MHz, 0.4º per 180 MHz,… 1.0º per 180 MHz. In the plots, the impulse functions have been shifted in time to align the kicking peaks and rescaled to agree in amplitude with the nominal kick. Full (horizontal) scale in the figures is ±100 ps. As before, the full bandwidth in the impulse function is ±180 MHz.

Again, it is the first unkicked bunch that is most susceptible to problems: amplifier phase errors (for errors that increase linearly with distance from the center frequency) should be kept smaller than ~1º over the full ±180 MHz band.

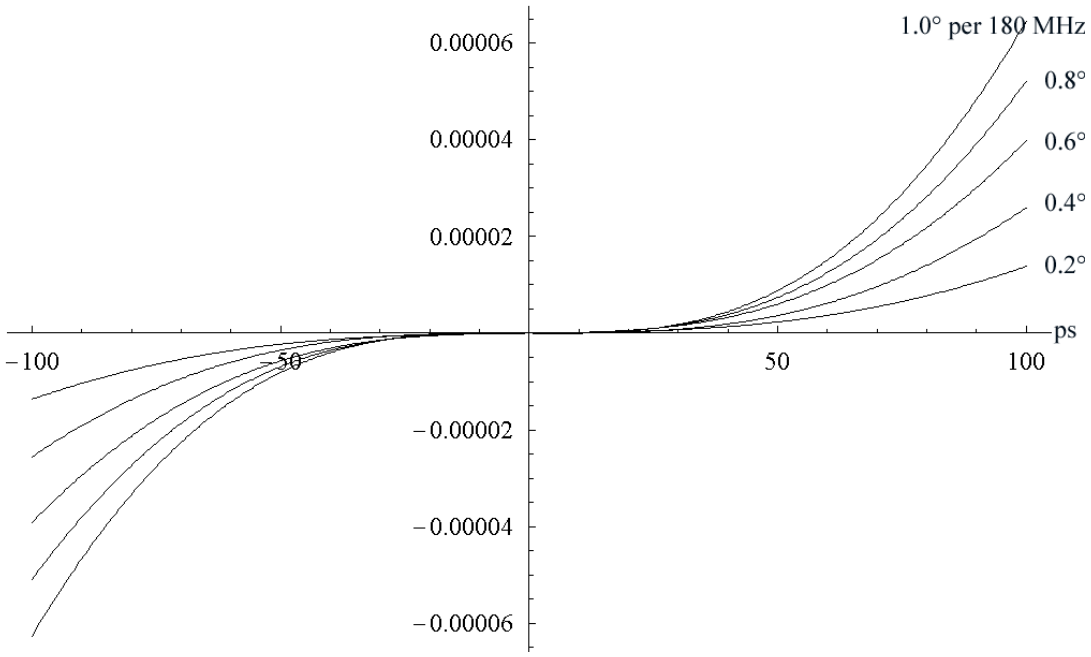

Figure 35. Effects of an amplifier phase error that grows linearly with frequency. The curves represent the difference between delivered and ideal impulses as functions of time. The time region in the plot is centered on the arrival time of the kicked bunch. Full (horizontal) scale is ±100 ps. The impulse functions have been shifted in time to align the kicking peaks at $t = 0$ and rescaled to agree in amplitude with the nominal kick.

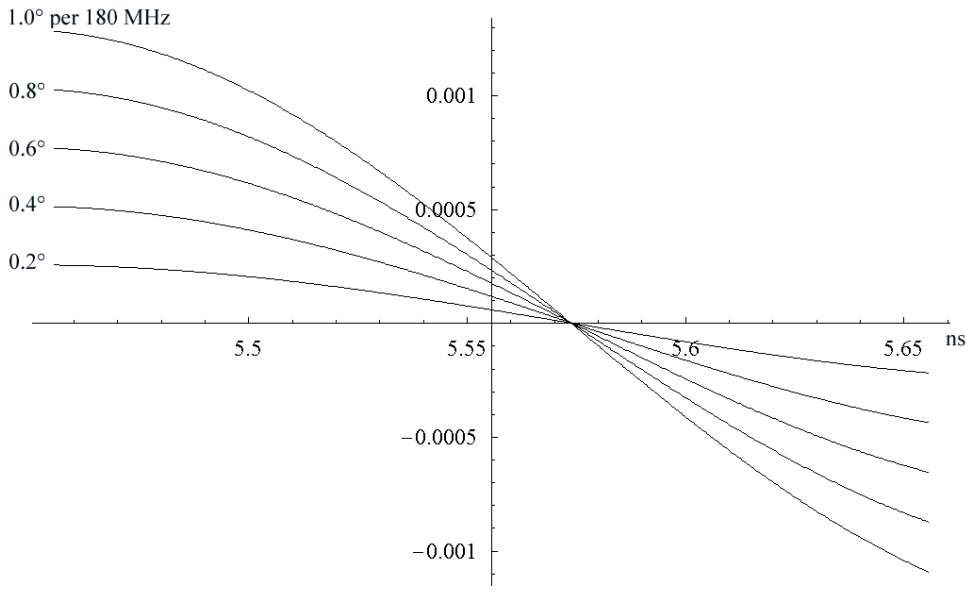

Figure 36. Effects of an amplifier phase error that grows linearly with frequency. The curves represent the difference between delivered and ideal impulses as functions of time. The time region in the plot is centered on the arrival time of the first unkicked bunch.

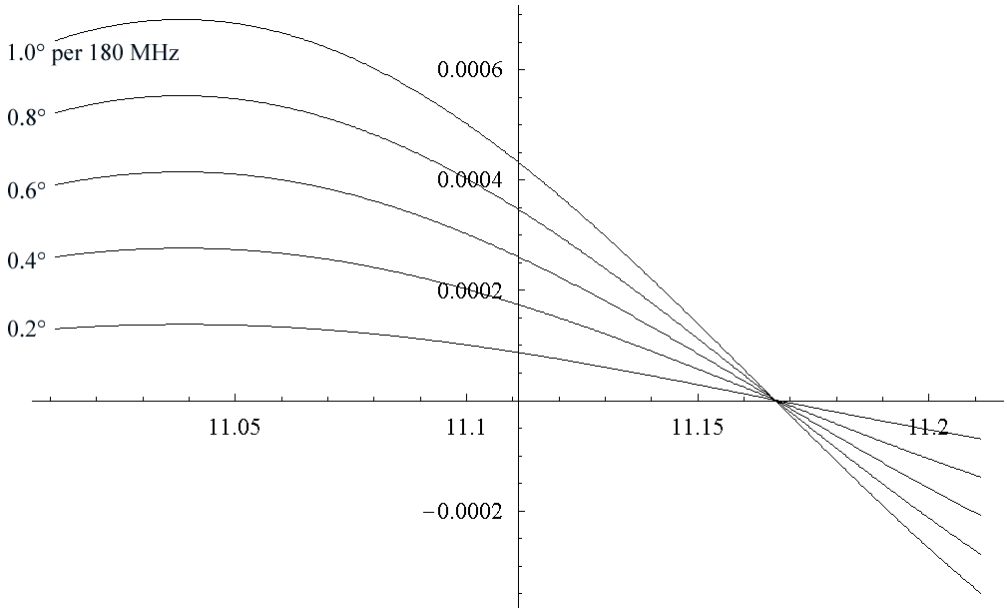

Figure 37. Effects of an amplifier phase error that grows linearly with frequency. The curves represent the difference between delivered and ideal impulses as functions of time. The time region in the plot is centered on the arrival time of the second unkicked bunch.

A comment on errors

The errors in impulse function caused by the effects described above can be corrected through adjustment of the signal produced by the programmable function generator. Small corrections can be made through adjustment in overall amplitude and timing of the function generator signal; larger adjustments will require changing the mix of Fourier amplitudes and phases in the signal sent to the RF amplifier.

Not all problems can be remedied through clever use of a low-level RF system to recognize impulse inaccuracies: noise and amplifier nonlinearities can introduce errors that cannot be removed through reprogramming.

Sensitivity to noise

Amplifier noise

We model amplifier noise as flat in frequency spectrum from 300 MHz to 6 GHz, and random in phase. We do not simulate noise outside this frequency range. To represent the noise voltage in the time domain, we divide the frequency band into bins that are 300 kHz wide and assign a noise voltage $v_i(t) = v_0 \cos(\omega_i t + \phi_i)$ to each bin. The subscript i labels the bin; the phase ϕ_i is selected randomly with no correlation between the phases of individual frequency bins. The overall noise voltage $v_{noise}(t)$ is the sum of $v_i(t)$ over all bins i.

As can be seen in Figure 17c, the maximum amplifier output is ~0.015 in units where the kicking voltage inside the RF cavity has unit strength 1. In these units, an RMS amplifier noise voltage of 10^{-4} per $\text{GHz}^{1/2}$ produces the results shown in the next several graphs. Figure 38 illustrates a typical noise voltage, shown as a function of time, at the amplifier output. Note the presence of high frequency contributions to the noise amplitude.

Since the RF cavity does not store energy efficiently at frequencies far from 1.8 GHz, we expect that the noise voltage inside the cavity will show much less out-of-band contribution than is present in the simulated amplifier noise. This can be seen in Figure 39 where the high frequency noise present in Figure 38 is largely absent.

The noise distribution added to the kicking impulse corresponding to an amplifier noise level of 10^{-4} per $\text{GHz}^{1/2}$ is shown in Figure 40. Note that the RMS noise voltage in the cavity is 0.00044 (in units where the ideal impulse has unit amplitude), somewhat smaller than the limit set by the total noise budget.

The full bandwidth of the amplifier input signal is 360 MHz; restricted to this band, the rms noise associated with 10^{-4} per $\text{GHz}^{1/2}$ would be 6×10^{-5} in comparison with a maximum signal of ~.015, or a required signal/noise ratio of ~250, or 48 db. With a wider acceptance band (the RF cavity responds to out-of-band frequencies), the required signal/noise ratio is greater.

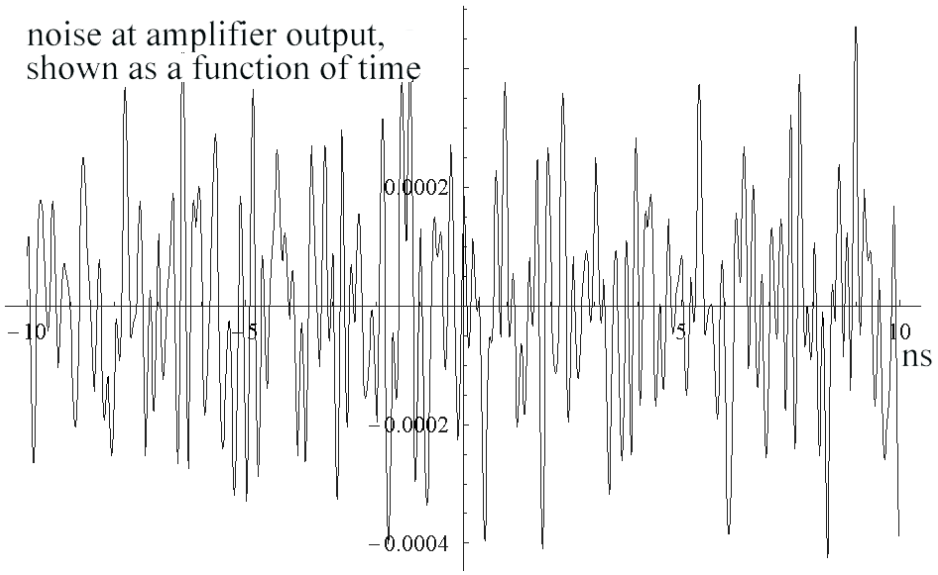

Figure 38. Effects of amplifier noise: the graph shows noise added to the amplifier's output signal as a function of time over the time period ±10 ns. The amplifier is assumed to generate an RMS noise voltage of 10^{-4} per $GHz^{1/2}$ in units where an ideal kick has unit amplitude. Noise is generated with constant amplitude and random phase in the frequency range 300 MHz to 6 GHz.

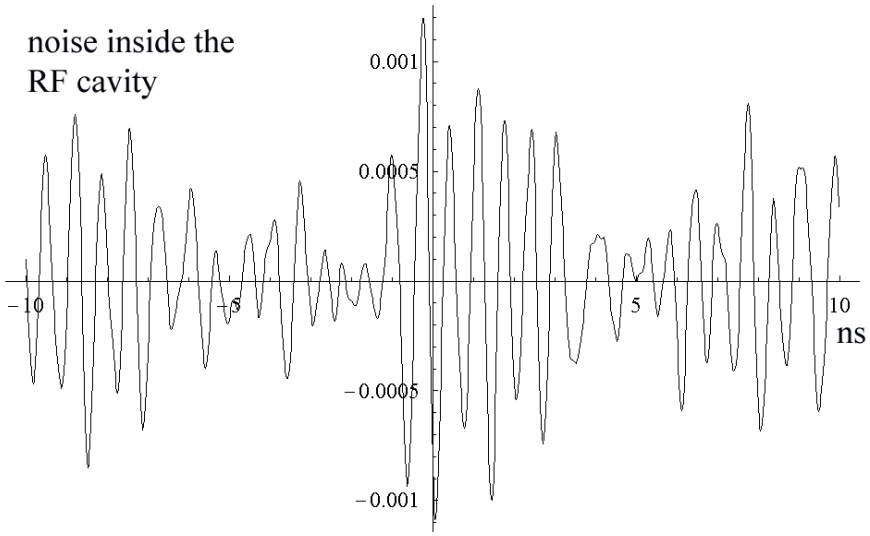

Figure 39. Effects of amplifier noise on kicking impulse: the graph shows the cavity's response to the amplifier noise plotted in the previous figure. Note the absence of the high frequency components evident in the previous figure. RMS noise voltage in the cavity is 0.00044, in units where the ideal impulse has unit amplitude.

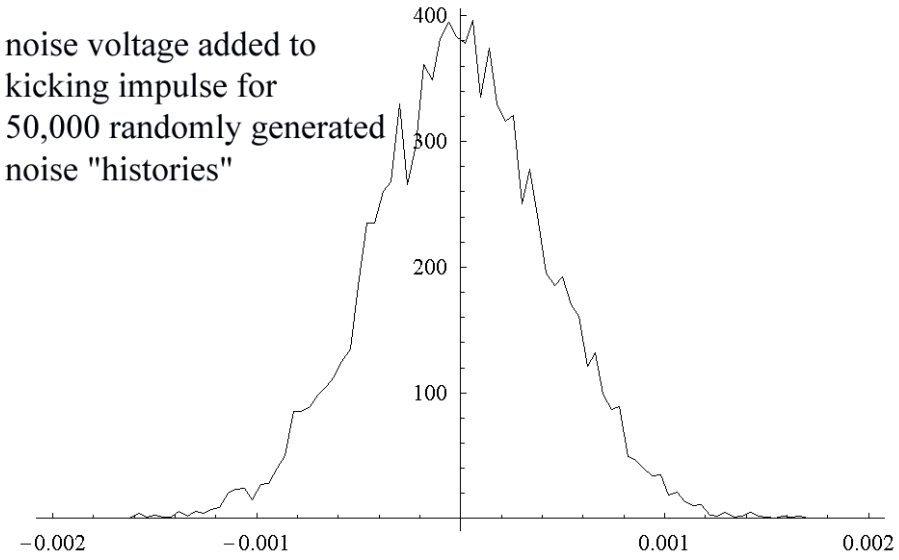

Figure 40. Noise voltages. RMS width of the distribution is 0.00044, in units where the ideal impulse has unit amplitude.

Arbitrary function generator noise

We do not yet model noise from the arbitrary function generator, instead including it in our naïve model for amplifier noise. It is reasonable to expect that the noise from a function generator will not be independent of frequency!

Nonlinear effects

Harmonic distortion

Our modeling of harmonic distortion is primitive, and should be further developed. At the present time we assume that harmonic distortion introduces an unwanted contribution to the amplifier output that is only a function of the amplifier's ideal (noise- and distortion-free) output signal as well as its output noise. We do not generate harmonic distortion associated with output frequency components introduced through other nonlinear effects such as intermodulation distortion. We do not model harmonic distortion arising from imperfections in the arbitrary function generator.

As was done with the simulation of amplifier noise, we model amplifier harmonic distortion as flat in frequency spectrum from 300 MHz to 6 GHz. Only the first harmonic is generated, using a fixed phase relationship between the parent signal voltage and distortion-induced harmonic. This is more clearly (and concisely) described in equations:

$$A_1 \cos\left(\omega_1 t + \varphi_1\right) \rightarrow \sum_{n=1}^{\infty} A_n \cos\left(n\omega_1 t + \varphi_1 + \delta\varphi_n\right)$$

$$\text{...where } A_n \equiv A_n\left(A_1, \omega_1\right) \text{ and } \delta\varphi_n \equiv \delta\varphi_n\left(A_1, \omega_1\right). \tag{11}$$

In our model,

$$A_n\left(A_1,\omega_1\right)=\begin{cases} aA_1 & n=2 \\ 0 & n>2 \end{cases} \qquad \text{and} \qquad \delta\varphi_n\left(A_1,\omega_1\right)=\begin{cases} b & n=2 \\ 0 & n>2 \end{cases} \tag{12}$$

where *a* and *b* are constants.

It would be natural to include more complicated dependences on amplitude and frequency; in the future we would like to refine these studies to incorporate more detailed properties of traveling wave tube amplifiers.

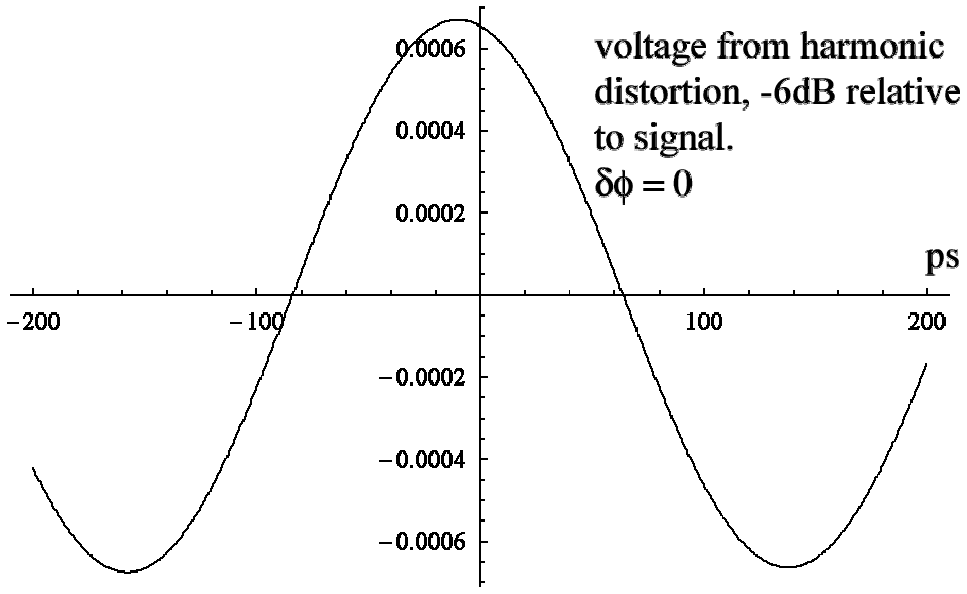

Figure 41. Voltages caused by (first) harmonic distortion. The coupling from fundamental into first harmonic is modeled to be independent of frequency as described in the text.

In our simple model, voltage arising from harmonic distortion scales linearly with *a* and shifts in time (without changing its shape) with *b*. Figure 41 illustrates the unwanted voltage added to an ideal signal in the case $a = 0.5$ and $b = 0$. In the figure contributions to the distortion signal from amplifier noise have been omitted: it seems likely that this is normally included in the quoted values of noise amplitude quoted by manufacturers of TWTA's.

The RF cavity response as a function of driving frequency was given in Equation 2. We see that the response to a driving signal at twice the center frequency ω_0 is

$$\frac{A_{cavity}}{A_{\omega_0}} = \frac{2\omega_0^2}{Q\sqrt{\left(\omega_0^2-\omega^2\right)^2+\left(\frac{2\omega_0\omega}{Q}\right)^2}} \xrightarrow[\omega=2\omega_0]{} \left.\frac{2}{Q\sqrt{9+\frac{16}{Q^2}}}\right|_{\omega=2\omega_0} \approx 0.027\,. \qquad (13)$$

Here A_{ω_0} is the cavity's response to a driving signal at its center frequency.

It is helpful that the cavity's response to signals far from its center frequency is small! Since the principal signal's full bandwidth is only ±10%, the distortion-induced harmonics are far from the signal band and are tolerable when $a < 0.5$, corresponding to -6dB.

Intermodulation distortion

Intermodulation (IM) distortion can introduce spurious signals at frequencies that are the sums and differences of frequencies present in the primary signal. As was true for harmonic distortion, the signal's ±10% full bandwidth and cavity's narrow frequency response will help suppress sensitivity to "second order" IM distortion. (Second order distortion signals primarily populate bands centered at 180 MHz and 3.69 GHz.) However, distortion-induced signals near 3.69 GHz can mix with signals in the primary band (centered at 1.845 GHz) to produce unwanted third order signals in the primary signal band.

Our modeling of IM distortion is unsophisticated at the present time. We assume that voltages created through second-order IM distortion arise from the sum of the amplifier's ideal signal, noise voltage, and harmonic distortion signal. We do not model IM distortion arising from imperfections in the arbitrary function generator. We calculate third-order harmonic distortion signals and then include them in the amplifier output presented to the simulation.

We model amplifier couplings between different frequencies to produce IM distortion as flat in frequency spectrum from 300 MHz to 6 GHz, generating distortion signals at both the sum and difference frequencies. We describe the second order IM signals this way:

$$\begin{aligned} A_1\cos\left(\omega_1 t+\varphi_1\right)+A_2\cos\left(\omega_2 t+\varphi_2\right) \rightarrow\; & A_1\cos\left(\omega_1 t+\varphi_1\right)+A_2\cos\left(\omega_2 t+\varphi_2\right)+ \\ & A_+\cos\left(\left[\omega_1+\omega_2\right]t+\varphi_+\right)+A_-\cos\left(\left[\omega_1-\omega_2\right]t+\varphi_-\right) \end{aligned} \qquad (14)$$

In our model,

$$A_+\left(A_1,\omega_1,A_2,\omega_2,\varphi_1-\varphi_2\right)=a_+A_1A_2 \quad \text{and} \quad \varphi_+\left(A_1,\omega_1,A_2,\omega_2,\varphi_1,\varphi_2\right)=\left(\frac{\varphi_1+\varphi_2}{2}\right)+b_+$$
$$A_-\left(A_1,\omega_1,A_2,\omega_2,\varphi_1-\varphi_2\right)=a_-A_1A_2 \quad \text{and} \quad \varphi_-\left(A_1,\omega_1,A_2,\omega_2,\varphi_1,\varphi_2\right)=\left(\frac{\varphi_1+\varphi_2}{2}\right)+b_- \tag{15}$$

where a_+, a_-, b_+, and b_- are constants. The same expressions are used to generate third-order IM distortion.

Work on modeling of intermodulation distortion is in progress.

Beam dynamics: effects associated with multiple passes through the kicker

Most bunches pass through the kicker several times after injection, or before extraction. There are a variety of effects that enter into a calculation of the kicker's influence on a bunch that orbits the damping ring several times during the injection/extraction cycle. In the extraction scheme under consideration, a bunch arrives at the kicker one "click" later each time it begins its next orbit of the damping ring until finally being ejected. As a result, it passes through the kicker during zeroes that are progressively closer to the kicking peak.

In a naïve description of the damping ring, the effects on a bunch associated with multiple zero crossings would be unimportant due to the field integral's zero first derivative. But imperfections in the kicker can introduce distortions to the impulse function that could cause coherent effects that will spoil beam emittance. Oscillations of the beam about a closed orbit, as well as the effects of synchrotron oscillations of particles inside the bunch relative to the bunch center, can be included in a beam dynamics simulation of the kicker.

Prototyping and tests

We have had discussions with Fermilab's RF group and Technical Division about studies of some of the technical challenges associated with the Fourier series kicker. After our simulations are finished we will collaborate with the lab on the engineering studies necessary to see if the concept is workable. We have submitted an expression of interest[8] to Fermilab to test devices in the A0 photoinjector beamline.

[8] G.D. Gollin, M.J. Haney, and J.B. Williams, An Expression of Interest Concerning Investigation of TESLA Damping Ring Kickers using the A0 Photoinjector Beam, May 24, 2004, http://www.hep.uiuc.edu/home/g-gollin/Linear_collider/Fermilab_kicker_A0_proposal.pdf .

UIUC Budget for LCRD 2.22

Item	FY04	FY05	FY06
Summer + academic year salary, 2 undergraduates (assume 750 hours/year/student, $6.15/hr)	$9,225	$9,225	$9,225
Indirect costs on undergraduate salaries (53.05%)	$4,894	$4,894	$4,894
Desktop computers for the students	$6,000	-	-
Periodic student travel to Fermilab during summers	$1500	$1500	$1500
Other travel (one trip to SLAC each year)	$1,200	$1,200	$1,200
Totals	$22,822	$16,822	$16,822

2.25: Investigation and prototyping of fast kicker options for the TESLA damping rings

(progress report)

Accelerator Physics

Contact person
Gerry Dugan
gfd1@cornell.edu
(607) 255-5744

Institution(s)
Cornell

Funds awarded (DOE)
FY04 award: 7,900
FY05 award: 135,000
FY06 award: 135,000

Investigation and prototyping of fast kicker options for the TESLA damping ring

April 11, 2005

Personnel and Institution(s) requesting funding

G. Dugan, D. Rubin, Laboratory of Elementary Particle Physics, Cornell University

Collaborators

D. Finley, C. Jensen, G. Krafczyk, V. Shiltsev, Fermilab

G. Gollin, T. Junk, University of Illinois at Urbana-Champaign

W. Decking, DESY

Project Leader

G. Dugan
gfd1@cornell.edu
(607)-255-5744

1 Project Overview

The large number of bunches (2820) and the relatively large inter-bunch spacing (337 ns) in the TESLA linear collider design give a bunch train which is more than 200 km long. A damping ring of this size would be very costly, and so the bunch train is damped in a compressed form, with a bunch spacing of 20 ns, leading to a damping ring with a circumference of 17 km.

In the TESLA baseline, the rise and fall time of the damping ring injection and extraction kickers determine the circumference of the ring. There is considerable leverage in developing faster kickers, as this translates directly into a smaller circumference ring. The baseline system for 500 GeV (cm) parameters has a 20 ns specification for the kicker pulse width; this becomes about 12 ns for the 800 GeV (cm) parameters. Designs and prototype results exist [1] for conventional kickers with widths of 7 ns, and design have been developed for more novel ultrafast schemes [2] using electron beams.

We propose to further explore the feasibility of the kicker designs described in the references cited above, particularly the very fast stripline kicker[1]. We will also develop new ideas for fast kickers. For example, we will explore the possibility of the use of the ponderomotive force from a high-intensity laser pulse to provide a very short kick to the beam. We will work closely with our collaborators from the University of Illinois and Fermilab in exploring their novel fast kicker concept.

In the TESLA baseline design, both the injection and extraction kickers must be fast. The injection kicker is considerably more difficult than the extraction kicker, because of

the larger beam size at injection. We will investigate the possibility of single-turn injection of beam into the damping rings, which would eliminate the need for a fast injection kicker.

It should be noted that, in addition to the small pulse width (of order ns) required for the kicker, extremely good pulse-to-pulse reproducibility is required in order to avoid beam jitter at the collision point. The fast intra-train feedback at TESLA cannot compensate for pulse–to-pulse jitter introduced by the extraction kicker. Part of the evaluation of the feasibility of any new kicker scheme must include an evaluation of the expected pulse-to-pulse jitter.

If a new fast kicker scheme is found to be technically feasible on paper, we propose to do an engineering design of a prototype, build the device, and test it using a high energy electron beam.

If the development of a fast kicker is successful and the ring size can be reduced, the average current will go up and at some point multibunch beam stability becomes the limiting factor to a further reduction in the ring size. This has been explored for two specific cases in prior work [3], for an earlier set of TESLA beam parameters. We propose to update and expand on these considerations, including our current understanding of critical stability issues such as the electron cloud, and to determine the minimum ring size permitted by beam dynamics considerations.

2 Progress Report

As noted above, the original proposal suggested that we would explore the physics issues associated with the use of damping rings of a much smaller circumference than the baseline TESLA TDR design, in order to determine the smallest feasible circumference for the damping ring. This circumference determines the required rise and fall time for the kickers, which is a key element of the specification.

However, a number of other groups are also engaged in these physics studies. Given the number of researchers already addressing these issues, we felt that it would be more efficient to choose a circumference which is the smallest that one could realistically consider, and to use this to determine the rise and fall time requirements of the kickers. If a kicker could be built to this specification, then it would easily serve for any larger circumference ring. This strategy decouples the physics studies of the ring from the kicker development, allowing both to proceed in parallel.

We have chosen a ring circumference of 3 km (similar to the PEP-II ring) as the smallest feasible circumference, and focused on the development of a kicker, with its associated pulser, appropriate for this ring. We assume the baseline ILC parameter of 2820 bunches. In a 3 km ring, these bunches, equally spaced, will have a 3.5 ns bunch spacing, so to allow the injection and extraction of individual bunches, the overall time-dependent kick seen by the beam must have a duration of less than 7 ns.

2.1 Specification for kicker and pulser

Bunch-by-bunch manipulation in a 3 km ring can be accomplished using a system of stripline kickers (for an example of an early design, see[1]), driven by synchronized very fast pulsers, capable of delivering pulses in the multi-kV regime. The rise time and fall times of the pulser can be about 0.5 ns, with a pulse width of about 4 ns. Individual bunches must be injected or extracted from the ring approximately once every 337 ns, forming a train of 2820 bunches, with an overall train duration of about 1 ms. The train is injected into a linac for subsequent acceleration. This process is repeated at a cycle rate of 5 Hz.

2.1.1 Kicker

As the basic module of the kicker, we consider a 0.36 m long stripline kicker, similar to that described in [1]. The kicker can be represented essentially as a vacuum parallel-plate transmission line, and can be designed to have an impedance in the range of 50-100 Ω. It will be terminated in its characteristic impedance, to suppress any reflections. Two synchronized pulses, of opposite polarity, injected onto the stripline plates at one end of this line, traveling opposite to the beam, will deliver a transverse kick to the beam. See Fig. 1 for a schematic illustration of the kicker. The cross section of a prototype design is shown in Fig. 2

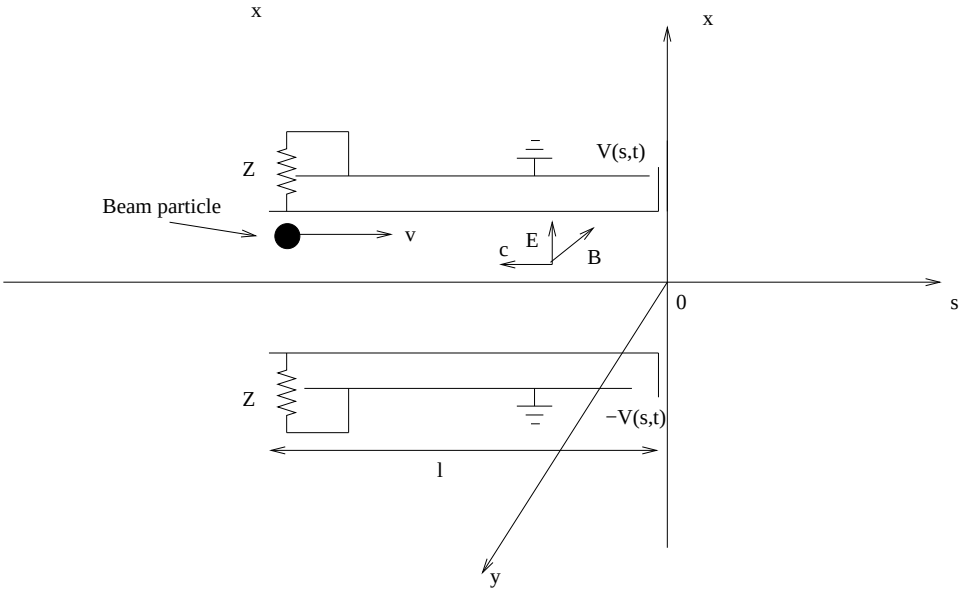

Figure 1: Stripline kicker

In Fig. 3, a possible pulse waveform is given, together with the resulting time variation

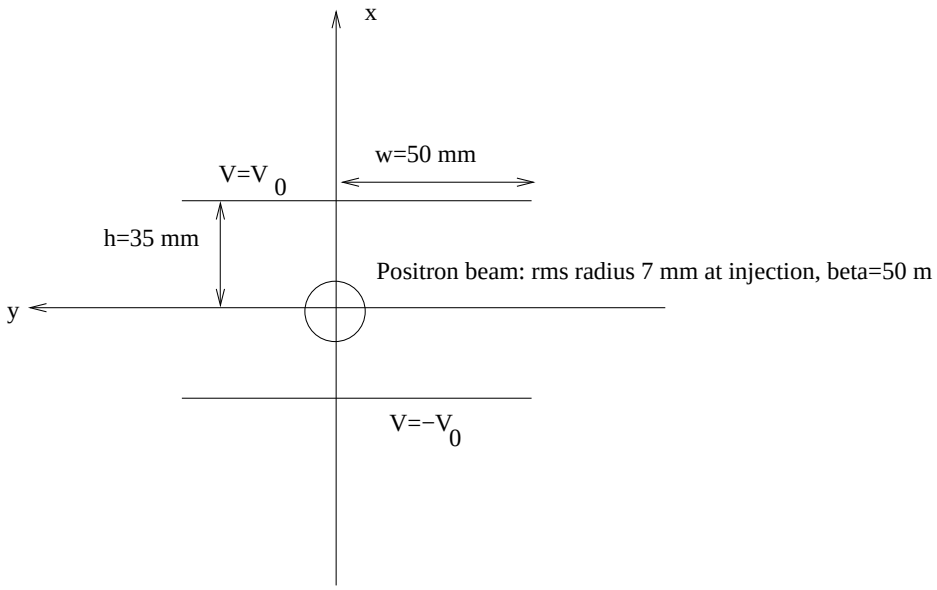

Figure 2: Stripline kicker cross section. The kicker is 360 mm long.

of the kick. The pulse rise time and fall time (10% to 90%) is 0.64 ns, and the pulse flat top (90% to 90%) is 2.96 ns. The time-dependent kick, $K(t)$, is related to the voltage pulse, $V(t)$, by

$$K(t) \propto \int_{t-t_k}^{t+t_k} V(t')dt',$$

in which t_k is the length of the stripline, which is 1.2 ns in this case. The time-dependent kick has rise and fall time (10% to 90%) of 1.97 ns, and the kick flat top (90% to 90%) is 1.63 ns. This time-dependent kick at ± 3.5 ns is 0.09% of the peak value, so it satisfies the requirement of being less than 7 ns in duration.

Note that other shapes are possible for the pulse, provided that the overall duration of the kick is less than 7 ns, and there is a flat-top for $K(t)$ of duration at least equal to the duration of the beam bunch (20 ps) plus any timing synchronization jitter between the pulsers. Generally, the overall pulse duration will need to be roughly at least $2t_k$ in order for the kicker to be fully efficient. This is because the pulse must be long enough to completely fill the kicker before the beam enters (t_k) plus it must remain there during the beam's passage (another t_k.)

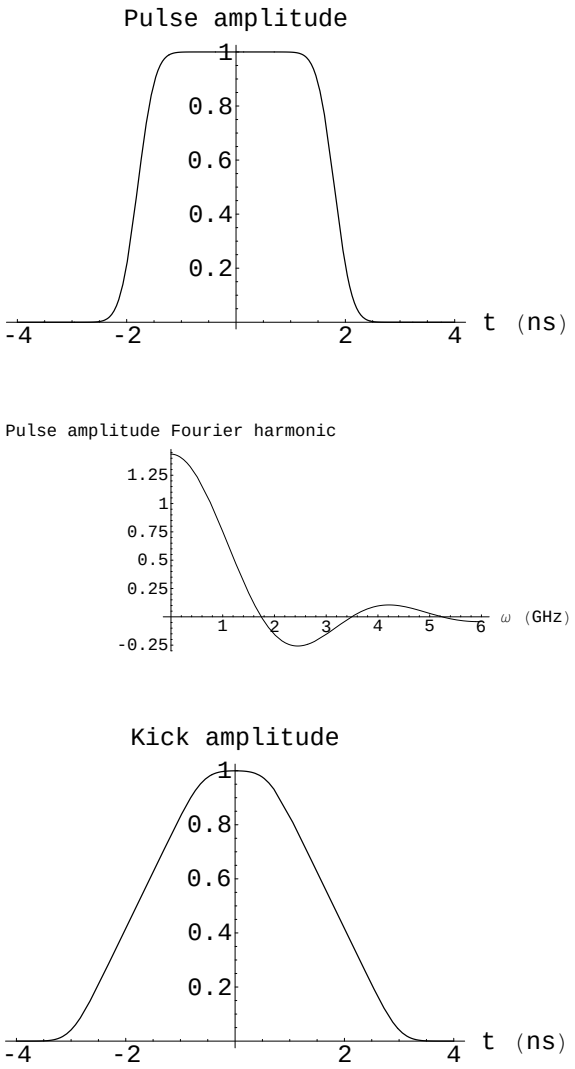

Figure 3: Top, symmetric pulse, $V(t)$. The pulse rise and fall time (10% to 90%) is 0.64 ns, and the pulse flat top (90% to 90%) is 2.96 ns. Center, Fourier spectrum of the voltage pulse $V(t)$. Bottom, resulting time-dependent kick, $K(t)$. The kick rise and fall time (10% to 90%) is 1.97 ns, and the kick flat top (90% to 90%) is 1.63 ns.

2.1.2 Time structure of a pulse train

The pulses described in the previous section must be delivered to the fast kicker with a pulse train structure illustrated in Fig. 4. The pulses are separated by 337 ns, and occur

in a train of 2820 successive pulses, with a total duration of 0.950 ms. The burst pulse rate during this train is 2.97 MHz. These trains are separated by a gap of 200 ms; i.e., the train rate is 5 Hz. The average pulse rate is $2820 \times 5 = 14,100$ Hz.

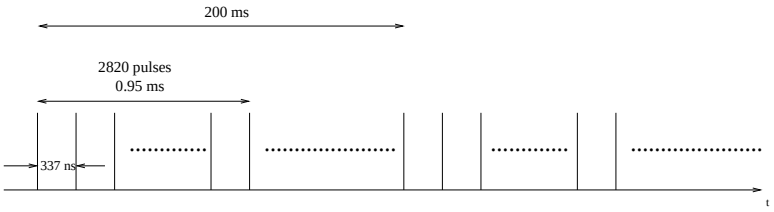

Figure 4: Pulse train structure. The pulses are separated by 337 ns, and occur in a train of 2820 successive pulses, with a total duration of 0.950 ms. The burst pulse rate during this train is 2.97 MHz. These trains are separated by a gap of 200 ms; i.e., the train rate is 5 Hz. The average pulse rate is $2820 \times 5 = 14,100$ Hz.

2.1.3 Pulse voltage, current, and synchronization requirements

The overall requirement for the system of fast kickers is to deliver a kick of 0.6 mrad to a 5 GeV electron beam. The kick angle is related to the kicker parameters by

$$\theta = \frac{2eV_0}{mc^2}\frac{l}{h}\frac{1}{\gamma}\tanh\frac{\pi w}{2h},$$

in which V_0 is the kicker voltage (per electrode), l is the kicker length, h is the kicker half-gap, w is the half-width of the electrodes, and $E = \gamma mc^2$ is beam energy. For the example considered here, $h = 35$ mm, $w = 50$ mm, and $E = 5$ GeV.

The length l of a single kicker module is constrained due to the requirement for a rapid rise time. Consequently, a number N_k of kickers will be required in series. The pulsers for these kickers must be synchronized, as is the case for the two pulsers which drive a single kicker, as discussed in Section 2.1.1.

In Table 1, two possible sets of pulser voltage, current, and power parameters are given, one corresponding to 3 kV pulses, and one to 10 kV pulses. In the former case, 50 kickers (100 pulsers) are required. In the latter case, 15 kickers (30 pulsers) are needed. The 10 kV pulser dissipates about 100 W in the terminating load. If higher voltages than 10 kV are available, such a pulser, which requires even fewer kickers than 15, would be preferable.

2.1.4 Pulse-to-pulse stability requirements

In a given pulse train, the relative pulse-to-pulse repeatability requirement on the total kick angle given to a beam bunch is 7×10^{-4}. If N_k kickers are used, and the pulsers driving

Table 1: Possible fast kicker parameters. The total kick angle required is taken to be 0.6 mrad. The kicker is assumed to have a 50 Ω impedance. The voltage V_0 refers to the peak amplitude of the voltage pulse $V(t)$.

V_0 [kV]	l [mm]	θ[mrad]	N_k	I [A]	P_{peak} [kW]	E_{pulse} [mJ]	f_{avg} [kHz]	P_{avg} [W]
3.0	360	0.012	50	60	90	0.648	14.1	9.2
10.0	360	0.040	15	200	2000	7.2	14.1	102

each kicker have random voltage fluctuations about an average over the train, with an rms value of σ_V, then we require

$$\sigma_V \leqslant \sqrt{N_k} \times 7 \times 10^{-4}.$$

For example, for the case of $N_k = 15$, we need $\sigma_V \leqslant 0.27\%$.

In addition, in order to not disturb the neighboring bunches, the amplitude of the kick $K(t)$ at the time of the neighboring bunches must be less than 0.3% of the peak kick amplitude.

2.2 Implementation of the fast pulser

To implement the fast pulser, we need a very fast rise and fall time device, capable of delivering voltage pulses in the kilovolt range, with an burst pulse repetition frequency of 3 MHz, capable of 1 ms bursts at 5 Hz, and extremely high pulse-to-pulse reproductibility. Meeting these demanding requirements is very challenging. Compared to gas-filled amplifiers, solid-state devices can potentially have very good reliability and reproducibility, but have difficulty meeting the high-power-pulse rise and fall time requirements.

We have begun to investigate a relatively new high-power ultra-fast-switch technology, based on a 4-element npnp structure called a fast ionization dynistor[4, 5, 6, 7, 8, 9, 10, 11, 12]. Ultra-fast high voltage pulse generators based on this technology are now commercially available[13, 14]. We have contacted a commercial firm, FID Technology, Ltd., which makes these pulse generators, and made them aware of the pulser requirements discussed in Section 2.1. They have responded with several sets of possible pulser specifications that they feel they can meet. These are presented in Table 2.

After much discussion, we focused on the pulser FPG2-3000-MC2, to procure as a prototype. It has specifications are close to what is required. The pulse is asymmetric, with the fall time being somewhat longer than the rise time. Nevertheless, the resulting time-dependent kick may be acceptable. A model of an asymmetric pulse having features similar to those of the FID pulser, and the resulting time-dependent kick, is shown in Fig. 5. The details of rise and fall times for this model are given in Table 3.

Pulses from a 4 kV pulser built by FID Technology, for another application, illustrating the achievable rapid rise and fall times, are shown in Fig. 6 and Fig. 7.

We have ordered the pulser FPG2-3000-MC2 from FID Technology, using a combination

Table 2: FID Technology Pulser Specifications[15]

Pulser	FPG2-3000-MC2	FPG1-3000	FPG3-3000	FPG10-3000
Output impedance[Ω]	50	100	100	100
Maximum output per channel [kV]	±1	1	3	10
Number of channels	2	1	1	1
Rise time 10-90% of amplitude [ns]	0.6-0.7	0.6-0.7	0.6-0.7	0.6-0.7
Pulse duration at 90% of maximum [ns]	2-2.5	2.5-3	2.5-3	2.5-3
Fall time 90-10% of amplitude [ns]	1-1.5	1-1.5	1-1.5	1.2-1.7
Maximum PRF in burst mode [MHz]	3	3	3	3
Maximum PRF in continuous mode [kHz]	15	15	15	15
Triggering - internal, external 5-10 v [ns]	20	20	100	100
Amplitude stability in burst mode [%]	0.3-0.5			
Pre- and after-pulses [%]	0.3-0.5			
Timing jitter, relative to trigger [ps]	20			

Table 3: Timing features of calculated symmetric and asymmetric pulses and kicks

Feature	Symmetric	Asymmetric
Pulse rise time (10% to 90%) [ns]	0.64	0.64
Pulse flat top (90% to 90%) [ns]	2.96	2.40
Pulse fall time (90% to 10%) [ns]	0.64	1.15
Kick rise time (10% to 90%) [ns]	1.97	1.91
Kick flat top (90% to 90%) [ns]	1.63	1.0
Kick fall time (90% to 10%) [ns]	1.97	2.1
Kick at 3.5 ns/Peak kick [%]	0.088	0.09

of funding from this proposal and from other sources. Delivery is estimated for June or July, 2005.

2.3 Future plans

Once the prototype pulser described above arrives, we will test it with a 50 Ω dummy load, and check that the performance specifications are met. In particular, we will measure the amplitude stability, and the pre- and after-pulse levels, as well as the detailed shape of the current pulse.

Subsequently, we are currently planning to test the pulser on a 100 Ω stripline kicker which has been built by Fermilab and the University of Illinois. This stripline kicker will be installed in the 16 MeV electron beam at the Fermilab A0 photoinjector facility. Measurements of the kick delivered by the pulser to the beam will allow the time-dependence

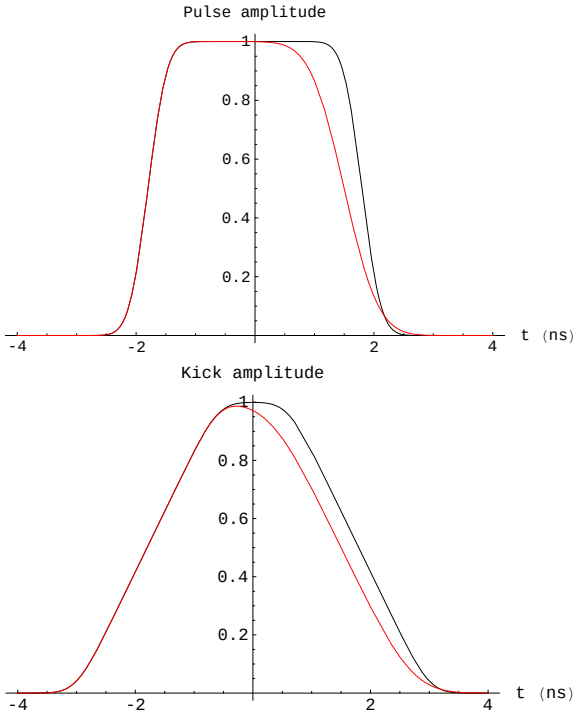

Figure 5: Top, symmetric pulse (black) and asymmetric pulse (red) $V(t)$. Bottom, resulting time-dependent kick, $K(t)$, in both cases. The timing features of the pulse and the kick are given in Table 3.

of the kick to be studied in detail.

Provided that the FID pulser performs according to requirements, we will continue development of the fast kicker system as planned in the original proposal. We will build a 50 Ω kicker, suitable for the ILC damping ring, along the lines of the design described above. We will procure a higher voltage FID pulser, probably in the ±5 kV range. We will test this kicker-pulser combination, which will be a true prototype for the ILC damping ring system, using the electron beam from the Cornell linac.

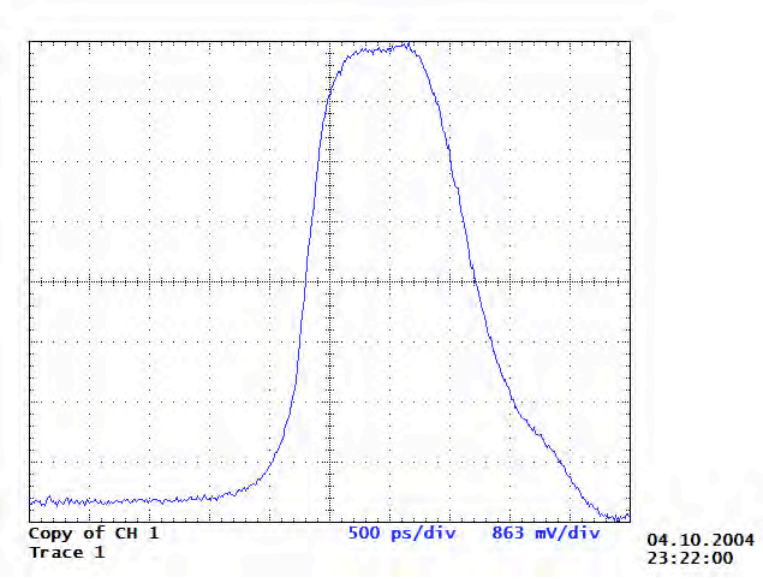

Figure 6: 4 kV fast pulse from FID Technology pulser[15] Rise time (10% to 90%): 0.4 ns. Flat top (90% to 90%): 0.9 ns. Fall time (90% to 10%): 1.1 ns

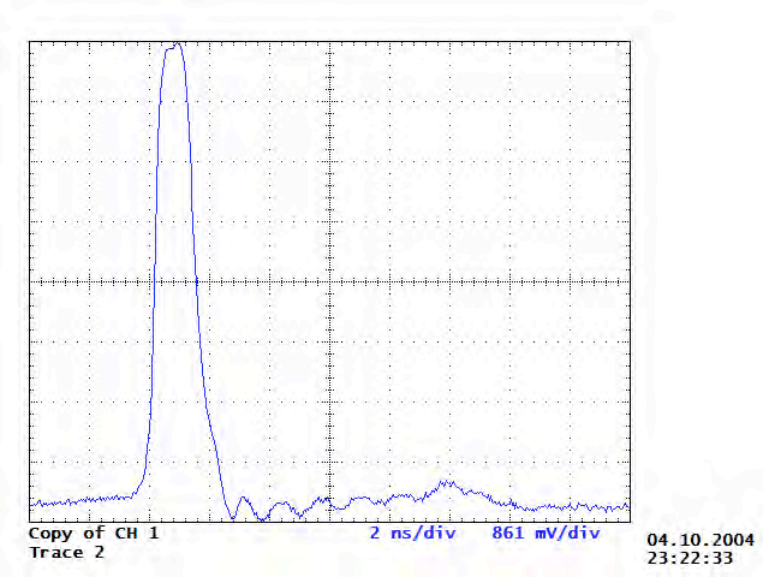

Figure 7: 4 kV fast pulse from FID Technology pulser. [15]

References

[1] B. I. Grishanov *et. al.*, "Very Fast Kicker for Accelerator Applications", TESLA 96-11 (Nov., 1996)

[2] V. Shiltsev, "Beam-beam Kicker for Superfast Bunch Handling", NIM A374, p. 137 (1996)

[3] V. Shiltsev, "TESLA Damping Ring Impedances: Preliminary Design Consideration", TESLA note 96-02 (1996)

[4] V. M. Efanaov *et. al.*, "New superfast power closing switched-dynistors on delayed ionization", in Proceedings of the 1996 International Power Modulator Conference, pp. 22-25,

[5] V. M. Efanaov *et. al.*, "Powerful Semiconductor 80 kV Nanosecond Pulser", in Proceedings of the 11^{th} International Pulsed Power Conference, pp. 985-987

[6] I. V. Grehkov *et. al.*, "Physical Basis for High-Power Semiconductor Nanosecond Opening Switcher", in IEEE Transactions on Plasma Science, Vol. 28, No. 5, pp. 1540-1544 (Oct, 2000)

[7] T. M. Podlesak, "Single Shot and Burst Repetitive Operation of Thryristors for Electric Launch Operations", in IEEE Transactions on Magnetics, Vol. 37, No. 1, pp. 385-388 (Jan, 2001)

[8] P. Rodin *et. al.* , "Tunneling-assisted impact ionization fronts in semiconductors ", Journal of Applied Physics, Vol. 92, No. 2, pp. 958-965 (July, 2002)

[9] P. Rodin *et. al.* , "Superfast fronts of impact ionization in initially unbiased layered semiconductor structures", Journal of Applied Physics, Vol. 92, No. 4, pp. 1971-1981 (Aug., 2002)

[10] I. V. Grehkov *et. al.*, "High Power Semiconductor-based Nano and Subnanosecond Pulse Generators with Low Delay Time ", in Proceedings of the 2004 Power Modulator Conference, ,O-SS Sw 4-7

[11] V. M. Efanaov *et. al.*, "FID Solid State Switches with Gigawatt Peak Power ", in Proceedings of the 2004 Power Modulator Conference, O-SS Sw 4-8

[12] 2nd European Pulsed Power Symposium (See booklet of abstracts, pp. 36, 42, 47)

[13] FID Technology

[14] MegaPulse, Pulse Systems group

[15] V. M. Efanaov, B. O'Meara, private communication

2.26: Continuing Research and Development of Linac and Final Doublet Girder Movers

(new proposal)

Accelerator Physics

Contact person
David Warner
Warner@lamar.colostate.edu
(970) 491-1035

Institution(s)
Colorado State
SLAC

New funds requested
FY05 request: 57,000
FY06 request: 66,400
FY07 request: 58,400

Continuing Research and Development of

Linac and Final Doublet Girder Movers

Classification:

Accelerator Science

Institution and Personnel requesting funding:

Colorado State University

David W. Warner, Engineer

Collaborators:

Stanford Linear Accelerator Center:
Gordon Bowden (staff scientist)

Project Leader:

David W. Warner
warner@lamar.colostate.edu
(970) 491-1035

Project Overview

This proposal is a continuation of the magnet mover R&D which was supported in the 2003 LCRD program. The project was not selected for funding in the 2004 round of LCRD grants, but we were given a no-cost extension to our existing grant and strongly encouraged to apply again in the next round. This extension has allowed us to continue research at a very low level.

We are requesting funds for a three-year R&D program, which will continue our investigations of the resolution attainable with mechanical movers similar to those produced at SLAC for the FFTB, and our efforts to reduce the costs associated with manufacturing them. We will also mount piezoelectric movers to the FFTB magnet mover to possibly reduce cost and/or improve the precision of the design while maintaining the required range of motion. After selecting the optimal design choice, we will produce production mover designs and a prototype device, with an emphasis on manufacturability and cost reduction. Vibration isolation and temperature control requirements are beyond the scope of this project—we are investigating the feasibility of manufacturing movers capable of meeting the motion precision required by the accelerator.

Two important decisions taken in the last year have had a major impact on magnet mover requirements. First, the selection of cryogenic RF technology for the linac has reduced the number of magnet movers required. Rather than the approximately 10,000 movers which would have been required for the full linac, we are now developing movers for only the warm magnets used in the beam delivery system of the accelerator, which will require approximately 1000 movers. The reduction in the number of movers has lowered the relative importance of cost while increasing the importance of performance. We are in the process of re-evaluating our initial plans in light of this change in requirements. Second, the requirement for 10nm step size for the final focus girder movers has been changed to 50nm, allowing us to use the same basic mover design throughout the beam delivery system.

Basic Mover Requirements

Every magnet and structure girder in the ILC beam delivery system will sit on movers to allow it to be positioned accurately. Depending on the requirements of the component in question, the movers will be required to position the beam components in either three degrees of freedom (two linear positions and one angle) or five degrees of freedom (two linear positions and three angles). Beam delivery system movers will typically be adjusted every few minutes, and must have a resolution or "step size" of approximately 50nm. It is not required that each step be precisely 50nm, simply that the average step size over a series of 10-20 steps achieve this limit. The movement will be relative, with the motion required by the mover and achieved in operation determined by beam position monitors. Since approximately 1,000 movers will be required, cost reduction, manufacturability and reliability are important for this component.

Gordon Bowden has developed and produced movers used in the FFTB which have been demonstrated to meet the requirements for final focus component movers except for resolution (they were measured to achieve a position resolution of approximately 300nm) and cost (a 5-degree of freedom mover would probably cost at least $5000 each to manufacture in their current design, at least in small quantities). These movers are mechanical, utilizing a kinematic support concept providing motion by rotation of bearings mounted on an eccentric shaft, which are in contact with wedge-shaped anvils supporting the linac component (See Fig. 1). Rotation of the shaft is accomplished by means of a 200 step per rotation stepper motor driven through a 100:1 harmonic drive. Mechanical movers such as these have several desirable features, including potentially lower cost (due to reduced requirements for feedback and control circuitry), reliability, and the ability to retain a set point without active compensation. Position monitoring can be accomplished by simply mounting a rotary encoder on the shaft.

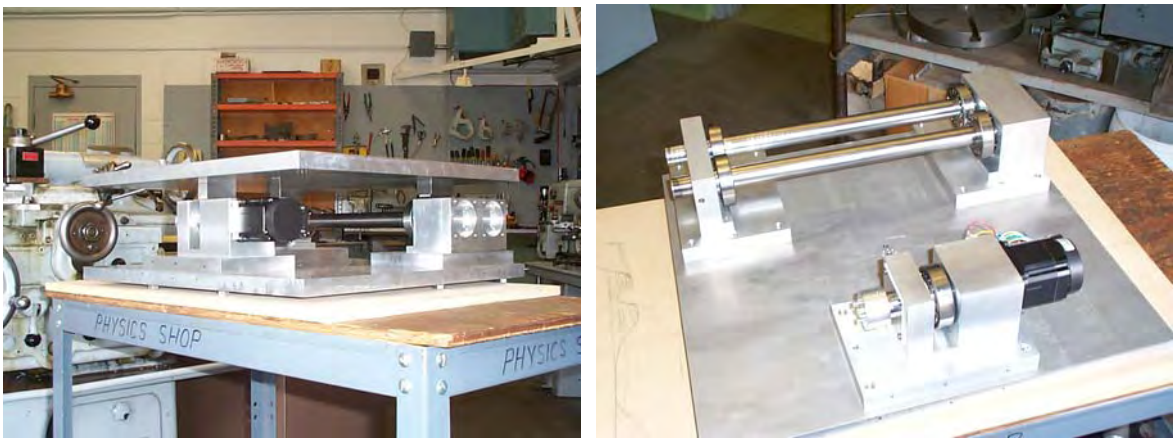

Figures 1A and B: Magnet mover prototype built at CSU from modified SLAC drawings

In order to meet the 50 nm step size requirement, the rotation of the eccentric shaft must be controlled in approximately 60 microradian intervals, or about 100,000 steps per rotation. This is challenging. One possibility for achieving the desired position resolution with the existing mover design is to increase the step resolution of the stepper motor to at least 2000 steps per rotation with a micro-step motor controller. This concept remains untried, and testing is required to determine if a purely mechanical mover of this type can provide 50 nm resolution.

The stepper motors and the harmonic drives are the cost drivers for this system. Any cost reduction effort for the mover must begin here. One way to accomplish this is to use stepper motors more efficiently, with less expensive mechanical reduction to replace the harmonic drives. It may even be possible to eliminate the mechanical gear reduction altogether, if it is possible to drive the stepper motor itself with sufficient precision and maintain sufficient stopped torque from the stepper motor. A second option is to use the mechanical mover to achieve rough positioning (with micron-scale precision) and achieve the 50nm precision motion using piezoelectric stacks. A final option is to use other mechanical options for driving the shafts with the required precision, such as DC actuators or combinations of stepper motors with worm gears, vertical wedges, piezoelectric inchworm movers or other systems.

Broader Impact and Student Involvement

This project will involve both graduate and undergraduate students in developing and testing the LabVIEW control software used to actuate the stepper motors and also the motion control software required to change the rotational motion of the shafts into physical motion of the magnet through two linear and three angular degrees of freedom. The precision movers developed for this project may be useful for other accelerator projects, as well as for optics and other high precision applications.

Results of Prior Research

In September 2003 the Technical Design facility at CSU received funds from the Linear Collider R&D program to develop linac magnet movers and final doublet girder movers. At that time, work began on procuring a prototype mover, refining our understanding of metrology techniques which will be used to qualify the mover, and exploring other shaft drive options that might prove more cost-effective. Our request for continued funding as part of the 2004 LCRD program was not supported, although a no-cost extension to our existing LCRD grant was approved allowing us to continue work on this project at a greatly reduced rate.

In the past year we have built a prototype mechanical mover system and are currently working on the stepper motor microstep control system and rotational encoder systems. We have made progress in identifying candidate metrology systems, but are awaiting the results of this funding request before reaching a decision on the extent of the system we will purchase.

Prototype mover system:

Unfortunately it was not possible to get an existing mover from SLAC, so we have replicated a modified version based on the original design and drawings for the SLAC three-axis mover. Our variant initially includes only three motors (as in the original FFTB mover), which will allow us to control two linear dimensions and one angle (X and Y and roll), but our model was designed to be expanded to 5 motors, allowing us to control all three angles (Pitch, yaw and roll) and two linear dimensions (X and Y, not along the beam axis). The prototype mover combines harmonic drive reducers and a micro-stepped stepper motor to drive the mount shafts, which should allow us to achieve the required step resolution.

Stepper Motor & Control System:

We have purchased and are studying the performance of a stepper motor system using Lin Engineering Model 5704M stepper motors, with a resolution of 0.45 degrees per step, or 800 steps/revolution. These motors are driven with Intelligent Motion Systems Inc. IM483 microstep drivers, which have a published resolution of 256 microsteps per full step. The combination of the motor and driver gives us a theoretical resolution of 204,800 microsteps per revolution. Using this motor/driver combination, it may be possible to eliminate the mechanical harmonic drive mechanical step reduction. If we can achieve sufficient precision and torque to drive the system, this would be a great simplification to mechanical assembly and cost.

The rotational position of the drive shafts is measured using a Micro-E Chip Encoder, with a resolution of 163,840 counts/revolution, allowing angular measurement with the required precision.

In preliminary bench-top testing we achieved very nearly the theoretically predicted precision through a small (few hundred) number of microsteps, but the rotation became less accurate as larger numbers of steps were moved. After further investigation it was determined that driver cards were a major source of our difficulties, due to electronic noise generated as the micro step driver crossed a full step boundary for the stepper motor. We are replacing them with a new model recommended by Lin Engineering, and expect better performance from our new system.

In addition to replacing the drivers as mentioned above we plan to acquire a Trinamic TMCM-302 3-axis controller. This controller will act as the interface between the drivers, encoders and a PC running Labview software.

Metrology:

We are investigating a metrology system based on capacitive position measuring, using a system from Lion Precision that will allow measurements with a precision of approximately 10 nm over a range of 50 microns. Additionally, each of the five drive shafts (after harmonic drive reduction) will be read out using rotary encoders with 3mr resolution. Together, this will allow us to measure the entire range of motion of the mover. We are also investigating linear encoder measuring systems such as those available from RSF electronics, which can achieve a resolution of approximately 100 nm.

We have a quote on a one sensor system that we will buy for our initial measurements, and plan to expand to a full 5 sensor system after we have proven the system works.

This metrology is for use in testing our prototype movers, and would not be part of a production design.

Facilities, Equipment and Other Resources

Our proposal is greatly enhanced by the mover prototype already funded by earlier LCRD funds. Our group also has significant experience with PC-based control systems and experienced LabVIEW programmers. We also have sufficient laboratory space with power, internet access etc. and low cost access to a machine shop with precision lathes, milling machines, etc., provided by the university.

This project is an excellent fit to the capabilities of the technical design facility at Colorado State University. The facility has been involved in manufacturing many components for HEP applications that require cost optimization due to the large number of items to be procured, as well as a great deal of prototype development and fixturing work. Through Prof. Wilson, the CSU HEP group has a long history of participation in the Linear Collider Detector development. The group is fully supportive of the technical design facility proposals to contribute to Linear Collider Accelerator development. Additionally, there is a precision measurements group in the department working on laser atom lithography projects lead by Prof. Siu Au Lee, which can provide advice and assistance as required.

Proposed Project

The work already funded by the LCRD program in our first proposal will be completed by the end of the summer of 2005. Our new proposal expands on the work already funded, taking advantage of the FFTB mover and metrology equipment we will build, and the experience we will have gained to move towards final mover designs.

Year one of this new proposal continues the initial project, investigating rotary motion drivers and motion encoders in an attempt to find a cost-effective version of the FFTB mover with sufficient resolution. We now have an operational mechanical prototype, and shortly will have the micro-stepped stepper motors in place and tested. We also hope to have the metrology equipment in place to allow us to measure its motion by early summer 2005. By October 2005, we will have determined if we can meet the step resolution required with a mechanical three-motor microstepped mover, what type of rotation reduction system will be required, and a preliminary indication of the cost per mover and the difficulties in producing this type of mover

A LabVIEW-based control system and motion control software will be developed with student assistance to allow us to move the magnet platform through a specified range of motion.

Additionally, we plan to purchase a full 5-axis capacitive position measuring system (actually an expansion of the system we are ordering for 1-axis measurements under our current grant) in order to be able to fully monitor the 5-axis movement of the stage simultaneously.

Deliverables:

-Measurements of the resolution achievable using the micro-step driven FFTB mover, both for three-motor and five-motor configurations.
-Development of a metrology system capable of measuring the 5-axis motion of the mover with better than 50 nm precision.
-Results from feasibility of alternate shaft driver options.
-Software and hardware for mover control system
-Designs for magnet mounts for a five-motor system

Year two goals are to evaluate the incorporation of piezoelectric movers and active feedback into a reduced-precision mechanical mover, with feedback based on the capacitive metrology system we are investigating for measuring the system performance or strain gauges.

Our experience during the first year of the project will give us a solid understanding of the limitations of the mechanical mover, and based on this platform we will develop a piezoelectric stack to attach to the mover, and begin to investigate the resolution, vibration isolation, and stability achievable with such a system.

Additionally, we will investigate the possibility of using other mechanical movement devices or alternate motor options, such as DC actuators or piezoelectric inchworm devices to try to reduce costs by eliminating the harmonic drive.

Deliverables:

-A design for a feedback system to stabilize a piezoelectric stack add-on to a mechanical mover capable of achieving 50 nm precision.
-A prototype mover system including these additions, and measurements of the resolution and stability achievable by such a system.

Year three of the project will move towards manufacturability of the beam delivery system mover at a low price, involving redesign of the components in collaboration with manufacturing firms to reduce price and to determine the most cost effective option for the driver system. Year three will also include development of any special mounts required for the final focus girder cryostat.

Deliverables:

-An optimized-for-manufacturability design report for the beam line movers, including an optimized shaft driving system, measurements of system performance, and projected costs
-A design for a final focus element mover.

Budget Justification

There is no HEP base program grant support for Warner. All costs, including travel, associated with this proposal must be provided by the project. Warner's salary is charged through the CSU Technical Design Facility at a flat rate of $50/hour. Fringe benefits charges are included in this hourly rate. Technician support and machine shop labor are also charged at flat hourly rates of $30/hour and $33/hour respectively, with fringe included in these rates as well.

In Year 1 (FY 05) our labor costs include: 2.5 months support for Warner; technical support funds in the form of machine shop and technician time for additional prototype development work; and summer salary support for a one graduate student to assist with control software development and system testing. We are requesting equipment and M&S funding for the metrology system, computer control hardware, and continued stepper motor development costs. We are requesting travel funds to support 3 trips, typically to SLAC and/or FNAL, to consult with LINAC development experts and report results.

In Year 2 (FY 06) our labor costs include: 3 months support for Warner; technician support; and summer salary for one grad student to assist with measurements and metrology software improvements. We are requesting equipment support for the piezo-electric mover; this equipment cost includes labor (including undergraduate student

labor), materials and supplies, but will be capitalized as a single piece of equipment at CSU. We are requesting travel funds to support 3 trips, typically to SLAC and/or FNAL.

In Year 3 (FY 07) our labor costs include: 3 months support for Warner; and technician support for testing the mechanical prototype. We are requesting equipment funds to build an industrial prototype mover in conjunction with a local manufacturing firm; as Year 2, this equipment cost includes development and M&S expenses (including undergraduate student labor) which will be capitalized as a single piece of equipment. We are requesting travel funds to support 3 trips, typically to SLAC and/or FNAL.

Three-Year Budget, in then-year K$

Item	FY2005	FY2006	FY2007	Total
Other Professionals	26.8	33.0	28.5	88.3
Graduate Students	4.5	4.5	0.0	9.0
Undergraduate Students	0.0	0.0	0.0	0.0
Total salaries & Wages	31.3	37.5	28.5	97.3
Fringe Benefits	0.2	0.2	0.0	0.3
Total Salaries, Wages and Fringe Benefits	31.5	37.7	28.5	97.6
Equipment	14.0	12.0	16.0	42.0
Travel	1.5	1.5	1.5	4.5
Materials and Supplies	0.0	2.5	2.5	5.0
Other Direct Costs	0.0	0.0	0.0	0.0
Total Direct Costs	47.0	53.7	48.5	149.1
Indirect Costs	10.1	12.7	9.9	32.7
Total Direct and Indirect Costs	57.0	66.4	58.4	181.8

2.27: Effects of CSR in Linear Collider Systems: A Progress Report

(progress report)

Accelerator Physics

Contact person
James Ellison
ellison@math.unm.edu
(505) 277-4613

Institution(s)
New Mexico

Funds awarded (DOE)
FY04 award: 36,758
FY05 award: 36,758
FY06 award: 36,758

Effects of CSR in Linear Collider Systems: A Progress Report

Classification (subsystem)

Accelerator

Personnel and Institution(s) requesting funding

James A. Ellison, Professor of Mathematics, U. of New Mexico

Gabriele Bassi, PostDoc, Mathematics Department, U. of New Mexico

Klaus Heinemann, Research Assistant, Mathematics Department, U. of New Mexico

Collaborators

Robert Warnock, SLAC

Collaborating personnel will work on CSR but are not requesting funding here.

Project Leader

James A. Ellison
ellison@math.unm.edu
505-277-4110

Guide for Reviewer

This is a progress report on a DOE/LCRD proposal which was funded in May 2004 for 3 years at \$36.8K/year. The award is in the form of a supplement to the project leaders DOE grant, DE-FG03-99ER41104 for "Investigations of Beam Dynamics Issues at Current and Future Accelerators" which is on the cycle April 1 - March 31. The supplementary award for 4/1/04-3/31/05 arrived at UNM in late August 2004.

In this report we have followed the Dugan format as much as possible. To make the progress report self-contained we have inserted the original four page proposal into the Project Overview Section (adding only several references that should have been there). Since this is a DOE progress report we have not included a "Broader Impact" section. The "Results of Prior Research" contains our progress report. The three year plan was contained in the initial proposal, however we make some additional remarks about activities for the second and third years in a section entitled: Project Activities and Deliverables for Years Two and Three. A reference section follows which contains the references from the original proposal as well as some new references related to the progress report.

Project Overview

I. Motivation

There are two points at which coherent synchrotron radiation (CSR) could be of concern in linear colliders. First, it may cause transverse x-emittance degradation in bunch compressors, since energy changes due to CSR get mapped into transverse coordinates through dispersion. Second, it might cause longitudinal bunch instabilities in the damping rings at high current, possibly leading to a quasi-periodic, sawtooth behavior of the bunch length. Damping ring designs contain many meters of wigglers (for instance 46 m at NLC and 432 at TESLA), to

reduce the damping time to a manageable value. The coupling impedance from CSR in the wigglers, combined with that from bending magnets, could induce the feared instability. For a review of microbunch instabilities due to CSR see [1].

II. Bunch Compressors and Computation of CSR from Arbitrary Orbits

Preliminary estimates of emittance growth in bunch compressors have been made by Emma and Woodley [2]. They have done calculations for the Stage 1 and Stage 2 compressors (BC1 and BC2) of the NLC and for the Tesla bunch compressor (TBC) [3]. For BC1, BC2, and TBC their figures for emittance growth $\Delta\epsilon_x/\epsilon_x$ due to CSR were 2.4%, 5.5%, and 1%, respectively. Although these values are regarded as reasonably small compared to other sources of emittance growth, they are based on a simplified model of the CSR field, and cannot be considered a definitive conclusion. The field calculation, as implemented in M. Borland's code ELEGANT [4], treats the source of the radiation as a line charge. In a macroparticle simulation the transverse charge distribution is projected onto a longitudinal line to produce an effective radiation source. Moreover, the formula for the field is for a source moving on a trajectory which is straight except for a single bend. Consequently there is no proper integration of single bends to make a true chicane orbit. Actually, there should be a residual field after a bend which does not decay completely before the next bend is reached.

There exist large codes to compute CSR from an arbitrary charge/current distribution on fairly general orbits (by Dohlus [5] at DESY and Rui Li at JLAB [6]), but these have proved to be cumbersome for actual design work and are not much used for that purpose. We have devoted considerable effort to finding a better calculational method, intended to be useful both for bunch compressors and rings, and perhaps also for wigglers.

III. Ongoing and Proposed Work on Bunch Compressors and Computation of CSR from Arbitrary Orbits

IIIA.
One approach that we have explored in recent months is to make a Fourier analysis of fields and sources in all spatial dimensions, with account of the large-wavelength shielding of CSR by the vacuum chamber (in a perfectly conducting parallel plate model). This avoids the tricky integrations over singularities of the Green function that make the usual approach in space-time quite difficult. The price to pay is in dealing with fast oscillations of the integrand in the inverse Fourier transform to compute the field. We hoped that this problem could be handled by the method of stationary phase, but it turns out that this method is only partially effective. Since it still might be used in combination with other procedures, we are currently writing a careful report on our experience.

IIIB.
We have recently made what appears to be great progress by using a Fourier series only in the vertical coordinate y, perpendicular to the plane of the orbit. This makes it trivial to satisfy the field boundary conditions on the parallel plates that model the vacuum chamber. The resulting 2D wave equation has a "mass" term, the mass being the vertical wave number, and a remarkably simple Green function with a softer singularity than the usual Green function for the 3D wave equation. We think that this should provide an efficient and simple numerical method, and propose the implementation of such a method as a main item of research. We will first study a chicane bunch compressor with the charge/current source coming from a bunch with energy chirp, evolving only in response to the fields of the dipoles. Horizontal transverse spread of the charge distribution is fully accounted for, whereas the vertical distribution is arbitrary but constant in time. Later we hope to make the calculation self-consistent, allowing

the phase space distribution to be affected by CSR. This could be done in a macroparticle simulation, or preferably in a less noisy Vlasov treatment if that could be done in reasonable computation time.

IV. Damping Ring Instabilities

A representation of the impedance for CSR in wigglers has been proposed by Wu, Raubenheimer, and Stupakov (WRS)[7]. Wu, Stupakov, Raubenheimer and Huang (WSRH) [8] have combined this impedance with the usual impedance for CSR in dipoles to discuss the longitudinal instability threshold in damping ring designs for NLC and TESLA, and for the existing prototype damping ring at the KEK ATF. The instability study is done with coasting beam theory for a line-charge beam, and without shielding of CSR. The conclusion is that the instability is indeed worrisome. The threshold is close to the nominal current for NLC and ATF. On the other hand, the dipole and wiggler impedances scale differently with frequency, and that leads to a possibility of optimizing the damping ring design to raise the threshold, perhaps by a factor of 4.

V. Proposed Work on Damping Ring Instabilities

Although the work of WSRH is a valuable first survey of the problem, it involves some serious assumptions that one would like to avoid. We propose to pursue the following improvements:

1. Avoid coasting beam theory by applying our program for numerical integration of the nonlinear Vlasov-Fokker-Planck (VFP) equation [9, 10]. We would begin with the Haïssinski equilibrium distribution, and see whether it becomes unstable under time evolution by the VFP integrator. As the authors WSRH point out, the coasting beam theory is doubtful in this instance, because the Boussard criterion does not apply: the bunch length is not much larger than the unstable wave lengths.
2. Study possible saturation of any instability, again using the VFP code. That code has proved to be very useful for long term simulations, giving plausible results over several damping times.
3. Include shielding of CSR, which will be necessary in studying dynamics of unstable cases, and may have some effect on thresholds as well. We are not yet sure how to describe shielding for the wiggler radiation, and there is the complication that the vacuum chamber has different sizes in bends and wigglers. Some innovative approximations will certainly be necessary.
4. Criticize the mathematics and physics of the model of the wiggler impedance in WRS. This is for an infinite wiggler, and takes as its starting point results of Saldin *et al.* [11]. As far as we know the complicated Saldin analysis has not been verified by other authors, and in any case there are some puzzling singularities in the result that we would like to understand. After becoming familiar with the problem, perhaps we can treat the case of a wiggler of finite length, which of course would be more relevant for the prediction of thresholds.
5. Try to include non-zero transverse extent of the bunch. This would relate to work on the 2D Green function mentioned above.

VI. Budget and Personnel

Warnock is a retired SLAC physicist with several years experience in CSR, see, for example,[10]. The proposal is based on his recent work, our joint progress over the last few months, and

discussions with other experts at SLAC. Ellison has some modest experience with radiation by moving charges from his work on channeling radiation at CERN and Aarhus in the late eighties and is now deeply involved in the basic issues of CSR from particle bunches on more or less arbitrary orbits. Bassi has been hired as a PostDoc, as of mid June 2003, after completing a Ph.D. at DESY and the University of Bologna. He is making a substantial contribution to our CSR work.

Warnock is not asking for financial support; he finds it sufficient to get theoretical and numerical collaboration from Ellison and Bassi. Ellison is not asking for financial support either as CSR is one item in the research of his current DOE grant - DE-FG03-99ER41104 for "Investigations of Beam Dynamics Issues at Current and Future Accelerators". In addition, Ellison has funds in his DOE grant to partially support the CSR work of Bassi. We are requesting \$36.8K/year for the 3 year period June 1, 2004 to May 31, 2007 to fill out the support of Bassi's CSR work and to partially support a graduate research assistant. The \$36.8K includes salary, fringe benefits, tuition, health insurance and the 50% indirect cost rate. Our current LCRD/DOE funding arrived too late to support a graduate student in the fall, however we have just hired a student who will begin work in January.

The proposal outlines an ambitious program that we find quite challenging.

Results of Prior Research: Progress Report on DOE/LCRD Award

A. Bunch Compressor and Computation of CSR from Arbitrary Planar Orbits

Considerable progress has been made on the computation of CSR from arbitrary planar orbits as proposed in IIIA above.

A detailed report [12] on the approach based on the full Fourier method has been written as promised in IIIA. Our conclusion is that the method of stationary phase, applied to reduce the number of integrations and the field calculation time, is not a good approximation in a large enough region of Fourier space and thus the computation time is too long for practical use. Although a negative result, we gained a great deal of understanding and it was helpful in the implementation of the method based on the 2D wave equation of IIIB. Nevertheless, the method of stationary phase may be useful in combination with other procedures and might be effective in a third variant of the Fourier method (1D wave equation after a Fourier transform in x).

In IIIB we proposed work on a new approach based on a 2D wave equation. To date, we have focused primarily on the important task of the field calculation and we have reported on our results in [13]. The fields exited by the bunch are computed in the laboratory frame from a new formula that leads to much simpler computations than the usual retarded or Lienard-Wiechert potentials. This computation is much faster than the full Fourier method above. Work has begun on the fully self-consistent calculation in which the Vlasov equation will be integrated in the beam frame interaction picture as discussed in [13]. Important to this is the transformation from lab to beam frame. This is somewhat complicated and we have a draft of a paper on this [14]. Our progress on the fully self-consistent calculation will be presented at PAC 2005.

In addition, we have studied low order moments using particle simulation in a first order perturbation theory, i.e., the field is calculated from the distribution evolving in response to the fields of the dipole magnets only. We have compared our results for the mean energy loss with results of Emma and Kabel (see figures in [13]). Our semi self-consistent results are in

reasonable agreement with [15] which gives us confidence in our field calculation. The next step will be to compare our fully self-consistent calculation with the Zeuthen benchmark.

B. Damping Ring Instabilities

The work on damping ring instabilities as proposed in IV and V above is in its initial stages. As mentioned, the award didn't arrive at UNM until late August 2004 and so we weren't able to hire an RA for the fall. However, we have now hired a research assistant, Klaus Heinemann, and he is focusing his attention on the wiggler problem and the Saldin approximations. He has a good background in beam dynamics and some experience with renormalization, which should be helpful in understanding and improving upon the Saldin approximations. Prior to the current LCRD award we had a $20K award. A significant part of this was used to support an RA for the spring semester of 2004. His task was to work through the Saldin papers however it took considerable time to get the proper background which didn't leave much time for understanding Saldin. However he did come to some useful insights on which Heinemann is building.

Facilities, Equipment and Other Resources

Our only needs are office space and computing facilities. We have good work stations from DOE money and UNM has a high performance computing laboratory which we can access. At some point we might like access to NERSC.

Project Activities and Deliverables for Years Two and Three

A. Bunch Compressor and Computation of CSR from Arbitrary Planar Orbits

We will continue our work on CSR from arbitrary planar orbits. As mentioned above considerable progress has been made in the context of the Bunch Compressor. Now, our main focus is on the implementation and testing of the fully self-consistent algorithm outlined in [13]. The algorithm is based on a standard technique of numerical analysis, namely spline approximation [16], to represent charge and current densities and the phase space distribution function. Splines are extremely convenient and have well understood convergence properties. As far as we know, other investigators have not used general methods of numerical analysis, instead preferring special techniques such as a representation of the bunch as a superposition of small Gaussian macro-particles [5]. We will focus on the construction of a good serial code, afterwhich we will look for ways to take advantage of parallel platforms. The code will be applied first to study CSR effects in a bunch compressor and carefully compared with the Zeuthen benchmark case. We will then take steps to study the nonlinear chirp and non-Gaussian case both in a semi and self-consistent approach. Next we will apply the code in the context of the ILC.

B. Damping Ring Instabilities

Because the money for the first year arrived late, the work on wigglers and undulators is just beginning. Here we will do as discussed in part V of the proposal. As mentioned above, Heinemann has been hired and his initial charge is to study the Saldin and Stupakov papers, to give more insight into the line charge models mentioned above. In addition once the code of A is developed, we will consider modifications needed to apply it to the wiggler/undulator problem as mentioned in part V5 of the proposal.

The bunch compressor work was partially supported by Ellison's DOE grant DE-FG03-99ER41104 for "Investigations of Beam Dynamics Issues at Current and Future Accelerators", which was awarded at $145K per year for the period April 1, 2002 to March 31, 2005.

The grant topics are Vlasov dynamics, nonlinear collective effects, collective and weak-strong beam-beam and spin dynamics in addition to CSR.

References

[1] G. Stupakov, R. Warnock, Microbunch Instability Theory and Simulations, to be published in ICFA-newsletter.

[2] P. Emma and M. Woodley, Coherent Synchrotron Radiation Emittance Growth in the NLC and TESLA Bunch Compressors, SLAC, May 3, 2002, unpublished report available from the authors.

[3] P. Emma, Cost and Performance Optimization of the NLC Bunch Compressor Systems, SLAC report LCC-0021, August, 1999.

[4] M. Borland, Simple Method for Particle Tracking with Coherent Synchrotron Radiation PRST-AB, **4**, 070701 (2001).

[5] A. Kabel, M. Dohlus, and T. Limberg, Numerical Calculation of Coherent Synchrotron Radiation Using TraFiC4, Nuc. Instrum. Methods Phys. Res., Sect.A **455**,185 (2000); M. Dohlus, A. Kabel, and T. Limberg, Efficient Field Calculation of 3D Bunches on General Trajectories, *ibid.* **445**, 338 (2000).

[6] R. Li, Self-Consistent Simulation of the CSR Effect on Beam Emittance, Nuc. Instrum. Methods Phys. Res., Sect. A **429**, 310 (1999).

[7] J. Wu, T. O. Raubenheimer, and G. V. Stupakov, Calculation of the Coherent Synchrotron Radiation Impedance from a Wiggler, PRST-AB, **6**, 040701 (2003).

[8] J. Wu, G. V. Stupakov, T. O. Raubenheimer, and Z. Huang, Impact of the Wiggler Coherent Synchrotron Radiation Impedance on the Beam Instability and Damping Ring Optimization, PRST-AB, **6** 104404 (2003).

[9] R. Warnock and J. Ellison, A General Method for Propagation of the Phase Space Distribution, with Application to the Saw-Tooth Instability, in *Proc. 2nd ICFA Advanced Workshop on Physics of High Brightness Beams*, UCLA, November 9-12, 1999 (World Scientific, Singapore, 2000) and SLAC-PUB-8404 (2000).

[10] M. Venturini and R. Warnock, Burst of Coherent Synchrotron Radiation in Electron Storage Rings: a Dynamical Model, Phys. Rev. Lett. **89** 224802 (2002).

[11] E. L. Saldin, E. A. Schneidmiller, and M. V. Yurkov, Radiative Interaction of Electrons in a Bunch Moving in an Undulator, Nucl. Instr. Meth. Phys. Res. A **417**, 158 (1998).

[12] G. Bassi, Note on the Full Fourier Method for the Field Calculation of Coherent Synchrotron Radiation from Arbitrary Planar Orbits. See LCRD papers at `http://www.math.unm.edu/~ellison`.

[13] R. Warnock, G. Bassi and J.A. Ellison, Vlasov Treatment of Coherent Synchrotron Radiation from Arbitrary Planar Orbits, Proc. ICAPC2004, St. Petersburg, Russia (to be published in Nucl. Instr. Meth. Sci. Res.), available as SLAC preprint SLAC-PUB-10760 (2004) and under LCRD papers at `http://www.math.unm.edu/~ellison`.

[14] G. Bassi, J.A. Ellison and R. Warnock, On the Relation of Lab and Beam Frame Densities, to be submitted. See LCRD papers at http://www.math.unm.edu/~ellison.

[15] ICFA Beam Dynamics Mini-Workshop on CSR, Berlin-Zeuthen, 2002. See http://www.desy.de/csr.

[16] C. de Boor, A Practical Guide to Splines, (Springer, New York, 2002).

Budget justification:

The budget justification is included in the original proposal. See VI above.

Three-year budget

The three year budget is as in the original proposal, see VI above. It is \$36.8K/year for partial support of Bassi's CSR work and for Heinemann.

2.30: Beam simulation: main beam transport in the linacs and beam delivery systems, beam halo modeling and transport, and implementation as a diagnostic tool for commissioning and operation

(progress report)

Accelerator Physics

Contact person
Dave Rubin
dlr@cesr10.lns.cornell.edu
(607) 255-3765

Institution(s)
Cornell

Funds awarded (DOE)
FY04 award: 16,060
FY05 award: 21,000
FY06 award: 32,000

2.30. Beam simulation: main beam transport in the linacs and beam delivery systems, beam halo modeling and transport, and implementation as a diagnostic tool for commissioning and operation (UCLC)

Accelerator Physics

Contact person: Dave Rubin
email: dlr@cesr10.lns.cornell.edu
phone: (607) 255-3765

Cornell

Year 1: $16,060
Year 2: $21,060
Year 3: $32,640

Beam simulation: beam transport in the bunch compressor main-linacs and beam delivery systems, beam halo modeling and transport, and implementation as a diagnostic tool for commissioning and operation

Personnel and Institution(s) requesting funding
G. Dugan, L. Gibbons, B. Heltsley, M. Palmer, R. Patterson, D. Rubin, D. Sagan, J.Smith
Laboratory of Elementary Particle Physics, Cornell University

Collaborators
A. Seryi, P. Tenenbaum - SLAC

Contact Person
D. Rubin
dlr@cesr10.lns.cornell.edu
(607)-255-3765, -8183

Project Overview

This project will cover simulations of main beam transport in linear colliders, with an emphasis on integrated damping ring to IP simulations; studies of the sources and transport of beam halo from its origin to the IP; implementation of modeling tools as a diagnostic for addressing commissioning and operational issues. Each of these topics is discussed in turn in the following paragraphs. Complete and robust simulation and modeling tools are critical to the evaluation of design and commissioning of ILC, and our goal is to develop software with the flexibility to investigate and evaluate design alternatives.

Main beam transport

One of the most essential features of a linear collider is the need for the preservation of a very small vertical emittance during beam transport from the damping ring to the IP. The best estimate of what is required to do this comes from integrated simulations of beam transport from the damping ring to the IP. Elaborate simulation programs have been developed at SLAC, DESY and CERN for the linear collider projects, in which errors can be incorporated, and realistic tuning algorithms can be explored, based on the expected performance of diagnostic systems. The errors are both static and dynamic, and include initial alignment errors, instrumentation resolution, ground motion and mechanical noise. Dynamic stabilization schemes and linac-based and IP feedback can be incorporated.

The worldwide effort in this area could benefit from additional manpower working in collaboration with the existing investigators to refine the simulation tools and develop improved tuning algorithms. We propose to join these ongoing beam simulation efforts, providing additional manpower, as well as fresh perspectives.

We will work closely with our collaborators, who have extensive experience in beam simulation, to identify critical issues which, in the context of the worldwide effort, require attention.

Particular areas of interest to us include the exploration of the tolerance of the baseline emittance preservation schemes to diagnostic faults, realistic modeling of the bunch compressors, and the effects of lattice mismatches. Also, one of our aspirations is to develop the machine model so that it can eventually interact with the control system in such a way that we can use it to diagnose and correct machine errors. Until a real control system exists, we can simulate that as well and begin to understand how the operational problems will become evident and then how they might be addressed.

We would also like to explore the utility of simulations of beam transport from the source to the damping ring. Our group has considerable experience developing computer models to study the properties of stored and accelerated beams, and for the evaluation of machine performance and diagnosis and correction of guide

field errors etc. We have done extensive simulation of single particle dynamics, beam-beam interaction, long range interaction of multiple bunch beams, and of the injection process for both CESR (5.3GeV) and for CESR-c(1.9GeV). We also created a detailed simulation of the positron production process in our linac in order to improve efficiency, and a rudimentary model of a superconducting linac to explore the dependence of single and multi-bunch stability on cavity parameters. We are well equipped to contribute to the effort to model beam transport in a high energy linac.

Machine commissioning and operation

During machine commissioning, interpretation of measurements of beam position monitors, beam size monitors, cavity higher order modes, etc. will be critical to identification of component failures and implementation of correction algorithms. Typically a simulation is used to compute the effects of the guide field on the beam so that the consequence of various field errors, misalignments, etc. can be anticipated. But during commissioning we must first measure the guide field errors, so that with the help of the models, appropriate corrections can be determined. We plan to develop the modeling tools to extract information about the guide field from the beam instrumentation, so that we can simulate the diagnosis and optimization of machine performance.

Beam halo modeling and transport

Understanding and control of beam halo is a crucial issue for linear colliders. The extent of the beam halo impacts the design of the collimation systems and muon spoilers, which in turn determine background conditions at the detector. The collimation systems are also an essential part of the machine protection system, a key issue for machine reliability.

One of the principal open issues in the baseline linear collider designs is the absence of a fully developed pre-linac collimation system. Working with our collaborators, we propose to develop a realistic design for such a system.

Beam halo typically explores regions of the vacuum chamber far from the central axis, where magnetic field nonlinearities, often ignored in main beam transport simulations, may be important. We propose to study the transport of halo particles, represented as longitudinal and transverse beam distribution tails, from the damping ring to where the halo is intercepted, exploring, for example, the effects of nonlinear field errors.

The baseline linear collider collimation systems have been designed to cope with a relatively high level of beam halo, based on previous linear collider experience. This level is typically much larger than simple estimates would indicate. A more basic understanding of the origin of beam halo would allow a better optimization of the collimation system design. We propose to simulate the sources of beam halo (e.g, due to scattering processes in the damping rings, dark current in the linac cavities, etc.) and track these particles from their sources to the collimation systems, where they are removed from the beam. Comparisons will be made to the assumed halo used for the design of the baseline collimation systems for ILC, and to the SLC beam halo experience.

Progress Report

The BMAD library of beam physics modeling routines is the basis for simulation, modeling, and diagnosis of CESR beam dynamics[1]. The library has been extended to include the physics of linacs. Implementations of the library routines, TESLAV and NLCV, have been developed to benchmark the BMAD code against studies based on the existing codes, LIAR, MERLIN, and PLACET. For a detailed description of the implementation see

D.Sagan, J.C.Smith, *The TAO Accelerator Simulation Program Environment*, Proceedings 2005 Particle Accelerator Conference

Calculation of machine parameters, multi-turn simulation of dynamic aperture, and multiparticle simulation

of emittance dilution are all in good agreement with other codes. We have computed sensitivies, specifically emittance dilution, to various misalignments, and find excellent agreement with the established codes. Documentation of the results will appear as

L.Fields, J.Urban, *Comparisons of BMAD with Three Other Simulation Programs*, Proceedings 2005 Particle Accelerator Conference

Although not as important for the superconducting 1.3Ghz linac as the X-band room temperature structure, both short and long range wakefields have been implemented with algorithms optimized for efficiency and speed. Experimentation with various tracking methods, macro-particle vs single particle tracking, numbers of particles, sensitivity to wakes etc. has allowed us to identify configurations that are both accurate and efficient.

The dispersion free steering alignment algorithm has been implemented and results are in good agreement with calculations based on Tenenbaum's implementation[2]. We are investigating sensitivity to BPM misalignemnt, convergence and efficiency of the fitting procedure. We are implementing and testing alternative algorithm's including ballistic alignment and Kubo's method[3] We are studying the effects of stray fields on emittance preservation in general and consequences for the various alignment methods. The status of the study of alignment methods will be presented at PAC05.

J.C.Smith, L.Gibbons, R.Patterson,D.Rubin,D.Sagan,P.Tenenbaum, *Comparison of Beam-Based Alignment Algorithms for the ILC*, Proceedings 2005 Particle Accelerator Conference

We use the same BMAD library of subroutines and data structures to model all accelerators of the linear collider, including injector, damping ring, bunch compresser and main linac and final focus. It is straightforward to link the accelerators together and propagate particles through the entire chain of machines. This flexibility will permit a thorough investigation of beam halo beginning with formation in the damping ring, propagation through bunch compressor and main linac to its fate in the beam delivery system.

Extensive investigation of the sensitivity to various misalignments, efficiency of alignment methods, the fate of halo particles, etc. is cpu intensive. We have implemented MPI (message passing interface) routines on two linux clusters that are available to us to enable parallel processing for the study of both beambeam effects in CESR and dynamic aperture in ILC damping rings. We plan to exploit this capability for main linac simulation as well.

We are members of the US ILC Low Emittance Transport working group and we are reporting progress and coordinating our studies through that forum.

References

[1] D.Sagan, *http://www.lns.cornell.edu/∼dcs/bmad*

[2] P. Tenenbaum, Proceedings European Particle Accelerator Conference, 2002

[3] K.Kubo, *http://lcdev.kek.jp/ kkubo/reports/MainLinac-simulation/*

2.32: Supplementary Damping Systems for the International Linear Collider

(renewal)

Accelerator Physics

Contact person
S. Mtingwa
mtingwa@ncat.edu
(336) 334-7423

Institution(s)
NCA&T

Funds awarded (NSF)
FY04 award: 22,600

New funds requested
FY05 request: 160,200
FY06 request: 193,700
FY07 request: 207,000

Supplementary Damping Systems for the International Linear Collider

Classification (subsystem)

Accelerator: Damping Systems

Personnel and Institution(s) requesting funding

S. Danagoulian, Department of Physics, North Carolina A&T State University

Collaborators

S. Mtingwa, Department of Physics, North Carolina A&T State University
Gerald Dugan, Cornell University
Andrzej Wolski, Lawrence Berkeley National Laboratory

Project Leader

S. Danagoulian
danagous@ncat.edu
(336) 334-7646

Project Overview

Indispensable subsystems of the International Linear Collider (ILC) will be the damping rings, which will shrink the emittances of the electron and positron beams. This idea was first proposed by Amaldi [1]. Once the beams enter their respective main linacs, the ultra low emittances should already have been achieved in the damping rings, where the equilibrium emittances are determined by the balancing of radiation damping, quantum excitations, and intrabeam scattering. For the TESLA superconducting linac design, one wants horizontal/vertical normalized emittances of 10/0.03 μrad. Given the long TESLA bunch trains, 2820 particles per bunch with 337 nsec between bunches, the damping ring is driven to a large circumference, 17 km. Also, various schemes require kickers with fast rise and fall times. There are also the challenges of achieving good dynamic aperture and beam stability during the long damping period. Any methods of alleviating some of these difficulties deserve serious study.

One possibility was proposed some time ago by Dikansky and Mikhailichenko. They suggested using a linear wiggler system to achieve small emittances at VLEPP [2]. There, they found that 15 GeV electron beams required about 1 km of wigglers and accelerating structures to decrease emittances the equivalent of a few damping times. Recently, Dugan [3] and Braun, Korostelev, and Zimmermann [4] have revived interest in this technique. As noted by Dugan, the length of the bunch train does not determine the length of a linear damping system (LDS). Also, unlike a damping ring, an LDS has no arcs contributing to quantum excitations. Moreover, as noted by Braun *et al.*, putting the LDS at higher energies greatly reduces the effect of intrabeam scattering.

Dugan considered alternating damping and accelerating structure sections. In order to completely replace the conventional ILC damping rings, Dugan showed that an electron or positron beam of 23 GeV would require 10 Tesla wiggler fields, an 11 cm wiggler period, and a total damping/accelerating length of 18 km to achieve the TESLA designed normalized

emittances. However, he noted that high-field, short period wigglers could be challenging technologically and the small beta functions and high wiggler fields could lead to severe tolerances and should be studied. Though it may not be feasible to replace completely the conventional damping ring with an LDS, it may be advantageous to supplement the conventional damping ring with a less ambitious LDS.

Braun *et al.* considered alternative, unconventional damping schemes, because the CLIC design as it stood did not achieve the desired electron and positron beam emittances. While the goal for normalized rms horizontal/vertical emittances was 450/3 nm, the designed damping ring only achieved 578/8.1 nm. First, they considered substituting rf wigglers and rf undulators for the conventional wiggler magnets in the damping ring. Since quantum excitations scale as the square of the wiggler period, the wiggler period is reduced by using these alternatives to magnets. Rf undulators, which have been considered in the past for synchrotron light sources [5-6], are defined by the regime where $\lambda_u B_0 < 0.01$ T-m, where λ_u is the undulator period and B_0 is the peak magnetic field. Braun *et al.* found that rf wigglers performed better than rf undulators. They also considered an LDS and obtained even better results, achieving horizontal/vertical normalized emittances of 400/3.7 nm, requiring a peak magnetic field of 10 T and a wiggler period of 1.5 cm. The additional linac length necessitated by the LDS was only 2.6 km.

This project describes research that is complementary to the baseline International Linear Collider (ILC) design. It will be divided into three phases.

PHASE I

Quantify the Impact of Supplementary Damping Schemes on Various ILC Designs

A number of damping ring designs have been proposed for the ILC, such as the 17 km dogbone design from the TESLA proposal and the 6 km design from Fermilab, both at a beam energy of 5 GeV. Each lattice has its own set of challenges; thus, we would like to determine how best to supplement the promising ILC designs with alternative damping systems. We will determine whether it would be advantageous to employ supplementary damping systems that are situated before and/or after the conventional damping rings. We will study such issues as dynamic apertures of the supplementary systems, the effect on vertical emittance of the opening angle effect of synchrotron radiation, the effect of small vertical dispersion in the supplementary systems, and other aspects of coupling such supplementary systems to a conventional damping ring.

For rf wigglers, Braun *et al.* examined the case of a rectangular waveguide in the TE_{10} mode. We will perform calculations of the effect of using disk-loaded and other promising geometric structures.

There are many issues that must be examined, and we will obtain a better overall assessment than currently exists about the utility of employing supplementary damping systems. We anticipate that PHASE I will take about a year and a half to complete.

PHASE II

Propose and Analyze Solutions to the Physics and Technological Challenges

Alternative damping schemes, such as the LDS, have a number of physics and technological challenges for which we will propose and analyze solutions. For example, Dugan has pointed out the challenge of implementing high-field, short period wigglers. We want to delve further into this question. We will evaluate the tolerance issues due to small beta functions and

high wiggler fields in an LDS. We will determine how best to avoid beam instabilities and the adverse effects of coherent synchrotron radiation due to high peak currents that result from bunch compression. These are some of the challenges that have been identified so far [3]. Other challenges surely will be discovered and we will address them as they arise. We anticipate Phase II to last about a year.

PHASE III

Design the Best-Case Supplementary Damping System and Propose Experiments at Existing Damping Rings

This final phase will draw upon the knowledge gained in Phases I and II. By that time, a viable conventional damping ring most likely will be settled upon by the worldwide ILC community. Thus, it will be clear how to complement such a system with one or more of the alternative damping schemes. We will design the specifications for such a system. Finally, we will propose experiments to be performed at currently operating damping rings to test the alternative damping ring concepts. This phase of the project should require about half a year.

Broader Impact This research will be performed with the assistance of two graduate students and two undergraduate students from North Carolina A&T State University (NCA&T). NCA&T has a Masters program in physics; thus, the graduate students working on this project would use their work to satisfy the thesis requirement. For the undergraduate students, the project would provide invaluable research opportunities so that they could appreciate firsthand the art of basic scientific research. For both the graduate and undergraduate students, the goal would be to encourage them to proceed to the doctorate in physics.

NCA&T is a public institution that is part of the University of North Carolina System. More importantly, it is one of the Historically Black Colleges and Universities, with both graduate and undergraduate enrollments containing in excess of ninety percent (90%) African-American students. Moreover, the physics program enrolls a number of women students, in some years comparable in number to the number of men students. Thus, this research project would proceed within a student environment that is composed of sizable numbers of underrepresented gender and ethnic groups.

NCA&T's partnership with Penn State, SLAC, and UC-Berkeley would be extremely advantageous for all involved. Not only would those institutions become better acquainted with the students' abilities, hopefully leading to future recruitment opportunities, but the students would gain a better appreciation of what is needed to perform at such institutions at the next level of their studies.

Hopefully, the research results from this project will be implemented at the ILC. In the meantime, the results will be presented at physics conferences and workshops and published in premier physics journals.

Results of Prior Research

We recently made substantial progress on linear collider research under two NSF grants: Planning Grant Award number PHY-0303702 (9/15/03 - 8/31/04) and the current Grant number PHY-0355182 (9/1/04 - 8/31/06). North Carolina A&T was a subcontractor with Cornell University, and the grants were for an accelerator project entitled, Damping Ring Studies for the LC. The goal was to derive more computationally friendly formulas for the phenomenon

of intrabeam scattering (IBS). IBS involves multiple small-angle Coulomb scatterings of particles within a bunch. To compute emittance growth rates due to IBS, the theory involves a series of matrix inversions and computations of the determinants of matrices at each of the many lattice points in the damping ring. To compute emittance growth rates versus bunch charge, popular mathematical codes take many hours to give results. Thus, approximations to the theory are necessary to reduce greatly the time needed to compute emittance growth rates. We derived such computationally-friendly approximations and showed that they give excellent agreement with the full theory for damping rings corresponding to both warm and cold linear collider designs.

For the lower energy damping rings for the warm linear collider designs, IBS would be the most important impediment to achieving ultra low beam emittances. Now that the decision has been made to use cold linear collider technology, the damping ring energies are sufficiently high that IBS does not seem to be a big problem, although in some designs it is not negligible and should always be checked.

The results of that work are now being revised for publication in Physical Review ST AB. Also, it has much broader applicability than to just the ILC. It can be applied readily to proton accelerators and other electron accelerators, such as synchrotron light sources.

Facilities, Equipment and Other Resources

This project will involve analytic calculations and computer simulations. As such, the main resource will be the computational facilities available at North Carolina A&T. The university offers main frames and personal computers in computer labs across the campus, with sufficient computer assistance to satisfy student and faculty needs. Moreover, the Department of Physics has its own computer lab with local workstations that are available to students and faculty. However, the computer labs are sometimes oversubscribed; thus, annually we would like to purchase two (2) personal computers and computational software to assist with this project.

FY2005 Project Activities and Deliverables

We will evaluate methods of supplementing the three (3) most promising genres of conventional ILC Damping Rings with alternative damping systems. We will evaluate the effects of including rf wigglers in damping rings and the effects of adding linear damping systems before and/or after them.

We will study disk-loaded rf wigglers in addition to simpler rectangular structures. We will determine dynamic apertures and study various beam stability questions. We will complete most of Phase I, and we will detail the progress on Phase I in a written report. Moreover, we will submit some aspects of our work to refereed journals for publication.

FY2006 Project Activities and Deliverables

By the end of Phase I of the project, which should be completed halfway through FY2006, a number of physics and technological challenges will have been identified. We will propose and analyze solutions. Among the solutions, we will make progress on settling the issues surrounding bunch compression and coherent synchrotron radiation. We will complete Phase I and half of Phase II, and we will provide a detailed written report of our results.

FY2007 Project Activities and Deliverables

During the final year of the project, we will complete Phases II and III. We will propose a design for an alternative damping system to complement the damping ring that the worldwide ILC community chooses. Finally, we will survey existing damping rings around the world and determine how best to devise experiments to test the concepts proposed for the supplementary damping systems. We will provide a final written report of our accomplishments.

Budget justification:

The entire project will consist mainly of computational and theoretical calculations, with heavy use of simulation codes. The first year's budget will provide research assistantships for two (2) graduate students and two (2) undergraduate students; travel for domestic and international conferences and the Principal Investigator, consultant, and collaborators to visit each other's institutions for the purpose of working on the project; materials and supplies in the form of two (2) personal computers, computer software and other miscellaneous materials; consultant services for S. Mtingwa at the rate of $524 per day for 41.1 days; and tuition support for two (2) graduate students. Note that individual items such as the PCs, which cost less than $5,000, are not considered equipment under NCA&T's regulations.

During the second year, we provide two (2) months summer salary for the PI and we include the same funds as requested the first year, increased mostly for inflation.

During the third year, we include the same funds as requested the second year, increased mostly for inflation.

Fringe benefits are 24% of faculty salaries and 7.65%of $6,000 graduate student summer salary. Other direct costs are tuition for two graduate students. Indirect costs are calculated at North Carolina A&T's 40% rate on modified total direct costs, which excludes tuition.

Three-year budget, in then-year K$

Institution: Institution 1

Item	FY2005	FY2006	FY2007	Total
Faculty (Summer)	0	13.0	13.6	26.6
Other Professionals	0	0	0	0
Graduate Students	30	32	34	96
Undergraduate Students	14	15	16	45
Total Salaries and Wages	44.0	60.0	63.6	167.6
Fringe Benefits	0.5	3.6	3.7	7.8
Total Salaries, Wages and Fringe Benefits	44.5	63.6	67.3	175.4
Equipment	0	0	0	0
Travel	15	16	18	49
Materials and Supplies	12	14	16	42
Consultant Services	21.5	22.6	23.7	67.8
Other direct costs	30	31	32	93
Total direct costs	123.0	147.2	157.0	427.2
Indirect costs	37.2	46.5	50.0	133.7
Total direct and indirect costs	160.2	193.7	207.0	560.9

References

[1] U. Amaldi Phys. Lett. 61B, 313 (1976).

[2] N. Dikansky and A. Mikhailichenko, EPAC'92, 848 (1992).

[3] G.Dugan, private discussions with a Damping Ring Working Group, also see " Linear Damping Systems for the International Linear Collider," Abstract for PAC'05.

[4] H. Braun, M. Korostelev, and F. Zimmermann, CLIC Note 594 (2004)/CERN- AB-2004-017-ABP and APAC'04.

[5] T. Shintake et al., Proc. Linac Conference, Tsukuba (1982), Japanese Journ. Appl. Phys. 21:L601 (1982), T. Shintake et al., Japanese Journ. Appl. Phys. 22:844 (1983).

[6] M. Seidel DESY-TESLA-FEL-2001-08 (2001).

2.34: Experimental, simulation, and design studies for linear collider damping rings

(renewal)

Accelerator Physics

Contact person
Gerry Dugan
gfd1@cornell.edu
(607) 255-5744

Institution(s)
Cornell
Minnesota

Funds awarded (NSF)
FY04 award: 45,133

New funds requested
FY05 request: 46,839
FY06 request: 72,006
FY07 request: 0

Experimental, simulation, and design studies for linear collider damping rings.

Classification (subsystem)

Damping rings

Personnel and Institution(s) requesting funding

G. Dugan, M. Palmer, D. Rubin, D. Sagan, LEPP, Cornell University.
R. Poling, A. Smith, University of Minnesota.

Collaborators

W. Decking, DESY
S. Mtingwa, North Carolina A&T State University
M. Ross, SLAC
J. Urakawa, KEK
A. Wolski, LBNL

Project Leader

G. Dugan
gfd1@cornell.edu
(607)255-5744

Project Overview

Studies of wiggler-related dynamic aperture limitations.

Two classes of circular electron accelerators will generate damping almost entirely in wiggler magnets: linear collider damping rings and some low-energy e^+e^- factories, such as CESR-*c*. Wigglers are unlike typical accelerator magnets in that they have longitudinal magnetic fields which are comparable to their transverse fields. Also, the design orbit has an angle and a displacement relative to the wiggler axis. The combination of the longitudinal field and the angle through the wiggler produces an effective field error, as does the combination of the field roll-off near the wiggler edge and the displacement from the wiggler axis. The effective field nonlinearity is quite strong, severely limits dynamic aperture in linear collider damping ring designs, and may decrease the damping rate for large-amplitude particles. We intend to develop and test a design algorithm for wigglers and lattices which preserves the dynamic aperture, and test this algorithm with beam measurements in CESR-*c*. We will apply the same techniques to the International Linear Collider (ILC) damping ring designs to demonstrate that they have adequate dynamic aperture and amplitude-dependent damping rate (or optimize those designs until they do).

Studies of space charge effects.

The large density of particles in the ILC damping rings creates a significant space charge tune shift. The tune shift is not the same for all particles, and the area of the tune footprint is significant. If this tune footprint overlaps strong resonance lines, particles may be lost, or

the emittance may grow. To evaluate the effects of space charge, we will incorporate suitable algorithms into our particle-tracking simulations and modeling codes.

Development of simulation and modeling tools

We have begun the development, at Cornell and at Minnesota, of simulation and modeling tools to support the measurements in CESR-*c* and the analysis of ATF data. The hardware to be used will be an Intel-architecture computing farm (`http://www.hep.umn.edu/~cleo3/`) consisting of 48 dual-processor systems in 1U rack-mount enclosures. An undergraduate student will be supported to act as operator and to participate in code development. While operating the farm for linear collider simulations, the high energy physicists at Minnesota will continue to develop expertise in accelerator physics to allow contributions to algorithm development and simulation-based benchmarking of designs for the damping ring project.

The modeling code is based on an existing object-oriented particle-tracking library, Bmad [1], that has been extensively tested against an operating machine, CESR. To understand the significance of measurements in CESR-*c*, we will make detailed comparisons of the simulated properties of the linear collider damping rings with CESR-*c*, including dynamic aperture with wiggler nonlinearities, space charge, and other collective effects. We will also use the models to explore coupling and dispersion correction schemes that can then be tested in CESR-*c*. Our study will include an independent evaluation of the characteristics of the ILC damping rings.

Development of high-quality beam diagnostics systems

High-quality beam diagnostics are required for the measurement of small beam sizes and short bunch lengths, and are critical to the development of any linear collider damping ring. We plan to improve the following existing CESR diagnostic systems, which are also important for linear collider damping rings: high-resolution beam size diagnostics (interferometric technique), and streak camera bunch length and shape monitoring.

Review of ILC damping ring design and optics.

The large number of bunches (2820) and the relatively large inter-bunch spacing (337 ns) in the TESLA ILC design gives a bunch train which is more than 200 km long. A damping ring of this size would be very costly, and so the bunch train is damped in a compressed form, with a bunch spacing of 20 ns, leading to a damping ring with a circumference of 17 km. This ring is still quite large, and, apart from the cost issue, has some technical disadvantages (such as large space charge effects) related to its large size. We will investigate other technical solutions for the damping rings, and compare the advantages and disadvantages relative to the baseline design.

Investigation of the superferric option for the ILC damping ring wigglers.

The baseline design of wigglers for the ILC damping rings is based on permanent magnet technology. Superconducting wigglers were also considered. At LEPP, we have experience both with permanent magnet systems, and, in connection with CESR-*c*, have developed expertise in the design and fabrication of superferric wigglers. We will re-examine the possibility

of superferric wigglers for the ILC damping rings. We will re-evaluate the technical and cost advantages and disadvantages of each technology choice.

Studies of beam-based alignment and emittance correction algorithms.

The ILC damping rings designs have an unprecedented low vertical emittance. Coupling and vertical dispersion must be very well corrected. It is likely that beam-based alignment (BBA) will be needed to reference the beam position monitors to the magnets with high precision. We plan to model BBA and correction algorithms in the ATF damping ring at KEK and in CESR-*c* with the simulation code Bmad, with special attention to the role of systematic errors in BBA. We will compare the simulation results with observations at ATF and at CESR-*c*. The goal is to produce improved BBA and emittance correction algorithms.

Broader Impact

Much of the research described in this proposal is synergistic with efforts to improve the performance of low-energy e^+e^- factories, such as CESR-*c* and DAΦNE. The simulation and modeling tools described above, as well as the diagnostic systems, will have applications in the design and operation of any high-performance circular electron accelerator systems, such as synchrotron radiation sources.

This proposal will support graduate and undergraduate students training in accelerator physics. Most accelerator work is carried out in national labs, which do not have the strong training mission of a university. The national shortage of accelerator physicists is related to the relatively poor representation of this discipline in the university community. This shortage affects not only high energy physics, but also many other fields, such as solid state physics, materials science, biophysics, and medical science, which have come to depend on accelerators as their front-line research tools. This proposal will contribute to the education of accelerator physicists, and consequently can have a broad impact on all these fields.

Results of Prior Research

Prior research in this area has been supported as part of the current grant NSF PHY-0355182, entitled "University-based Accelerator R&D for a Linear Collider", in the amount $128,315, covering the period 9/1/04-8/31/06. Under this grant, the specific activity entitled "Experimental, simulation, and design studies for linear collider damping rings" is supported at the level of $45,133. Results of this prior research are described below.

Studies of dynamic aperture of wiggler-dominated damping rings

Work performed thus far in studying the dynamic aperture of the various ILC damping ring designs has been focused on the development of simulation tools and methods to be used for the accurate calculation of the dynamic aperture of a wiggler-dominated ring. Using Bmad, we have optimized the application of conventional dynamic aperture calculations to a damping ring lattice. A new dynamic aperture calculation which we have also implemented to study the damping ring, is a frequency map analysis which shows the dynamic aperture while also highlighting the chaotic nature of the particle orbits.

These simulation tools have been used on the TESLA dog-bone damping ring lattice using a full non-linear representation of the wiggler magnets which are the predominant limiter of the dynamic aperture. The non-linear modeling of the damping ring wigglers has been done

using the same techniques developed at Cornell for modeling CESR-*c* wigglers, now modified for application to the linear collider damping rings.

With simulation tools and algorithms in place, evaluating the robustness of the different ILC damping ring designs will be a straightforward application of the simulations. Future work will also be performed to maximize the dynamic aperture of a wiggler-dominated ring by varying the physical geometry of the wiggler magnets and studying these new wiggler magnets in the proposed damping ring designs.

Alternate designs for the ILC damping rings

We are investigating a method for manipulating a compressed bunch train in the damping ring using RF deflectors and multiple transfer lines. Bunches in the injection/extraction line are four times as far apart as bunches in the main ring, thereby reducing the size of the ring by approximately a factor of four without increasing requirements for the injection/extraction kicker.

In order to model these rings, we have implemented deflecting cavity elements in Bmad. These elements use realistic EM fields including spatial and temporal nonlinearities. We are currently testing this scheme in a 4 km ring based upon the TESLA dogbone design and the KEK-B deflecting cavities. Early results suggest that we can obtain the necessary emittance and damping time without a significant compromise of the dynamic aperture.

Development of simulation and modeling tools.

In the past year we have completed the assembly and commissioning at Minnesota of an Intel-architecture computing farm (`http://www.hep.umn.edu/~cleo3/`) consisting of 48 dual-processor systems in 1U rack-mount enclosures. Funding for this system was provided by the Department of Energy and the University of Minnesota primarily to provide large-scale simulations for the CLEO-*c* experiment, but with a planned 10% share for linear collider accelerator simulations. The processors are Pentium 4 Xeons operating at ~ 2.5 GHz. with hyper threading enabled. Each worker node is equipped with 1GB of memory, modest local disk space (40GB), and Gbit Ethernet. Libraries, and input and output files reside on a dedicated 3.5-terabyte fiber-channel disk array. The operating system is Scientific Linux and all nodes are network-administered in a PXE boot environment.

CLEO-*c* simulations are currently carried out under the Condor system, while accelerator simulations are run in the LAM/MPI parallel computing environment. So far linear collider simulations on computers at Minnesota have been limited to demonstration jobs with Bmad and the TESLA Dog-Bone Damping Ring Lattice from W. Decking of DESY. CESR-*c* simulations are being run intensively, taking advantage of significant excess processing capacity beyond the current needs of the CLEO-*c* program.

Development of high-quality beam diagnostics systems

Improved beam diagnostics capability is critical to our understanding of CESR-*c* as a wiggler-dominated storage ring and for the measurement of small beams and short bunch lengths at CESR. A general upgrade of CESR instrumentation is presently underway. Two aspects of this upgrade that are particularly applicable to experiments for damping ring development are upgrades of CESR's streak camera and beam profile monitor systems.

The data acquisition system for our Hamamatsu C1587 streak camera has recently been upgraded. The camera is located at the end of an optical transport system which accepts synchrotron light from both the electron and positron beams in CESR originating from source points in two equivalent dipoles. The streak camera provides resolutions down to 1.6 ps for bunch measurements in CESR where bunches are spaced at 14 ns intervals. The device is presently undergoing *in situ* calibration and is in regular use for both low and high energy CESR operation.

Double-slit interferometer hardware, operating on the principle of the Michelson Stellar Interferometer, has been installed in the optics systems of both the electron and the positron vertical beam profile monitors in CESR. The system makes use of horizontally polarized synchrotron light originating in a standard CESR arc bend magnet. The depths of the observed interference fringes can be measured with a CCD camera and used to determine the vertical source size. With our current slit arrangement, a vertical resolution limit of approximately 50 μm is obtained. We are presently expanding the capability of this device for fast bunch-by-bunch readout by installing a new optics line for a Hamamatsu H7260 multianode photomultiplier. This device consists of a 32 channel linear array of anodes with 1 mm pitch and 0.6 ns rise-time. The fast response of this device makes it an excellent choice for distinguishing the 14 ns spaced bunches in CESR. With suitable imaging optics, our simulations indicate it is capable of making beam size measurements with a resolution of several percent in fewer than 10 passes of a single bunch. As such it can provide a unique probe of multi-bunch beam dynamics in CESR. Turn-by-turn multi-bunch readout electronics has been designed, built, and is currently being tested. We expect to start full system tests of the positron monitor prototype during the first half of 2005. The addition of an optics line and a second device for electron monitoring should follow shortly thereafter.

Due to the small beam sizes expected in a linear collider damping ring, beam profile measurement devices with improved intrinsic resolution are highly desirable. There is an ongoing effort at LEPP [2] to develop a beam profile monitor using Si and/or GaAs PIN diode devices to image X-rays. Our development of turn-by-turn multi-bunch readout electronics for our existing beam profile system will provide critical hardware for use in the testing of such devices. At present we are developing suitable analog front-end electronics to read out the proposed prototype detectors. The remainder of the electronics package will be a copy of that developed for our visible light beam profile monitor.

Facilities, Equipment and Other Resources

The facilities of the Cornell Laboratory for Elementary-Particle Physics (LEPP) include an accelerator complex (linac, synchrotron, storage ring, and insertion devices), the CLEO detector, substantial computer facilities with a computing support staff, an electronics shop equipped with a variety of sophisticated electronic test equipment, electronic design and fabrication support staff, machine shops, and other related facilities.

FY2005 Project Activities and Deliverables

During the first year we plan to:

1. Develop a space charge element for particle tracking simulations.

2. Make active use of the streak camera bunch length and shape monitor, and complete upgrades to the interferometric beam size monitor, including integration into the CESR control system.
3. Continue to investigate alternative damping ring solutions for the ILC.
4. Continue to benchmark the design algorithm and particle-tracking code for a wiggler-dominated ring by measuring the dynamic aperture, orbit-dependent tune shifts, decoherence, phase space distortion, and amplitude-dependent damping rate in CESR-*c*.
5. Perform an evaluation of the technical and cost advantages of permanent magnet and superferric wigglers for the ILC damping rings.
6. Continue to develop the infrastructure for supporting accelerator simulations on the Minnesota farm. This will include investigating the MPICH implementation of multi-processor parallel computing under Condor. This will have the benefit of more effective utilization of resources within a cluster that is serving both CLEO-*c* and accelerator simulations, and will allow the linear collider simulations to take advantage of the fault tolerance, administrative resources, and other features of high-throughput computing that Condor provides.

The first year deliverables are technical reports on the items described above.

FY2006 Project Activities and Deliverables

During the second year we plan to:

1. Complete the benchmarking of our design algorithm and particle-tracking code for a wiggler-dominated ring.
2. Using this code, perform a complete simulation (tune plane scan) of candidate ILC damping ring designs, including wiggler nonlinearities and space charge, to determine the optimum operating points and particle loss rates.
3. Develop well-optimized correction algorithms for BBA and vertical dispersion and coupling correction that can be applied to the ILC damping rings and to tests in CESR-*c* and possibly ATF.
4. Continue to develop the infrastructure for supporting accelerator simulations on the Minnesota farm.

The second year deliverables are technical reports on the items described above.

Budget justification: Cornell University

The activities will require the involvement of Cornell LEPP staff members and graduate students. One graduate student will be supported half-time from this grant in the first year, and full-time in the second year. The activities at Cornell will require travel funds for consultation with collaborators at DESY, SLAC, KEK, and LBNL. Indirect costs are calculated at Cornell's 58% rate on modified total direct costs.

Three-year budget, in then-year K$

Institution: Cornell University

Item	FY2005	FY2006	Total
Other Professionals	0	0	0
Graduate Students	9.067	19.767	28.834
Undergraduate Students	0.0	0.0	0.0
Total Salaries and Wages	9.067	19.767	28.834
Fringe Benefits	0.0	0.0	0.0
Total Salaries, Wages and Fringe Benefits	9.067	19.767	28.834
Equipment	0.0	0.0	0.0
Travel	4.0	4.0	8.0
Materials and Supplies	0.0	0.0	0.0
Other direct costs	9.183	17.964	27.147
Minnesota subcontract	13.5	13.5	27.0
Total direct costs	35.75	55.231	90.981
Indirect costs*	11.089	16.775	27.864
Total direct and indirect costs	46.839	72.006	118.845

* Includes 26% of first $25K subcontract costs

Budget justification: University of Minnesota

The budget for the Minnesota component of the project assumes that all support for scientific personnel (Poling, Smith) will be provided by the Department of Energy through grant DE-FG02-94ER40823. This grant also covers maintenance and software-licensing costs for the Minnesota simulations farm. Salary support is requested for one undergraduate work-study student to aid in programming and operation of this facility for linear collider applications. The budget is based on the expectation of 10 to 15 hours of work per week during the academic year and double that during the summer. A typical level of work-study support is assumed. Funds are also requested for travel to three or four linear collider meetings per year. DOE-supported travel to Cornell for CLEO-*c* work will also provide opportunities to consult with collaborators. Indirect costs are computed using the University of Minnesota's rate for on-campus research (49.5%). Undergraduate student salaries do not incur fringe-benefit costs.

Three-year budget, in then-year K$

Institution: University of Minnesota

Item	FY2005	FY2006	Total
Other Professionals	0	0	0
Graduate Students	0	0	0
Undergraduate Students	5.0	5.0	10.0
Total Salaries and Wages	5.0	5.0	10.0
Fringe Benefits	0	0	0
Total Salaries, Wages and Fringe Benefits	5.0	5.0	10.0
Equipment	0.0	0.0	0.0
Travel	4.0	4.0	8.0
Materials and Supplies	0	0	0
Other direct costs	0	0	0
Total direct costs	9.0	9.0	18.0
Indirect costs	4.5	4.5	9.0
Total direct and indirect costs	13.5	13.5	27.0

References

[1] D.L. Rubin and D. Sagan, "CESR Lattice Design", Proc. 2001 Particle Accelerator Conference, Chicago, paper RPPH121 (2001).

[2] J. Alexander, J. Ernst,"Design for a Fast Synchrotron Radiation Imaging System for Beam Size Monitoring", a component of the grant NSF PHY-0355182, "University-based Accelerator R&D for a Linear Collider"

2.37: Demonstration of Undulator-Based Production of Polarized Positrons at FFTB at SLAC

(progress report)

Accelerator Physics

Contact person
William Bugg
bugg@slac.stanford.edu
(865) 974-7799

Institution(s)
Princeton
South Carolina
Tennessee

Funds awarded (DOE)
FY04 award: 65,000
FY05 award: 40,000
FY06 award: 0

E166(2.37) Update as of 4 April, 2005

A) Equipment and Readiness Status

Item	Responsible Institution	Status
Beamline equipment		
Undulator and power supply	Cornell	Completed and delivered to SLAC, August 2004.
Undulator collimator, beampipe, beam postion monitors,undulator table, photon collimator, positron production target, positron vacuum chamber.	SLAC	Nearly complete. Some installation and alignment to be done immediately before run.
Special purpose magnets		
Photon transmission magnets(2) for photon and positron lines.	DESY	Completed and shipped to SLAC, August, 2004. Installed in FFTB.Not tested
Positron focusing solenoid and transport magnets.	Design Princeton-Construction SLAC	To be installed just prior to run.
Detectors		
Photon line-		
Aerogel photon counter(2)	Princeton	Completed and installed-March 2005. not yet tested
SiW photon counters(2+spare)	Tennessee	Completed and installed-June2004. Commisioned
Segmented SiW calorimeter	Tennessee	Completed and installed-June 2204. Commisioned
Positron line-		
CsI Calorimeter	DESY	Completed and installed Commissioned
Silicon positron counter	Tennessee	Completed and tested. To be installed after vacuum chamber installation.
Faraday cup	SLAC-Princeton	Installation after vacuum chamber installation
Background monitors-		
CsI crystal	SLAC	All detectors installed tested and operated in FFTB to
CsI crystal	DESY	study FFTB background during E164-5, SPPS runs.
SiW calorimeter	Tennessee	Installed in FFTB for >1.5 years.
SiW photon counter	Tennessee	No beam with E166 run conditions was available
Scintillator Paddles(5)	SLAC/Tenn	during these experiments.
DAQ		
Labview system, VME, CAMAC electronics, HV control,	SLAC	Completed >2 years. Recently updated to include controlled voltage ramp runs for transmission magnets
Analysis Software Output of DAQ is Ascii file		
Ntuple creation for event data	Tennessee	Used extensively for background studies and detector
PAW analysis files-	Tennessee	calibrations.
Data quality, calibration, photon and positron transmission for polarization measurement.		Polarization programs as yet untested.
Magnet ramp control analysis	DESY	Tested with simulated ramp. Actual magnet ramp not yet implemented
Root analysis software	DESY	Not yet used..

B) Estimated Schedule.

E166 actually began a scheduled run in early October, 2004. The goal was to align the system, calibrate the detectors, install and commission the undulator and if possible to make a first measurement of photon polarization On October 8,9 we received the first low energy (28 GeV) test beam All detectors except the photon line Aerogel detectors, the Silicon positron detector and the positron Faraday cup were in place and background data were recorded. The following week was scheduled for undulator installation to be followed by alignment and calibration studies and increase to 50 GeV. However, the electrical accident at SLAC resulted in cancellation of all activities and shutdown of the accelerator.

Current expectations are that permission to reactivate the FFTB beam will be forthcoming in late April or early May. It has been agreed that the SPPS experiment will run initially for a few (3-4) weeks and followed by E166 at which time we will resume the program planned for last October. A one week shutdown is required to install those items which cannot be in place during the SPPS run. We hope to achieve in Phase 1 measurement of the undulator photon intensity and polarization. A later run is planned for Fall, 2005 to measure the positron polarization.

The SPPS run will be used to thoroughly recheck detectors and DAQ system prior to E166 run

Linear Collider Accelerator Physics R&D Progress Report 2.37a
April 14, 2005

Undulator-Based Production of Polarized Positrons
(SLAC Experiment E-166)

Changguo Lu, Kirk T. McDonald

Joseph Henry Laboratory, Princeton University, Princeton, NJ 08544

Summary

Princeton University is participating in SLAC experiment E-166 [1], an international accelerator-physics project involving 15 institutions to demonstrate undulator-based production of polarized positrons for a linear collider. This effort, and that of U. Tennessee, forms LCRD 2.37 of the Linear Collider Accelerator Physics R&D Program [2]

The full exploitation of the physics potential of future linear colliders such as the JLC, NLC, and TESLA will require the development of polarized positron beams. In the scheme under study in experiment E-166, a helical undulator is employed to generate photons of several MeV with circular polarization which are then converted in a relatively thin target to generate longitudinally polarized positrons.

To characterize the success of this technique, the experiment includes diagnostics of the polarization of both the MeV-scale photons and positrons, based on the polarization dependence of the rate of transmission of photons through magnetized iron. Princeton University has responsibility for construction of a magnetic spectrometer for the positrons, and also for construction of a pair of siilica aerogel counters for use in the polarimeter to diagnose the undulator photons.

All of the hardware construction for experiment E-166 is now complete. In addition, Princeton has purchased tungsten shielding for the positron spectrometer, a waveform generator to control the reversal of magnetic field of the photon polarimeters, a 4-channel digital oscilloscope for use with the 3 Faraday cup diagnostics of the positron spectromter, and two PC's for use in the E-166 data acquisition system.

The LCRD budget award for Princeton was \$30k in FY05, with the anticipation of a renewal of \$40k in FY06. Because the experiment is to run in FY05, it has been necessary to spend about \$60k to date, with another \$10k needed to cover travel expenses for the coming run of the experiment.

Experiment E-166 had taken two days of beam at SLAC in October 2004, before the lab was shut down due to an electrical accident. As of today, we believe the experiment can run again from May 15-June 4, 2005, and for an additonal 3 weeks around Sept. 1, 2005.

Section 1 presents some relevant extracts from the E-166 proposal [1]. Section 2 reviews the Princeton effort on E-166.

1 Introduction

The full exploitation of the physics potential of future linear colliders such as the JLC, NLC, and TESLA will require the development of polarized positron beams.

In the proposed scheme of Balakin and Mikhailichenko [3] a helical undulator is employed to generate photons of several MeV with circular polarization which are then converted in a relatively thin target to generate longitudinally polarized positrons.

To advance progress in this field, a new experiment, SLAC E-166 [1, 4] (approved June 30, 2003), will test this scheme to determine whether such a technique can produce polarized positron beams of sufficient quality for use in future Linear Colliders. The experiment will install a 1-meter-long, short-period ($\lambda_u = 2.4$ mm, $K = 0.17$), pulsed helical undulator in the Final Focus Test Beam (FFTB) at SLAC. A low-emittance 50-GeV electron beam passing through this undulator will generate circularly polarized photons with energies up to a cutoff energy of about 10 MeV. These polarized photons are then converted to polarized positrons via pair production in thin targets.

1.1 Undulator Based Production of Polarized Positrons

A polarized positron source for a Linear Collider was first proposed by Balakin and Mikhailichenko in 1979 in the framework of the VLEPP project [3]. The concept, schematically sketched in Fig. 1, sends the high energy ($\geq$ 150 GeV) electron beam of a Linear Collider through a ($\sim$ 200 m-long) helical undulator to produce circularly polarized photons with energies of about 11 MeV. While the electrons are further accelerated and brought into collision after passing through the undulator, the photons are converted in a thin target into electron-positron pairs. Here the polarization state of the photons is transferred to the positrons and electrons. Only the on-axis photons of the helical undulator radiation are completely circularly polarized; the degree of polarization is decreasing with increasing emission angle. Hence, the polarization of the photons and of the generated positrons can be increased at the expense of the total number of positrons by collimation. The positrons are captured behind the target similarly to the case of a conventional positron source [5, 6], and fed into a linac.

This undulator-based positron source concept offers the additional advantage that the heat load on the target is less than that of a conventional source, and so the former is very well suited for the production of high intensity positron beams [7]. An undulator-based polarized positron source can in principle be realized independently of the linac technology, *i.e.*, independently of the details of the required pulse structure, because the number of produced positrons scales with the number of the electrons in the drive linac, and the pulse structure of the electrons is directly copied to that of the positrons. In this sense it is an option for all Linear Collider projects.

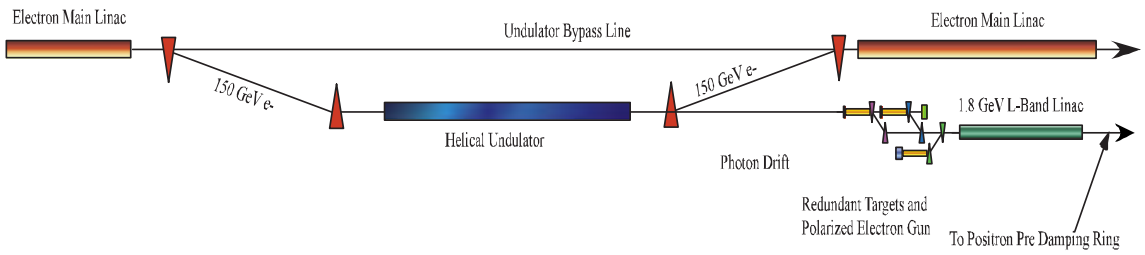

Figure 1: Conceptual scheme for undulator-based production of polarized positrons.

1.2 Physics Opportunities at a Linear Collider with Polarized Electrons and Polarized Positrons

Polarized electrons have been a part of each of the different Linear Collider proposals for a long time. Recently much scrutiny has been given to the case for polarized positrons in addition to polarized electrons. A consensus has emerged that polarized positrons are a highly desirable option for a Linear Collider.

The importance of beam polarization in general was demonstrated e.g., at the SLAC Linear Collider (SLC). Because of the high degree of electron polarization (during its last run in 1997/98, an average longitudinal beam polarization $P_{e^-} = 74\%$ was reached [8]) one of the world's most precise measurements of the weak mixing angle at Z-pole energies was performed.

Having both beams polarized offers a number of advantages:

- Higher effective polarization.
- Increased signal to background in studies of Standard Model Physics.
- Enhancement of the effective luminosity.
- Precise analysis of many kinds of non-standard couplings.
- The option to use transversely polarized beams.
- Improved accuracy in measuring the polarization.

1.3 The Need for a Demonstration Experiment

The aim of the proposed experiment E-166 is to test the fundamental process of polarization transfer in an electromagnetic cascade. For this, a simplified version of the scheme shown in Fig. 1 will be used, in which a 50-GeV electron beam passes through a 1-m-long undulator as shown in Fig. 2. The resulting photon beam of MeV energy is converted to positrons (and electrons) in a thin target, after which the polarization of the positrons (and photons) is analyzed.

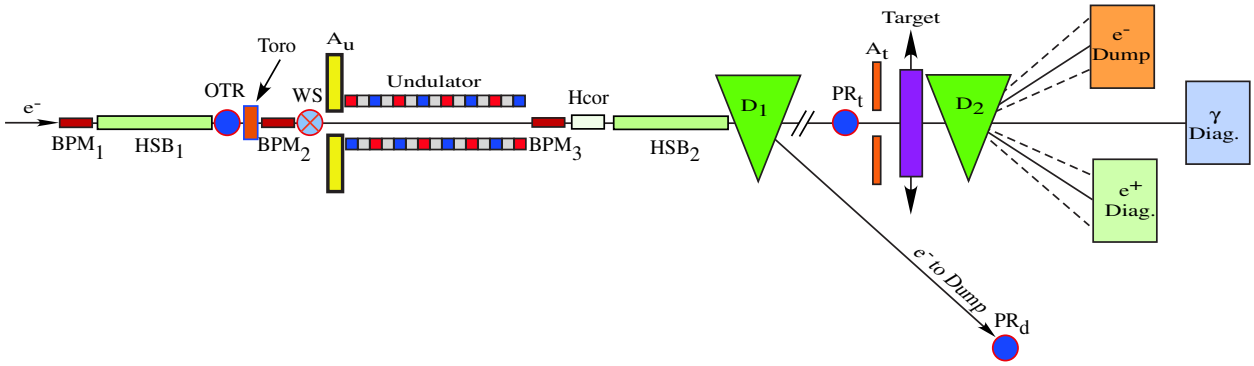

Figure 2: Conceptual layout (not to scale) of the experiment to demonstrate the production of polarized positrons in the SLAC FFTB. 50-GeV electrons enter from the left and pass through an undulator to produce a beam of circularly polarized photons of MeV energy. The electrons are deflected away from the photons by the D_1 magnet. The photons are converted to electrons and positrons in a thin target. The polarization of the positrons, and of the photons, are measured in polarimeters based on Compton scattering of electrons in magnetized iron. BPM_i = beam-position monitor; HSB_i ="hard" soft bend; OTR = optical-transition-radiation beam-profile monitor; Toro = beam-current toroid; WS = wire scanner; A_i = aperture limiting collimators; Hcor = horizontal steering magnet; D_1 = FFTB primary beam dump bend-magnet string; PR_d = dumpline beam-profile monitor; PR_t = e^+ target beam-profile monitor; D_2 = analyzing magnet.

While the basic cross sections for the QED processes relevant to polarization transfer were derived in the late 1950's, experimental verification of the polarization development in an electromagnetic cascade is still missing. From this point of view, the proposed experiment has some general scientific aspects in addition to its importance for Linear Colliders.

Each approximation in the modeling of electromagnetic cascades seems to be well justified in itself, but the complexity of polarization transfer in cascades makes the comparison with an experiment desirable, so that the decision whether a Linear Collider should be built with or without a polarized positron source can be based on solid grounds. The achievable precision of the proposed transmission polarimetry of 5-10% is sufficient for this purpose. This experiment, however, will not address detailed systems issues related to polarized positron production for a Collider, such as capture efficiency, target thermal hydrodynamics, radiation damage in the target, or an undulator prototype suitable for use at a Linear Collider; such issues are well within the scope of R&D by a Linear Collider project that chooses to implement a polarized positron source based on a helical undulator.

1.4 Overview of Experiment E-166

The goal of the experiment is

- To measure the yield and polarization of the photons produced by passing an electron

beam through a helical undulator.

- To measure the yield and polarization of the positrons produced by conversion of undulator photons in a thin target.
- To compare the results to simulations.

A schematic layout of the experiment is shown in Fig. 2 with emphasis on the particle beams, while Fig. 3 shows the layout of the detectors to measure the flux and polarization of the photons and positrons.

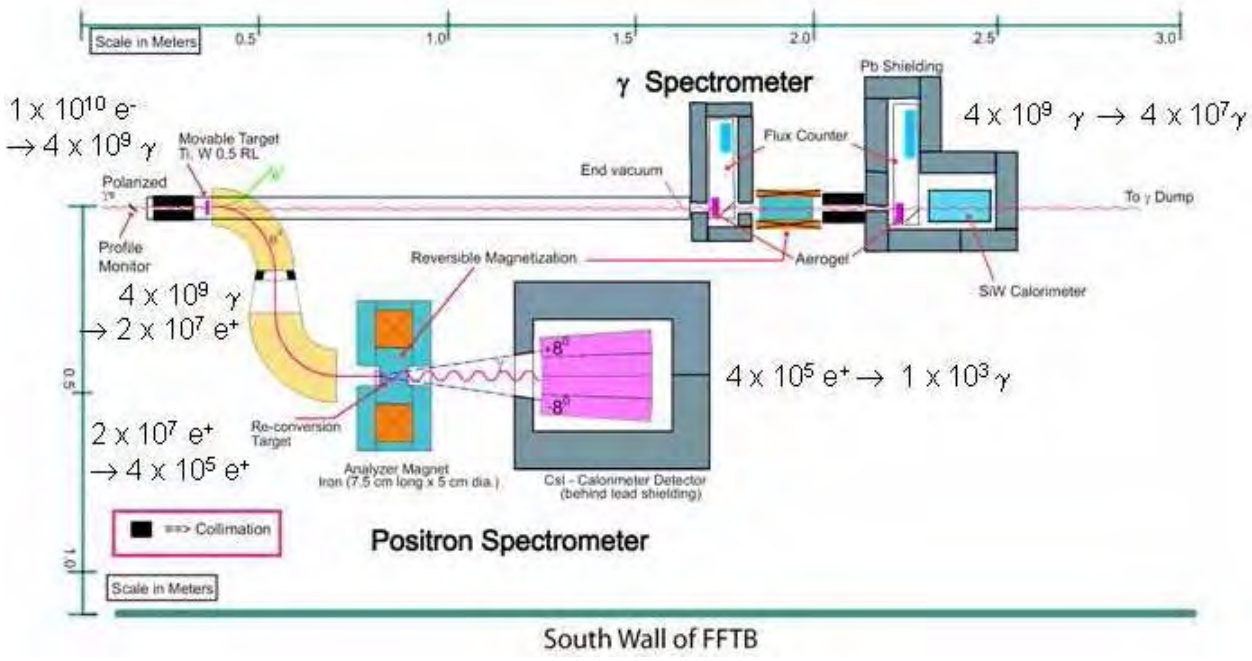

Figure 3: Conceptual layout of the E–166 positron generation and photon and positron diagnostic systems. Representative rates of photons and positrons, per electron pulse, are shown in various regions of the apparatus.

The experiment uses a low-emittance, 50-GeV electron beam in the SLAC Final Focus Test Beam (FFTB) plus a 1-meter-long, short-period ($\lambda_u = 2.4$-mm, K=0.17), pulsed helical undulator, to produce circularly polarized photons of energies up to 10 MeV. These polarized photons are then converted to polarized positrons through pair production in a Ti target which has a nominal thickness of 0.5 rad. len. The polarizations of the photons and positrons are measured by the Compton transmission method using a magnetized iron absorber [9].

This experiment is a demonstration of undulator-based production of polarized positrons for Linear Colliders at a scale of 1% in length and intensity:

- Photons are produced in the same energy range and polarization as in a Linear Collider;
- The same target thickness and material are used as in the Linear Collider;

- The polarization of the produced positrons is expected to be in the same range as in a Linear Collider.
- The simulation tools being used to model the experiment are the same as those being used to design the polarized positron system for a Linear Collider: EGS4 [10] and GEANT3, both modified to include spin effects for polarized e^+ production, and BEAMPATH [11] for collection and transport.

1.5 The Photon Polarimeter

Measurements of the circular polarization of energetic photons are most commonly based on the spin dependence of Compton scattering off atomic electrons [12, 13]. One can either observe the scattered electrons and/or photons emerging from a thin, magnetized iron foil [14], or measure the transmission of unscattered photons through a thick, magnetized iron absorber [9, 15, 16]. Experiment E-166 uses the latter technique, which is sketched in Fig. 4. The basic components are a magnetized iron absorber and a detector that measures the photons that penetrate through the absorber.

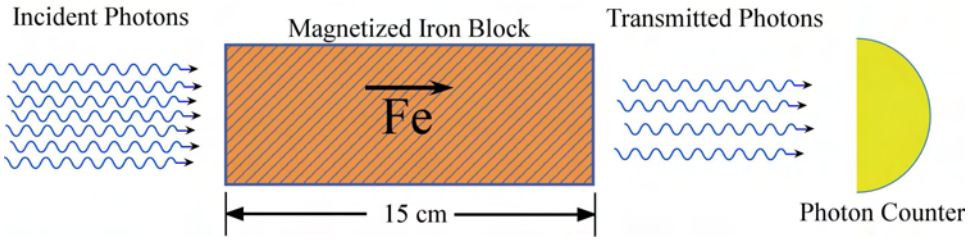

Figure 4: The concept of transmission polarimetry, in which the survival rate is measured for photons that pass through a magnetized iron absorber.

On reversing the sign of the magnetization of the absorber, an asymmetry $\delta = P_\gamma P_{e^-} A_\gamma$ is measured in the rate of transmitted photons, where P_γ is the photon polarization, P_{e^-} is the polarization of the electrons in the iron, and A_γ is the so-called analyzing power which is proportional to the spin-dependent part of the Compton scattering cross section [1].

The implementation of the photon polarimeter for E-166 is sketched in Fig. 3. The photon polarimeter will include two types of photon detectors, a total absorption calorimeter and a Čerenkov detector.

1.5.1 Silicon-Tungsten Calorimeter

The total absorption calorimeter for the transmitted photons is a silicon-tungsten sampling calorimeter, similar to that employed in SLAC experiment E-144 [18]. As shown in Fig. 5, this device consists of 20 plates of tungsten, each 1 rad. len. thick, separated by silicon detectors in the form of a 4×4 array of pads, each 1.6×1.6 cm^2 in area. The pads are read out in longitudinal groups of 5, for a total of 64 readout channels. The resulting transverse

and longitudinal segmentation of the calorimeter will permit confirmation that the energy deposited in the calorimeter has the profile expected from the signal of undulator photons, rather than that of possible backgrounds of scattered electrons and photons.

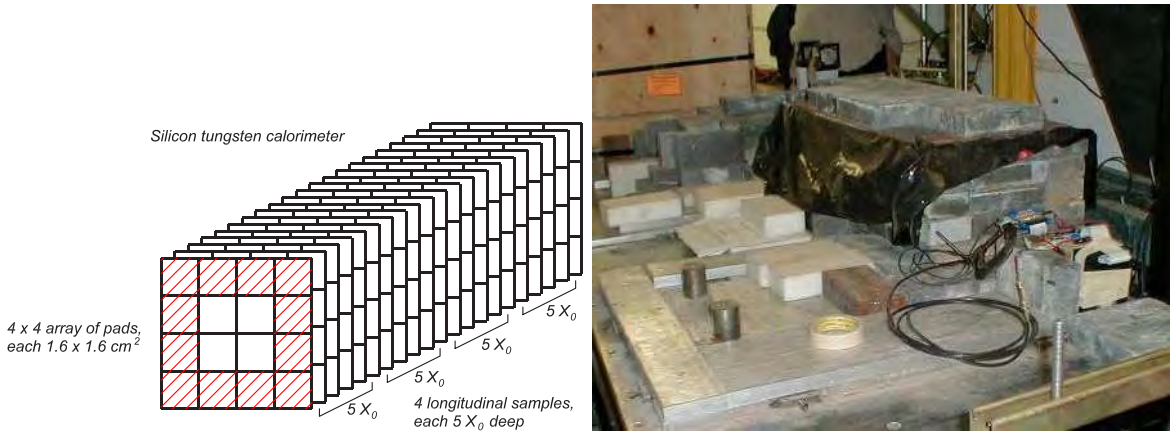

Figure 5: a) The silicon tungsten calorimeter consists of 20 longitudinal samples of 1 X_0 each, grouped into 4 segments of 5 X_0 each. The transverse sampling is via a 4×4 array of pads, each 1.6×1.6 cm^2 each. b) View of E-166/T-467 test apparatus in the FFTB: the silicon tungsten calorimeter is the small object (with cabling)at the right; a CsI counter is under the lead brick shield in the center; the aerogel flux counters are at the top center.

The resolution of a similar sampling calorimeter has been measured to be [18]

$$\sigma_{\mathcal{E}}^2 = (0.19)^2\mathcal{E} + (0.4)^2, \tag{1}$$

where $\mathcal{E}$ is the electron energy in GeV. For a pulse of 10^{10} electrons, some 4×10^7 photons of average energy 5 MeV reach the calorimeter, depositing about 200 TeV. Hence, the relative error on that energy of only 0.06 %.

1.5.2 Aerogel Flux Counters

A complementary measurement of the transmitted photon flux will be made with a pair of aerogel Čerenkov counters with index of refraction $n = 1.009$ [19]. This extremely low-index material is available from the BELLE experiment. The two flux counters are deployed before and after the magnetized iron absorber, as shown in Fig. 3.

The signal in the aerogel flux counter is generated by conversion of undulator photons in the aerogel, after which electrons and positrons of energy greater than 4.3 MeV will emit Čerenkov light. This light is observed in a photomultiplier that views the aerogel through an air light pipe, as shown in Fig. 6.

Because of their threshold energy of 4.3 MeV, the aerogel flux counters are insensitive to synchrotron radiation in the beam. Hence, a pair of aerogel flux counters that are placed upstream and downstream of the magnetized iron absorber, as shown in Fig. 3, can confirm

Figure 6: a) Sketch of the photon flux counter, consisting of a 2-cm-thick block of aerogel of index $n = 1.009$, viewed by a photomultiplier tube at the end of an air light pipe. b) Photograph of the two aerogel flux counters. c) A block of aerogel mounted in a Michelson interferometer in order to measure its index of refraction [19].

the attenuation of this absorber on photons of energy above 5 MeV, independent of possible backgrounds of lower-energy photons.

The conversion probability of an undulator photon in the 1-mm-thick Al cover plate of the detector will yield about 1 electron or positron per 300 photons, but only 1/3 of these will have energy above Čerenkov threshold. The number of photons of energy that penetrate the iron absorber is about 4×10^7 per pulse of 10^{10} electrons, so the number of useful conversions is about 4×10^4. There will be about 50 $\theta_C^2 \approx 5$ ŏptical Cerenkov photons per conversion, leading to about 1/2 photoelectron per conversion in a photomultiplier whose photon collection efficiency times quantum efficiency is 10%. Hence, the expected signal in the Čerenkov counter downstream of the magnetized iron absorber is about 2×10^4 photoelectron per electron beam pulse.

1.6 The Positron Polarimeter

The measurement of positron polarization is to be made by first transferring the polarization to photons, and then using a photon-transmission polarimeter [17]. Measurements of the asymmetry $\delta = P_{e^+} P_{e^-} A_{e^+}$ in the rate of transmitted photons can be related to the positron polarization P_{e^+} and the polarization P_{e^-} of the electrons in the magnetized iron absorber via a calculable analyzing power A_{e^+} [1].

The layout of the positron polarimeter has been shown in Fig. 3, and is shown again in Fig. 7. A double 90°-bend magnet transports a ±20% momentum bite of the positron spectrum to the reconversion target (0.5 rad. len. of tungsten). The photons that emerge from the target are then incident on an 7.5-cm-long magnetized iron absorber. The photons that are transmitted through the absorber ($\approx 10^3$ per pulse) are detected in a CsI array. The latter device was chosen, rather than a Si-W calorimeter, because the typical energy of

photons reaching the detector in the positron polarimeter is only about 1 MeV; the energy resolution of a CsI calorimeter for such energies is about 2.5%, compared to 20% for a Si-W device.

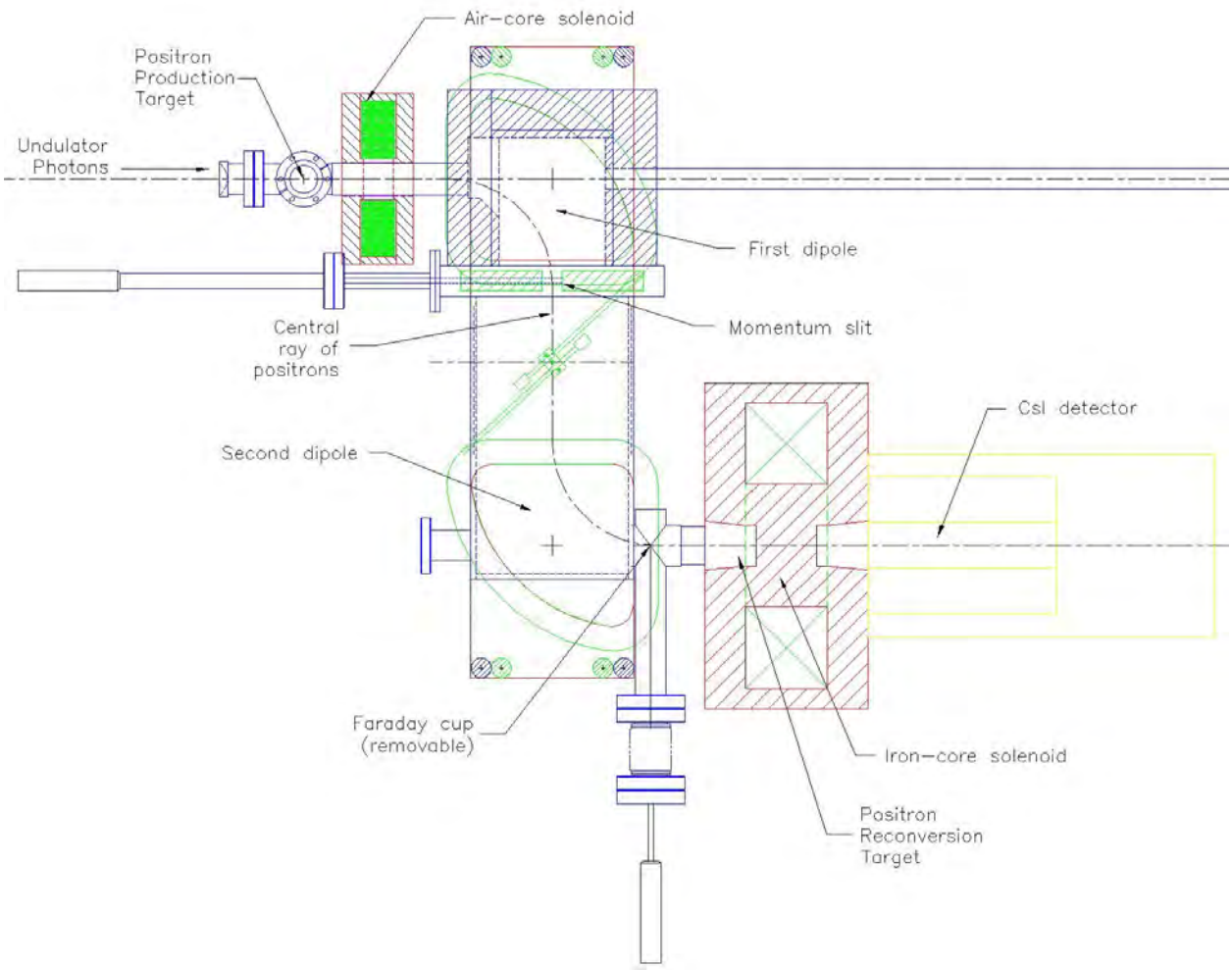

Figure 7: Layout of the positron polarimeter.

2 Princeton Activities on E-166

1. K. McDonald is Co-Spokesperson of E-166 (along with J. Sheppard of SLAC).

2. The solenoid and dipole pair for the positron spectrometer were fabricated at Princeton, and are now installed in the FFTB tunnel (Fig. 8).

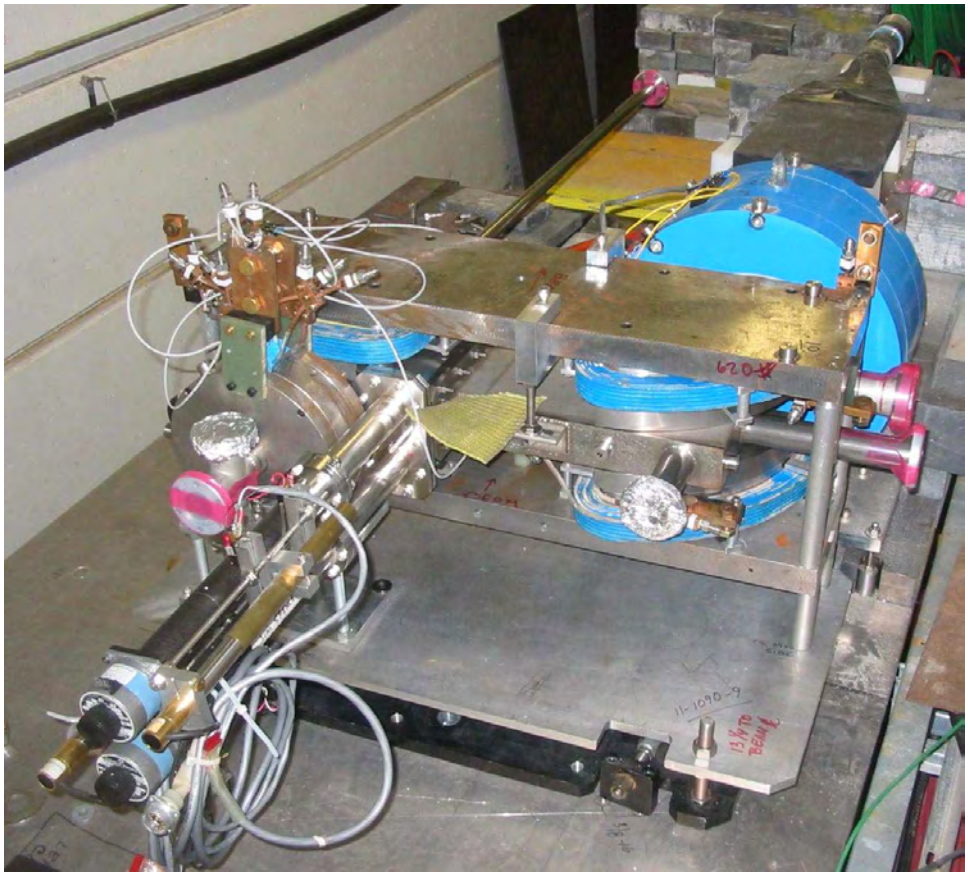

Figure 8: The positron spectrometer in the FFTB tunnel.

3. Princeton participated in the mechancial design of the vacuum chamber for the positron spectrometer (Fig. 9).

4. Princeton participated in the mechancial design of the Faraday "cup" at the end of the positron spectrometer (Fig. 10).

5. Princeton participated in the design and fabrication of the temporary articulated bellows system that permits use of two parallel beam pipes at the location of the unulator (Fig. 11).

6. Princeton fabricated a pair of silica aerogel detectors (index of refraction $n = 1.09$) for use with the undulator photon polarimeter (Fig. 12).

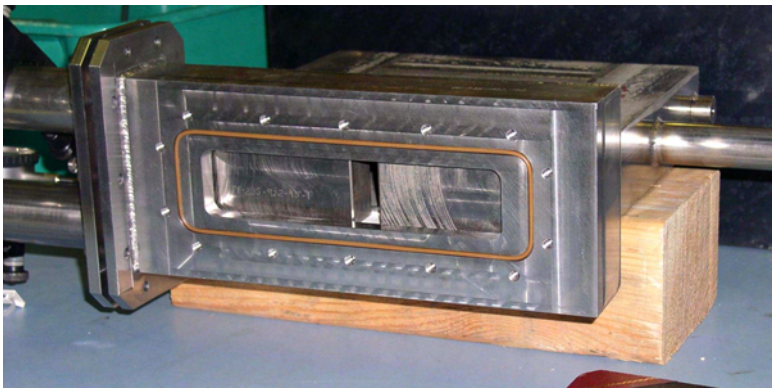

Figure 9: The half of the vacuum chamber that fits inside the first dipole of the positron spectrometer. The tungsten jaws of the momentum slit are visible.

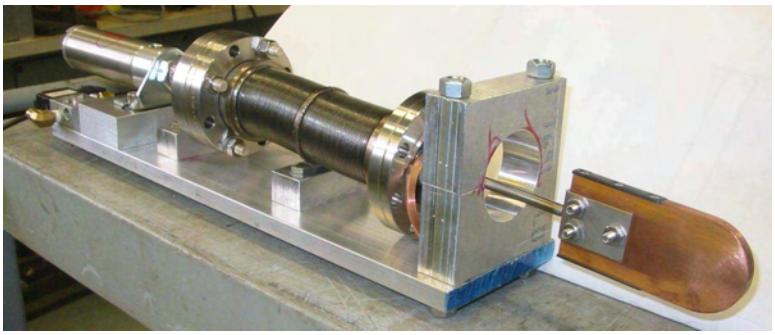

Figure 10: The Faraday cup and associated motion control, to be placed at the downbeam end of the positron spectrometer.

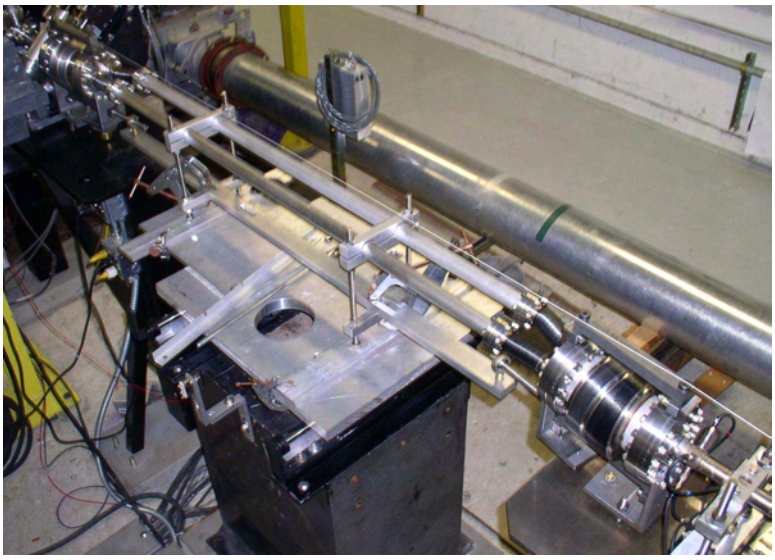

Figure 11: The temporaty articulated bellows system at the eventual location of the undulator in the FFTB tunnel.

Figure 12: The aerogel detectors in the FFTB tunnel, surrounding the undulator-photon polarimeter solenoid.

7. Princeton purchased 3 sets of tungsten (heavimet) shielding of various geomtries for use in and around the positron spectrometer.

8. Princeton purchased an Agilent 33220A arbitrary function generator to control the ramping of the iron-core solenoids, when their field directions are reversed during the polarimetry measurements.

9. Princeton purchased a Tektronix TDS5504N 4-channel digitial oscilloscope for use with the 3 Faraday cup diagnostics of the positron spectrometer.

10. Princeton purchased to PC's for use in the E-166 data acquisition system.

3 References

[1] G. Alexander *et al.*, *Undulator-Based Production of Polarized Positrons. A Proposal for the 50-GeV Beam in the FFTB* (June 7, 2003; approved as SLAC E-166 on June 30, 2003), http://www-project.slac.stanford.edu/lc/local/PolarizedPositrons/E-166bis.pdf

[2] See sec. 2.37 of *A University Program of Accelerator and Detector Research for the Linear Collider*, Vol. II, G.D. Gollin ed. (Nov. 24, 2003), http://www.hep.uiuc.edu/LCRD/pdf_docs/LCRD_UCLC_Big_Doc/big_doc_2_accel.pdf

[3] V.E. Balakin and A.A. Mikhailichenko, *The Conversion System for Obtaining High Polarized Electrons and Positrons*, Budker Institute of Nuclear Physics, Preprint BINP 79-85 (1979), http://puhep1.princeton.edu/~mcdonald/e166/Mikhailichenko/balakin83.pdf

[4] K.P. Schüler and J.C. Sheppard, *E-166. Undulator-Based Production of Polarized Positrons*, presented to the SLAC EPAC (June 12, 2003), http://www.slac.stanford.edu/grp/rd/epac/Meeting/200306/sheppard.pdf

[5] K.C. Moffeit, *Positron Source: First Fifty Nanoseconds*, SLAC-CN-268 (May 1984); F. Bulos *et al.*, *Design of a High Yield Positron Source*, SLAC-PUB-3635 (April 1985), IEEE Trans. Nucl. Sci. **NS32**, 1832 (1985), http://www.slac.stanford.edu/pubs/slacpubs/3000/slac-pub-3635.html

[6] The NLC Collaboration, N. Phinney ed., *2001 Report on the Next Linear Collider*, SLAC-R-571 (June 2001), sec. 5.4, http://www.slac.stanford.edu/pubs/slacreports/slac-r-571.html

[7] K. Floettmann, *Investigations Toward the Development of Polarized and Unpolarized High Intensity Positron Sources for Linear Colliders*, Ph.D. Thesis, DESY 93-161.

[8] P. Raimondi *et al.*, *Recent Luminosity Improvements at the SLC*, 17th Intl. Conf. on High-Energy Accl (HEACC 98), Dubna, Russia, SLAC-PUB-7955 (September 1998), http://www.slac.stanford.edu/cgi-wrap/getdoc/slac-pub-7955.pdf

[9] H. Schopper, *Measurement of Circular Polarization of γ-rays*, Nucl. Instr. and Meth. **3**, 158 (1958), http://www-project.slac.stanford.edu/lc/local/PolarizedPositrons/doc/ClassicalPapers/Schopper.pdf

[10] W.R. Nelson, H. Hirayama and D.W.O. Rogers, *The EGS4 Code System*, SLAC-Report-265, (1985).

[11] Y. Batygin, *Particle-in-cell code BEAMPATH for Beam Dynamics Simulations with Space Charge*, ISSN 1344-3877, RIKEN AF-AC-17 (2000).

[12] L.W. Fagg and S.W. Hanna, *Polarization Measurements on Nuclear Gamma Rays*, Rev. Mod. Phys. **31**, 711 (1959).

[13] H. Frauenfelder and A. Rossi, *Determination of the Polarization of Electrons and Photons*, in *Methods of Experimental Physics. Nucl. Physics, Part B***5**, ed. by L.C.L. Yuan and C.-S. Wu (Academic Press, New York, 1963), pp. 214-274.

[14] J.C. Wheatley *et al.*, *Circular Polarization of Gamma Radiation Emitted by Oriented Co-40 Nuclei*, Physica **21**, 841 (1955).

[15] S.B. Gunst and L.A. Page, *Compton Scattering of 2.62 MeV Gamma Rays by Polarized Electrons*, Phys. Rev. **92**, 970 (1953).

[16] M. Fukuda et al., *Polarimetry of Short-Pulse Gamma-Rays Produced through Inverse Compton Scattering of Circularly Polarized Laser Beams*, Phys. Rev. ST Accel. Beams **6**, 091001 (2003).

[17] M. Goldhaber, L. Grodzins, and A.W. Sunyar, *Evidence for Circular Polarization of Bremsstrahlung Produced by Beta Rays*, Phys. Rev. **106**, 826 (1957).

[18] C. Bamber *et al.*, *Studies of Nonlinear QED in Collisions of 46.6 GeV Electrons with Intense Laser Pulses*, Phys. Rev. D **60**, 092004 (1999).

[19] T. Dimofte, *Measurement of the Index of Refraction of an Aerogel* (Aug. 2003), http://viper.hep.princeton.edu/~mcdonald/e166/Dimofte/aerogel_index.pdf

[20] K.T. McDonald *et al.*, *Study of Polarized Positron Production for the LC* (Sept. 3, 2002, approved as part of the FY03 LCRD Accelerator Physics Program), http://www-project.slac.stanford.edu/lc/local/PolarizedPositrons/internal/doc/2002/sctennloi-aw03.pdf

2.40: Development of Polarized Photocathodes for the Linear Collider

(progress report)

Accelerator Physics

Contact person
Richard Prepost
prepost@hep.wisc.edu
(608) 262-4905

Institution(s)
SLAC
Wisconsin

Funds awarded (DOE)
FY04 award: 34,616
FY05 award: 34,600
FY06 award: 34,600

April 13, 2005

Development of Polarized Photocathodes for the Linear Collider

Accelerator Physics - Year 1 of Continuing Proposal

Contact Person: Richard Prepost
University of Wisconsin, Madison, WI 53706
EMail: prepost@hep.wisc.edu
Phone: 608 262-4905

Results of Prior Support

The proposal submitted in Oct. 2003 was approved for funding on Oct. 2004. The research is focussed on producing photocathodes which have polarization in excess of 90% and a peak output charge meeting the charge requirements of the ILC. The technical decision for the superconducting version of the linear collider has a favorable impact on this R&D program. The cathode surface charge limit problem is much less for the cold machine since the bunch spacing is 300 ns compared to the much shorter bunch spacing of 1.4 ns that was proposed for the warm machine.

The research to date has been successful in achieving higher polarization and higher QE, but the goal of $> 90\%$ polarization has not been achieved. The polarization appears saturated at 85% and a material-specific spin-depolarization mechanism appears to be present. Consequently, we have embarked on a program to study several types of superlattice structures.

To address material-specific spin depolarization mechanisms and achieve higher polarization, we will continue to study a superlattice stucture proposed by the Russian St. Petersburg group of Y. Mamaev. The Mamaev group has had CDRF funds in partnership with SLAC to study and grow certain superlattice structures. The two year CDRF grant ended Nov. 2004 and resulted in an interesting structure which requires additional study. The stucture developed is a InAlGaAs/GaAs superlattice of about 18 periods. This particular stucture has a lattice matched buffer layer which should result in higher quality with less dislocations and a smaller conduction band offset which should result in greater electron transport. The previous GaAsP/GaAs superlattice structures we have studied do not have these particular beneficial characteristics. The structure has several parameters which require systematic study.

We have placed an order for several of the InAlGaAs/GaAs stuctures with SVT Associates in Minneapolis. This company has grown other structures for us and we are pleased with the quality of their work.

Another structure we plan to study is a superlattice based on GaAs and InGaP. A GaAs/InGaP superlattice structure differs from the previously studied GaAs/GaAsP superlattice structure in that GaAsP superlattice barrier layers are replaced by InGaP. The GaAs strained wells remain the same.

The new strained superlattice is expected to increase the polarization because the spin relaxation rate in InGaP is less than in GaAsP. Since the band-gap energy of InGaP is larger than that of GaAsP, an enhancement of the Quantum Efficiency is also expected.

Proposal to the University Consortium for a Linear Collider

October 21, 2003

Proposal Name

Development of Polarized Photocathodes for the Linear Collider

Classification

Accelerator (New Proposal)

Personnel and Institution requesting funding

Richard Prepost, University of Wisconsin, Madison WI 53706

Collaborators

SLAC
J. Clendenin
E. Garwin
R. Kirby
T. Maruyama

Contact Person

R. Prepost
prepost@hep.wisc.edu
608 262 4905

Project Overview

The development of high current polarized photocathodes is very important for the Linear Collider (LC) project. Physics requirements call for highly polarized electron beams with a goal of at least 90% polarization.

A Wisconsin-SLAC collaboration has been developing and studying polarized photocathodes which have been used for the SLAC SLD and fixed target programs. A more recent goal is the development of photocathodes with a polarization in excess of 90% which meet the NLC charge requirements. This work started as a SLAC-Wisconsin collaboration (E. Garwin, T. Maruyama of SLAC and R. Prepost of Wisconsin) and has evolved into a formal SLAC collaboration called the Polarized Photocathode Research Collaboration (PPRC).

SLAC personnel now also include J. Clendenin, R. Kirby, D. Luh, A. Brachmann, and S. Harvey

To date, well over 80% polarization has been achieved with strained gallium arsenide photocathodes which have been used in past SLAC experiments. The 1994-1998 SLC operation with the SLD detector and subsequent fixed target experiments E-142, E-143, E-154, E-155, and E-155X used strained gallium arsenide cathodes which produced at least 80% polarization at the source. More recently, a newly developed high current polarized photocathode used for SLAC experiment E-158 achieved a polarization of about 85% with a charge approaching that required for the NLC.

These applications were the world's first use of strained photocathodes specifically designed for a polarized electron source, resulting in record polarization for a high intensity electron linac. The research and development program will continue to focus on studying the properties of these cathodes with respect to spin relaxation, quantum efficiency, and charge saturation, with the goal of developing photocathodes for use with the LC.

Early research efforts focused on the development of strained photocathodes since electron spin polarization higher than 50%, approaching 100%, is theoretically possible using cathode structures which have less crystal symmetry than unstrained GaAs. As long as GaAs or any zinc blende type structure is used for cathodes, the electron polarization is limited to $\leq$50% due to the degeneracy of the valence bands.

Since the seminal studies with strained InGaAs, research has been carried out with strained GaAs epitaxial layers grown on a GaAsP buffer layer. Electron spin polarizations approaching 85% were observed at low quantum efficiency (QE), decreasing to about 80% at high QE. A variety of layer thicknesses and strains were studied using MOCVD grown samples commercially obtained from the SPIRE Corporation in Bedford, MA. The samples were of high quality, and all samples studied to date have shown a significant polarization enhancement in excess of the unstrained maximum polarization of 50%. The epitaxial layer thicknesses varied from 0.1 μm to 0.3 μm and the strains of approximately 1% resulted from phosphorous concentrations ranging from 21% to 28%. Even the 0.3 μm thick sample, well in excess of theoretical estimates for the critical thickness for pseudomorphic growth, reached an electron spin polarization of 75% at low QE and 70% at high QE, demonstrating significant persistance of lattice strain.

We have continued R&D efforts on cathode structures to address certain issues, specifically 1) fundamental properties of materials, 2) higher polarization, and 3) higher charge limit. The cathode charge limit, was not a limiting factor for the SLAC SLD and fixed target programs but is an issue for a LC polarized source with an NLC micro-bunch structure. The LC with an NLC micro-bunch structure requires higher peak current than can be obtained from the photocathodes that were used for the SLAC SLC program. Provided that the photocathode output charge is not limited by the space charge limit of the electron gun, the output charge is limited by charge saturation of the photocathode itself. Charge saturation occurs because a photovoltage develops at the cathode surface at high currents acting as a potential barrier for further charge emission

One possible cure for this problem is to increase the p-type doping in the epitaxial surface

layer. Over the past two years systematic studies have been made of strained GaAs samples where the electron polarization was measured as a function of the high doped surface layer thickness. The results showed, as expected, that the polarization increases as the high doped layer thickness is reduced. From these studies it was concluded that greater than 80% polarization could be obtained with about 5-10 nm of a surface layer doping of 5×10^{19} cm^{-3}.

High surface layer doped samples have been grown to our specifications by the Bandwidth Semiconductor Corporation (former SPIRE Corporation). The basic structure was a 0.1 μ GaAs active layer highly doped for the first 10 nm of surface and strained by a GaAsP buffer layer. The highly doped surface layer is kept very thin so as not to decrease the electron polarization. The high doping surface layer has the effect of decreasing the band gap near the surface, resulting in a small potential barrier. A small amount of phosphorus (5%) was added to the active layer to compensate the energy difference in the conduction band resulting from the high gradient doping.

This structure was tested with a long pulse laser system to simulate the NLC 190 microbunch train of total length 266 ns. The NLC charge requirement for the source is 2.2 nC in each microbunch for a total of 420 nC, about 25 times the SLC maximum charge. A short YAG-Ti laser pulse was superimposed on the long flash-Ti laser pulse to simulate the peak charge requirement of a single microbunch. The resultant measurements of extracted charge vs laser energy showed no charge saturation up to the maximum laser energy. Both the microbunch peak charge and the total charge of the macrobunch nominally approach the NLC charge requirements. This new cathode structure was used for the first two runs (2002) of the fixed-target experiment E-158 which required about 80 nC in a 300 ns pulse, a higher charge requirement than previous cathodes have been able to deliver. The electron polarization was in excess of 80%, in accord with polarization measurements measured in the test lab.

Another approach to obtain higher photocathode output charge is to increase the thickness of the photocathode active layer, ordinarily limited to about 0.1 μ. Larger thickness of the active layer results in serious degradation of the strain. Superlattice structures can in principle overcome the inherent thickness limitation of single heterostructures. Molecular Beam Epitaxy (MBE) superlattice structures have been grown for us by SVT Associates through an SBIR award with SLAC as the technical partner. Measurements of these structures during 2002-2003 have shown both good QE and high polarization. These measurements are continuing during 2003-04 with the goal of fine-tuning the superlattice parameters. To this date, peak polarizations of 85% and QEs of about 1% have been achieved. Fig. 1 shows polarization and QE vs. laser wavelength for several different SVT photocathode structures with varying superlattice parameters. The peak polarizations and QE are consistent with superlattice computer simulations. The superlattice structures shown here are typically 16 periods of 3-4 nm $GaAs_{1-x}P_x$ barriers alternating with 3-4 nm GaAs wells with a phosphorus fraction of x = 0.35. The extracted charge nominally meets NLC peak charge requirements. One of these superlattice photocathodes was used successfully for the final run of E-158 in 2003.

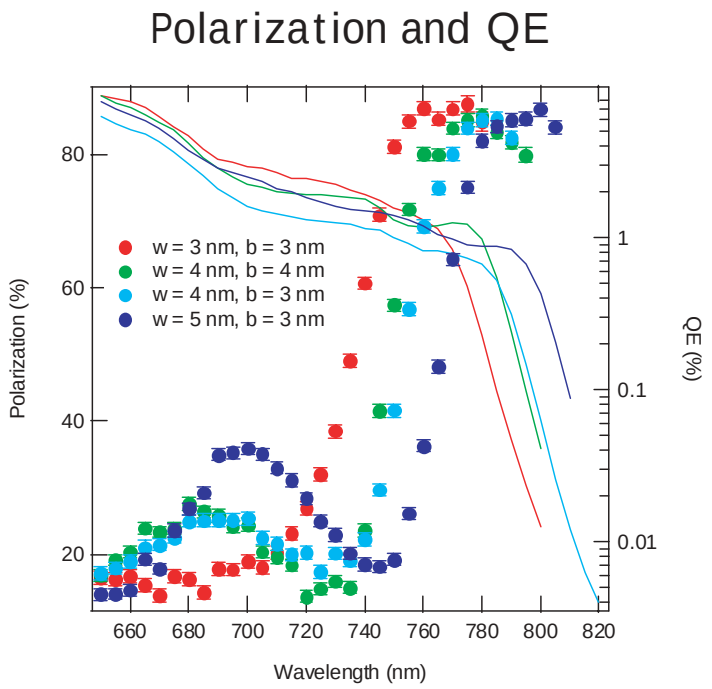

Figure 1: Polarization and QE for several SVT GaAsP/GaAs superlattice samples vs. laser excitation wavelength. Here w is the well width and b is the barrier width.

Another problem which has been addressed during 2003 is the dopant loss and strain relaxation during the relatively high temperatures used for heat-cleaning. This factor tends to prevent the achievement of ultimate performance from the photocathodes. To this end we have tested an atomic hydrogen cleaning system based on a Jefferson Lab design. The goal of atomic hydrogen cleaning is to achieve high QE using a heat cleaning temperature of 450°C. This temperature is in contrast to the normal heat cleaning temperature of 600°C which results in the degradation effects mentioned above. Our studies have shown that when hydrogen ions are prevented from reaching the photocathode, the performance goals are achieved.

Description of Project Activities

The research and development program divides into several well defined parts as follows:

1. **Fabrication**
   The cathode structures are grown by a commercial or academic partner who has the

facilities required for structure growth. Currently we receive structures from SVT Associates with whom SLAC currently has a Phase II SBIR award, now in the final year, and from a Russian group at St. Petersburg Technical University with whom SLAC shares a CRDF grant.

2. **Photocathode Characterization**
   The parameters of the photocathodes must be measured, requiring a variety of techniques including, but not limited to, X-Ray Bragg measurements, Electron Microscopy, Secondary Ion Mass Spectroscopy (SIMS), Auger analysis and Photoluminescence measurements.

3. **Measurement of Polarization, Quantum Efficiency (QE), and Charge Limits**
   SLAC has the facilities for these measurements using a cathode test system (CTS) for measurements of polarization and QE, and a HV gun test lab for measurement of charge saturation properties.

4. **Structure Design**
   The design of a photocathode structure requires computer programs to calculate the parameters for a band structure which calculations show have the desired polarization and charge. The analysis of X-Ray curves also requires X-Ray simulation software.

0.1 Results of Prior Support

The proposal submitted in Oct. 2003 was approved for funding on Oct. 2004. The research is focussed on producing photocathodes which have polarization in excess of 90% and a peak output charge meeting the charge requirements of the ILC. The technical decision for the superconducting version of the linear collider has a favorable impact on this R&D program. The cathode surface charge limit problem is much less for the cold machine since the bunch spacing is 300 ns compared to the much shorter bunch spacing of 1.4 ns that was proposed for the warm machine.

The research to date has been successful in achieving higher polarization and higher QE, but the goal of $> 90\%$ polarization has not been achieved. The polarization appears saturated at 85% and a material-specific spin-depolarization mechanism appears to be present. Consequently, we have embarked on a program to study several types of superlattice structures.

To address material-specific spin depolarization mechanisms and achieve higher polarization, we will continue to study a superlattice stucture proposed by the Russian St. Petersburg group of Y. Mamaev. The Mamaev group has had CDRF funds in partnership with SLAC to study and grow certain superlattice structures. The two year CDRF grant ended Nov. 2004 and resulted in an interesting structure which requires additional study. The stucture developed is a InAlGaAs/GaAs superlattice of about 18 periods. This particular stucture has a lattice matched buffer layer which should result in higher quality with less dislocations and a smaller conduction band offset which should result in greater electron transport. The

previous GaAsP/GaAs superlattice structures we have studied do not have these particular beneficial characteristics. The structure has several parameters which require systematic study.

We have placed an order for several of the InAlGaAs/GaAs stuctures with SVT Associates in Minneapolis. This company has grown other structures for us and we are pleased with the quality of their work.

Another structure we plan to study is a superlattice based on GaAs and InGaP. A GaAs/InGaP superlattice structure differs from the previously studied GaAs/GaAsP superlattice structure in that GaAsP superlattice barrier layers are replaced by InGaP. The GaAs strained wells remain the same.

The new strained superlattice is expected to increase the polarization because the spin relaxation rate in InGaP is less than in GaAsP. Since the band-gap energy of InGaP is larger than that of GaAsP, an enhancement of the Quantum Efficiency is also expected.

Project Activities and Deliverables–FY2004-2006

Research will continue with the goal of producing photocathodes which have polarization in excess of 90% and a peak output charge meeting the charge requirements of a LC with the microbunch structure of the NLC LC. Some of the structures studied to date are excellent candidates for meeting these requirements. The current research is with superlattice structures. Superlattice structures are particularly difficult to design since there are many parameters, making it difficult to simultaneously optimize QE and polarization. The target parameters for a structure are not always met during the fabrication process, making it very important to have many samples and high quality characterization techniques. One of the key studies is how to achieve maximum possible polarization while still satisfying the peak charge requirements.

Work will also continue with studies of atomic hydrogen cathode cleaning which results in being able to use lower heat cleaning temperatures. Lower heat cleaning temperatures result in lower dopant loss, dopant diffusion, and strain relaxation. We propose to build a hydrogen cleaning system with a load-lock system which will enable the transfer of cathodes between test systems.

Budget Justification

We propose a budget for the following items:

1. **Purchase of photocathode structures from a commercial source** The commercial source is presently SVT Associates which has the facilities for MBE growth with Be doping. The request for each FY is for 5 cathode structures @ 3K$ each, representing about 1/2 of the research requirements.

2. **Facility Upgrade** We plan to upgrade the photoluminescence facility which Robin Mair, a former Wisconsin student, used for his PhD work on the study of strained

photocathodes. The photoluminescence facility has proven to be very valuable for structure characterization. The photocathode structures discussed above require an expanded wavelength range which will be accomplished by obtaining more diode laser heads. The request is for two laser heads for year 1 with a similar amount for additional photoluminescence diagnostic equipment in years 2 and 3.

3. **Characterization Studies** X-Ray and SIMS analyses are done off-site and payment is required. We have in the past done X-Ray analyses at Wisconsin and currently use a facility on the Stanford campus. We run the analyses but pay to use the facility. SIMS analyses are done by a commercial vendor. SIMS analyses measure the doping profile of the samples. The request is for 1/2 of the anticipated research needs.

4. **Travel** The travel request is for 1/2 of the Prepost trips to SLAC.

Budget (K$)

Item	FY2004	FY2005	FY2006
Cathodes	15	15	15
X-Ray Analyses	5	5	5
SIMS Analyses	3.6	3.6	3.6
Laser Heads	3	0	0
Diagnostic Equipment	0	3	3
Travel	5	5	5
Total Direct Costs	31.6	31.6	31.6
Indirect Costs	3.0	3.0	3.0
Total	34.6	34.6	34.6

References

[1] "Atomic Hydrogen Cleaning of Polarized GaAs Photocathodes", T. Maruyama et al., Appl. Phys. Lett. **82**, 4184 (2003).

[2] "A Very High Charge, High Polarization Gradient Doped Strained GaAs Photocathode", T. Maruyama et al., Nucl. Instrum. Meth **A492**, 199 (2002).

[3] "Photovoltage Effects in Photoemission from Thin GaAs Layers", G.A. Mulhollan et al., Phys. Lett. **A282**, 309 (2001).

[4] "Measurement of the Deformation Potentials for GaAs Using Polarized Photoluminescence", R. Mair, R. Prepost, E.L. Garwin, and T. Maruyama, Phys. Lett. **A 239**, 277 (1998).

[5] "Anisotropies in Strain and Quantum Efficiency of Strained GaAs Grown on GaAsP", R. A. Mair et al., Phys. Lett. A **212**, 231 (1996).

[6] "Electron Spin Polarization in Photoemission from Thin $Al_xGa_{1-x}As$", T. Maruyama, E. L. Garwin, R. A. Mair, R. Prepost, J. S. Smith, and J. D. Walker, J. Appl. Phys. **73**, 5189 (1993).

[7] "Electron Spin Polarization in Photoemission from Strained GaAs Grown on GaAsP", T. Maruyama, E. L. Garwin, R. Prepost, G. H. Zapalac, Phys. Rev. **B46**, 4261 (1992).

[8] "Observation of Strain Enhanced Electron Spin Polarization in Photoemission from InGaAs", T. Maruyama, E. L. Garwin, R. Prepost, G. H. Zapalac, J. S. Smith, and J. D. Walker, Phys. Rev. Lett. **66**, 2376 (1991).

[9] "Enhanced Electron Spin Polarization in Photemission from Thin GaAs", T. Maruyama et al., Appl. Phys. Lett. **55**, 1686 (1989).

2.43: Investigation of acoustic localization of rf coupler breakdown

(new proposal)

Accelerator Physics

Contact person
Jeremy Williams
jbw@mail.lns.cornell.edu
(217) 649-8481

Institution(s)
University of Illinois
SLAC

New funds requested
FY05 request: 14,600
FY06 request: 24,300
FY07 request: 24,700

Investigation of acoustic localization of rf coupler breakdown

Classification (subsystem)

Rf couplers

Personnel and Institution(s) requesting funding

J. Williams, Department of Physics, University of Illinois at Urbana-Champaign

Collaborators

G.D. Gollin, M.J. Haney, J. Calvey, M. Davidsaver, J. Phillips, Department of Physics, University of Illinois at Urbana-Champaign

W.D. O'Brien, Department of Electrical and Computer Engineering, University of Illinois at Urbana-Champaign

M. Ross, Stanford Linear Accelerator Center

Contact Person

J. Williams
jbw@mail.lns.cornell.edu
(217)-649-8481

Project Overview

Electrical breakdown in accelerating structures produces electromagnetic and acoustic signals that may be used to localize (in a non-invasive fashion) the breakdown site inside a cavity. Other indications of breakdown (microwave, X-ray, and dark current measurements) have proven insufficient to elucidate the basic physics of cavity breakdown. During tests of the ILC design it will be important to record information describing electrical breakdown in order to understand why cavities break down, and how cavity design and operating conditions influence accelerator reliability.

The goal of this project is to understand the acoustic properties of coupling structures with a substantial (over 300K) temperature gradient, in order to relate the acoustic signatures of breakdown events to the underlying electromagnetic catastrophes taking place inside the structures. We would do this by deriving (whether explicitly or implicitly) a time-dependant, invertible, acoustic Green's function for an individual structure. This Green's function could be used to predict the signals arriving at various sensors as functions of the acoustic excitation caused by a cavity breaking down. The inverse function, derived from data from a sufficiently large number of sensors, can be used to localize and classify breakdown modes in TESLA rf couplers.

Two years of investigation have so far been conducted at UIUC. The first year of investigation concentrated on building software tools and developing a small amount of laboratory

infrastructure so that we could begin learning about the problems we are confronting. Our second year of investigation continued these developments, increasing the sophistication of the simulation and testing the simulation's fidelity to the underlying physical system.

We have developed an understanding of acoustic events propagating forward in time. In addition to deepening this understanding, our purpose now is to trace backward from effects to causes. We have three methods that may be able to identify the source of an event from signals received at sensors. Each method still needs testing – both simulated and actual – before we can use it to understand electrical breakdown.

Broader Impact

Williams is currently involved in a search for a faculty position at an undergraduate institution. This proposal will be updated when the results of that search are known. Undergraduate institutions are underrepresented for purposes of high-energy physics (HEP) research; most have no active HEP programs. Because the effects of breakdown events are well described by classical mechanics, the research has proved ideal for participation by undergraduates – even undergraduates in the early stages of their higher education. The UIUC students involved have been remarkably productive and insightful; they are continuing LCRD involvement, but shifting their emphasis to a different project. Williams plans to recruit students to continue this project.

Results of Prior Research

Our investigation has begun with examining NLC rf accelerating cavities. Although these cavities are simpler in structure, they have electromagnetic breakdown problems similar to those of TESLA rf couplers; they were a good place to begin investigations prior to the decision on an accelerating technology. Since the NLC structures are held at high temperature when they are assembled by brazing, the copper's grain size grows so that sound waves must propagate through a crystalline medium with randomly oriented, irregularly shaped grains a few millimeters in size. We have worked with two sets of copper dowels on loan from the Fermilab NLC structure factory. The copper stock is from a shipment of material used to construct actual NLC test structures. One set of dowels has been heat-annealed to bring up its grain size; the other has not and consequently has microscopic grains.

We have borrowed several 1.8MHz transducers and associated signal conditioning electronics from Bill O'Brien's lab as well as purchasing a pair of 500kHz Panametrics transducers. A variety of measurements (including speed of sound, attenuation length, and beam spread) for dowels of different lengths provide us with a nice set of experimental inputs with which to confront our acoustic models. Instead of a transducer, we can also use a mechanical tapper to produce acoustic waves in the dowels; this avoids cross-talk between transmitting and receiving transducer channels, although at the cost of not knowing the exact timing of the initial impulse.

We have developed a model for the propagation and detection of acoustic waves in copper. The model describes copper as a (possibly irregular) grid of mass points connected by springs.

We can vary the individual spring constants and the arrangement of interconnections to introduce irregularities representing grains in our simulated material. We can alter the spring constants over larger regions to model varying materials with different speeds of sound. This model, although it may seem simplistic, is able to support a variety of complex phenomena; we are able to tune various physical properties (such as the speeds of sound for compression- and shear-acoustic waves through adjustments of the model's parameters.

Our model, written by two students, performs a fourth-order Runge-Kutta numerical integration to compute the response of mass points to acoustic perturbations. Our early model systems were two-dimensional grids of roughly 10^5 points. We "drive" signals into them using a transducer model in which the piezoelectric device is described as a damped oscillator excited by shocks of short duration. Because of reflections at the ends of the cable used to drive the real transducers, the actual drive signal is complicated; we find we can model it adequately as a series of four closely-spaced impulses. We have used the first echo to guide our selection of drive parameters; the shape of the second echo is well reproduced. We can simulate the transducer signal as a function of time by summing the amplitudes at the "face" of a transducer as it experiences the effects of the acoustic pulse. Figure 1 shows propagation of a simulated acoustic wave in a homogeneous 250×650 point grid. Figure 2 compares a real oscilloscope record of transducer signal vs. time to the results of this two-dimensional simulation. These results are promising but need a considerable amount of refinement.

Scattering off grains produces very complicated effects and it is important to confirm that our calculations are accurate. We have used *MatLab* as a computational engine to generate an analytic solution to the coupled equations describing the forces acting on each mass point. The numerical integration model is able to handle considerably larger systems than is possible with *MatLab*. However, when applied to smaller systems (with a few hundred mass points), the analytical calculation agrees with our model to an accuracy consistent with integration step size and machine precision.

The effect of inhomogeneities on an acoustic wave is dramatic. The disruption suffered by a pulse in an inhomogeneous crystal dumps a significant amount of acoustic energy into the bulk of the copper. This produces an acoustic glow that washes over the transducer site. Figure 3 shows this effect in the (real) heat-treated dowels when we drive them with our 1.8MHz transducers. The existence of the glow implies that transducers monitoring rf couplers are not limited to detecting acoustical breakdown in select regions, but can sense breakdown wherever it occurs.

There are two limitations on transducer placement for our investigations. One limitation is the cost of transducers, making it desirable to choose a method that requires fewer transducers to isolate a breakdown event. The second limitation is the geometry of the systems we are

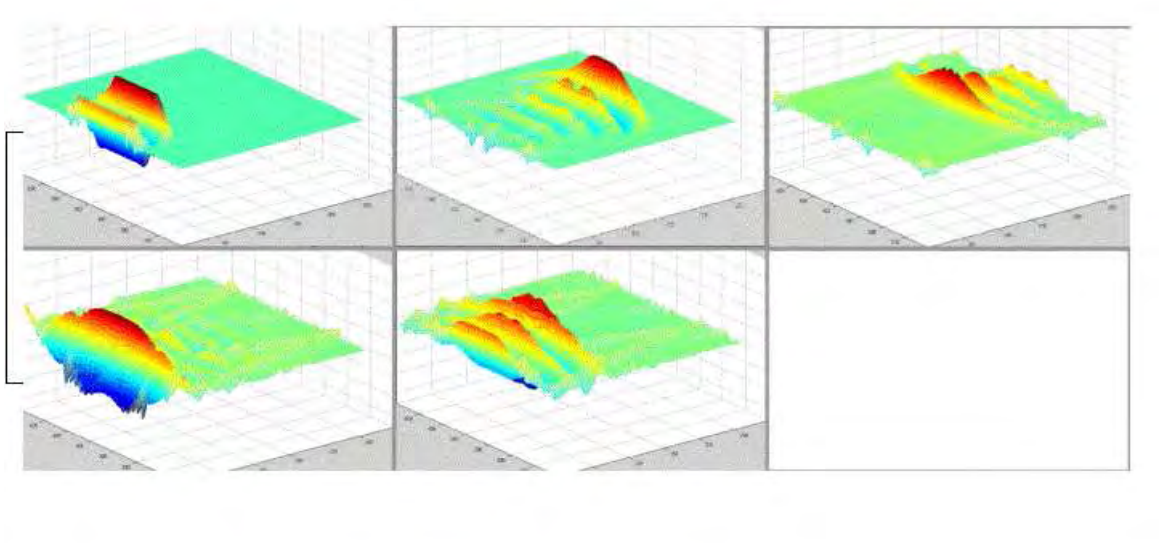

Figure 1: Acoustic wave propagating in a homogenous 250x650 point grid.

studying; even if cost were not a barrier to tiling the outside of NLC cavities or rf couplers with transducers, cooling pipes and power connections still would be.

We are investigating three methods of isolating the source of an acoustic event. One method uses the time-dependent transducer outputs of a simulation as inputs and runs the simulation backward in time. The waves detected by multiple transducers can then be used to isolate the place and time of the original impulse. A small number of transducers (three or four) is capable of isolating the source of an event if they have complete information about the behavior of the small area of the copper surface with which they are in contact. However, because the real transducers we use only receive information about the component of acoustic waves perpendicular to their surface, directional information is lost. Additional information is lost compared to the simulation because, unlike the mathematical points in the simulation, real transducers are extended objects that average over their surface. Better reconstruction may be possible with a large number of transducers. Also, transducers capable of measuring all three directional components of acoustical waves exist, but are custom-made and considerably more expensive than the transducers we use. In order to test the usefulness of transducers capable of sensing motion in three dimensions for isolating acoustic events, it may be possible to rent or borrow such transducers built for another purpose.

A second method is to triangulate the source of an event based on relative arrival times of glow at various transducers. Because arrival time is susceptible to analytic treatment, it is possible to pursue source triangulation both in conjuntion with and independently of our

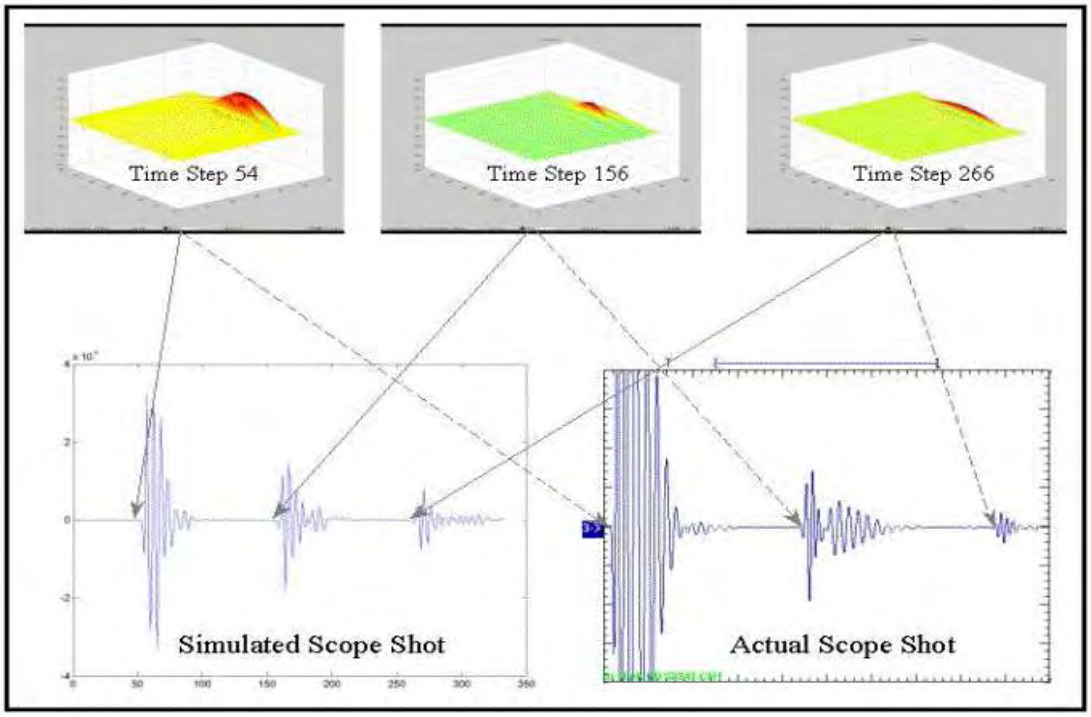

Figure 2: Real transducer output compared to a simulation.

simulations. Without *a priori* knowledge of the absolute time of the event, a minimum of four transducers is necessary to define a point source uniquely by this method. If the source is not pointlike, additional transducers are necessary to determine its location and extent. Propagation of direct signals precedes that of the glow; the process of triangulation could be disrupted by early responses by transducers in the direct path of an event. The geometry of the material in which the acoustic waves propagate can create discrete ambiguities in signal source. So far, we have only considered triangulation in a simplified model of an NLC accelerating cavity; we do not yet know how well this method will work in systems of more complicated geometry (such as TESLA rf couplers).

Our third method uses not only the leading edge of the acoustic glow but also its time-evolution. Figure 4 shows simulated responses for four transducers staggered in both axial (z) and azimuthal (ϕ) directions along an NLC cavity. Shown for each transducer are responses to signals from five sources at the same ϕ but separated in z by intervals of 2 cm. This method requires us to build a library of transducer responses to various breakdown modes, and then use a fitting program such as MINUIT to distinguish among the modes. By using the complete time-dependent record (rather than just the arrival time) from each transducer, we can treat the transducer responses as linear combinations of breakdown modes, and thus distinguish point sources from extended sources without requiring additional transducers.

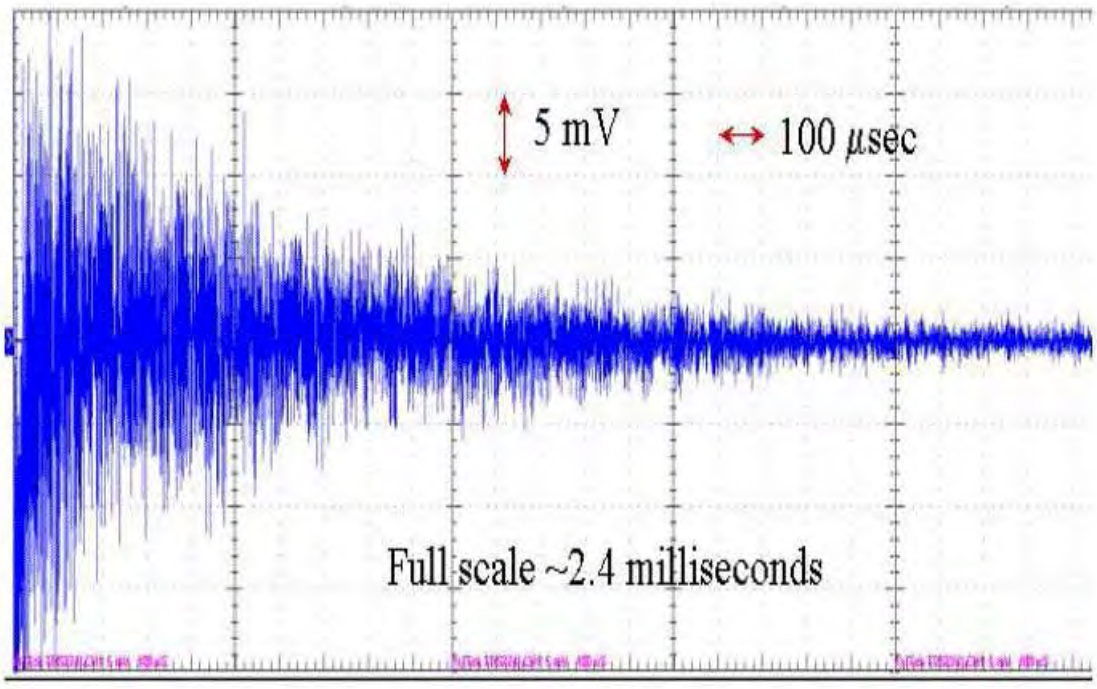

Figure 3: Acoustic glow at long times observed in a heat-treated, long, copper dowel. Note that the scope trace is not showing noise; the fine structure is reproducible from shot to shot.

We have solved several of the immediate challenges that faced us one year ago. We have made improvements in the efficiency of the simulation code, allowing us feasibly to simulate systems with a larger number of mass points, including three-dimensional systems. We have moved from simulation of simple geometrical regions to models of accelerating structures. The simulation is now able to handle multiple grains in the simulated medium (a year ago, at most one grain was possible). We have added a mechanical tapper as an alternate source of signals for the laboratory setup. We have improved our simulation of the transducers.

We will continue to pursue this investigation on several levels. Our models of accelerating structures still have room for additional refinements, modeling both temperature dependence and the more complex makeup of the TESLA rf coupler (the latter is shown in Fig. 5). We need a more quantitative understanding of grain structure and its effect on signal transmission. All three methods of source localization appear promising, and it is not yet clear which will yield the best resolution; each has its own particular challenges. The test of our methods is not merely internal self-consistency nor simulation benchmarks, but external validation by testing with real systems including the couplers.

Facilities and Resources

The University of Illinois High Energy Physics group has excellent computing, networking, and electronics design infrastructure. Our group includes three electrical engineers and two technicians; Haney heads this electronics group. Another member of the group's technical staff manages the group's computing, which comprises a mixture of unix, linux, and Windows machines as well as file and print serving resources. Some of our laboratory instrumentation is managed by realtime systems such as VxWorks running in VME processors; a number of groups use PCI bus modules installed in lab Windows machines which run LabVIEW to control devices.

FY2005 Project Activities and Deliverables

The collaborators' work on this project is already funded as part of LCRD. Williams, a UIUC postdoc, is currently seeking a faculty position; this proposal will be updated when the results of this search are known. A principal activity of the first year of this proposal, therefore, will be transplanting the project to a different institution and recruiting new students to participate. During the first year, we also plan to:

- Develop a geometrical description of TESLA rf couplers suitable for use in our simulations.
- Ensure the isotropy of signal propagation in three-dimensional simulations.
- Determine the precision with which the source of a breakdown event can be located in rf couplers by profile matching.
- Develop a quantitative description of how wave behavior (e.g. propagation speed, dispersion, attenuation) varies in the simulation with grain size.
- Determine the minimum number of transducers needed for the location of a point source in a rf coupler to be unambiguously determined by signal arrival time.

FY2006 Project Activities and Deliverables

For the second year, we plan to:

- Adapt our simulations to include the temperature dependence of ultrasound propagation.
- Develop a method to measure ultrasound in materials at temperatures below the operating range of the transducers, perhaps by coupling acoustically without thermal coupling.
- Expand our model of rf couplers to include material and temperature variations.
- Acquire (preferably by renting or borrowing) transducer(s) capable of two- or three-dimensional measurements to test their use with our back-propagation technique.
- Match wave attenuation between simulation and bench tests.
- Investigate the possibility of field-testing our methods in conjunction with tests of rf couplers at ANL and FNAL.
- Complete such other studies as are suggested by our first-year objectives.

FY2007 Project Activities and Deliverables

By the third year, we plan to have at least one functioning method (and preferably more) to localize breakdown in rf couplers and determine optimum placement of transducers.

Budget justification: Unidentified Institution

The largest component of budget is student wages. This figure is based on two students each working 750 hours/year at a rate of $ 6.50 / hour. Because new students have not yet been recruited, we halve the number of hours for FY2005.

Equipment is a second large component of the budget. In FY2005, this includes two PCs on which to run simulations. In later years, we require transducers for bench tests. Conventional 500 kHz transducers cost $ 500 each; to locate an acoustic event requires at least four. Conventional transducers are sensitive to one component of an acoustic wave; one of our methods requires transducers sensitive in two or three dimensions. Such sensors are custom-built at a price of about $ 1500 each.

We include travel funds sufficient for one trip to a national laboratory in the first year and two trips per year thereafter.

Three-year budget, in then-year K$

Institution: [University of Illinois at Urbana-Champaign]

Item	FY2005	FY2006	FY2007	Total
Other Professionals	0	0	0	0
Graduate Students	0	0	0	0
Undergraduate Students	4.9	9.8	10.1	
Total Salaries and Wages	4.9	9.8	10.1	
Fringe Benefits	0.1	0.2	0.2	0.5
Total Salaries, Wages and Fringe Benefits	5.0	10.0	10.3	
Equipment	6.0	7.0	7.0	20.0
Travel	0.7	1.4	1.4	3.5
Materials and Supplies	0	0	0	0
Other direct costs	0	0	0	0
Total direct costs	11.7	18.4	18.7	48.8
Indirect costs	2.9	5.9	6.0	14.8
Total direct and indirect costs	14.6	24.3	24.7	63.6

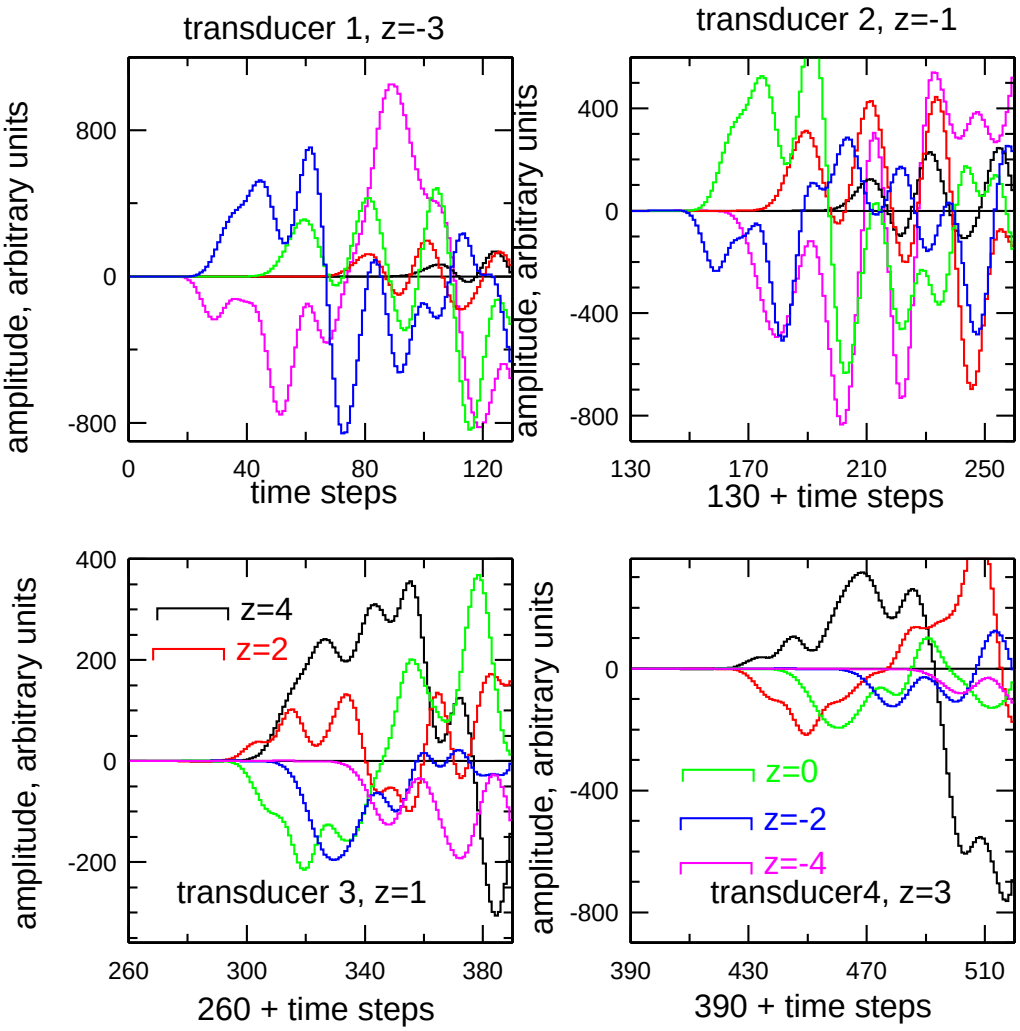

Figure 4: Amplitude vs. time for four simulated transducers staggered in both ϕ and z about a cylinder. The time range is the same for each of the four transducers. For each of the transducers, response to signals from five different z positions (colors) is shown.

2.44: 20-MW Magnicon for ILC

(new proposal)

Accelerator Physics

Contact person
J.L. Hirshfield
jay.hirshfield@yale.edu
(203) 432-5428

Institution(s)
Budker Institute
Omega-P Inc.
Yale

New funds requested
FY05 request: 60,507
FY06 request: 64,875
FY07 request: 65,850

20 MW Magnicon for International Linear Collider ILC

Classification (subsystem)

linear accelerator RF system

Personnel and institution requested funding

J. L. Hirshfield, M. A. LaPointe, S. Finkelshteyn; Yale University

Collaborators

O. A. Nezhevenko, Omega-P, Inc.
V. P. Yakovlev, Omega-P, Inc.
E. V. Kozyrev, Budker Institute of Nuclear Physics, Novosibirsk

Project leader

J. L. Hirshfield
jay.hirshfield@yale.edu
(203) 432-5428

PROJECT OVERVIEW

Introduction

The overall goal of the R&D program outlined here is to design, build, and test a magnicon amplifier at 1.3 GHz with a peak power output in the range of 20 MW, for the future International Linear Collider ILC that is based on superconducting RF technology. This overall project is to evolve into a collaboration between the Yale Beam Physics Laboratory (YBPL), Omega-P, Inc., and Budker Institute of Nuclear Physics, Novosibirsk. Three-year funding for YBPL in the present proposal is mostly to provide infrastructure needed to accommodate the magnicon experimental test facility; further funding for YBPL is anticipated from a Phase II DoE STTR grant to Omega-P, to follow a pending Phase I SBIR grant for refinement of the design of the 1.3 GHz, 20 MW magnicon, and/or from other sources.

There is broad agreement in the high energy physics community that a linear e^+-e^- collider with a center-of-mass energy E_{cm} = 500-1000 GeV and a luminosity above 10^{34} $cm^{-2}s^{-1}$ is of fundamental importance for the future development of particle physics; it is in many respects

expected to be complementary to the Large Hadron Collider LHC (under construction at CERN), and is anticipated to be built as the next large accelerator facility. In 2004, the International Committee for Future Accelerators (ICFA) formed the International Technology Recommendation Panel (ITRP) to evaluate the two competing technologies and to recommend a single choice on which to base ILC. One approach, developed by the TESLA collaboration [1], accelerates beams in 1.3 GHz (L-band) superconducting cavities. The second approach, a result of joint research by the NLC and GLC collaborations [2], accelerates beams using 11.4 GHz (X-band) room temperature copper structures. ITRP recommended that ILC be based on superconducting L-band RF technology [3].

In TESLA [2], considered to be the basis for ILC, the two main linacs would each be constructed from about 10^4 one-meter long, nine-cell superconducting cavities operating at 1.3 GHz. Groups of twelve such cavities would be installed in a common cryostat. The accelerating gradient would be about 25 MeV/m and the final center-of-mass (c.m.) energy would be 500 GeV. RF-power would be generated by some 600 klystrons, each feeding 36 nine-cell cavities. Required peak power per klystron is 9.5 MW, including a 10% overhead for correcting phase errors during the beam pulse which arise from Lorentz force detuning and microphonics. RF pulse length is 1.37 ms, which includes the beam pulse length of 950 μs, and the cavity fill time of 420 μs. The repetition rate is 5 Hz for the major part of the linac, but the 5-50 GeV section stations will run at 10 Hz to alternate between XFEL and linear collider operation. Three versions of 10 MW multibeam klystrons (MBK) have so far been designed and built as candidate RF source for TESLA. The MBK TH1801 (Thales) [4] having a beam voltage of 117 kV and an efficiency of 65% was tested; three tubes were built and one tube is now in use at the TESLA Test Facility. However, the tube still has a problem caused by arcing in the gun [5] and needs improvements in order to achieve stable operation. Another MBK, VKL-8301 (CPI) [6] that demonstrated efficiency of 60%, but with an achieved pulse width of only 10 μs, is under test at this writing. The third MBK, E3736 (Toshiba) has demonstrated parameters close to full design values, namely a peak power of 10 MW, an efficiency of 65%, and operation with a 1 msec pulse width [7]. The major differences between ILC and TESLA are (*i*) a higher accelerating gradient for ILC of 35 MeV/m, which has already been achieved [8], or possibly a yet higher gradient of about 40 MeV/m [9]; and (*ii*) ILC should be upgradeable to a c.m. energy of 1 TeV.

The requirement for the capability of an upgrade in c.m. energy to 1 TeV represents a serious challenge for the RF system, especially for the high-power RF sources. In the simplest scenario of upgrade, the collider would require about 1200 - 10 MW klystrons. The high cost and complexity of this approach have led to suggestions of other scenarios, some which require development of an RF amplifier with a peak power about 18 MW [10]. However, regardless of the details of a given scenario, the availability of a 20 MW amplifier would allow lowering the number of tubes to 300 in the 0.5 TeV option, and to 600 in the 1 TeV option, representing an important step towards reducing the complexity and cost for ILC. But despite its evident appeal, this option has not been realized because development of a 20 MW, 1.3 GHz, 1.5-2 msec pulse-width tube represents a highly serious technical challenge. Even at the 10 MW power level, the three MBK developers are faced with problems caused mainly by breakdown in the gun, impossibility to achieve the desired beam area compression, and increased level of beam current interception. In principle, a single beam klystron (SBK) could be designed for this parameter range, but it will be impractical due to its enormous length.

The program proposed here has as its ultimate goal the laboratory demonstration a 20-MW, 1.3 GHz magnicon amplifier* that would replace two MBK′s, and thus reduce by a factor-of-two the number of tubes required for ILC. The magnicon is a deflection-modulated RF amplifier, which has already demonstrated in a wide range of frequencies from 915 MHz to 34.3 GHz a capability for producing multi-megawatt peak power, very high efficiency, and high gain [11-15]. The interaction mechanism of the magnicon does not require beam bunching, and consequently does not require long drift spaces between the RF cavities. As a result, the RF system of a 20-MW magnicon can be substantially shorter than that of an SBK, and similar in size to the RF system employed in 10 MW MBK′s that are now contemplated for ILC.

In the Yale portion of the program as outlined here, laboratory infrastructure would be established in YBPL to allow installation and operation of the magnicon. This infrastructure includes provision of sufficient mains power and of adequate chilled water flow to dissipate the spent power, re-arrangement of an existing access door to provide necessary x-ray shielding, instrumentation to monitor x-ray dose, and data processing instrumentation for monitoring magnicon performance. Under a pending Phase I DoE SBIR grant that would run through April, 2006, Omega-P will on its own carry out design refinements for the magnicon. It is anticipated that joint support for collaborative R&D would then materialize under a follow-on two-year Phase II DoE STTR grant to Omega-P, with Yale as the participating research institution. Until July 2006, the Yale and Omega-P activities would be closely coordinated, but formally independent of one another. Until establishment of the STTR, no Yale facilities will be used for research tasks originating with Omega-P. In the proposal for the Phase II STTR grant that would run until about June 2008, formal linkage is to be established in the manner that is customary between universities and R&D companies operating under STTR auspices. But, because of the long lead time for realization of the infrastructure installations, and since physical modifications of Yale research space should be undertaken with funds directly administered by Yale, independent support is needed to prepare the facilities in advance of final engineering design, installation, and testing of high-power components of the magnicon setup. The modulator, electron gun and beam collector are the first components that would be so tested.

Technical Approach

Several versions of the magnicon have been built, from the decimeter to the millimeter wavelength domains, operating in the first, second and third harmonic modes. The first magnicon gave a power of 2.6 MW at 915 MHz with a pulse length of 30 μsec and electronic efficiency of 85% [11]. That tube, a first harmonic (fundamental) amplifier, was successfully tested in 1985 not only with absorbing loads, but with also a resonant accelerating structure, without use of a ferrite circulator [17]. This success led to projects for development of magnicons at wavelengths from decimeter to millimeter wavelength ranges. A second magnicon is a frequency doubler (or second harmonic amplifier), operating at a frequency of 7 GHz [18,19]. This tube has demonstrated experimentally an output power of 55 MW, an efficiency of 56%, and a gain of ~70 dB in 1 μsec pulses, in very good agreement with simulation results [13,20]. Another frequency-doubling magnicon amplifier at the NLC frequency of 11.424 GHz has been designed and built in a collaboration between Omega-P, Inc. and Naval Research

*Design simulations for the 20-MW, 1.3 GHz magnicon shown in this proposal were obtained by V. P. Yakovlev and O. A. Nezhevenko, of Omega-P, Inc.

Laboratory (NRL). The tube is designed to produce ~60 MW at 60% efficiency and 59 dB gain, using a 470 kV, 220 A, 2 mm-diameter beam. At present, the tube is conditioned up to power level of 25 MW for 0.2 μsec pulse widths. The power is limited by oscillations in the beam collector [14]. Construction of a new collector was completed recently, and the collector is scheduled to be installed in January 2005. Operation of this latter magnicon has established a research facility located at NRL as only the second laboratory in the USA, after SLAC, where high-power microwave development at X-band can take place. A high power third-harmonic magnicon at 34.272 GHz has been designed and built as a microwave source to develop RF technology for a future multi-TeV electron-positron linear collider. After preliminary RF conditioning, this tube produced an output power of 10 MW in 0.25 μs pulses, with a gain of 54 dB [15]. These preliminary results already constitute record values for a millimeter-wave accelerator-class amplifier. While the second and third harmonic magnicon amplifier concepts were introduced in order to achieve high power in the cm- and mm-wave ranges, the first harmonic amplifier has higher efficiency and smaller size than harmonic versions; this can be especially critical at decimeter wave lengths.

Preliminary design parameters of a 20 MW, 1.3 GHz first-harmonic magnicon design for ILC are presented in Table I, and the schematic arrangement is shown in Fig. 1.

The electron gun injects a small diameter pencil beam into a chain of cavities forming the RF system. The deflection system consists of a drive cavity (#1 in Fig. 1) and gain cavities (#2 to #7) to provide the required deflection angle. The external magnetic field provides both beam focusing and coupling between the electrons and the RF fields in the cavities. The scanning beam rotates at the frequency of the drive signal, then enters the output cavity (#8) and emits radiation by interacting with the TM_{110} mode. All cavities of the RF system oscillate in the circularly polarized TM_{110} mode at 1.3 GHz. The proposed magnicon amplifier will operate with a 300 kV, 100 A electron beam to meet the requirements for operation in ILC, namely 20 MW peak output power with a 1.5 ms pulse duration, and a 10 Hz repetition rate. The average power level for this beam is thus 450 kW.

Table I. Preliminary design parameters of 20 MW, 1.3 GHz magnicon amplifier.

operating frequency, MHz	1300
output peak power, MW	~21
average power, kW	300
pulse duration, msec	1.5
repetition rate, Hz	10
efficiency, %	~70
gain, dB	>44
FWHM bandwidth, MHz	~2
beam power, MW	30
beam voltage, kV	300
beam current, A	100
beam perveance, $A/V^{3/2}$	0.61×10^{-6}

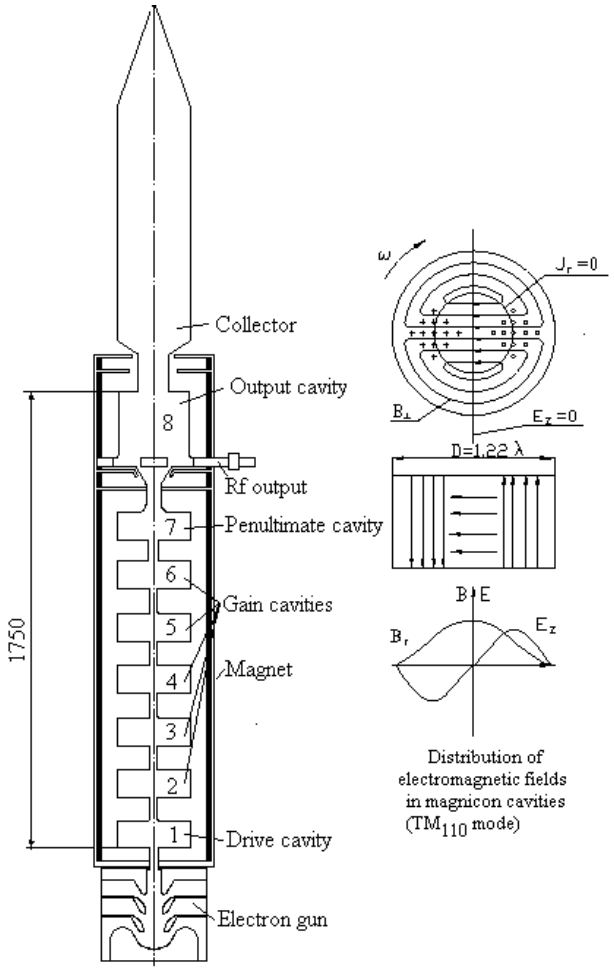

Figure 1. Schematic of 20 MW, 1.3 GHz magnicon amplifier. Note that the 1.75-m length of the RF system is about the same as for the 10 MW Thales MBK TH1801 [4].

The shapes of the cavities are carefully designed to get high efficiency with the smallest possible magnitude of RF fields in the cavities. The maximum surface electric fields in the penultimate and output cavities do not exceed 75 kV/cm. All cavities in the deflection system (#1 to #7 in Fig. 1) are 280 mm in diameter and 100 mm long. For efficient interaction the RF electric and magnetic fields in the output cavity (#8 in Fig. 1) must have nearly similar profiles along the axis, as shown in Fig. 2. Such profiles were obtained by increasing the diameter of the cavity near its entrance [21] as can be seen in Fig. 2. Increase in diameter of the output cavity to 306 mm is also advantageous when using four output waveguides and windows, which may be desirable at the high power level (e.g. as suggested in [10]).

Fig. 3 shows the required magnetic field profile (top) and the coil configuration and iron yoke geometry to achieve this profile (bottom). For effective deflection, the magnetic field in the deflection system should be about 930 Gauss. However, in the output cavity, for efficient extraction of energy, the magnetic field should be about 650 Gauss. One can see that the required levels of magnetic field are quite modest.

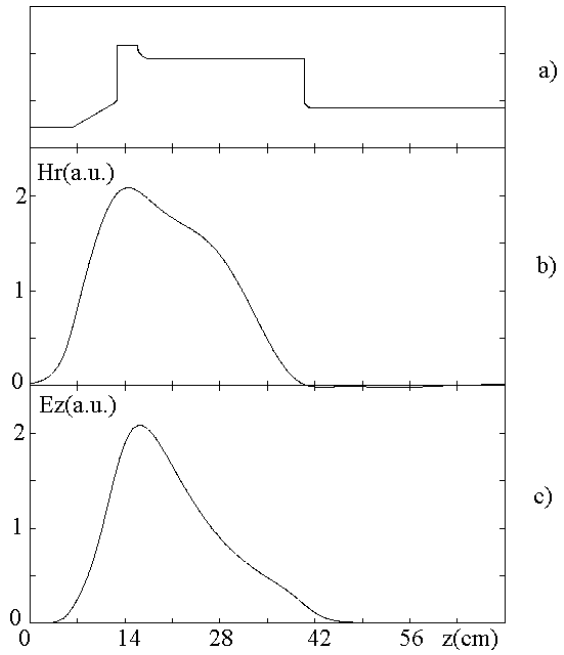

Figure 2. (a) The output cavity layout, (b) transverse magnetic field and (c) longitudinal electric field distribution along the cavity axis at a radius of 20 mm.

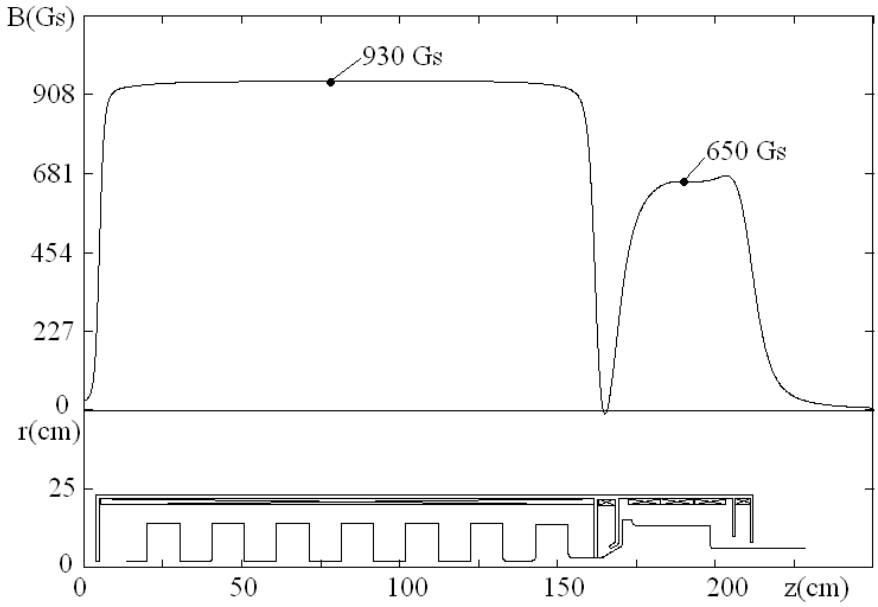

Figure 3. Required axial magnetic field profile (top), coils and iron yoke layout (bottom). Cavity chain is also shown at the bottom.

In Fig. 4 are shown the results of magnicon steady-state simulation. One can see that the deceleration is relatively uniform, and that the beam loses a substantial part of it's energy (>70% on average). The beam trajectories indicate that there is no current interception in the tube. The absence of current interception was proven experimentally in different tested versions of magnicons [11-15].

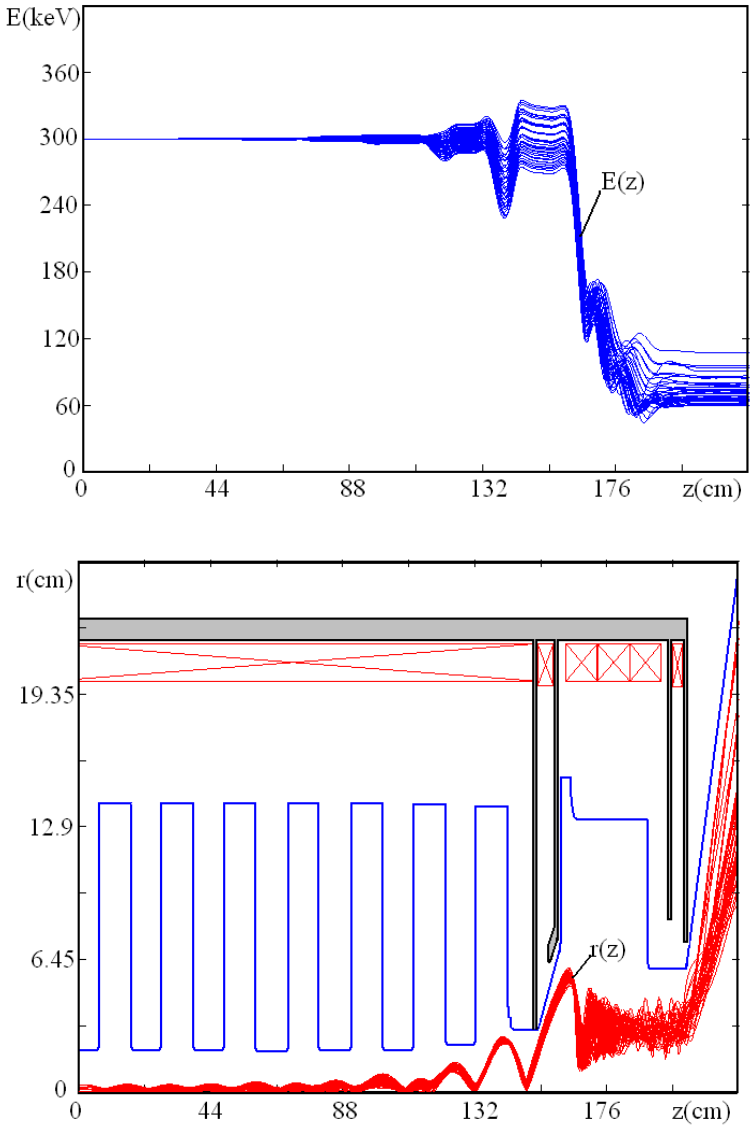

Figure 4. Results of preliminary simulations for a 20 MW, 1300 MHz magnicon. Shown is an outline of the RF cavities, energy *E* and radial coordinates of beam electrons *r*, all as functions of coordinate *z* along the axis of the tube.

Results of time-dependent simulations of transient process in this magnicon amplifier are shown in Figure 5. One can see that the transient process is smooth, and that the build-up time for steady oscillations is about 0.8 μsec. The calculated dependence of the drive curve, i.e. output power *vs.* input power, is shown in Figure 6. The drive curve is monotonic, indicating that the tube operates stably within the full range of output power. Calculated magnicon output power *vs* drive frequency is shown in Figure 7. It indicates that the tube's FWHM bandwidth is about 2 MHz.

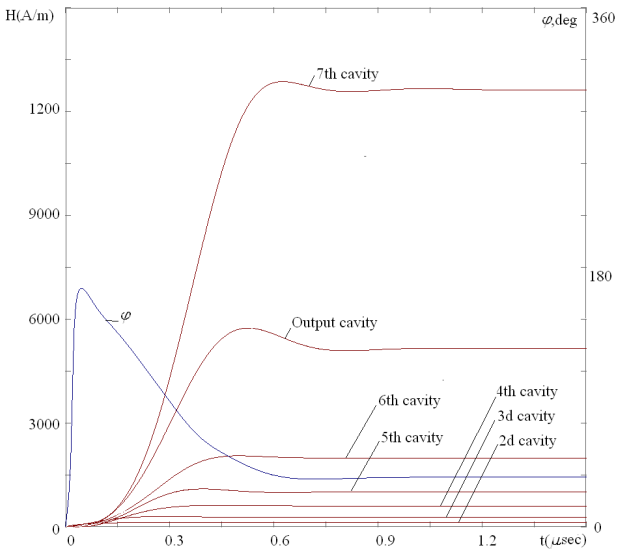

Figure 5. Example of transient processes in the magnicon. Shown are the computed RF amplitudes in the cavities and phase φ in the output cavity, *vs* time from the start of the RF pulse.

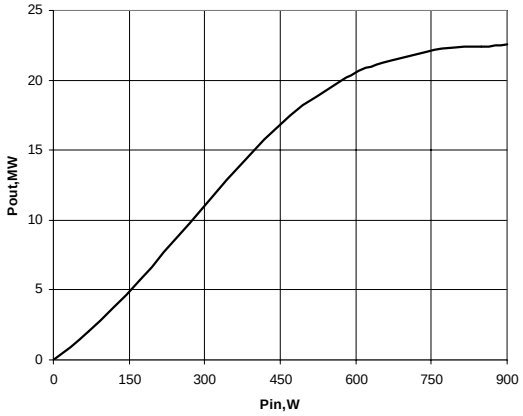

Figure 6. Output power *vs*. input power. Note, in this example, that the output power actually rises to > 22 MW.

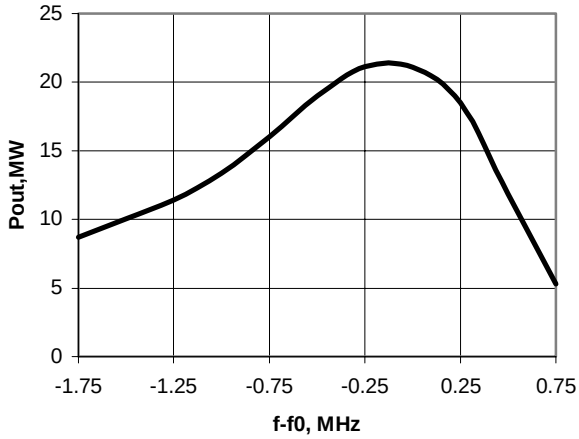

Figure 7. Output power vs. frequency. FWHM bandwidth is about 2 MHz.

Due to the long pulse, the acceptable electric field in the gun must be relatively low. For pulse lengths longer than about 1.0 msec, an empirical relation on the high voltage breakdown condition is given by $E_s V_e$ < 800 kV^2/mm, where E_S is surface electric field on the electrode at lower potential and V_e is the voltage between two electrodes [22]. This requirement represents a challenge in the gun design which can be overcome by using a multi-gap (multi-anode) gun concept. In the proposed magnicon, the beam parameters are: beam voltage of 300 kV and beam current of 100 A. To provide these parameters with a pulse-width of about 2 msec, a triple-anode gun with a spherical cathode 8 cm in diameter has been designed, as shown in Fig. 8. The maximum cathode loading doesn't exceed 2.7 A/cm^2, which allows one to expect good cathode longevity of ~100,000 hours according to [23].

Due to the long pulse, the acceptable electric field in the gun must be relatively low. For pulse lengths longer than about 1.0 msec, an empirical relation on the high voltage breakdown condition is given by $E_s V_e$ < 800 kV^2/mm, where E_S is surface electric field on the electrode at lower potential and V_e is the voltage between two electrodes [22]. This requirement represents a challenge in the gun design which can be overcome by using a multi-gap (multi-anode) gun concept. In the proposed magnicon, the beam parameters are: beam voltage of 300 kV and beam current of 100 A. To provide these parameters with a pulse-width of about 2 msec, a triple-anode gun with a spherical cathode 8 cm in diameter has been designed. A layout of the electrode configuration for the gun and sample electron trajectories are shown in Fig. 8. The maximum cathode loading doesn't exceed 2.7 A/cm^2, which allows one to expect good cathode longevity of ~100,000 hours according to [23]. Current density distribution over the cathode surface is shown in Figure 9. In the present gun design, E_S = 51 kV/cm on the focus electrode and $E_S V_e$ = 510 kV^2/mm between the first anode and the focus electrode. On the first anode E_S = 45 kV/cm and $E_S V_e$ = 450 kV^2/mm between the two anodes. On the second anode E_S = 50 kV/cm and $E_S V_e$ = 500 kV^2/mm between the two anodes. These values are comfortably below the breakdown limit. Long life cathode operation can be expected with these levels of surface field in the gun [23]. Preliminary gun design parameters are listed in Table II.

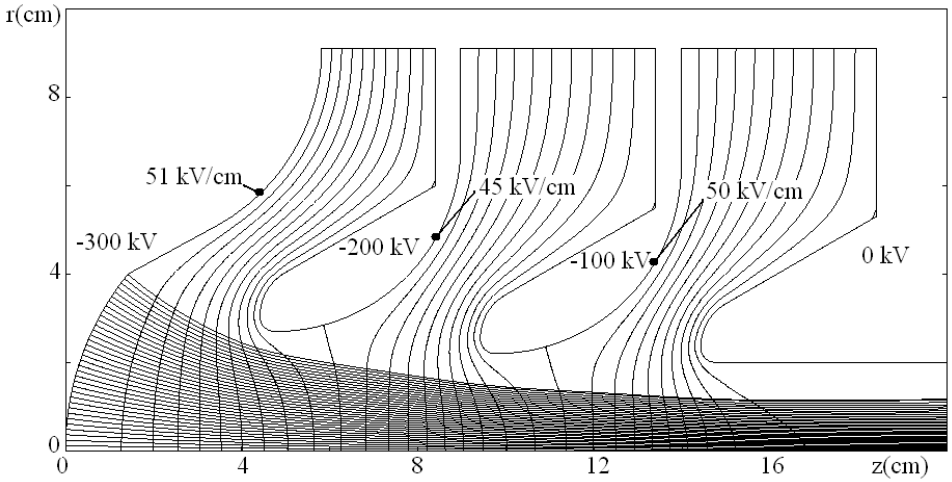

Figure 8. The triple-anode gun layout, trajectories and equipotential lines.

These preliminary design results show that no fundamental impediment exists to realization of a 1.3 GHz magnicon amplifier with a peak power of 20 MW in a pulse-width of 1.5 msec. Logistical issues in the realization of a prototype involve detailed engineering designs and fabrication for the components of the tube, namely the electron gun, RF cavity system, magnetic field, system, and beam collector. A suitable modulator must be obtained, although some compromise in average power (below the 450 kW design beam power) might be required due to ac mains power limitations in YBPL, and to specifications of the modulator that can be acquired within budgetary limitations; however tests at the full pulse width of 1.5 ms are deemed essential for validation of the design. But before engineering designs can be deemed final, space, utility, and radiation shielding parameters must be fixed. Infrastructure needs can be met within an unused 1200 sq. ft. vault in YBPL, a drawing of which is shown in Figure 10. The x-ray shielded control area encloses a 12′×24′×8′ high RF shielded room with two access doors.

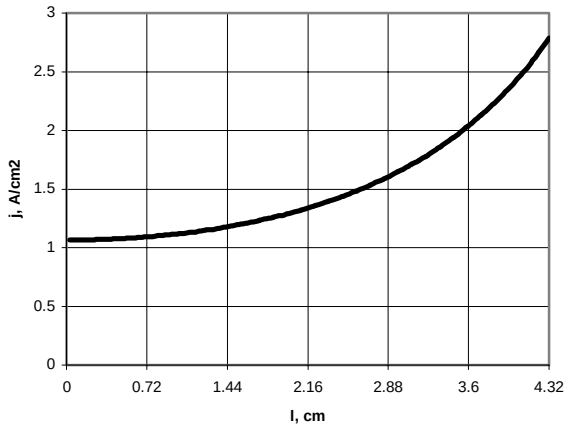

Figure 9. Current density distribution along the cathode surface; *l =0* corresponds to the cathode center.

Table II. Design parameters of the electron gun for a 20 MW, 1.3 GHz magnicon.

beam voltage, kV	300
beam current, A	100
beam power, MW	30
beam perveance, $A/V^{3/2}$	0.61×10^{-6}
pulse duration, msec	1.5
repetition rate, Hz	10
cathode diameter, mm	80
maximum cathode loading, A/cm^2	2.7
number of anodes	3
voltage between the cathode and the 1st anode, kV	100
maximum electric field on the focus electrode (the 1st gap), kV/cm	51
voltage between the 1st anode and 2d anode, kV	100
maximum electric field on the 1st anode (the 2d gap, kV/cm)	45
voltage between the 2d anode and 3d anode, kV	100
maximum electric field on the 2d anode (the 3d gap), kV/cm	50
electrostatic compression	11:1

At present, only 72 kW of 208-V, 3-phase mains power is wired into in the test vault. One goal of the infrastructure up-grade that is proposed is to increase the mains power as much as possible by re-directing power from the 1.5 MW sub-station that powers some of the other areas in YBPL, with the goal of operating the magnicon at a repetition rate of at least 2 Hz. It will also be necessary to install a closed-loop cooling system to dissipate spent power; it is proposed to accomplish this by installing a cooling tower on the laboratory roof (at a position above the 3′ shielding wall) which, together with a pump and heat exchanger, will provide the cooling. An additional modification is needed to allow the large radiation shielding door shown in Fig. 10 to close; it is now blocked by water pipes that were thoughtlessly installed before re-use of the vault was contemplated. These infrastructure changes should be in place before engineering design for the 20-MW, 1.3 GHz magnicon is completed, so that specifications for the mains power needs

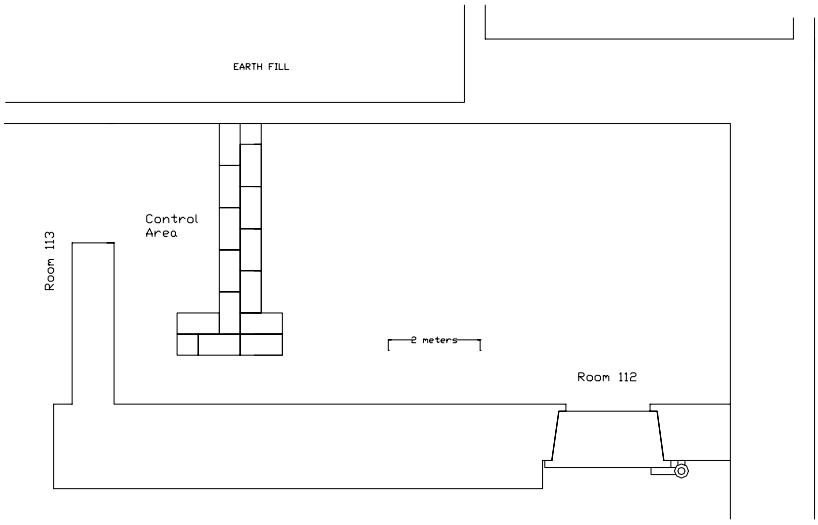

Figure 10. Test vault available within the Yale Beam Physics Laboratory.

will match needs of the available modulator, and so that the physical arrangement in the vault of the (relatively) large experimental magnicon tube and associated components can be optimized. As stated on p. 2 of this document, this would require the infrastructure improvements for the vault to be fully designed, with installations underway by July, 2006, when the formal collaboration sets in between Yale and Omega-P, assuming timely award of a Phase II STTR grant to Omega-P for this project. The third-year portion of the Yale grant requested here is for acquisition, installation, and calibration of instrumentation to monitor x-ray dosage in designated areas of the laboratory, and to diagnostic signals from the magnicon under test. It is appropriate that the costs for these infrastructure installations and instrumentation come from a research award directly to Yale, as they would become integrated as permanent facilities of YBPL.

RESULTS OF PRIOR SUPPORT

There has been no prior support for development of the specific magnicon described in this proposal. However, prior support has been provided by DoE and BINP for a number of versions of the magnicon to be designed and built from the decimeter to the millimeter wavelength domains, operating in the first, second and third harmonic modes. The first magnicon was built and tested in 1985 in Novosibirsk [11]. A power of 2.6 MW was obtained at 915 MHz with a pulse length of 30 μsec and electronic efficiency of 85%. That tube is a first harmonic (i.e., fundamental) amplifier. The device was successfully tested not only with absorbing loads, but with a resonant accelerating structure as well, without use of a ferrite circulator [17]. This success led to projects for development of magnicons at wavelengths from decimeter to millimeter ranges for different accelerator projects. A second magnicon, also developed in Novosibirsk, is a frequency doubler (or second harmonic amplifier), operating at a frequency of 7 GHz [18,19]. This tube has demonstrated experimentally an output power of 55 MW, an efficiency of 56%, and a gain of ~70 dB in 1 μsec pulses, in very good agreement with simulation results [13,20]. Another frequency-doubling magnicon amplifier at the NLC frequency of 11.424 GHz has been designed and built in a collaboration between Omega-P, Inc.

and Naval Research Laboratory (NRL). The tube is designed to produce ~60 MW at 60% efficiency and 59 dB gain, using a 470 kV, 220 A, 2 mm-diameter beam. At present, the tube is conditioned up to power level of 25 MW for 0.2 μsec pulse widths. The power is limited by the oscillations in the beam collector [14]. Construction of a new collector was completed recently, and the collector is scheduled to be installed in January 2005. Operation of this latter magnicon has established a research facility located at NRL as only the second laboratory in the USA, after SLAC, where high-power microwave development at the X-band frequency can take place. A high power third-harmonic magnicon at 34.272 GHz has been designed and built as a microwave source to develop RF technology for a future multi-TeV electron-positron linear collider. After preliminary RF conditioning, this tube produced an output power of 10 MW in 0.25 μs pulses, with a gain of 54 dB [15]. Higher power currently obtains, as RF conditioning progresses. These preliminary results constitute record values for a mm-wave accelerator-class amplifier.

FACILITIES, EQUIPMENT, AND OTHER RESOURCES

Since 1992, efforts have been underway in the Physics Department at Yale to establish and equip the Yale Beam Physics Laboratory. Space in the Wright Nuclear Structure Laboratory (WNSL) on the Yale campus vacated by decommissioning of a 50 MeV L-band electron linear accelerator was made available by the Physics Department for beam physics research. However, the Room 112 vault within the Beam Physics Laboratory shown in Fig. 10, used at present for staging and preparation of experiments, requires the refurbishment described above. Utilities include dedicated use of a 2 MW power company substation (1.5 MW at 480 V; and 0.5 MW at 208 V). Approximately 3500 sq. feet of shielded laboratory space has been refurbished so far, including a 10′×10′×100′ buried tunnel, wherein high voltage, high power rf accelerator operations are conducted without danger of human exposure to penetrating radiation. Areas for a control room, experimental staging, cold testing, electronics assembly, and some staff offices are also part of the laboratory. A copious supply of chilled re-circulating deionized water is available for disposal of at least 100 kW of waste heat, with distribution installed along the tunnel from overhead feed and return lines. Experiments that have been carried in this facility include a 10 MW *CARA* (Cyclotron Autoresonance Accelerator), a 4th harmonic 11.424 GHz multi-MW gyroharmonic converter, a 6 MeV rf gun and 17-element beamline, microwave inverse free-electron laser accelerator *(MIFELA)* and microwave inverse Cerenkov accelerator *(MICA).* It is within this laboratory that the 34-GHz magnicon is installed, together with its 100 MW, 1.5 μsec modulator, data analysis, and test equipment. Other installations include a 24 MW XK-5 former SLAC 2.856 GHz klystron, that is powered by a 65 MW modulator providing 3 μsec, 250 kV, 250 A pulses at up to 10 pps. A 3 MW modulator provides 100 kV, 31.4 A pulses synchronized with the klystron pulses to drive the *CARA* injector. Test equipment is available for S-, X-, and Ka-band measurements, including a scalar network analyzer operating up to 40 GHz. The Yale group also carries out experiments on wake field acceleration in dielectric-lined structures and on LACARA at Brookhaven National Laboratory, Accelerator Test Facility in collaboration with Columbia University and Omega-P, Inc. A fully equipped machine shop is located in Yale Gibbs Laboratory, a few steps from WNSL, where a wide range of operations for the fabrication and vacuum brazing of experimental components can be carried out. Other machining, hydrogen brazing, e-beam welding, waveguide fabrication and internal pipe honing necessary for

specialized steps in equipment fabrication can be carried out at small shops close to New Haven. Mechanical design can be carried out by mechanical engineers at the Gibbs shop. Electronics design, construction and repair operations are performed by a full-time YBPL technician.

STATEMENT ON BROAD IMPACT

The R&D program proposed here has as its goal the design of the 20 MW, 1.3 GHz magnicon amplifier that would replace two multi-beam klystrons, and thus reduce by a factor-of-two the number of high-power tubes required for ILC. This would allow significant simplification of the RF architecture and reduction in cost of ILC, as well as strengthened participation by US entities in RF source R&D and manufacturing in what is so far fragmented between US, European, and Japanese firms. The technical challenges that will be addressed during the proposed R&D will provide training in high-power vacuum electronics to young researchers and students that is only available at a select few universities, and which is needed to provide know-how and experience required to maintain US capability in this field. Results of the R&D can be applied in the industrialization of the 1.3 GHz, 20 MW magnicon, should it be selected for use in the ILC test accelerator; and in the development of similar magnicons for applications in nuclear physics and high-power microwave systems for defense. Costs to support students are not provided for in the budget presented here. Nevertheless, it is anticipated that opportunities for undergraduate and graduate participation in the program will occur. Such participation could include senior research projects required of all Yale physics majors, and summer employment for graduate students prior to their selection of a Ph.D. thesis topic.

REFERENCES

1. R. Brinkmann K. Flöttmann J. Roßbach, *et al.*, "TESLA Technical Design Report," *http://tesla.desy.de/new_pages/TDR_CD/start.html*
2. International Linear Collider Technical Review Committee, 2[d] Report, SLAC-R-606, SLAC,2003.
3. Final Intern National Technology Recommendation Panel Report, September 2004, *www.fnal.gov/directorate/icfa/ITRP_Report_Final.pdf*
4. A. Beunas, G. Faillon and S. Choroba, "A High Power Long Pulse High Efficiency Multi- Beam Klystron," *http://tdserver1.fnal.gov/8gevlinacPapers/Klystrons/Thales_multi_beam_Klystron_MDK2001.pdf*
5. S. Choroba, "Status of RF System," International Technology Recommendation Panel. *ITRP Meeting Two*, April 5 - 6, 2004. DESY – Hamburg, *tesla.desy.de/new_pages/hamburg_meeting_4_2004/talks/ITRP_Choroba_RF.pdf*
6. E. Wright, A. Balkcum, H. Bohlen, *et al*., "Test Results for a 10 MW, L-Band Multiple Beam Klystron For TESLA," *Proceedings of 2004 European Particle Accelerator Conference*, Lucerne, July 2004, pp. 1117-1119.
7. S. Choroba, "RF Power Sources from TESLA for ILC and XFEL," *First ILC Workshop*, KEK, November 2004, *http://lcdev.kek.jp/ILCWS/WG2.php*
8. C. Pagani, "Technical Issues for Large Accelerators based on High Gradient SC Cavities," *9th European Particle Accelerator Conference***,** July 2004, Lucerne, *a**cc**el**c**onf.web.**c**ern.**c**h/A**cc**elConf/e04/HTML/WEYCH.HTML*
9. J. Zekutovicz, "New Cavity Shape for Higher Gradient," *First ILC Workshop*, KEK, November 2004, *http://lcdev.kek.jp/ILCWS/WG5.php*
10. Y.H. Chin and V. Vogel, "Simple-Minded Upgrade Paths to 800 GeV or Higher," *First ILC Workshop*, KEK, November 2004, *http://lcdev.kek.jp/ILCWS/WG1.php*
11. M.M.Karliner, E.V.Kozyrev, I.G.Makarov, O.A.Nezhevenko, G.N. Ostreiko, B.Z.Persov, and G.V.Serdobintsev, "The Magnicon - An Advanced Version of the Gyrokon," *Nucl. Instrum. Methods Phys. Res.* A **269**, 459-473 (1988).

12. O.A. Nezhevenko, "Gyrocons and Magnicons: Microwave Generators with Circular Deflection of the Electron Beam," *IEEE Trans. Plasma Sci.* **22** pp. 765-772, Oct., 1994.
13. E.V. Kozyrev, O.A. Nezhevenko, A.A. Nikiforov, G.N. Ostreiko, G.V. Serdobintsev, S.V. Schelkunoff, V.V. Tarnetsky, V.P. Yakovlev, I.A. Zapryagaev, "Present Status on Budker INP 7 GHz Pulsed Magnicon", RF98 Workshop, Pajaro dunes, October 5-9, 1998, AIP Conference Proc. 474, Woodbury, N.Y., 1999, pp.187-194.
14. O.A. Nezhevenko, V.P. Yakovlev, J.L. Hirshfield, E.V. Kozyrev, S.H. Gold, A.W. Fliflet, and A.K. Kinkead, "Performance Of X-Band Pulsed Magnicon Amplifier," *Proc. 2003 Particle Accelerator Conf.*, Portland, May 11-16, 2003, pp.1128-1130
15. O.A. Nezhevenko, M.A. LaPointe, V.P. Yakovlev, J.L. Hirshfield, "Commissioning of the 34-GHz 45-MW Pulsed Magnicon," *IEEE Trans. Plasma Sci.*, vol.32 pp. 994-1001, June, 2004.
16. G.I. Budker, M.M. Karliner, I.G. Makarov, S.N. Morosov, O.A. Nezhevenko, G.N. Ostreiko, and I.A. Shekhtman, "The Gyrocon—An Efficient Relativistic High–Power VHF Generator," *Part. Accel.*, vol. 10, pp. 41–59, 1979.
17. V.E. Akimov *et al.*, "Accelerating system of the racetrack microtron", Preprint INP 89-162, Novosibirsk, 1989 (in Russian). Deposited into NTIS database.
18. O.A. Nezhevenko, *Proc. 1991 Particle Accelerator Conf.*, San Francisco, 1991, (IEEE, Piscataway, NJ, 1992), p. 2933.
19. V.E. Akimov, Yu.V. Baryshev, B.S. Estrin, M.M. Karliner, I.V. Kazarezov, E.V. Kozyrev, G.I. Kuznetsov, I.G. Makarov, O.A. Nezhevenko, G.N. Ostreiko, B.E. Persov, G.V. Serdobintsev, M.A. Tiunov, V.P. Yakovlev, and I.A. Zapryagaev. *Proceedings of 1990 European Particle Accelerator Conference*, Nice, 1990, (World Scientific, Singapore, 1991), p. 1000.
20. E.V. Kozyrev, O.A. Nezhevenko,A.A. Nikiforov, G.N. Ostreiko, B.Z. Persov,G.V. Serdobintsev, S.V. Schelkunoff, V.V. Tarnetsky, V.P. Yakovlev, I.A. Zapryagaev, "New Results of 7 GHz Pulsed Magnicon Amplifier Investigations", *Proceeding of 1998 EPAC*, Stockholm, June 22-26, 1998, p.1897.
21. A. Nezhevenko, V.P. Yakovlev, and A.K. Ganguly, "Long-Pulse 1.3 GHz Magnicon", *Proc. 1998 European Particle Accelerator Conference*, Stockholm, June 22-26, 1998, p.1906.
22. High Voltage Vacuum Insulation, Edited by R.V. Latham, Acad. Press, N.Y., 1995, pp. 403-429.
23. E. Wright, A. Balkcum, H. Bohlen, *et al*., "Development of 10-MW, L-Band Multiple-Beam Klystron For TESLA," *Proc. 2003 Particle Accelerator Conf.*, Portland, 2003, pp.1144-1146.

PROJECT ACTIVITIES AND DELIVERABLES

As stated above, activities to be supported under the grant requested here include infra-structure improvements in the Yale Beam Physics Laboratory YBPL necessary to accommodate an experimental 20 MW, 1.3 GHz, 1.5 ms pulsed magnicon amplifier intended as an RF power source for the superconducting linacs for the future International Linear Collider ILC. Activities would be distributed over the three-year duration of the grant as follows:

FY2005 Project Activities would include redistribution of electrical power that is now available to YBPL from a nearby power vault, so as to provide sufficient power to a modulator to allow generation of an average beam power of at least 90 kW (corresponding to operation at a pulse repetition rate of at least 2 Hz), plus ancillary power needed for the tube's < 1 kG solenoid magnet and other loads. In addition, runs of water piping that now block the x-ray shielding door shown at the bottom right in Fig. 10 would be relocated so as to allow the door to close. **FY2005 Deliverable** would include a written annual report, plus whatever other presentation(s) are requested by the sponsor, or that are appropriate for dissemination at scientific conferences.

FY2006 Project Activities would include installation of a cooling tower on the building roof above the experimental area shown in Figure 10, of a suitable circulating pump, and of a heat exchanger in the experimental area that can be used to dissipate the > 120 kW of heat expected to be generated from operation of the magnicon at a pulse repetition rate of at least 2 Hz. **FY2006**

Deliverable would include a written annual report, plus whatever other presentation(s) are requested by the sponsor, or that are appropriate for dissemination at scientific conferences.

FY2006 Project Activities would include acquisition of instrumentation required to monitor and record x-ray dose levels in areas of the laboratory occupied by radiation-certified personnel during operation of the magnicon, and adjacent areas open to the general public. It is also useful to monitor radiation levels in areas that are never occupied during experimental runs, and to monitor for the presence of any detectable activation. In addition, instrumentation would be acquired for installation in the control area shown in Figure 10 to allow monitoring of diagnostic signals from the operating magnicon. **FY2007 Deliverable** would include a written annual report, plus whatever other presentation(s) are requested by the sponsor, or that are appropriate for dissemination at scientific conferences.

BUDGET JUSTIFICATION

The budget given below includes salary and fringe benefits for one month each per year for Dr. Michael A. LaPointe, Yale Research Scientist; and Mr. Saveliy Finkelshtyen, Yale Research Technician; these are listed together in the category "Other professionals." Levels are based on current Yale salaries, with a 5% increase each year for FY2006 and FY2007. Fringe benefit rate for DoE grants is 42.3% for all three years. No salary request is made for the Principal Investigator, Dr. Jay L. Hirshfield. Equipment acquisitions include $18,000 for a heat exchanger and pump in FY2005; $22,000 for a cooling tower in FY2006; and $25,000 for radiation monitors ($5,000) and signal processing instrumentation ($20,000) in FY2007. These costs are extrapolated from costs in a facilities study carried out for YBPL by Yale Physical Plant Department in 2001. For FY2005, $5,500 is for costs of re-routing plumbing installations, and in FY $6,000 for installation of the chilled-water cooling circuit in FY 2006. Materials and supplies include electrical, electronic, plumbing, and other infrastructure parts and components needed for the installations. Indirect costs are 63.5% of all direct costs, excluding equipment.

Three-Year Budget Request

Item	FY2005	FY2006	FY2007	Total
Other professionals	10,188	10,698	11,233	32,119
Graduate students				
Undergraduate students				
Total salaries and wages	10,188	10,698	11,233	32,119
Fringe benefits	4,310	4,525	4,752	13,587
Total salaries, wages and fringe benefits	14,498	15,223	15,985	45,706
Equipment	18,000	22,000	25,000	65,000
Travel				
Materials and supplies	6,000	5,000	9,000	20,000
Other direct costs	5,500	6,000		11,500
Institution 2 subcontract				
Total direct costs	43,998	48,223	49,985	142,206
Indirect costs	16,509	16,652	15,865	49,026
Total direct and indirect costs	60,507	64,875	65,850	191,232

2.45: SCRF Low-Level RF (LLRF) Development for ILC-SMTF

(new proposal)

Accelerator Physics

Contact person
Nigel Lockyer
lockyer@physics.upenn.edu
(215) 898-5806

Institution(s)
University of Pennsylvania

New funds requested
FY05 request: 21,794
FY06 request: 95,232
FY07 request: 98,089

SCRF Low-Level RF(LLRF) Development for ILC-SMTF

Classification (Cryomodule LLRF)

Personnel and Institution(s) requesting funding

N. S. Lockyer
University of Pennsylvania

Collaborators

There are several groups interested in working on the project and others that are willing to consult based on their significant experience. Those presently interested in working on the project include a group from Fermilab (Helen Edwards, Philippe Piot, Ralph Pasquinelli, Brian Chase, Bill Foster), the Pisa group led by Giorgio Bellettini, and the University of Pennsylvania. Experts being consulted include Stefan Simrock from DESY, Larry Doolittle from LBNL, Mark Champion from Oak Ridge, Matthias Liepe Cornell, and Marc Ross from SLAC.

Project Leader

N. S. Lockyer
rutherford.hep.upenn.edu
215-898-5806

Project Overview

We are planning to participate in a new national initiative in Superconducting Radio Frequency (SCRF) research. A Expression of Interest (EOI) or pre-proposal has been submitted to Fermilab outlining the ambitious plan. The proposal is entitled "Superconducting Module Test Facility" or SMTF. The proponents (except Penn) are all accelerator physicists. This proposal is intended to help establish a new direction of research in the particle physics group in the Physics Department, SCRF research in accelerator physics. We propose to collaborate on instrumentation for the LLRF and controls for the "capture cavity" and future energy upgrades planned for the electron beam test facility at Fermilab called the A0 photoinjector and SMTF in general. The photo injector will be the injector for the SMTF in Meson East at Fermilab. Several upgrades to the injector are planned. The purpose of the instrumentation is to control the frequency, phase, and amplitude of the RF electric field in the superconducting cavity, commonly referred to as the RF Control System or Low Level RF (LLRF). A new "capture cavity" will be commissioned beginning this summer at the meson lab at Fermilab as "Phase Zero" of the SMTF program. The Penn instrumentation group has extensive expertise in instrumentation, especially FPGAs (Field Programmable Arrays) as well as analog and digital electronics and this allows us to contribute uniquely to the hardware and firmware aspects of the project, while at the same time allowing the physicists an opportunity to learn the essential physics of the impact of SCRF cavities on low emittance electron beams. This project is intended to help begin to establish the researcher at Penn in accelerator physics instrumentation and educate a number of students and postdocs in the accelerator physics and prepare them for participation in future accelerator projects, hopefully the ILC. The two students, entering graduate school fall 05 at Penn, have been identified and they explicitly asked to work on an ILC based project for summer 05.

Prior Support

There is no prior support for this activity. Thus far, the preparation for making this transition from particle physics to accelerator physics has really just begun. I am co-editing the SMTF proposal, have sent Penn post-doc Chris Neu to the accelerator school at Berkeley last month(EPICS controls course), organized a video meeting with the world LLRF experts, and interacted mostly with Philippe Piot and to a lesser extent Helen Edwards on the subject. Penn instrumentation engineer Mitch Newcomer has started to read documentation and spent two days at Fermilab understanding the needs of the A0 injector. The instrumentation at A0 would benefit from Penn's involvement. I created a WEB page with much of the documentation available on the TTF LLRF. The URL is

`http://rutherford.hep.upenn.edu/~lockyer/llrf.html`

Broader Impact

This proposal will train accelerator physicists. In particular, it is my intention to co-supervise a Ph.D student with my colleagues at Fermilab, hopefully Helen Edwards or Shekhar Mishra. In addition, I plan to train students during the summer, both undergraduates and graduate students.

Facilities, Equipment and other resources

The Penn High Energy Physics group is well supported by DOE HEP. We have one of the best instrumentation groups at a university in the country. The group provides integrated circuits as a by product of our own program, custom designed at Penn, to other groups around the world, at cost, as a service to the community. The ASDQ chip, used for drift chamber readout, is one example. It is the frontend readout chip for the CDF Central Outer Tracker(30,240 channels), that was my main responsiblity to CDF. We design and build circuit boards (Cadence), program FPGAs, and design numerous electronic systems. Penn has excellent computing available and substantial lab space for the HEP group.

FY2005 Project Activities and Deliverables

Since 1992, Fermilab has been engaged in the production of high-brightness electron beams. In conjunction with the TESLA collaboration, it has constructed and operated an L-band (1.3 GHz) photo injector, a copy of which was installed at the TESLA test facility in DESY Hamburg, for various tests, especially for the proof-of-principle UV SASE free-electron laser experiment. The Fermilab/NICADD photo injector laboratory (FNPL) is used as a test facility for beam dynamics studies associated to high brightness beam and its associated diagnosis, along with application to advanced accelerator physics.

We plan to start by preparing the LLRF for the SCRF 1.3 GHz "capture cavity" this summer. We will also begin evaluation the LLRF system used by DESY and design by Stefan Simrock and collaborators. We may use this system for SMTF but we do not yet have enough knowledge of that system to understand whether it meets the needs of SMTF.

We propose to implement the RF control system for the 3rd harmonic accelerating structure after the capture cavity and evaluation is complete. The 3rd harmonic 3.9 GHz accelerating structure planned for the photo injector is necessary to linearize the energy of the electron bunch after acceleration in the preceding RF cavity and is this important for optimal bunch

compression.

The RF control system fulfills several functions. It stabilizes the frequency, amplitude, and phase variations induced by sources such as the RF drive, beam current variations, Lorentz force detuning, and microphonics. The typical loaded Q of superconducting cavities is chosen to be a few 10^6. The resulting narrow bandwidth makes superconducting cavities much more sensitive to mechanical vibrations (microphonics). The RF field in a cavity also interacts with the RF wall current resulting in a Lorentz force which causes a deformation of the cavity shape which results in a change in the cavity resonant frequency.

The precision and stability of the combined resonant frequency, amplitude, and phase control determines the energy spread in the beam of the linear accelerator. The energy spread is critical to measuring the mass of new elementary particles as well as the top quark. These precision mass measurements are essential to the understanding of dark matter candidates. The high Q value of these cavities makes the LLRF system crucial for the success of the program. Interestingly, the criteria are not as stringent as needed at the X-FEL at DESY. Their experience will be important for us to monitor. (private communication Hasan Padamsee)

Deliverables: Commissioning of the LLRF and controls for the new "capture captivity" by the end of summer 05. Evaluate the DESY LLRF system and recommend whether it should be used for the 3rd Harmonic accelerating cavity and SMTF cryomodules.

FY2006 Project Activities and Deliverables

The activities in year two will be to complete and expand the plans for year one. A "Chechia" horizontal test facility is planned for the Meson East area. We will need to install the controls and LLRF for that facility. This will be a prototype SMTF cryomodule system, but it will work for only one 9-cell cavity.

We will be working toward preparing the controls and LLRF for the first US-ILC 8-cavity 1.3 GHz cryomodule that we expect to arrive during FY07.

Deliverable: LLRF for "Chechia" horizontal test facility at Fermilab. Install and commission the controls and LLRF for the first full cryomodule at SMTF.

FY2007 Project Activities and Deliverables

The following section is from the SMTF plan.

Electron Beam Tests:

We outline below possible studies with an electron beam. First, the RF performance of the cavities can be measured directly with beam and secondly, the impact of the cavity on the beam can be assessed. Note that item three below is primarily the responsibility of Penn and the control system performance. However, we plan to be involved with many measurements with the facility. An initial set of measurements would include:

Beam energy: a spectrometer would provide an independent and accurate measurement of the accelerating gradient (RF based techniques are not as accurate). Long Range wake-field

characterization: Measure frequency spectra of bunch positions downstream of cryomodule to search for high Q cavity dipole modes that could cause beam break-up in the ILC. Correlate these data with HOM power measurements. Tests of low-level RF system: demonstrate that a $< 0.1\%$ bunch-to-bunch energy spread can be achieved in a 1 msec bunch train. (Penn proposed responsibility) Impact of the SCRF cavity on transverse beam dynamics: measure the beam kicks caused by the fundamental mode fields. Study beam centering based on HOM (higher order modes) dipole signals.

To study basic cavity performance during beam operation, the photo injector should provide bunch trains comparable to those envisioned for the linear collider. The main requirements include:

bunch charge: up to 2e10 electrons bunch length: as low as 300 microns rms bunch spacing: nominally 337 ns with option of halving this. bunch energy stability $< 1\%$ rms average (Penn) current stability $< 1\%$ rms (preferably $< 0.1\%$ rms) number of bunches: up to 2820 pulse rep rate = up to 5 Hz.

This broad range of measurements will present several technical challenges, the details of which have to be worked out.

Deliverables:

Operate the full LLRF system with a crymodule and begin to understand the beam and cryomodule performance. We expect to make many measurements on the cryomodule with and without beam.

(Budget justification)

The first year budget is for two incoming graduate students for one summer. Travel and subsistence is included.

The second and third year we request additional funds for a postdoc as well as continued summer support for the students.

(Three-year budget)

Year 1: $\$21,794$
Year 2: $\$95,232$
Year 3: $\$98,089$

Total: $\$215,115$

Item	FY2005	FY2006	FY2007	Total
Other Professionals	0	43000	44290	87290
Graduate Students	8750	9012	9282	27046
Undergraduate Students	0	0	0	0
Total Salaries and Wages	8750	52012	53572	114334
Fringe Benefits	0	4171	4296	8467
Total Salaries, Wages and Fringe Benefits	8750	56184	57869	122803
Equipment	0	0	0	0
Travel	5000			5000
Materials and Supplies	0	0	0	0
Other direct costs	0	3900	4017	7917
Institution 2 subcontract	0	0	0	0
Total direct costs	13750	60084	61886	135720
Indirect costs(1)	8044	35149	36203	79396
Total direct and indirect costs	21794	95232	98089	215115

2.46: Polarized Positron Sources

(new proposal)

Accelerator Physics

Contact person
Mayda Velasco
mvelasco@lotus.phys.nwu.edu
(847) 467-7099

Institution(s)
Livermore
Northwestern

New funds requested
FY05 request: 36,209
FY06 request: 0
FY07 request: 0

Polarized Positron Sources

Classification (subsystem)

Accelerator

Personnel and Institution(s) requesting funding

Northwestern University, Department of Physics and Astronomy:
Mayda Velasco (Assistant Professor),
Armen Apyan (Research Associate).

Collaborators

Lawrence Livermore National Laboratory:
Jeff Gronberg

Project Leader

Mayda Velasco
mvelasco@lotus.phys.northwestern.edu
847 467 7099

Project Overview

Future high energy e^+e^- linear colliders require high intensity positron beams with low emittances and a high degree of longitudinal polarization. Low emittance is essential to attain high luminosity, while the beam polarization expands the physics capabilities of the machine.

How to produce polarized electrons is well understood. It is known that we can get longitudinal polarization that is as high as 75-80% for electrons produced by photo-emission in a semiconductor photocathode. However, although the polarization of positron beams is very useful, the technical progress to produce intense polarized positron sources has been rather slow, and significant R&D is needed.

A few methods to produce polarized positrons are being considered by the linear collider (LC) community. For example:

- to use β decay of naturally existing radioactive isotopes or short-lived isotopes produced by an accelerator.
- to use e^+e^- pairs created by converting circularly polarized γ rays. The main concept is to produce circularly polarized photons, followed by the collection of longitudinally polarized positrons produce in a target that acts a converter. The circularly polarized γ's come from one of these sources:

- Helical undulator radiation by unpolarized electron beams [1].
- Compton scattering of circularly polarized laser-light off a high-energy electron beam [2].
- Bremsstrahlung of longitudinally polarized electrons in high-Z amorphous targets [3].

Each of these three concepts have their own problems connected with their cost and/or technical complexity.

We propose to investigate and develop a simple alternative method which is also cost effective. It is based on a two-target scheme:

- *Target#1: uses an aligned single crystal diamond as a radiator ($e^- \rightarrow e^-\gamma$) for a polarized electron beam to make the polarized photon source instead of using an amorphous target.* We will exploit the enhancement of photon radiation via the mechanism of Coherent Bremsstrahlung (CB). In addition, photons produced by the interaction of longitudinally polarized electrons with a crystalline targets are circularly polarized due to conservation of angular momentum [4], just like radiation in an amorphous material.

  We will perform detailed Monte-Carlo (MC) simulations of the photon production by the CB of an electron beam in a diamond crystal. MC simulations will provide the optimum crystal thickness, crystal orientation and expected photon yield and circular polarization. All these studies will take into account the multiple scattering of the electrons inside the crystal, beam divergence and photon emission angle.

  In addition, we will investigate the effect of radiation damage on the degradation of CB. A significant energy will be deposited in the crystal when high energy electron beam passes through the crystal. This can leads to crystal stress, heating and damage. This could be the main problem for using the diamond crystal as a photon source. Synthetic diamonds look promising, but needs to be checked [5].

- *Target#2: produce polarized positrons from the conversion of circularly polarized photons in a high Z material.*

  We plan to carry out the calculations for the positron yield and polarization for several high and low Z materials, such as W,W-Re, Ti etc. after taking into account the characteristics of the photon beam produced above.

  We need to take into account the depolarization of the positrons in the photon converter.

Broader Impact

In the past, we have already worked with, both undergraduate and prospective graduate, students on the NA59 physics simulations. These students enjoyed their work and participated in our research for a significant amount of time. An example is Mengkai Shieh, now in medical school at Stanford. He was interested in using the knowladge that he was getting from us to make imaging devices for medical purposes. The NA59 collaboration studies the coherent interactions of high energy electrons and photons in an oriented single crystal, which

are the basis for the positron production scheme that we want to investigate next. Therefore, we plan to hire undergraduate students to participate in this project again.

Results of Prior Research

We have carried out preliminary MC simulations where we compare the photon yield from electrons radiating from a 1 cm thick single crystal diamond and 0.2 mm thick tungsten. The simulations were done assuming that the initial electron energy is 10 GeV.

The photon yield for the chosen crystal orientation is shown in Fig. 1 along with the expectation from the chosen amorphous material.

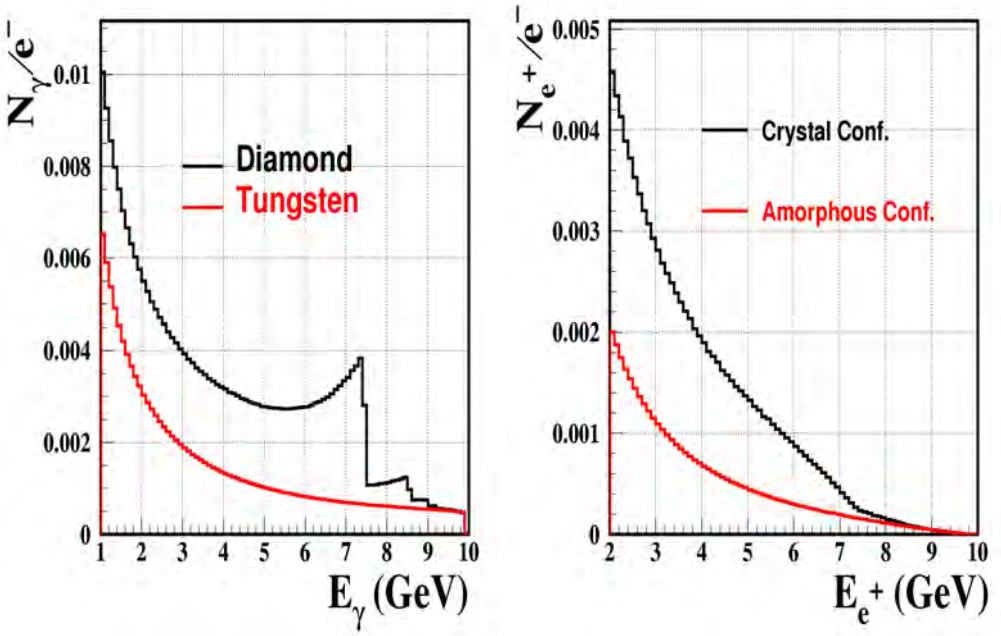

Figure 1: Number of photons per incident electron.

For the chosen parameters, 90% of the photons are from the first generation of radiated photons in the energy range between 6.5 -7.5 GeV. This was the condition used to select the target thickness because only the first radiated photon 'remembers' the electron polarization. However, the electron can radiate several photons as it passed through the target leading to a decrease in polarization of the incident electron beam. The thickness of the photon converter was chosen in the same manner. We chose a 0.3 mm amorphous Tungsten as photon converter.

With this configuration we have $0.007\gamma/e^-$ from Tungsten radiator and $0.03\gamma/e^-$ from single crystal Diamond. As shown, the crystal scheme provides ~ 3 times larger photon yield than amorphous configuration with the same beam parameters. This leads to increase of positron yield. In addition, the emittance of the photon beam is 6 times smaller in the useful energy range. For example, photon emission angles for amorphous Tungsten is $\sim 50\mu rad$, while for

aligned diamond is $\sim 8\mu rad$ in the photon peak.

In the Fig. 2, we show the expected circular polarization of photons produced by the CB of longitudinally polarized electrons in aligned diamond crystal (LEFT), and the degree of polarization for the positrons produced from pair production in the Tungsten target (RIGHT).

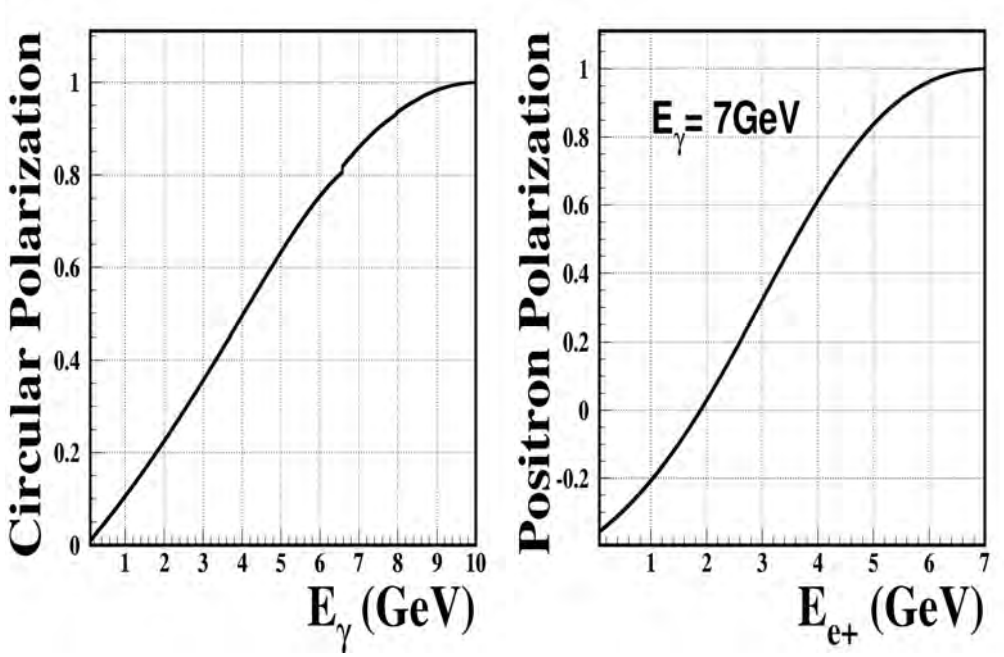

Figure 2: Circular polarization of photons and Longitudinal polarization of positrons

The expected polarization of the positron beam in the energy range 6 GeV -7.5 GeV is about 45 %, as show by our preliminary MC simulations.

All the results require detailed calculations taking into account the influence of the all processes arising in the targets when charged particles traverse them, and details of the beam.

Preliminary results were presented at the ICAR meeting in Argonne May 2004, see `http://www.capp.iit.edu/ icar/ANLWorkshop5-04/Workshop-agendaMay04.html`, and Fermilab Accelerator Physics and Technology Seminars, October 2004, see `http://www-bd.fnal.gov/ADSeminars/references.html#Armen`.

This research was funded by a grant from the state of Illinois to do accelerator development, ICAR.

Facilities, Equipment and Other Resources

The work will use the computer resources of the high energy group at Northwestern University.

FY2005 Project Activities and Deliverables

Year	Period	Activity
2005	May-July	Prepare MC simulation codes for the photon beam production. Production and formation of the circularly polarized photon beam.
	July-October	Preparing detailed MC code for polarized positron production. Formation and capture in accelerator of the positron beam. Write up and Publication

FY2006 Project Activities and Deliverables

N/A

FY2007 Project Activities and Deliverables

N/A

Budget justification: Institution 1

We are requesting financial support for a six months period for the successful fulfillment of the planned studies of the project. The financial support will cover the salary of the post-doc researcher who will work on the project.

Three-year budget, in then-year K$

$32,209

Institution: Institution 1

Item	FY2005	FY2006	FY2007	Total
Other Professionals	23,484	0	0	23,484
Graduate Students	0	0	0	0
Undergraduate Students	0	0	0	0
Total Salaries and Wages	23,484	0	0	23,484
Fringe Benefits	5,253	0	0	5,253
Total Salaries, Wages and Fringe Benefits	28,737	0	0	28,737
Equipment	0	0	0	0
Travel	0	0	0	0
Materials and Supplies	0	0	0	0
Other direct costs	0	0	0	0
Institution 2 subcontract	0	0	0	0
Total direct costs	28,737	0	0	28,737
Indirect costs(1)	7,472	0	0	7,472
Total direct and indirect costs	36,209	0	0	36,209

(1) Includes 25% of first $28,737 subcontract costs

References

[1] V. E. Balakin and A. A. Michailichenko, Preprint INP 79-85 (1979).

[2] T. Okugi et al., Jpn. J. Appl. Phys. **35**, 3677 (1996).

[3] A. P. Potylitsin, Nucl. Instr. and Meth. **A398**, (1997) 395-398.

[4] H. Olsen *et al.*, Phys. Rev., **114** (1959) 887.

[5] A. Apyan *et al.* [NA59 Collaboration], "Coherent pair production by photons in the 20-GeV - 170-GeV energy range incident on crystals and birefringence," arXiv:hep-ex/0306028.

2.47: Magnetic Investigation of High Purity Niobium for Superconducting RF Cavities

(new proposal)

Accelerator Physics

Contact person
P. Lee
lee@engr.wisc.edu
(608)263-1760

Institution(s)
Fermilab
University of Wisconsin

New funds requested
FY05 request: 66,702
FY06 request: 69,262
FY07 request: 71,941

Magnetic Investigation of High Purity Niobium for Superconducting RF Cavities

Proposal for LCRD/UCLC 2005

Classification (subsystem)

Material science on niobium for superconducting cavities of main linac

Personnel and Institutions requesting funding
P. J. Lee (PI), D. C. Larbalestier (Co-PI), A. Polyanskii, A. Squitieri, A. Gurevich,
Applied Superconductivity Center, University of Wisconsin at Madison

Collaborators
P. Bauer, L. Bellantoni, Fermilab

Project Leader
P. J. Lee
lee@engr.wisc.edu
(608)263-1760

Project Overview

Introduction

Fermilab is developing superconducting RF cavities for a future high-energy electron-positron linear collider as the next international, large-scale high energy physics discovery machine [1]. More than one year ago Fermilab and the Applied Superconductivity Center (ASC) of the University of Wisconsin-Madison (UW) have joined forces to investigate high purity niobium used in the cavity fabrication. As a mission statement the work agreement between Fermilab and the ASC/UW states that the goal of the collaborative effort is:

"… to improve the understanding of the effects of chemical composition and surface topology (grain size, grain boundaries) in Niobium for superconducting RF applications and possibly to explain the so-called Q-slope observed in superconducting resonators."

Motivation

The study of the magnetic properties of high purity niobium is extremely important for the advancement of the understanding of performance limitations of this material in the high gradient superconducting RF cavities for a future linear collider. During RF operation the high power RF fields penetrate only into a very thin layer on the surface of the cavity. This penetration layer is approximately 50 nm thick. It is currently believed that the penetration of only a few magnetic flux quanta into this layer will lead to a break-down of the superconducting state as a result of local heating due to the oscillation of the flux lines in the RF fields. The onset of flux penetration is believed to occur, in the best case, at a field close (or related) to the thermodynamic critical field (~180 mT in niobium). No niobium-based cavities have surpassed that surface field to this date. Grain boundaries and normal-conducting defects are potentially regions of suppressed superconductivity, allowing the penetration of magnetic flux lines even at low external magnetic fields. Therefore the assessment of the local shielding behavior of the superconductor in magnetic

fields is paramount for a better understanding of the performance limits of SRF cavities. The investigation of the effect of DC fields, such as with magneto-optics is the first step in this direction. The magneto-optical technique together with transport measurements can be used to quantify the possible suppression of superconductivity in grain boundaries or other surface defects. These two measurement techniques will be described next.

Magneto-Optics and Transport Measurements at the ASC/UW

We have been the first to show that the magneto-optical technique, a remarkable tool that can image local field penetration into a superconductor, can be applied to the study of high purity Nb for SRF application. The magneto-optical (MO) technique is described in detail in [3]. It uses the strong Faraday effect in YFe garnet to measure the vertical magnetic field component above a sample, in this case of superconducting material. The spatial resolution attained is ~5-10 microns. The garnet is placed on the face of the sample to retain the highest possible sensitivity. The technique is able to resolve fields of the order of 1 mT. The sample is typically a 5x5 mm^2 rectangle. Via indirect cooling with a cold finger containing liquid helium the sample temperature was held at temperatures between 5.6 and 7 K. An external solenoid is used to apply a vertical magnetic field on the sample.

We propose to also use grain-boundary critical current and grain boundary resistance (in the normal state) measurements to further support the magneto-optical measurements of the penetration of RF magnetic flux. The grain-boundary critical current measurements (as a function of external field) give an independent assessment of flux penetration into the grain boundaries. Normal state grain boundary resistivity measurements measure the electron scattering at the grain boundaries and therefore give further information about the grain boundary properties. These so-called transport measurements are best performed in bi-crystal samples, that is samples which consist of two single crystals separated by a grain boundary. The experiments then consist of the measurement of the current/voltage characteristic of each grain and the grain boundary.

ASC/UW and Fermilab Collaboration Overview

The ASC/UW and Fermilab have agreed to collaborate on the study of the magnetic properties of bulk niobium for SRF cavities using magneto-optics, transport measurements, XPS and microscopy. According to the agreement, Fermilab will be responsible to provide samples for the studies conducted at the ASC/UW. Both parties share the efforts related to analysis and publication.

The following project goals have been defined:

1) to improve the understanding of the effect of the chemical composition and topology of the surface, in general, and the grain boundaries, in particular, of state of the art high purity niobium for SRF cavities, including e-beam weld regions, on the capability of the material to shield magnetic flux;
2) to provide quantitative estimates of the grain-boundary critical currents and grain boundary resistance (in the normal state) such as further characterize grain-boundaries;
3) to correlate surface and grain-boundary chemical composition with the RF performance of SRF cavities, such as for instance for the case of the observed improvement of performance following a low temperature, in situ bake-out;

To achieve the above-defined goals a series of samples need to be provided to the ASC/UW, which are optimized for the use of various measurement techniques, such as magneto-optics and

transport measurements, without compromising the chemical condition of the surface. In particular we would like to test samples of the following type:

1) samples representative of the e-beam weld region in the cavities (MO, SEM and XPS);
2) samples representative of the non-weld region in the cavities (MO, SEM and XPS);
3) single crystal samples to study grain boundary free material (MO, SEM and XPS);
4) bi-crystal samples for transport measurements of the grain boundary properties (transport, SEM and XPS);
5) samples obtained via sputtering of niobium on a copper substrate to study very small grain material (MO, SEM and XPS);

The samples should be prepared with different degrees of completeness (e.g. mechanically deformed and deeply etched vs mechanically deformed, deeply etched and heat treated, … etc) such as to allow measurement of the evolution of the magnetic and transport properties during the fabrication of the cavities. The polishing variants, i.e. using chemical etching and electro-polishing, should also be differentiated. Furthermore this series of experiments should also include the low temperature bake (~120C, 50 hrs) that was recently shown to improve cavity performance significantly.

Broader Impact

One of the primary goals of this work will be to introduce a graduate student, trained in metallurgy/materials science, to the field of superconducting cavities. The Applied Superconductivity Center has been very successful in training students who have gone on to make valuable contributions to superconducting materials fabrication in both industry and laboratories.

Results of Prior Work

Although we have not been previously funded under LCRD we have achieved the following with funds made available by FNAL:

1) SEM and optical microscopy analysis was performed at the ASC/UW on large and small grain samples provided by Fermilab. Large grain samples (produced both by welding and high temperature heat treatment) showed deep (~1 μm) groves at the grain boundaries. All BCP etched samples showed surface roughness associated with differing rates of etching from grain to grain resulting in localized height variations of up to 10 μm. New, computer software based techniques were successfully employed to make the quantitative topological estimates quoted above.
2) XPS analysis revealed no direct evidence of sub-oxides (sputtering rate 0.3 nm/step, penetration depth of X-ray photons: ~4 nm) in the case of the samples that were surface treated in the same way as cavities. After re-oxidation in air for 5 minutes following a complete sputtering cycle, however, evidence of sub-oxides was found.
3) Magneto-optical measurements revealed strong variations in the magnetic shielding between large and small grain samples. A large grain weld sample as well as a sample, which was heat-treated at high temperature to grow large grains, showed evidence of flux penetration deep into the sample, indicating a breakdown of shielding in the grain boundaries (more in [2]).
4) Successful measurements of magnetization (Fermilab and ASC/UW) and specific heat (ASC/UW) have been performed on some samples.

Most of these results were presented at the "Pushing the Limits of RF Superconductivity" workshop at the Argonne National Laboratory in Sept. 2004 and at the Applied Superconductivity conference in Jacksonville in Oct. 2004 [2]. Our presentations at ANL can be viewed at the workshop website and a paper will be published in the proceedings. The measurements mentioned above raised several questions, which need to be resolved. Among them is the question of what caused the flux penetration into the large grain samples and whether this condition is present in e.g. the e-beam welds of SRF cavities, which similarly have very large grains. The collaboration between Fermilab and the ASC/UW has already provided new and interesting insights into the properties of chemically polished Nb for SRF cavities in magnetic fields and provides a model for University-National Laboratory collaboration in this field.

Facilities, Equipment and Other Resources

At the University of Wisconsin-Madison Applied Superconductivity Center we have comprehensive facilities for superconducting materials testing and microstructural characterization (including adjacent Materials Science Center). A comprehensive list can be found at http://www.asc.wisc.edu/facility/facility.htm. For electromagnetic testing we have 14-16 T and 15-17 T Oxford Instruments magnets with Variable Temperature operation from 2 to 120 K, a 5.5 T Quantum Design SQUID magnetometer, an Oxford Instruments 14 T Vibrating Sample Magnetometer with Cantilever Torque magnetometer, a Quantum Design 9 T Physical Property Measurement System with DC and AC susceptibility and specific heat capability. We also have a Very-Low-Field Shielded Test Facility and extensive high-sensitivity electronics permitting nanovolt DC measurements.

Activities and Deliverables for this Proposed Work

Under this proposal we plan to recruit a graduate student to:

1) start transport measurements to derive the grain-boundary critical currents as well as the grain boundary normal state resistivity;
2) support this work with SEM (OIM for grain boundary orientation), XPS and light microscopy

The list of samples to be prepared by Fermilab and submitted to tests at the ASC/UW is outlined in Table 1. The preparation and testing of all the samples discussed in this table is a multi-year task.

Table 1: Run-plan for Fermilab/ASC-UW studies on niobium for SRF cavities. The roster of samples includes specimen prepared to different degrees of completeness. Also for each preparation condition there should be samples representative of the two different cavity areas (the weld and non-weld area) and/or the two main polishing techniques: BCP and EP (where BCP refers to "buffered chemical polishing" and EP stands for "electro-polishing").

Sample normal/weld/ sputtered/single-crystal	as received	deep drawn	100 μm etch (BCP/EP)	heat treatment (750C/5hrs)	20 μm etch (BCP/EP)	Low temp bake (120C/50hrs)
1	**X**					
2	**X**	**X**	**X**			
3	**X**	**X**	**X**	**X**		
4	**X**	**X**	**X**	**X**	**X**	
5	**X**	**X**	**X**	**X**	**X**	**X**

The deliverables for the next years are expected to be quantitative estimates of the DC flux penetration field in the various samples as well as the grain boundary critical currents and the grain boundary normal state resistance. The results of these studies should be published in a renowned journal such as Physical Review as well as in the important meetings of the SRF technology community.

Budget Justification

The activities outlined above will involve Fermilab staff members, whose salaries are not included in the budget request below. The budget request only includes salaries for the ASC/UW staff members participating in this study. The quoted amount includes a

3% of annual time Peter Lee to co-ordinate work at UW;
3% research fraction of Anatolii Polyanskii to train student for the magneto-optical measurements;
3% research fraction of A. Squitieri to train student for the transport measurements;

The following budgetary estimate is in $.

Table 2: Budgetary estimate for ASC/UW-Fermilab collaboration on the study of high purity niobium for SRF cavities.

Item	FY 2005	FY2006	FY2007
Other professionals	$9,164	$9,530	$9,530
Graduate Students	$22,253	$22,253	$22,253
Total Salaries (incl. fringe benefits)	$40,319	$41,927	$43,608
Equipment	0	0	0
Travel	$500	$500	$500
Materials and Supplies	$1000	$1000	$1000
Sample preparation	$200	$200	$200
Total direct costs	$47,583	$49,412	$51,326
Total indirect costs	$19,119	$19,850	$20,615
Total direct and indirect costs	**$66,702**	**$69,262**	**$71,941**

References

[1] L. Bellantoni, N. Solyak, I. Gonin, T. Berenc, H. Edwards, M. Foley, N. Khabiboulline, D. Mitchell "*Test Results of the 3.9 GHz Cavity at Fermilab*", presented at the LINAC 2004 Conference, Luebeck, Germany, Sept. 2004.

[2] P. Lee, P. Bauer, A. Polyanskii, C. Boffo, L. Bellantoni, H. Edwards, A. Gurevich, M. Jewell, D. Larbalestier, G. Perkins, A. Squitieri "*An Investigation of the Properties of BCP Niobium for Superconducting RF Cavities*", submitted to the proceedings of the "Pushing the Limits of RF Superconductivity" workshop, Argonne National Lab, Sept 2004.

[3] A. A. Polyanskii, D. M. Feldmann, and D. C. Larbalestier, "*Magneto-Optical Characterization Techniques* ", The Handbook on Superconducting Materials, Edited by David Cardwell and David Ginley, Institute of Physics UK , pp. 1551, 2003.

Peter J. Lee

Tel: 608 263-1760
EFAX: (503) 907-5676
email: peterlee@wisc.edu

Applied Superconductivity Center
Rm. 939, Eng. Res. Bld., 1500 Engineering Drive,
Madison WI 53706-1609

CURRENT POSITION

1994 - Senior Scientist in the Superconducting Materials Research Group of the Applied Superconductivity Center at the University of Wisconsin-Madison. Focus: Microanalytical and microstructural evaluation by transmission electron microscopy, Scanning Auger, field emission SEM and electron microprobes of superconducting composites Low Temperature Superconductors. Currently co-principal investigator with Prof. David C. Larbalestier for grants from the US Dept. of Energy Division of High Energy Physics (~$530,000 per annum), DOE-Office of Fusion Energy (~$100,000 per annum) and Fermi National Accelerator Laboratory ($75,000 to explore SRF Cavity work). Our analytical expertise has also attracted additional funding from industry for service work via the DOE-SBIR program.

COMMITTEE MEMBERSHIPS

Conductor Advisory Committee for High Energy Physics High Field Magnets (1999 - present).
Applied Superconductivity Conference, elected board member since 2002.
ICMC, elected board member 2004 (term expires 2011)

RECENT INVITED TALKS AND SEMINARS

"Advances in Superconducting Materials for Accelerator Magnet Application," 2003 Particle Accelerator Conference, Portland, OR, May 13th 2003.
"Microstructural and Microchemical Homogeneity for High Critical Current Density in Nb_3Sn," 1st International Workshop on Progress in Nb Based Superconductors, Tsukuba, Japan February 2-3, 2004.

PUBLICATIONS

Patent: "Artificial and Multiple Phase Micro-Electropolishing," US Patent Number 5,354,437, Oct. 11, 1994

Books: *"Composite Superconductors," ed. K. Osamura, T. Matsushita, P. J. Lee, S. Ochiai, pub. Marcel Dekker, New York, 1994.*
"Engineering Superconductivity, ed. Peter J. Lee, Wiley-Interscience, New York, 2001

Book Contributions: 21, most recently:

"Handbook of Superconducting Materials," Chapter 3.3: Conductor Processing of Low-T_c Materials: The Alloy Nb-Ti, Lance Cooley, Peter Lee, and David Larbalestier. A Pre-publication draft is available for download from http://128.104.186.21/asc/pdf_papers/630.pdf
"Superconductor: WIRES AND CABLES: MATERIALS AND PROCESSES," Peter J. Lee, in the ENCYCLOPEDIA OF MATERIALS: SCIENCE AND TECHNOLOGY - Update, Edited by K. H. J. Buschow, R. W. Cahn, M. C. Flemings, P Veyssiere, E. J. Kramer, S. Mahajan. Published on-line by Elsevier at the EMSAT website in 2003. To appear in the full electronic update of EMSAT in 2004.

Refereed Articles: 69 articles, most recently:

1 "Development Of Point-Array APC Nano-Structures In Nb-Ti Based Superconducting Strand," P. J. Lee, L. R. Motowidlo, M. K. Rudziak and T. Wong. Advances in Cryogenic Engineering, 50B, pp. 314-321, 2004. http://128.104.186.21/asc/pdf_papers/780.pdf

2 "Flux Pinning Properties In Nb-Ti Composites Having Nb And Ti Mixed Artificial Pins," O. Miura, D. Ito, P. J. Lee, and D. C. Larbalestier, Advances in Cryogenic Engineering, 50B, pp. 307-313, 2004. http://128.104.186.21/asc/pdf_papers/782.pdf

3 "Simulations of the effects of tin composition gradients on the superconducting properties of Nb_3Sn conductors," L. D. Cooley, C. M. Fischer, P. J. Lee, and D. C. Larbalestier, accepted for publication in *J. Applied Physics* (August 1st) 2004.

Further information available at: http://homepages.cae.wisc.edu/~plee

2.48: 3D Atom-Probe Microscopy on Niobium for SRF Cavities

(new proposal)

Accelerator Physics

Contact person
D.N. Seidman
d-seidman@northwestern.edu
(847) 491-4391

Institution(s)
Argonne
Fermilab
Northwestern

New funds requested
FY05 request: 43,500
FY06 request: 44,300
FY07 request: 45,100

3D Atom-Probe Microscopy on Niobium for SRF Cavities

Proposal for LCRD/UCLC 2005

Classification (subsystem)

Material science on niobium for superconducting cavities of main linac

Personnel and Institutions requesting funding

D. N. Seidman, Materials Science & Engineering Dept, Northwestern University (NU)

Collaborators

P. Bauer, Fermilab (FNAL)
J. Norem, Argonne National Lab (ANL)

Project Leader

D. N. Seidman, d-seidman@northwestern.edu, (847) 491-4391

Project Overview

Introduction

Fermilab (FNAL) is developing superconducting RF cavities for a future high-energy electron-positron linear collider as the next international, large-scale high energy physics discovery machine [1]. In this context FNAL has been steadily developing its SRF cavity expertise, infrastructure and technology base. Recently FNAL and the Northwestern University Center for Atom-Probe Tomography (NUCAPT), Evanston, Illinois, have joined forces to investigate the properties of the high purity niobium used in the cavity fabrication. The NUCAPT is among the world leaders in the field of three-dimensional atom-probe microscopy, particularly as result of the recent installation of a local-electrode atom-probe (LEAP) microscope, manufactured by Imago Scientific Instruments (http://www.imago.com) Currently only three other LEAP microscopes, with a comparable performance, exist throughout the world. Atomic-probe microscopy consists of dissecting a specimen on an atom-by-atom basis, employing pulsed field-evaporation, and determining the chemical identity of each field-evaporated atom by time-of-flight mass spectrometry, with single atom identification capability, using a 2D position sensitive delay line detector, which yields the position of each atom in a specimen with sub-nanoscale resolution. Analysis rates of upwards of 72 million atoms hr^{-1} have been achieved employing a LEAP microscope at NU. The collected data is used to reconstruct a specimen in three-dimensions, where the chemical identity of each atom is known. The collaboration between FNAL and NUCAPT will produce spectacular results with lasting impact and strongly advance the understanding of the surface chemistry in state of the art high purity niobium for superconducting RF cavities.

Motivation

The study of the surface chemistry of high purity niobium is extremely important for the advancement of the understanding of performance limitations of this material in the high gradient superconducting RF cavities for a future linear collider. During RF operation the high power RF fields penetrate only approximately 50 nm into the surface of the cavity. The interaction of RF photons with the complex electronic system in the surface of the superconductor produces the so-called BCS resistance loss, heating and ultimately thermal quenching. In niobium this surface resistance contribution is well understood for the "ideal" surface. It is less well understood in the case of "realistic" surfaces. It is known, however, that the presence of metallic oxides and hydrides (e.g. in grain-boundaries) strongly affect the BCS surface resistance because of a weakened superconducting state (reduced gap energy). The BCS resistance measured in state of the art bulk niobium cavities is consistent with a gap energy that is smaller than in the ideal case. This measurement, however, averages over the entire RF penetration layer and thus presumably includes ideal behavior at greater depths and strongly suppressed behavior in the first 10-20 nm of the material. The weakening of the superconducting state also reduces the shielding of magnetic flux associated with the RF electromagnetic fields. It is currently believed that the penetration of only a few magnetic flux quanta will lead to a break-down of the superconducting state as a result of local heating due to the oscillation of the flux lines in the RF fields. Therefore, the assessment of the surface chemistry at the microscopic level is paramount to better understanding the surface resistance of and magnetic flux penetration into a "real" niobium surface as in high performance RF cavities.

Previously the analysis of the surface chemistry was obtained mostly through x-ray spectroscopy [2, 3] or electron spectroscopy [4]. This research has already yielded a good understanding of the issues at hand. It became clear, for instance, that below the insulating (and therefore inert) Nb_2O_5 layer, a mix of Nb-O compounds with varying stoichiometries exist, which are usually referred to as sub-oxides. The role of these sub-oxides is not completely understood yet, but their mere presence can be a source of gap suppression and flux penetration. The XPS studies were not capable, however, to resolve the surface chemistry layer-by-layer (although new proposals exist to do just that), nor could they clearly resolve the chemistry of grain-boundaries. The 3D atom-probe technique we propose to use, would be the first attempt to reveal the surface and grain boundary chemistry in state-of-the-art niobium for SRF cavities at the most microscopic level possible, namely atom-by-atom. It needs to be stressed as well that the superior spatial resolution and analytical sensitivity of the atomic probe microscope also makes it possible to investigate how macro-processes, such as chemical polishing, heat treating, welding, exposure to gases,..etc, affect the micro-structure. Furthermore the high spatial resolution of the technique promises to allow the detection of field emitters, another performance limitation encountered in high gradient SRF cavities.

Project Goals

Northwestern University (NU) and Fermilab (FNAL) have agreed to collaborate on the study of the surface chemistry of bulk niobium for SRF cavities using the Imago LEAP microscope in NUCAPT. According to the agreement, FNAL will be responsible to provide samples for the 3DAP studies conducted at NU. Both parties will share the efforts related to analysis and publication.

The following project goals have been defined:

1) to improve the understanding of the chemical composition of the surface of state of the art high purity niobium for SRF cavities, including e-beam weld regions;
2) to improve the understanding of the chemical composition of the grain boundaries in state of the art high purity niobium for SRF cavities, including e-beam weld regions;
3) to correlate surface and grain-boundary chemical composition with the various macro-treatment steps used to prepare cavities for RF performance of SRF cavities, such as for instance the low temperature, in-situ bake-out, which was recently shown to significantly increase cavity performance;

To achieve the above-defined goals a series of samples need to be provided to the NU, which are optimized for the use of 3DAP without compromising the chemical condition of the surface. Therefore the initial phase of the project will be devoted to the test of different samples preparation techniques and sample shapes. Different possible techniques are wire erosion cutting of individual specimens from a bulk specimen combined with chemical etching. Alternatively, focused ion beam (FIB) milling of posts, to a diameter in the range 100 to 200 microns, in an initially flat surface, followed by sharpening of the tops of the posts to a radius of less than 50 nm. The samples will undergo the same surface preparation steps as the inner surfaces of cavities, including mechanical deformation, etchings and heat treatments. The weld-samples will be prepared from e-beam welded strips. Following the initial assessment of the best-suited sample preparation technique we will investigate the effect of all major cavity preparation steps on the surface chemistry. Samples prepared with different degrees of completeness (e.g. mechanically deformed and deeply etched versus mechanically deformed, deeply etched and heat treated, etc). The polishing variants, i.e. using chemical etching and electro-polishing, should also be differentiated. Furthermore this series of experiments should include the low temperature bake (~120ºC, 50 hrs) that was recently shown to improve cavity performance significantly.

Broader Impact

Toward attracting underrepresented groups and women for careers in science we will provide access to NUCAPT to students and professors at: (1) Harold Washington College, a minority serving institution in downtown Chicago (Profs. Thomas Higgins and Cecilia Lopez); (2) Saint Mary's College, Notre Dame, Indiana, a liberal arts women's college with a strong chemistry major (Prof. Deborah McCarthy); and (3) College of St. Benedict/St. John's University in St Joseph, Minnesota (Prof. Anna McKenna), which is also a liberal arts women's college with a strong undergraduate chemistry program. We will help Professor Higgins in the development of an Undergraduate Research Center (URC). Similarly we will open the doors of NUCAPT to Professors McCarthy and McKenna of Saint Mary's College and College of St. Benedict/St. John's University, respectively, and their students through NSF REU/MRI grants and faculty development awards. Furthermore, we will obtain REU/MRI students through Northwestern's NSF funded Nanoscience and Engineering Center (Prof. M. Hersam) and Material Research Center (Prof. M. Olvera). We will help Dr. Vondracek (Evanston Township High School (ETHS)) construct a field-emission microscope from components we are no longer using. This will allow ETHS students to see molecules on the surfaces of sharply pointed

wire tips. The members of my research group will provide Dr. Vondracek the necessary help to maintain these microscopes. In addition to supervising the research projects of women and underrepresented groups we will conduct a short course for all REU/MRI students each summer to explain to them how the LEAP™ microscope works and how it is employed for diverse research projects being performed throughout the world.

Results of Prior Research

Although not previously been funded by LCRD, NUCAPT has a long been involved in 3DAP. The following presents an example of results that employ three-dimensional atom-probe (3DAP) microscopy, [5],[6], which is the successor to so-called 1DAP microscopy [7]. The example we now focus on is that of an Al-2.2 at.% Mg-0.12 at.% Sc alloy, which is relevant for aerospace applications, where segregation during aging adversely affects the high-temperature creep properties, and as a model system for its microstructural properties. This alloy was prepared employing solidification and homogenization procedures. During aging at 300°C, the supersaturated solid-solution decomposes into an α-Al matrix and $4\pm2\times10^{22}$ precipitates m^{-3} of nanoscale Al_3Sc precipitates with radii <4.5 nm. HREM observations demonstrate that the α-Al/Al_3Sc interface remains coherent, that is, dislocation free, in both the binary Al-0.18 at.% Sc and ternary Al-Mg-Sc alloy, even for precipitates with radii of 4.5 nm. Without Mg, the precipitate shows pronounced facets on the {100}, {110}, and {111} planes, which tend to shrink with the addition of Mg. To investigate the behavior of Mg, we performed 3DAP microscopy resulting in solute composition profiles suitable to determine the Gibbsian interfacial excesses [8]. This demonstrates that segregation decreases the interfacial free energies, which concomitantly decreases the coarsening rate, thereby stabilizing the microstructure at elevated temperatures.

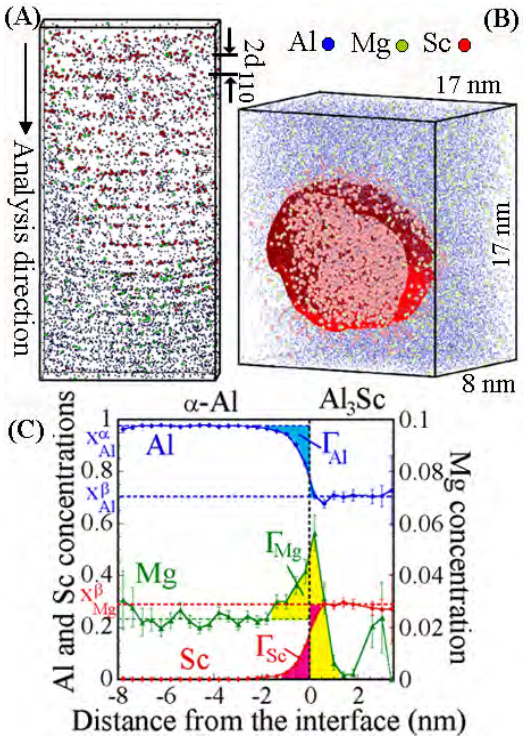

Fig. 1: (**A**) 3D reconstruction of an Al_3Sc precipitate with a slice taken through it showing the (110) planes. (**B**) 3D reconstruction of an analyzed volume from a specimen aged at 300°C for 1040 hours, showing the isoconcentration surface used to delineate the Al/Al_3Sc interface. Sc (Mg) atoms are in pink-red (light green), and Al is in blue. (**C**) Proximity histogram showing Al, Mg, and Sc concentrations with respect to distance from the interface, which is an average for many precipitates.

The spatial resolution of the 3DAP is illustrated in Fig. 1(A), where an analysis reveals the {220} atomic planes perpendicular to the analysis direction. The curvature of the planes comes from the projection of the hemispherical tip onto a planar detector. In the Al_3Sc precipitate, alternating planes containing 100% Al and 50% Al are visible, consistent with the $L1_2$ structure and stoichiometry of the Al_3Sc phase. A proximity histogram calculates average compositions in shells of 0.4 nm

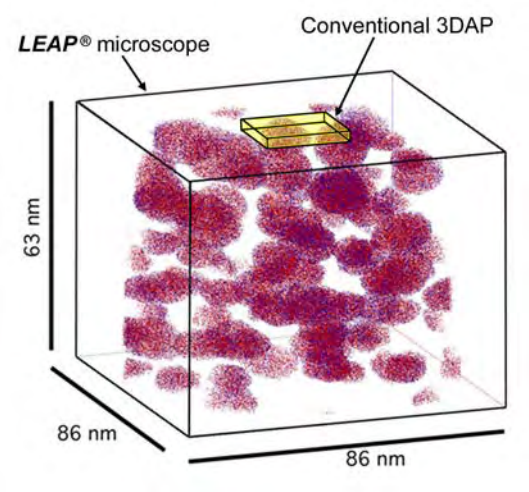

Fig. 2: Analysis volume containing 25 million atoms collected in approximately one hour on a Ni-5.2 Al-14.2 Cr at. % specimen aged for 256 h at 600°C using the LEAP microscope. The highlighted volume in yellow contains 50,000 atoms and marks the volume that would be collected in the same amount of time on a conventional 3DAP microscope. Only Al (red) and Cr (blue) atoms within gamma-prime precipitates are shown for clarity.

thickness at different distances from the α-Al/Al_3Sc interface; the interface is defined by an isoconcentration surface corresponding to 18 at.% Sc [Fig. 1(B)]. Interfacial Mg segregation was observed for all analyzed aging times, and the particular example of Fig. 1(C) exhibits a Mg concentration enhancement of 180%. First-principles calculations were conducted to investigate the energetics of Mg solute atoms in the vicinity of planar coherent α-Al/Al_3Sc interfaces. The agreement between the experimental and theoretical values of the relative Gibbsian interfacial Mg excess establishes that the measured interfacial Mg enhancement reflects pronounced segregation of Mg to coherent α-Al/Al_3Sc heterophase interfaces.

The analytical sensitivity and spatial resolution of 3DAP microscopy are well documented in the following example. Figure 2 displays a data set for a Ni-Al-Cr alloy recorded with a LEAP microscope; the nanoscale precipitates is the γ'-phase ($L1_2$ structure). The yellow parallelepiped indicates a typical data set recorded with a conventional 3DAP microscope. The LEAP microscope is capable of recording data a rate that can be a factor of 667 faster than a conventional 3DAP microscope and the volumes analyzed are concomitantly significantly larger.

Facilities, Equipment and other Resources

A. Atom-probe tomographic facility – Northwestern University Center for Atom-Probe Tomography (NUCAPT)

- A high mass resolution 1D-atom-probe field-ion microscope system: It utilizes a single-stage reflectron lens to determine the time-of-flight of the field evaporated ions, and it has a mass resolution of 800, full-width at half-maximum (FWHM) employing electrical pulses to field evaporate ions. The time-of-flight electronics allow for the measurement of up to 128 ions per field evaporation pulse. It also can be used as a pulsed laser atom probe (PLAP), which has a mass resolution of 900, FWHM. It is equipped with a pre-chamber that permits us to deposit controlled amounts of different metallic evaporants. This instrument is also completely computer controlled.
- An Imago Scientific Instruments local-electrode atom-probe (LEAP) microscope, which is a state-of-the-art tomographic atom-probe microscope. This instrument allows us to collect data at a rate of up to 20,000 ions sec-1 (72x106 ions hr-1) from a volume that can be 100 nm^2 x several microns. This instrument has a variable tip-to-detector distance (80 to 170 nm), which implies

that we can obtain wide-angle field-of-views, as well as analyzing smaller pre-selected areas. This instrument can also examine microposts on a wafer, which implies that we can sample sequentially different areas of the same region with atomic resolution

- A three-dimensional (3D) atom-probe microscope: This instrument has an ultrahigh vacuum system, with a specimen exchange system that holds ten specimens, which allows us to change specimens within approximately 20 minutes. It employs an optical detection system fabricated by Kindbrisk Limited and the capability of the detection system is 110,000 ions per hour with a 90% positioning efficiency (defined as the fraction of the detected ions that can be associated uniquely with a given x-y position and simultaneously a given mass-to-charge state ratio). This implies that data sets exceeding one million atoms can be collected in less than a day. The main chamber is equipped with a single-stage reflectron lens, which has a mass resolution ($m/\Delta m$) exceeding 300. This instrument can also be adapted for use as a pulsed laser atom probe (PLAP). This is a completely computer-controlled instrument.
- A versatile system for highly controlled electroetching or electropolishing of field-ion microscope specimens has been developed. This system is particularly useful for backpolishing an atom probe specimen to place a preselected Al/Al3Sc interface in the field-of-view of a field-ion microscope image. The preselection is performed by TEM in a specially fabricated double tilt stage for an Hitachi transmission electron microscope; this stage can hold a wire specimen about 1 cm long and about 125 to 200 μm in diameter.

B. High-resolution, scanning transmission, and analytical electron microscopes

- At Northwestern University, there is an Hitachi 2000 analytical electron microscope that is equipped with both a parallel electron energy loss spectrometer and an energy dispersive x-ray spectrometer; that latter has a thin window that makes possible the detection of oxygen. This microscope has a cold field-emission gun that produces an electron beam with a spot diameter of 1 nm under best operating conditions. It also has a recently installed GIF.
- At Northwestern University, there is also an Analytical Scanning Transmission Atomic Resolution (A STAR) electron microscope (JEOL JEM-2100F FAST TEM) with the following features: High brightness Schottky emitter operated at 200kV; BF/ADF STEM detectors, EDS system and EMISPEC system for atomic resolution Z-contrast imaging, sub-nanoscale resolution EDS and PEELS point analysis, and automated line scans and maps; UTW x-ray detector; Gatan TV-rate CCD camera; Top-hat aperture to eliminate hard x-ray; Several side-entry specimen holders; Standard single and double-tilt holder; Low-Z(Be) holder for analytical x-ray microanalysis
- At Argonne National Laboratory, there is a JEOL 4000EX, a 400 kV high-resolution microscope available for this project; this instrument has a point-to-point resolution of 0.165 nm and a line resolution of approximately 0.11 nm.
- At Argonne National Laboratory, there is a Vacuum Generators, VG 6032 advanced analytical electron microscope, operated in UHV with a field emission gun (FEG) at voltages up to 300 keV with a 0.28 nm point-to-point resolution. This instrument is equipped with EELS, XEDS, AES, SIMS, LEED and will be available for our use.

- In addition to the HREM instruments at Argonne, a number of conventional tools for structural and analytical observation are available. A listing of the instruments available is as follows: Philips CM 30-300 kV TEM, Energy dispersive x-ray analysis (EDX), PEELS, Philips 420, 120 kV TEM, EDX, EELSJEOL 100 CX 100 kV TEM, EDX.
- At Argonne National Laboratory there is also a dual beam FIB instrument, which is useful for preparing atom-probe microscope specimens from bulk specimens.

C. Heat-treatment and metallography facility

- Three resistive-convection furnaces (temperature capability: 1050˚C) in the P.I.'s laboratory, allowing precise temperature measurement (within 1˚C) for heat-treatment in air or vacuum of samples to be homogenized or aged.
- The Optical Microscopy and Metallography Facility (OMMF) is equipped for the metallographic preparation of specimens by producing strain-free surfaces usually examined by optical microscopy. Equipment includes fourteen optical microscopes bright field and dark field modes, and polarized light and digital image capture, a micro hardness tester (loads from 10 grams to 1000 grams with either Knoop or Vickers indentors), an interference microscope, and a hot stage (300 C maximum) for viewing optically clear specimens are available. A "digital" darkroom with AV Macintosh, scanner and a dye-sublimation printer capable of photographic quality prints and a standard darkroom are available. Metallographic specimens can be cut with diamond-tipped blades on either a slicer/dicer, low-speed, or high-speed cut-off saw. Samples can be encapsulated in either cold-mount acrylics or phenolic resins. Manual abrading with silicon carbide paper or with variable speed 12" diameter SiC platens can be done in the facility. Various 8" diameter platens for polishing are available with diamond paste sizes ranging from 30 to 0.1 micrometer. Alumina slurry polishing is also available with sizes from 1.0 to 0.05 micrometer. A semi-automatic Buehler Ecomet IV Abrasive and Polishing System is capable of preparing up to eight specimens simultaneously with reproducible parameters of platen speed, pressure, and diamond concentrations.

Project Activities and Deliverables

During the first year we plan to complete initial 3DAP measurements of different shape samples of weld and non-weld material, prepared by different methods to assess the general feasibility of the measurements. These initial measurements will not only serve to debug the measurement technique but most likely also deliver first publishable results and possibly also raise questions that will determine the course of the subsequent investigations. The first year deliverables are the technical reports describing how to successfully implement 3DAP measurements with high purity niobium for SRF cavities.

During the second year we plan to complete the experimental program outlined above. The list of samples to be prepared by Fermilab and submitted to tests at NU is outlined in Table 1. The second year deliverables are expected to be high quality 3DAP measurement results that should lead to a new understanding of the surface chemistry of bulk niobium and possibly leading to the suggestion of new or improved cavity surface

treatment procedures. Obviously such results should be published in a journal such as Physical Review.

Table 1: Run-plan for 3DAP microscopy studies on niobium for SRF cavities. The roster of samples includes specimen prepared to different degrees of completeness. Also for each preparation condition there should be samples representative of the two different cavity areas (the weld and non-weld area) and/or the two main polishing techniques: BCP and EP (where BCP refers to "buffered chemical polishing" and EP stands for "electro-polishing").

Sample normal/weld	as received	deep drawn	100 μm etch (BCP/EP)	heat treatment (750ºC/5hrs)	20 μm etch (BCP/EP)	Low temp bake (120ºC/50hrs)
1	**X**					
2	**X**	**X**	**X**			
3	**X**	**X**	**X**	**X**		
4	**X**	**X**	**X**	**X**	**X**	
5	**X**	**X**	**X**	**X**	**X**	**X**

During the third year we plan to address the issues that arose during the systematic testing of year 2. The effect of new preparation steps suggested as a result of this (or other work) on the surface chemistry should systematically be tested by 3DAP.

Budget Justification

The activities outlined above will involve NU and FNAL staff members, whose salaries are not included in the budget request below. The budget request includes only funding for Dr. Jason Sebastian, who will dedicate four months per year to this effort (including travel to meetings/conferences). Also included is the minimum operating cost of the LEAP microscope ($250/day), assuming a total of twenty days (listed under "Materials and Supplies"). Although FNAL will generally cover the cost of sample preparation, the budget also includes the projected cost of sample preparation outside of FNAL, should such a need occur. NU, as the general contractor for this proposal will also administer these funds. The following budgetary estimate is in k$.

Table 2: Budgetary estimate (in k$) for NU-FNAL collaboration on 3DAP microscopy of high purity niobium for SRF cavities.

Item	**FY 2005**	**FY2006**	**FY2007**
Other professionals	11.7	12.1	12.4
Total Salaries (incl. 24% fringe benefits)	14.3	14.8	15.4
Travel	5.0	5.0	5.0
Materials and Supplies	5.0	5.0	5.0
Sample preparation	5.0	5.0	5.0
Total direct costs	29.3	29.8	30.4
Total indirect costs (incl. 48%)	14.2	14.5	14.7
Total direct and indirect costs	**43.5**	**44.3**	**45.1**

References

[1] L. Bellantoni, N. Solyak, I. Gonin, T. Berenc, H. Edwards, M. Foley, N. Khabiboulline, D. Mitchell "*Test Results of the 3.9 GHz Cavity at Fermilab*", presented at the LINAC 2004 Conference, Luebeck, Germany, Sept. 2004.

[2] A. Dacca, G, Gemme, L. Mattera, R. Parodi, "*XPS Characterization of Niobium for RF Cavities*", Proc. of the 8th RF Superconductivity Workshop, Abano Terme, Italy, 1997;

[3] C. Antoine, A. Aspart, S. Regnault, A. Chincarini, "*Surface Studies: Method of Analysis and Results*", paper MA007, Proc. of the 10th RF Superconductivity Workshop, Tsukuba, Japan, 2001;

[4] R. Rosenberg, Q. Ma, "*Thermal and Electron Beam Irradiation Effects on the Surfaces of Niobium for RF Cavity Production*", paper PR007, Proc. of the 10th RF Superconductivity Workshop, Tsukuba, Japan, 2001;

[5] M. K. Miller, "*Atom Probe Tomography: Analysis at the Atomic Level*", Kluwer Academic/Plenum Publishers, New York, 2000;

[6] M. K. Miller, A. Cerezo, M. G. Hetherington, and G. D. W. Smith, "*Atom Probe Field Ion Microscopy*", Oxford Science Publications, Clarendon Press, Oxford, 1996;

[7] R. Wagner, "*Field-Ion Microscopy*", Springer-Verlag, Berlin, 1982;

[8] E. A. Marquis, D. N. Seidman, M. Asta, C. M. Woodward, and V. Ozoliņš, "*Segregation at Al/Al3Sc Heterophase Interfaces on an Atomic Scale: Experiments and Computations*", Physical Review Letters, 91, 036101-1 to 036101-4, 2003;

2.49: Experimental Study of High Field Limits of RF Cavities

(new proposal)

Accelerator Physics

Contact person
D.N. Seidman
d-seidman@northwestern.edu
(847) 491-4391

Institution(s)
Argonne
Northwestern

New funds requested
FY05 request: 64,800
FY06 request: 66,300
FY07 request: 67,900

Experimental Study of High Field Limits of RF Cavities

Classification (subsystem)

High gradient rf systems

Personnel and Institution(s) requesting funding

D. N. Seidman, Materials Science and Engineering Department, Northwestern Univ. (NU).

Collaborators

J. Norem, Argonne National Lab (ANL)

Project Leader

D. N. Seidman, Materials Science and Engineering Department, Northwestern Univ. (NU).
email: d-seidman@northwestern.edu
phone: (847) 491-4391

Project Overview

We want to understand how the maximum fields in high gradient systems depend on the surface material and explore the improvements that modifications can bring.

Although high electric fields have been used in DC and RF applications for many years, up to now there has been no fundamental agreement on the cause of breakdown in these systems [1]. Recently, a group from the Muon Collaboration doing accelerator R&D, computer modelers at Argonne, and materials scientists using Atom Probe Field Ion Microscopy (APFIM) at Northwestern, have had success understanding the process in terms of high mechanical stresses at local field emitters in cavities. We have published this work in Phys Rev STAB, Nuclear Instruments and Methods, and many accelerator conference papers over the 18 months [2][3][4] The most interesting discovery in this work has been that **the pre-breakdown environment we measured in rf cavities, (0.1 μm asperities, $\sim$10 GV/m electric fields) has been used in material science for years, for precisely the sort of measurements we would like to make**[5]. This technology has been aggressively developed and has had recent breakthroughs such as the Local Electrode Atom Probe (LEAP) microscope [6].

Our model predicts that high voltage systems will break down when the mechanical stress produced by the local electric field exceeds the tensile strength of the surface material. This model seems to agree with all the good data we can find on copper rf structures. The figure shows how data on the maximum gradients produced in CLIC, NLC, KEK, the Muon Collaboration and old linacs compare with superconducting rf systems optimized for the ILC[2][7]. (CLIC data tolerated higher breakdown rates, and claim to be consistent with our argument [8].) The model strongly argues that breakdown events are the result of fragments or clusters breaking off of the surface and rapidly being ionized in the electron beams from the field emitter. Within the active volume, the power involved in these beams is comparable to nuclear weapons. This model is also generally in agreement with the experience with APFIM samples at the high fields used. Tiny APFIM samples operate at fields about 5 times higher than the local E field limit we postulate, but they also frequently fail, however there has been no systematic study of these failure modes.

Although the limits of superconducting systems like the ILC may be dominated by magnetic field effects, this model applies directly to failures due to field emission, it describes high

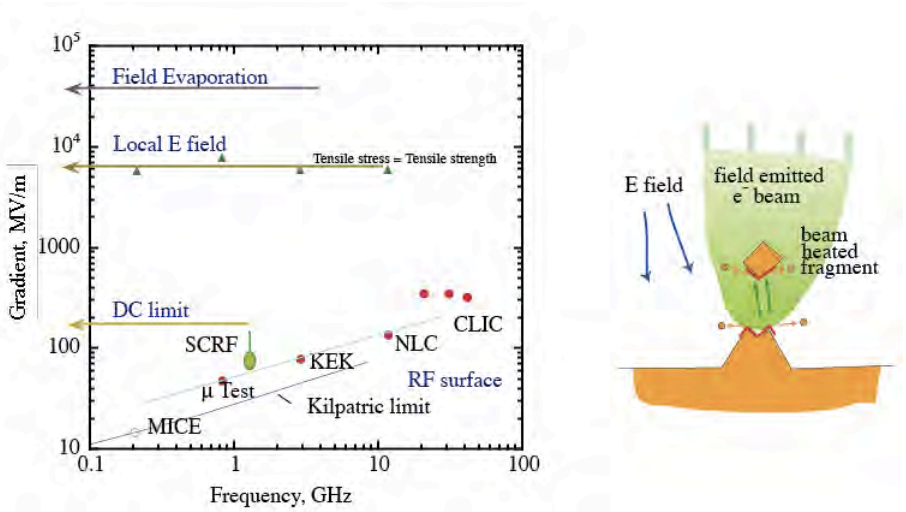

Figure 1: High field operating conditions for accelerator structures, and the trigger mechanism we propose compared to 50 - 100 year old DC data. Local tensile stresses and power densities can be very high.

power processing, and this work should be essential to the development of large quantities of superconducting surfaces running at the highest highest possible gradients.

The study of high fields proposed here is not an isolated effort. This work will involve a collaboration with the Muon Collaboration who are optimizing the surfaces in a working cavities at 805 and 201 MHz, with significant interests in converging on practical methods to operate at high accelerating fields in high magnetic fields. We will also be working with modeling experts at Argonne who are interested in showing how the basic mechanisms of breakdown work. A third interaction will be with superconducting rf programs at ANL and FNAL, who want metallurgical information on the surface configuration of superconductors, i.e. how the oxides, impurities, and supercurrents coexist in the top 50 microns of a superconductor.

The lack of basic knowledge of how the defining fields of the machine were produced was partially responsible for the catastrophes of ISABELLE (which could not produce magnets which matched the prototype), the SSC (which did not have the required data on conductor placement tolerances / good field region), and the NLC (which was plagued by breakdown events from then unknown causes). (The Tevatron, it seems, was sold as an "Energy Saver" and not as an energy frontier machine.) We believe an understanding of the basic processes of breakdown and the structure and influence of the conductor surface is essential to the credibility of the ILC design.

At the present time, the best experimental data for the high field breakdown thresholds of different materials is a Masters Thesis from Berkeley, in 1964, which was not done according to modern standards[9]. The environment of a APFIM permits this and other experiments under highly controlled conditions, over a wide range of parameters, which have never been possible for rf systems.

Broader Impact

We believe this work is of general interest to a very wide community. We had contacted

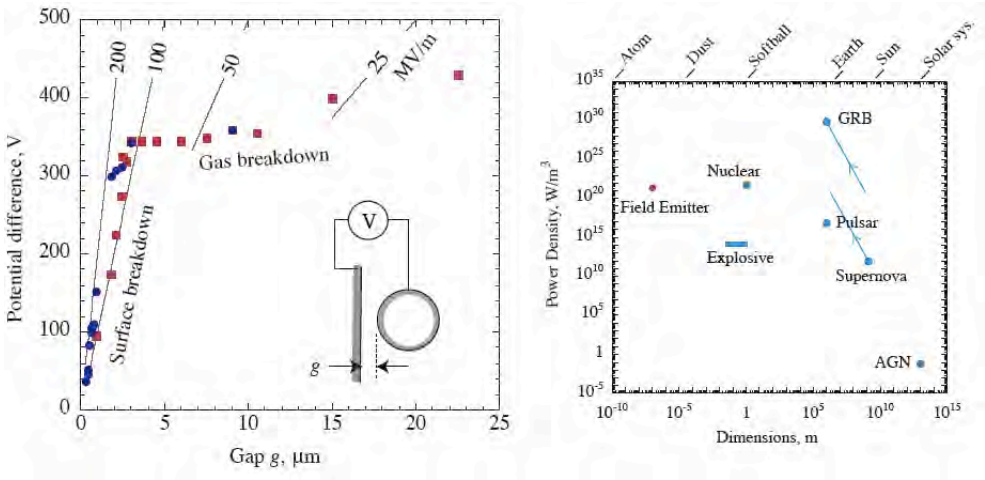

Figure 2: Early data (1900 -1905) on surface breakdown from Refs [10-11] showing ∼150 MV/m breakdown thresholds, and comparative power densities for astronomical and terrestrial power sources showing field emitted electrons generate very high power densities in small volumes.

the Argonne Office of Public Affairs and talked with them about issuing a Press Release three months ago, saying that we had a solution to one of the longest lasting problems in experimental physics, i.e. high voltage vacuum breakdown. We were diverted from this by the pressures of events, but we intend to get back to them as soon as things settle down a little. There is almost no interaction between "Big Science" and the general public on practical issues, and the connection we have made between very old data, common phenomena and very exotic physics should be interesting to a wide community. We think this work should be in the New York Times.

Breakdown at surfaces was discovered by Earhart and Michelson, at Chicago, in 1900 [10]. While checking the new "electron" theory of gas breakdown at small distances, they discovered that there were two mechanisms present, at large distances gas breakdown dominated, and at small distances breakdown of the surface was correctly identified as the mechanism. The break point where the two mechanisms met, at atmospheric pressure, occurs at about 300 V. This was confirmed 5 years later by Hobbs and Millikan [11], and is consistent with modern data on vacuum breakdown. Until our work, no theoretical understanding of this process developed over the last 100 years, although many papers have been written[1]. It is interesting to note that all consumer power switching takes place below 300 V, thus when switching on power in the home or lab, the initial contact is due to breakdown of a surface. This mechanism is thus accessible to everyone.

Another interesting feature of this mechanism is that the power densities involved are enormous. The numbers can be obtained from the values we measured for field emitted currents, electric field, the emitter dimensions, and volume for transferring electromagnetic field energy into electron kinetic energy[2]. Combining these gives, (10 GV/m)(10^{-7} m)(1 mA)/(10^{-7} m)^3= 10^{21} W/m^3, a value that seems to be greater than all other natural effects, except perhaps Gamma Ray Bursters (GRB's) [12]. The power density is comparable to nuclear weapons. Michelson and Millikan noticed the "hot sparks" in 1905, bought a vacuum pump, (which they didn't have), and invented vacuum ultraviolet spectroscopy. Both moved on, and did not look in detail at the mechanisms involved.

Combining these two ideas, however, one can conclude that: 1) this mechanism produces perhaps the highest power density commonly found in nature, and, 2) it is accessible to anyone with a wall switch or an electric light, and is used many times a day by everyone. These two facts should make this work almost irresistible to a wide spectrum of introductory physics courses, news media and science fair experiments. We believe it is very important for High Energy Physics to show that it can say interesting things to the general population. We want to experimentally verify the details first, however.

Vacuum breakdown affects many disciplines and technologies. Although there have been a variety of ways to work around this problem, a fundamental understanding of the mechanisms should be helpful, interesting and productive to a very wide community. In APFIM, like many branches of science and technology that use high voltages in vacuum, these mechanisms can also be an irritation. Although there are usually ways to work around problems, basic understanding of the problem is long overdue.

We have given a large number of talks on this subject in the last two years: FNAL (3 Acc. Sci. and Tech. Seminars), SLAC (Linear Collider Design Group), PAC03, Our High Gradient rf Workshop at Argonne, (3 talks), Northwestern (Mat. Sci. and Eng. Seminar), Argonne HEP (2 lunch seminars, 1 accelerator seminar), Univ of Chicago (Enrico Fermi Inst. Seminar), Int. Vac. Nanoelectronics Conf. EPAC04 and LINAC04.

The Northwestern University Center for Atom-Probe Tomography (NUCAPT) has an existing outreach program to involve women and legal minorities in the LEAP microscope work. There are many connections with local colleges (Harold Washington College) and with Evanston Township High School (ETHS).

Results of Prior Research

This work has grown from the study of cavities in a magnetic field done for the Muon Collaboration, to understand how cavities operated in a magnetic field and near sensitive single particle detectors. X rays were presumed to be a problem and in fact they have been. Prior funding for the breakdown studies has come from an Argonne LDRD.

We think we have developed a model of breakdown that explains the phenomenon in almost all environments, which can make quantitative, easily testable predictions. The data required for these predictions are also very easy to acquire, requiring only a radiation monitor and some way of measuring the relative electric field in the cavity at two values. We have tested these models in a variety of environments and published the results [2]. We are beginning to trust them.

While there has been extensive study of the time development of breakdown events from the first small local ionization to complete breakdown of a cavity, the trigger for breakdown, and how it was related to the metallurgy of surfaces has received very little attention until now. Our model predicts that the production of clusters and fragments is an essential component of breakdown. This is consistent with experience in Atom Probe Tomography, however there is almost no systematic data on sample failures under the high field environment used in data taking.

Our previous work has been published in three refereed papers and many conference papers. The Muon Collaboration summary of the results of our open cell cavity, an outline of the mechanisms of triggers for rf breakdown and a detailed calculation of the properties of clusters emitted from surfaces at high field. We have mentioned that one of the surprises of this work

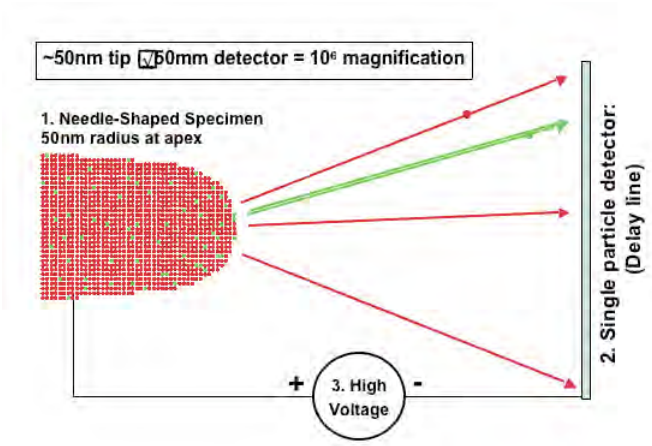

Figure 3: An Atom Probe Field Ion Microscope (APFIM) uses a pulsed voltage to evaporate single atoms from a sample and a microchannel plate plus a delay line detector to determine their position and velocity, enabling reconstruction of the positions of the atoms in the original solid.

was the discovery that Atom Probe Field Ion Microscopes studied the same environment that causes breakdown in rf cavities. Specific technical highlights of this work include:

- Understanding x ray production from rf cavities.[13]
- Identification of mechanical stress as the primary trigger for high field breakdown[2][3].
- Discovery of discontinuities in Voltage vs. time plots in APFIM data that confirm emission of fragments[3]. This is shown in Figure 3.
- Preliminary models of the early development of breakdown triggers in an rf field[3] [14].
- Successful comparison of this model with data from NLC, KEK, IPNS and ISIS linacs[2].
- Modeling of the emission of clusters at high fields[4].
- Identification of other mechanisms, 1) Production of GV/m fields by from interactions between surface current and defects [3]. 2) High stresses produced within emitters when field emission currents interact with high static B fields. These two mechanisms are less common under optimum conditions.
- Hosting an international workshop on High Gradient RF[15][16].
- Constructing a facility for applying and measuring surface properties (coatings) in an APFIM.

The environments where these systems have been tested have been the comparatively dirty, inaccessible and uncontrolled surfaces of rf cavities. While this is good for the understanding rf cavities, it is more interesting and valuable to test the models over a wide variety of materials, temperatures, surface treatments, and mechanical stresses, in a highly controlled environment with excellent instrumentation. This is what we want to do.

Facilities, Equipment and Other Resources

Atom probe tomography is a rapidly advancing field. The recent development of the LEAP microscope has extended the resolution, sensitivity, statistics and graphics of this technology.

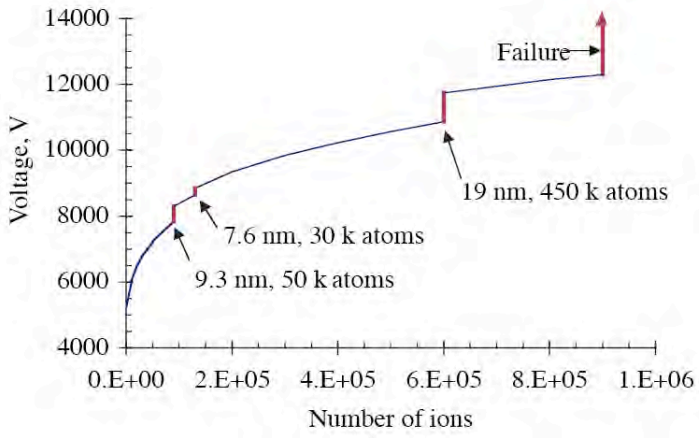

Figure 4: Discontinuities in the voltage vs. time (constant erosion rate) plot for an APFIM. During normal operation the voltage in these devices is controlled to maintain a stable evaporation rate, effectively determining a constant surface field. Since $E \sim V/r$, measured voltage is proportional to tip radius (∼50 nm). Size (in nm) assumes fragments are cubes.

In addition we have constructed a facility to do testing of coatings for the Muon Collaboration. The purpose of these tests is to test and measure coatings that can suppress dark currents in the Muon Ionization Cooling Experiment (MICE).

Recently ANL and the Northwestern University Center for Atom-Probe Tomography (NUCAPT), directed by Prof. David Seidman have joined forces to understand how the maximum fields in high gradient systems depend on the surface material. The NUCAPT is among the world leaders in the field of three-dimensional atom-probe microscopy, particularly as result of the recent installation of a LEAP microscope, manufactured by Imago Scientific Instruments [6] Currently only three other LEAP microscopes, with a comparable performance, exist throughout the world. Atomic-probe tomography consists of dissecting a specimen on an atom-by-atom basis, employing pulsed field-evaporation, and determining the chemical identity of each field-evaporated atom by time-of-flight (TOF) mass spectrometry, with single atom identification capability, using a 2D position sensitive delay line detector, which yields the position of each atom in a specimen with sub-nanoscale resolution. Analysis rates of upwards of 72 million atoms/hr have been achieved employing a LEAP microscope at NU[17][18]. The collected data is used to reconstruct a specimen in three-dimensions, where the chemical identity of each atom is known. In addition to the LEAP microscope there is also a pulsed-laser atom-probe (PLAP) microscope, which permits one to dissect a tip atom-by-atom using nanosecond laser pulses produced by a nitrogen laser or pulsed electric fields. The PLAP has a pre-chamber that permits us to deposit different metallic coatings on copper tips or other substrates, under ultrahigh vacuum (UHV) conditions. The collaboration between ANL and NUCAPT will produce spectacular results with lasting impact and strongly advance the understanding of how the maximum fields in high gradient systems depend on the surface material.

An example of the ability of our three-dimensional atom-probe (3DAP) microscope to reconstruct a specimen with subnanometer spatical resolution and chemical identification of individual atoms is shown in Figure 5 (left). This figure shows the nanostructure of an Fe-

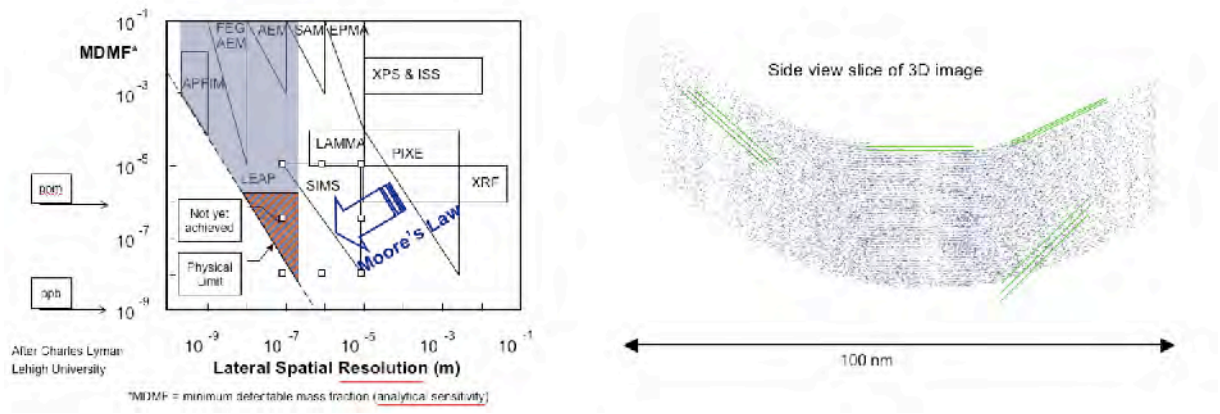

Figure 5: LEAP resolution and sensitivity, how it sees samples (note atomic planes and individual atoms). Compare the fragment dimensions in Fig. 3, with the 100 nm tip size to see the magnitude of discontinuities.

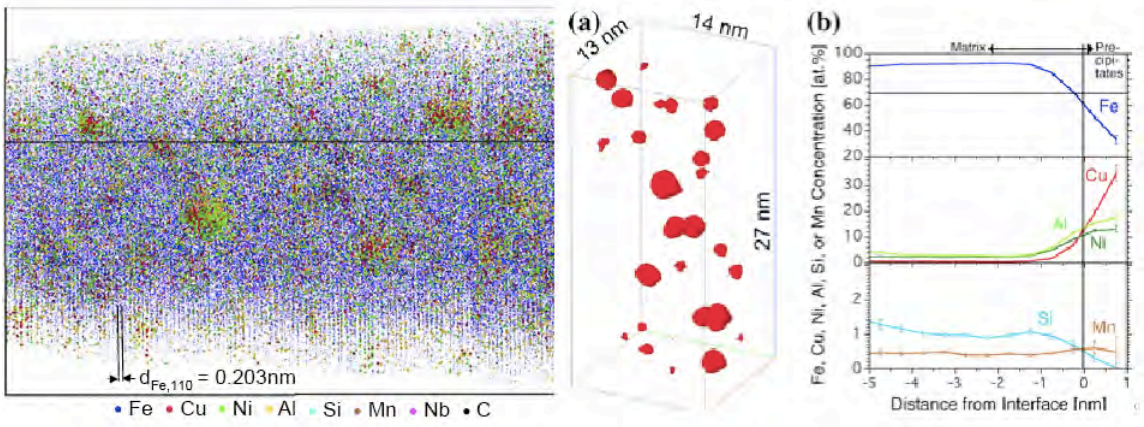

Figure 6: Left: 3DAP microscope reconstruction of an Fe-Al-Ni-Cu-2 steel, after austenitizing at 1050degC, quenching, and aging at 823 K for 2 hr. The reconstructed volume is 14x13x27 nm^3 and contains 204,000 atoms. The (110) planes, an interplanar spacing of 0.203 nm, are resolved. Right: (a) A 5 at. % Cu isoconcentration surface (red) delineates Cu-rich precipitates in Fe-Al-Ni-Cu-2 steel. (b) The proxigram concentration profile displays a quantitative compositional analysis of the precipitates shown in (a), together with the surrounding matrix.

Cu-Ni-Al-Si-Mn-C ferritic steel, developed to have blast-resistant properties, that had been heat treated to produce a high number density ($6x10^{24}/m^3$) of nanometer diameter (0.5 to 2 nm) copper-rich precipitates[19]. The 110 atomic planes are clearly resolved with an interplanar spacing of 0.203 nm. Also note that individual atoms within the 110 are resolved and their chemical identities obtained. This nanostructure yields excellent mechanical properties: A yield strength of 135 ksi (ca. 945 MPa) and an ultimate tensile strength of 145 ksi (ca. 1015 MPa) are obtained to below -40C and the ductility is 30%. Figure 5 (right) (a) (next one) exhibits Cu-rich precipitates in the same ferritic steel that are indicated by a 5 at. % Cu isoconcentration surface (red) in the indicated volume of material; note, no atoms are displayed in this representation [19]. The so-called proxigram of the different elements in this steel are displayed in Figure 5(b), which yields the concentration profiles as a function of distance from the matrix/precipitate interface; the latter is at 0 nm. This figure shows directly the variations of concentrations of all the elements both within the matrix and the copper-rich precipitate. There is currently no other way to obtain this type of chemical information with the same spatial resolution. The LEAP microscope will be employed to determine the chemical compositions of different coated substrates both before and after they have failed during pulsed field-evaporation with an electric field.

FY2005 Project Activities and Deliverables

We are presently funded from Argonne LDRD funds. These funds will allow us to present preliminary data at PAC05 and the Cornell superconducting workshop.

We understand that the behavior of surfaces under high fields depends partially on the top monolayer, (field emission) and partially on the bulk properties(breakdown). With our facilities we will be able to independently vary bulk and surface properties and measure a wide spectrum of behavior due to a wide spectrum of materials properties, preparations and variables such as temperature and exposure to gasses. There are a number of approaches we would like to begin in the first year:

- From the point of view of breakdown studies, the most important data would be the spectrum of failure of samples as a function of applied field. As there is no reliable, systematic data on breakdown thresholds for different materials, it would be desirable to do this with a large sample of materials, under a variety of conditions such as temperature, gas pressure and surface modification techniques. The coatings we would like to apply become one of the important variables here and these must also be studied systematically to determine the bonding of coating with substrate.
- Suppression of field emission. It has been shown that fractions of a monolayer of materials with different work functions will change the field emission by large factors. What is not known is how to apply these materials to real surfaces, and how the surfaces will stick in the presence of oxide layers, gasses and a variety of other real world effects. These can be experimentally checked. The materials with desirable work functions do not obviously bond strongly to the surfaces we would like to use, and it is possible to look at ways to improve this bonding with intermediate layers.
- Study of clusters and fragments. Our breakdown model implies that the emission of clusters and fragments from the surface is an important component of the breakdown trigger. There is a little published data that confirms that these effects exist. We would like to look at ways that an APFIM can be made more sensitive to this phenomena and look systematically for these clusters and fragments. We would also like to look at

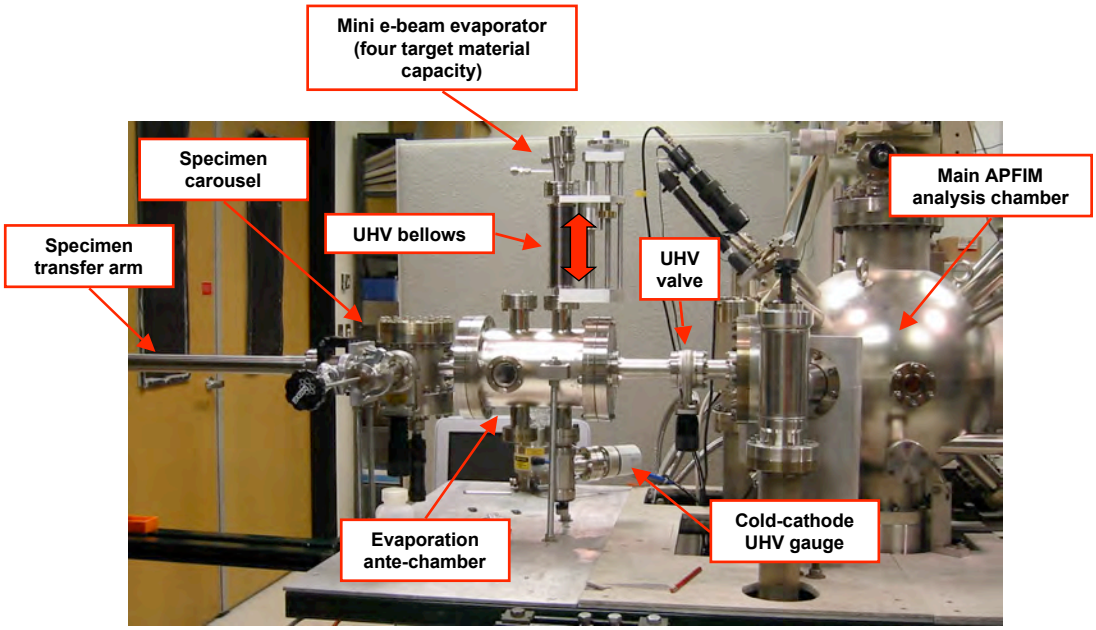

Figure 7: The evaporation chamber on the Pulsed Laser Atom Probe Microscope (PLAP), showing the evaporator, evaporation chamber and analysis chamber.

LEAP data to see if there is any evidence for cluster and fragment emission as part of sample failure modes.

- Find the constraints on the superconducting rf surface and see if there are ways of modifying the surface, for example with multilayer oxides, which would protect the ILC superconductor from the primary effects of O and H penetration, dust and other contaminants.

At the end of the first year we will have our coating facility operating and we should have presented some very preliminary data at PAC05, and the Cornell superconducting rf workshop in the early summer. At the end of the year we will also have some useful preliminary data from runs for other users on the LEAP microscope which will provide useful information on how to proceed most efficiently.

FY2006 Project Activities and Deliverables

- We will write up the results of these systematic studies. In FY 06 we will primarily do the systematic studies described in the previous section. At the end of this year we should have considerable data to compare with models and guide future experiments.
- We will develop a "best method" for suppressing dark currents and magnetic field induced breakdown events at the end of this period, with extensive documentation. The initial motivation of all this effort to understand the high gradient behavior of metals is to develop practical low frequency cavities for muon cooling. The work has expanded and become more general, but the need for better performance in muon cooling cavities remains. One goal of this work is to develop and justify an optimized coating technology that can be used in a variety of low frequency cavities, such as the 201 MHz structure,

presently under construction and soon to be installed in the Fermilab Muon Test Area. This practical goal should help to keep the studies focused.

FY2007 Project Activities and Deliverables

- We will finish final systematic scans, re-take particularly important data and write up the final papers. Since the experimental program we have outlined is all new, the goals in the third year will depend, to some extent, on what we have learned.
- We will modify the breakdown model as needed to accommodate the new data on breakdown. This will incorporate practical effects such as dust, coatings and practical suggestions for simplifying the construction of the ILC superconducting rf system.

Budget justification: Northwestern University

The primary costs involved are for support for Dr. Jason Sebastian for 8 months. We have also included some support for time on the LEAP microscope ($250 /day) and misc hardware for modifications to the coating facility and pulsed laser atom probe (PLAP) device. Work in all years will involve both the LEAP device and work with the coating deposition system. While there are no charges for the PLAP, maintenance and modifications must be included in the overall operating expenses.

Three-year budget, in then-year K$

Institution: Northwestern University

Item	FY2005	FY2006	FY2007	Total
Other Professionals	23.4	24.1	24.8	72.3
Graduate Students	0	0	0	0
Undergraduate Students	0	0	0	0
Total Salaries and Wages	23.4	24.1	24.8	72.3
Fringe Benefits	5.2	5.6	5.9	16.7
Total Salaries, Wages and (24%)Fringe Benefits	28.6	29.7	30.7	89
Equipment	0	0	0	0
Travel	5	5	5	15
Materials and Supplies	5	5	5	15
Hardware modifications	5	5	5	15
Total direct costs (incl 48%)	43.6	44.7	45.7	134
Indirect costs	21.2	21.7	22.2	65.1
Total direct and indirect costs	64.8	66.3	67.9	199

References

[1] 2001 Report on the Next Linear Collider, SLAC Report SLAC-R-571, (2001), p73

[2] J. Norem, V. Wu, A. Moretti, M. Popovic, Z. Qian, L. Ducas, Y. Torun and N. Solomey, Phys. Rev. STAB, **6**, 072001, (2003)

[3] J. Norem, Z. Insepov, I. Konkashbaev, Nucl Instr. and Meth. in Phys. Res. A 537 (2005) 510

[4] Z. Insepov, J. Norem, A. Hassanein, Phys. Rev. STAB, **7** 122001 (2004)

[5] M. K. Miller, *Atom Probe Tomography, Analysis at the Atomic Level*, Kluwer Academic / Plenum Publishers, New York, (2000)

[6] Imago Scientific Instruments, Madison Wisconsin, http://www.imago.com

[7] H. H. Braun, S. Dobert, I. Wilson and W. Wuensch, Phys. Rev. Lett. bf 90, 22401, (2003)

[8] W. Wuensch, CERN, Private Communication, (2004)

[9] P. Kranjec and L. Ruby, J. of Vac. Sci. and Tech. **4**, 94, (1967)

[10] R. F. Earhart, Phil Mag. **1** 147 (1901)

[11] G. M. Hobbs, Phil. Mag., **10**, 617 (1905)

[12] D. Q. Lamb, Phys Rep. **333-334** (2000) 505

[13] J. Norem, A. Moretti, M. Popovic. Nucl. Instr. and Meth. In Phys. Res. A **472**, 600, (2001)

[14] J. Norem, Z. Insepov, Proceedings of EPAC04, Lucerne, Sw. (2004)

[15] J. Norem, CERN Courier, **44** (Feb/Mar 2004) p21

[16] J. Norem, *Summary of the Workshop on High Gradient rf*, Proceedings of LINAC04, Lubeck, Germany (2004)

[17] C. K. Sudbrack, PhD Thesis, Northwestern University, (2004)

[18] S. S. A. Gerstl, PhD Thesis, Northwestern University, (2004)

[19] D. Isheim, M. Gagliano, M. E. Fine, D. N. Seidman, Submitted for publication, (2004)

2.50: Evaluation of MgB2 for Future Accelerator Cavities

(new proposal)

Accelerator Physics

Contact person
V. Nesterenko
vnesterenko@ucsd.edu
(858) 822-0289

Institution(s)
U.C. San Diego
LANL

New funds requested
FY05 request: 59,300
FY06 request: 59,300
FY07 request: 59,300

Evaluation of MgB_2 for Future Accelerator Cavities

Proposal for LCRD/UCLC 2005

Classification (subsystem)

RF Cavity in main linac

Personnel and Institutions requesting funding

V. F. Nesterenko, University of California, San Diego (UCSD)

Collaborators

T. Tajima, Los Alamos National Lab (LANL)

Project Leader

V. Nesterenko
vnesterenko@ucsd.edu
(858) 822-0289

Introduction

Superconducting RF technology was chosen for the International Linear Collider (ILC) in August 2004. While Nb technology is the baseline for the ILC design and associated R&D should be the first priority, it is still important to find a new superconducting material that can exceed the Nb performance.

Since the accelerating gradient (E_{acc}) of Nb cavities are theoretically limited at ~50 MV/m, finding a material that can exceed this limit would open up the possibility of increasing the achievable E_{acc}, leading to a shorter and more cost effective accelerator.

A material such as magnesium diboride (MgB_2), that has a higher superconducting transition temperature (T_c=39 K) than Nb (T_c=9.2 K), could not only provide a higher gradient but also give other benefits, such as a higher cavity Q_0 at the same operating temperature and increasing the quench margin due to the higher T_c. If the ILC can be operated with lower losses or at a temperature higher than 2 K, the capital and operational costs for the cryogenic system could be significantly lower.

Motivation

Superconductivity in the intermetallic compound MgB_2 was recently discovered with the T_c as high as 39 K (Nagamatsu et al., 2001). Although its T_c is not as high as of so-called high-T_c materials such as YBCO, its metallic nature and the ensuing simplifications in fabrication have triggered a number of studies.

Regarding the application to RF cavities, Collings et al. show the potential of MgB_2 having a ~50 % higher theoretical critical magnetic field than Nb [1]. Tajima proposed a method to form a bulk MgB_2 layer inside a copper cavity using a hot isostatic press (HIP)

technique [2]. In the field of MgB_2 fabrication, Nesterenko et al. have successfully developed a method to fabricate a dense MgB_2 using an ordinary HIP machine [3]. Fully dense material with a mirror-like surface quality is important for microwave devices such as RF cavities and for enabling fabrication of superconductor thin films with superior quality via laser ablation and sputter deposition.

The most important feature for a radio-frequency (RF) cavity for particle accelerators is RF loss at high surface magnetic fields. Unfortunately, oxide-based high-T_c materials such as YBCO show rapid increase of RF surface resistance (R_s) with higher magnetic fields and cannot be applied to RF cavities. MgB_2, however, has shown much less increase of R_s with higher magnetic fields [4]. For example, Figure 1 shows a recent result of the dependence of RF surface resistance (R_s) on the surface magnetic field [5]. As one can see, the R_s did not increase up to 60 Oe and showed small increase at ~120 Oe. These numbers are equivalent to E_{acc}~1.5 and 3 MV/m, respectively. In the experiment, the highest available field was limited by the available power.

Although the sample used in this experiment showed higher R_s than Nb, possibly because the film was not optimized, some good films have already shown lower R_s at 4 K. Figure 2 shows such an example. It indicates that further reduction is possible by reducing the residual resistance.

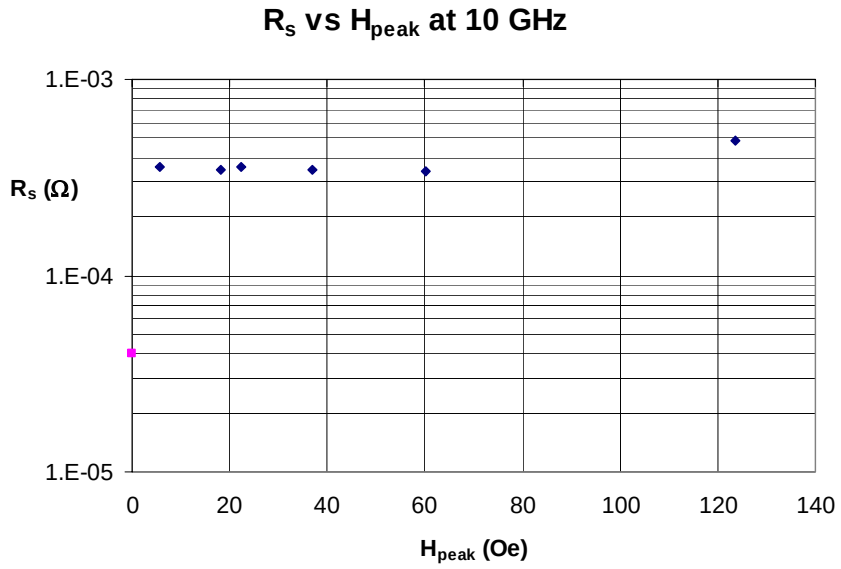

Figure 1: R_s dependence on surface magnetic field [5]. The purple dot shows the BCS resistance of Nb as a reference.

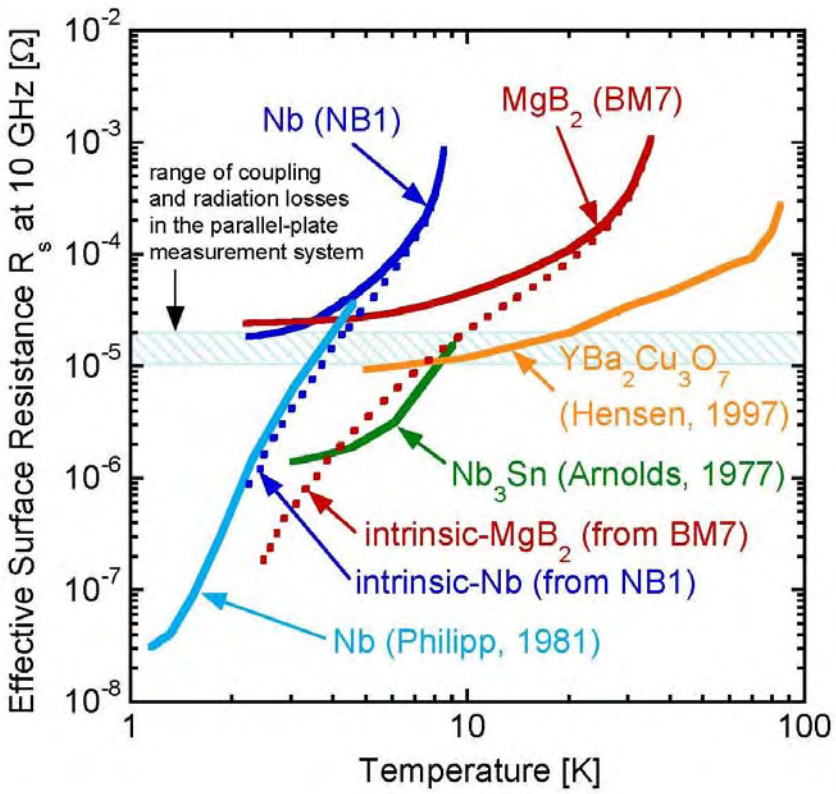

Figure 2: RF surface resistance of MgB_2 film measured at LANL a function of temperature. As a reference, Nb data are shown. Also, dotted lines are the prediction without residual resistance [6].

With much higher T_c of 39 K compared to 9.2 K for Nb, it is worthwhile to investigate the possibility of using this material for an RF cavity.

Capability of studying MgB_2 at UCSD

UCSD has unique expertise in hot isostatic pressing (HIPing) of magnesium diboride (bulk and wire) with excellent mechanical and superconducting properties [3, 7-17]**.** The PI laboratory has full scale processing equipment based on cold and hot isostatic presses and all steps starting with vacuum encapsulation are performed in house.

The UCSD team also has the expertise and equipment for the application of the Resonant Ultrasound Spectroscopy (RUS) method [18] for high accuracy measurements of elastic properties of magnesium diboride which can be used for tuning of the HIPing. The first published data on elastic properties of HIPed solid magnesium diboride are in good agreement with theoretical estimates. We plan to use RUS measurements of elastic moduli as a very accurate method to control the material quality. Another application of the RUS measurements will be the evaluation of elastic moduli of composite materials (such as the composite-structured, MgB_2 with improved surface resistance) and the quality of bonding between components based on measurements of *Q*.

Capability of testing MgB_2 samples and cavities at LANL

The SRF Structures Lab at Los Alamos Neutron Science Center (LANSCE) has a capability of measuring MgB_2 samples [19] and SRF cavities [20]. It has 200-600 Watt RF amplifiers from 0.2 – 4.0 GHz. Also, it has a number of 3-GHz Nb single-cell cavities on which a MgB_2 film can be coated as soon as a reasonable coating technique has been developed.

Project Overview

UCSD and LANL have agreed to collaborate on the evaluation of MgB_2 for the application to the RF cavities. According to the agreement, UCSD will be responsible for providing the samples of bulk magnesium diboride and possibly high-quality MgB_2 targets for the development of laser vapor deposition and/or magnetron sputtering techniques. LANL will be responsible for measuring the RF properties such as surface resistance, its field dependence and the critical magnetic field. Both parties are responsible for developing the techniques to fabricate MgB_2 cavities and will share the efforts related to analysis and publication.

The following project goals have been defined:

1) Establish the fabrication parameters to get an RF surface resistance lower than Nb at 4 K for bulk and film MgB_2.

2) Develop one or more technique(s) to deposit a high-quality MgB_2 film on the inner surface of a cavity made of Nb and/or Cu.

3) Develop one or more technique(s) to make a cavity with a high-quality bulk MgB_2.

4) Measure Q_0 versus E_{acc} curves of the cavities made of film MgB_2 and bulk MgB_2 to compare with Nb results.

5) Test critical magnetic field to compare the theoretical limits with Nb.

Broader Impact

The outcome of the proposed work will broadly contribute to the advancement of understanding of the relationship between processing, microstructure/defects, and superconducting microwave properties of MgB_2. Successful fabrication of fully dense superconductors and high-quality films in practical configurations, such as microwave cavity components, will have major impacts on applications of superconductors for communications and energy applications. Graduate students involved in this research will be educated and trained in the materials science of superconductors as well as in the forefront aspects of superconductor microstructural control, properties and applications. The outcome of this exciting superconductor materials/technologies research will broadly benefit the superconductor industries as well as stimulate research and development effort in academia and research institutes.

Project Activities and Deliverables

During FY05, we plan to complete the optimization of the MgB_2 fabrication technique to lower the residual resistance so that the RF surface resistance is reduced to less than that of Nb at 4 K. We also plan to complete fabrication of the targets to be used for laser ablation or magnetron sputter coating of MgB_2. In addition, we plan to measure the critical magnetic field using small samples.

During FY06, we plan to develop a method to fabricate a bulk MgB_2 cavity using a CIP/HIP technique. Also, in collaboration with other labs, we plan to develop a method to coat the inner surface of a cavity. Since there are 3-GHz Nb cavities at LANL, we will try to coat those cavities first, but our ultimate goal is to coat on a highly-thermal conductive metal such as copper. We also plan to complete the critical magnetic field measurement.

During FY07, we plan to demonstrate at least one method to either fabricate a bulk MgB_2 cavity or to coat MgB_2 on a Nb or copper cavity and measure the Q_0 versus E_{acc} curve.

Budget Justification

The budget request includes funding for salary of a graduate student, who will dedicate 6 months per year to this effort (including travel to meetings/conferences). Also included are some upgrades of the equipment for fabricating MgB_2 samples and its supplies at UCSD and costs for testing the samples at LANL. The following budgetary estimate is in k$.

Table 1: Budgetary estimate (in k$) for UCSD-LANL collaboration on the evaluation of MgB_2 for SRF cavities.

Item	FY 2005	FY2006	FY2007
Graduate student salary (6 months)	10.0	10.0	10.0
0.5 month PI summer salary (including academic summer salary benefits)	7.0	7.0	7.0
Total Salaries (incl. fringe benefits)	17.4	17.4	17.4
Travel	2.0	2.0	2.0
Materials and Supplies	4.0	4.0	4.0
Samples preparation	5.0	5.0	5.0
Tests at LANL	10.0	10.0	10.0
Total direct costs	38.4	38.4	38.4
Total indirect costs (incl. 54%)	20.7	20.7	20.7
Total direct and indirect costs	**59.3**	**59.3**	**59.3**

References

[1] E.W. Collings, M.D. Sumption, T. Tajima, "Magnesium Diboride Superconducting RF Cavities for High Energy Particle Acceleration," *Superconductor Science and Technology* 17 (2004) S595-S601.

[2] T. Tajima, "Possibility of MgB_2 Application to Superconducting Cavities," *Eighth European Particle Accelerator Conference (EPAC2002)*, Paris, France, June 3-7, 2002.

[3] V.F. Nesterenko, "Bulk Magnesium Diboride-Mechanical and Superconducting Properties", in *Processing and Fabrication of Advanced Materials XI, Proceedings of 11th International Symposium on Processing and Fabrication of Advanced Materials*, edited by T.S. Srivatsan and R. A. Varin, ASM International, ASM International, Materials Park, OH, 2003, pp. 29-43.

[4] A.T. Findikoglu et al., "Microwave Performance of Fully-Dense Bulk MgB_2," *Applied Physics Letters*, 83, pp. 108-110, 2003.

[5] T. Tajima et al, "MgB_2 RF Surface Resistance Dependence on Magnetic Field," *Applied Superconductivity Conference (ASC04)*, Jacksonville, FL, October 3-8, 2004.

[6] A. T. Findikoglu, unpublished. 400 nm film coated on Sapphire by B. Moeckly of Superconductor Technologies, Inc.

[7] S.S. Indrakanti et al., "Hot isostatic pressing of bulk magnesium diboride: mechanical and superconducting properties," *Philosophical Magazine Letters*, **81**, pp. 849–857, 2001.

[8] N.A. Frederick et al., "Improved superconducting properties of MgB_2," *Physica* C, **363**, pp. 1–5, 2001.

[9] A. Serquis et al., "Synthesis, characterization and aging of MgB_2. *Mat. Res. Soc. Symp. Proc*. **689**, pp. E2.7.1–E2.7.6, 2002.

[10] A. Serquis et al., "Influence of microstructures and crystalline defects on the superconductivity of MgB_2," *J. Appl. Phys*., **92**, pp. 351–356, 2002.

[11] A. Serquis et al., "Degradation of MgB_2 under ambient environment," *Appl. Phys. Letters*, **80**, pp. 4401–4403, 2002.

[12] M.P. Maple et al., "Critical scaling and flux dynamics in bulk MgB_2 and high-purity $YBa_2Cu_3O_{7-\delta}$ single crystals," *Physica* C, 382, pp. 132-136, 2002.

[13] S. Li et al., "Mixed-state flux dynamics in bulk MgB_2," *Physica C*, **382**, pp. 177-186, 2002.

[14] V.F. Nesterenko and Y. Gu, "Elastic Properties of Hot Isostatically Pressed Magnesium Diboride," *Applied Physics Letters*, 2003, **82**, pp. 4104-4106, 2003.

[15] V.F. Nesterenko, "Dependence of Elastic and Superconducting Properties of Magnesium Diboride on Conditions of Hot Isostatic Pressing", in *Processing and Fabrication of Advanced Materials XII, Proceedings of 12th International Symposium on Processing and Fabrication of Advanced Materials*, edited by T.S. Srivatsan and R. A. Varin, ASM International, Materials Park, OH, 2004, pp. 40-59.

[16] U. Harms et al., "Low Temperature Elastic Constants of Polycrystalline MgB_2," *Journal of Superconductivity*, **16**, pp. 941-944, 2003.

[17] A. Serquis et al., "Large Field Generation With Hot Isostatically Pressed Powder-in-Tube MgB_2 Coil at 25K," *Supercond. Sci. Technol., Rapid Communications*, **17,** pp. L35-L37, 2004.

[18] A. Migliori and J.L. Sarrao, "*Resonant Ultrasound Spectroscopy*," Wiley@Sons, Inc., 1997

[19] T. Tajima, F. L. Krawczyk, J. Liu, D. C. Nguyen, D. L. Schrage, A. Serquis, A. H. Shapiro, V. F. Nesterenko, Y. Gu, "RF Surface Resistance of a HIPped MgB_2 Sample at 21 GHz," *6th European Conference on Applied Superconductivity (EUCAS2003)*, Sorrento (Naples), Italy, September 14-18, 2003.

[20] T. Tajima et al., "Status of the LANL Activities in the Field of RF Superconductivity," *Proc. 11th Workshop on RF Superconductivity (SRF2003)*, Travemunde, Germany, September 8-12, 2003.

VITALI F. NESTERENKO, Professor
Department of Mechanical and Aerospace Engineering, University of California, San Diego
9500 Gilman Drive, La Jolla, California 92093-0411
Tel: (858) 822-02890; Fax: (858) 534-5698; E-mail: **vnesterenko@ucsd.edu**

PERSONAL: Date of birth: January 16, 1949, Russia; U.S. Citizen.

EDUCATION:

1971 -	Diploma with Excellence, Department of Physics, NSU, Novosibirsk, Russia.
1975 -	Ph.D. in Physics, Academy of Sciences, Russia
1989 -	Doctor of Physics and Mathematics, Academy of Sciences, Russia.

EXPERIENCES (last 10 years):

March 1996 – Present	Professor of Materials Science, University of California, San Diego.
October 1999 - January 2003	Director of UCSD Materials Science and Engineering Program.
March 1994 - March 1996	Visiting Scholar, Dept of Applied Mech. and Eng. Sciences, UCSD

5 PUBLICATIONS (most closely related to the proposed project)

S.S. Indrakanti, V.F. Nesterenko, M.B. Maple, N.A. Frederick, W.M. Yuhaz, and Shi Li, Hot Isostatic Pressing of Bulk Magnesium Diboride: Mechanical and Superconducting Properties, *Phil. Mag. Lett,*, **81**, 849-857, 2001.

N.A. Frederick, Shi Li, M.B. Maple, V.F. Nesterenko, and S.S. Indrakanti, Improved Superconducting Properties of MgB_2, *Physica C*, **363**, 1-5, 2001.

A.T. Findikoglu, A.Serquis, L. Civale, X.Z. Liao, Y.T. Zhu, M. Hawley, F.M. Muller, V.F. Nesterenko, and Y. Gu "Microwave Performance of Fully-Dense Bulk MgB_2", *Appl. Physics Lett.*, **83**, 108-110, 2003.

A.Serquis, L. Civale, D.L. Hammon, X.Z. Liao, J.Y. Coulter, Y.T. Zhu, M. Jaime, D.E. Peterson, F.M. Muller, V.F. Nesterenko, and Y. Gu, "Hot Isostatic Pressing of Powder in Tube MgB_2 Wires", *Appl. Phys. Lett.*, **82**, 2847-2849, 2003.

V.F. Nesterenko and Y. Gu "Elastic Properties of Hot Isostatically Pressed Magnesium Diboride", *Appl. Phys. Lett,*, **82**, 4104-4106., 2003

5 OTHER SIGNIFICANT PUBLICATIONS

A. Serquis, X.Y.Liao, Y.T. Zhu, J.Y. Coulter, J.Y. Huang, J. O. Willis, D.E. Peterson, F.M. Mueller, N.O. Moreno, J.D. Thompson, V.F. Nesterenko, and S.S. Indrakanti, Influence of Microstructures and Crystalline Defects on the Superconductivity of MgB_2, *Journal Applied Physics*, **92**, 351-356, 2002.

A.Serquis, L. Civale, J.Y. Coulter, D.L. Hammon, X.Z. Liao, Y.T. Zhu, D.E. Peterson, F.M. Muller, V.F. Nesterenko, and S.S. Indrakanti "Large Field Generation With Hot Isostatically Pressed Powder-in-Tube MgB_2 Coil at 25K", *Supercond. Sci. Technol., Rapid Communications*, vol. **17,** L35-L37, 2004.

V.F. Nesterenko, W. Goldsmith, S.S. Indrakanti, and Yabei Gu, Response of Hot Isostatically Pressed Ti-6Al-4V Targets to Normal Impact by Conical and Blunt Projectiles, *Int. .J. of Impact Eng.*, **28/2**, 137-160, 2003.

C. Daraio, V.F. Nesterenko and S. Jin "Highly Nonlinear Contact Interaction and Dynamic Energy Dissipation by Forest of Carbon Nanotubes", *Appl. Phys. Letters*, **85**, 5724-5726, 2004.

V.F. Nesterenko, Dynamics of Heterogeneous Materials, Springer-Verlag, NY, 2001.

Total number of publications in Archival Journals 107, two books.

RESEARCH INTERESTS

High pressure, high temperature powder-based processing of advanced materials (magnesium diboride, titanium alloy based materials, wafer bonding)

Strongly nonlinear wave dynamics in phononic metamaterials

Dynamic behavior of materials

Research supported by NSF, ONR, LANL, SRI, and von Liebig foundation.

AWARDS AND HONORS: Fellow of American Physical Society

2.51: Investigation of Secondary Electron Emission from Nb Surfaces with Different Surface Treatments

(new proposal)

Accelerator Physics

Contact person
Robert Schill
schill@ee.unlv.edu
(702) 895-1526

Institution(s)
U.N. Las Vegas

New funds requested
FY05 request: 81,248
FY06 request: 0
FY07 request: 0

Investigation of Secondary Electron Emission from Nb Surfaces with Different Surface Treatments

Proposal for LCRD/UCLC 2005

Classification (subsystem)

RF cavity for the main linac

Personnel and Institutions requesting funding

R. A. Schill, Jr., University of Nevada Las Vegas (UNLV)

Collaborators

T. Tajima, Los Alamos National Laboratory (LANL)

Project Leader

Robert A. Schill, Jr.
University of Nevada Las Vegas
Electrical and Computer Engineering Department
4505 Maryland Parkway
Las Vegas, Nevada 89154-4026
schill@ee.unlv.edu
(702) 895-1526

Introduction

Electron field emission and multipacting inhibit goals in achieving a high gradient in Nb superconducting rf (SRF) cavities. Understanding and characterization of the secondary electron emission (SEE) from Nb surfaces in the superconducting state and with various surface treatments are important for the design of SRF cavities.

Adsorbants, whether physisorbed or chemisorbed, change the surface characteristics of the niobium relative to the bulk. This affects the electronic properties of the material. These electronic properties, namely the true secondary electron, inelastically backscattered primary electron, and the elastically reflected primary electron properties, are surface material dependent and, consequently, are dependent of the cleaning protocols employed. [1-5]

The niobium cavities support significantly large electromagnetic fields that not only accelerate the beam but may undesirably promote field emission leading to electron acceleration and electron impacting with the niobium wall. This impact can lead to the generation of one or more secondary electrons (based on the electronic properties of the niobium walls) that, in turn, act as primary electrons, which may result in the generation of more electrons in a localized region. Once resonance is achieved with the fields supported by the cavity, the number of impacting electrons grows, yielding an avalanche growth of impacting electrons denoted as multipacting. [1] Consequently, RF power is

absorbed and/or dissipated in this multipacting beam, preventing the power in the supported cavity fields to increase as the power supplied to the cavity is increased. The electron collisions with the walls of the structure lead to a localized increase in temperature. When the localized temperature increases beyond a critical value, the superconductivity property of the localized region is compromised. Therefore, the Q_0 (quality factor) of the cavity is significantly reduced at the multipacting thresholds.

It becomes important to simulate the electronic properties or its effects in design codes to optimize the full potential of the material with surface structure and surface contaminants when designing cavity configurations.

Motivation

The Electromagnetics and Pulse Power groups at UNLV continue to develop and refine a novel technique to measure secondary electron emission from niobium under cryogenic temperatures in an ultra high vacuum (UHV). Ultra high vacuum pressures (~1.2×10^{-9} Torr without baking) attained by the vacuum system fits well within the parameter regime of interest. Conventional secondary electron emission techniques provide lumped secondary electron yields relative to incident primary electron energies.

The novel technique under development in the Electromagnetics Laboratory at UNLV should provide intimate knowledge of the initial conditions of the emitted secondary electrons. The current secondary electron emission system, Fig. 1, contains a particle position detector, a 50 eV to 5 keV pulsed electron gun, and a target on a rotatable cryostat. The resolution of the system is well characterized with particle tracking codes and controlled with a detector grid. [6] With the aid of a look-up table developed for the specific experimental setup, one can determine a family of initial conditions (momentum and energy) for secondary electrons emitted at the point of primary electron impact and terminating at the point of detector interception.

Varying the detector grid voltage offers one means to narrow the selection of all possible secondary electrons that may impact the detector at the same location. Because the SEE system contains no moveable parts, field perturbations from the measuring instrument are eliminated. Consequently, low energy secondary electrons may be characterized.

Preliminary experimental studies should commence in February of 2005. Experimental results are to be compared against an existing Monte Carlo code developed by Dr. Joy (ORNL and Univ. of Tenn.) [7] for scanning electron microscopy applications with ongoing enhancements incorporated by UNLV to handle surface impurity layers more rigorously. Single primary electron studies in the code complement the low current primary electron beam requirement in the experiment. The code's greatest asset, speed, stems from approximate calculations based on probabilistic techniques in lieu of time consuming exact calculations and hard to acquire parameter specifications.

Over 100's of thousands of trajectories may be followed in about one-minute duration. Based on Dr. Joy's experiences, [7] the code should be reasonably valid for electrons with energies from as low as 50 eV to those well over many ten's of keV. The code's accuracy, based on the programmed physical model, yields reasonable results for primary electron energies above 1 keV. The time and space resolution of the particle

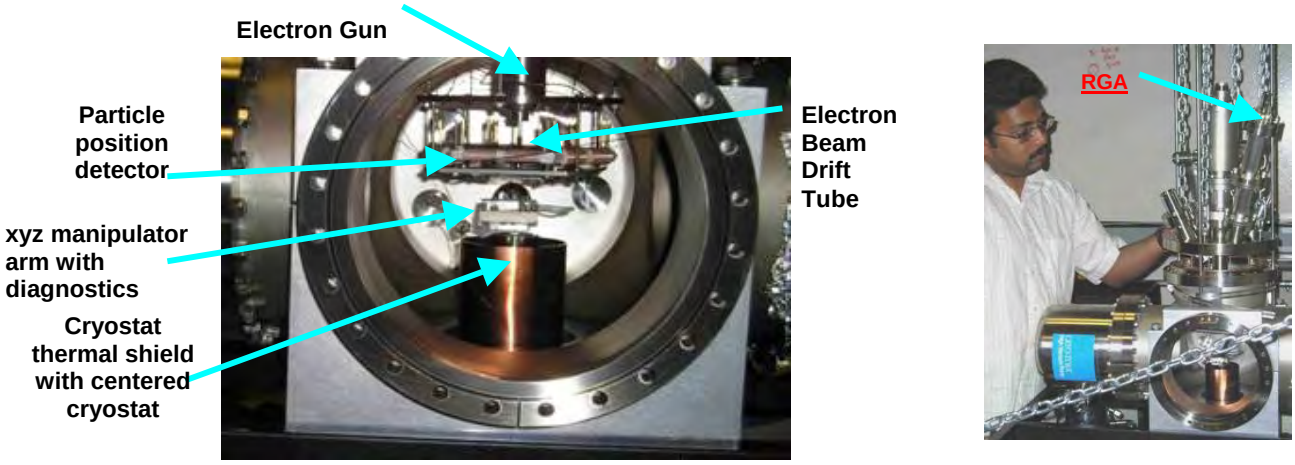

Figure 1. The SEE detection system showing the cryostat, xyz manipulator, electron gun, particle position detector, beam tube, residual gas analyzer, and vacuum chamber.

position detector place limits on the primary beam current. Only low beam currents may be employed.

The benefit of knowing the initial dynamics of the secondary electrons, whether of the true or of the backscattered type, leads to understanding how primary electrons deposit energy into the material. In studying the surface physics for the generation of SEE, minimal interactions among incident primary electrons internal to the target is desired. Low current electron beams accomplish this task. It is anticipated that the incident primary energy, angle of incidence, target material, and target temperature will map into a statistical distribution of secondary launch positions, momentums, and energies (dynamic surface statistics).

Knowledge on where and how energy deposition results may relax or guide design requirements. For example, high-energy primary electron beams will behave differently than low energy beams when interacting with a material containing a crystalline lattice structure. Electron diffraction can be significant at the higher energies. Heating the surface of the materials perturbs the crystalline structure resulting in a broadening of the diffracted electron beam. With flat energy profiles and low primary beam currents, changes in the scattering dynamics may be observed for each SEE mechanism. It is anticipated that energy deposition of low- and high-energy primary electron beams will differ.

Current UNLV Electromagnetics Laboratory Collaboration with LANL

The SEE system under development in the Electromagnetics Laboratory at UNLV is motivated by typical parameters for SRF cavities. Table 1 stipulates approximate parameter regimes that represent present and future needs for SRF cavities and the design capabilities of the SEE system in the UNLV Electromagnetics Lab. Interests and capabilities compare well.

One of the major thrusts of this proposal is to aid in the design of a thermal barrier to minimize large thermal gradients experienced by the cryostat support mount. As observed in Fig. 1, the secondary cooling stage surrounding the cryostat cylinder allows for line of sight access between the sample and the view ports and between the sample and the detector. At present, large thermal gradients exist that prevent the sample from reaching the desired temperatures. These gradients can not be avoided due to various operations that need to be performed by the system.

Table 1. Typical SRF cavity and UNLV parameter regimes interests and capabilities.

Parameter	Parameter Regime of Interest	Existing UNLV Setup
Incident e beam currents	on the order of nanoamps and higher	30 nA (50 eV) to 2.5 μA (5 keV)
Incident e beam energies	2 eV – 1.5 keV	50 eV – 5 keV
Beam repetition rate	100 Hz	100 kHz max.
Material temperatures	Liquid helium temperature ~2^{o} K or <9.2K	Cryostat cold head ~8.5^{o} K Cryostat support mount ~17^{o} K
Material types	BCP or EP Niobium	Any material can be mounted
Vacuum pressures	$<10^{-9}$ Torr	2.5×10^{-9} Torr
Pulse duration	1 ms - CW	0.5 μs to 10 μs

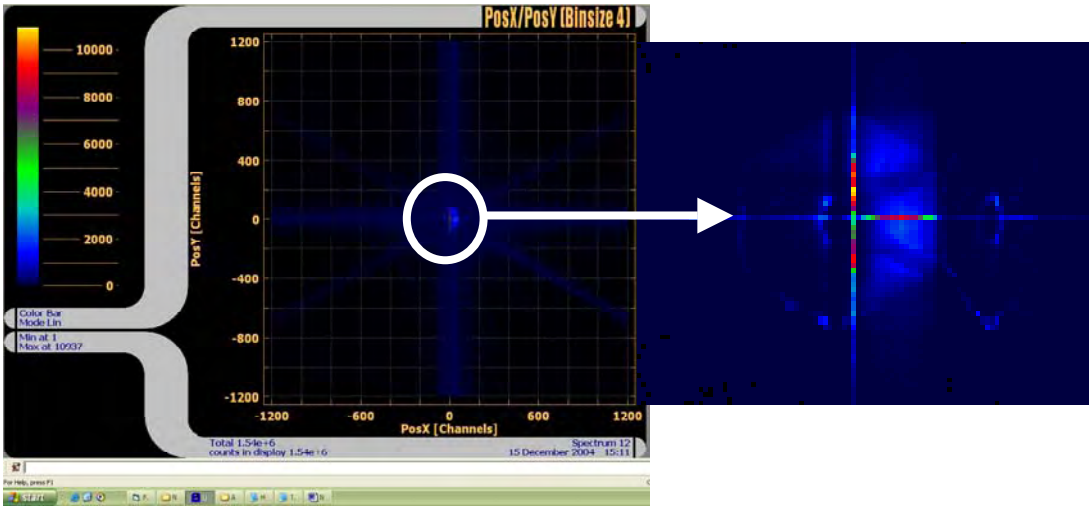

Figure 2 A first result obtained from the particle position detector. Undesired ghost images and loss of signal on the left half side of the detector is currently being corrected. The color intensity of the regions over the hexane shaped detector indicates the number of electrons detected at that position over time.

Figure 2 displays a first result from the particle position detector. The enlarged signal to the right indicates that some fine-tuning in the software and hardware is required. Even so, the detector responds to the secondary electrons emitted from a niobium sample at room temperature as initiated by a primary electron beam.

For a typical cavity design, particle trajectory studies over a large parameter space of initial conditions for secondary electrons launched from the niobium surface has been performed and stored in a large data base look-up table. Conventional particle tracking codes have been employed. To aid in verifying and limiting the family of particles with the same final conditions, a secondary electron emission Monte Carlo code has been secured and is being continuously enhanced.

The second major thrust of this proposal is to enhance the current code to allow for multiple layers of material to exist on a bulk medium in a more rigorous manner. Currently the code follows both the primary and all of the generated secondary electrons making use of cross-sections and mean free paths characterizing stopping powers and most probable types of collision (elastic or inelastic) for bulk mediums.

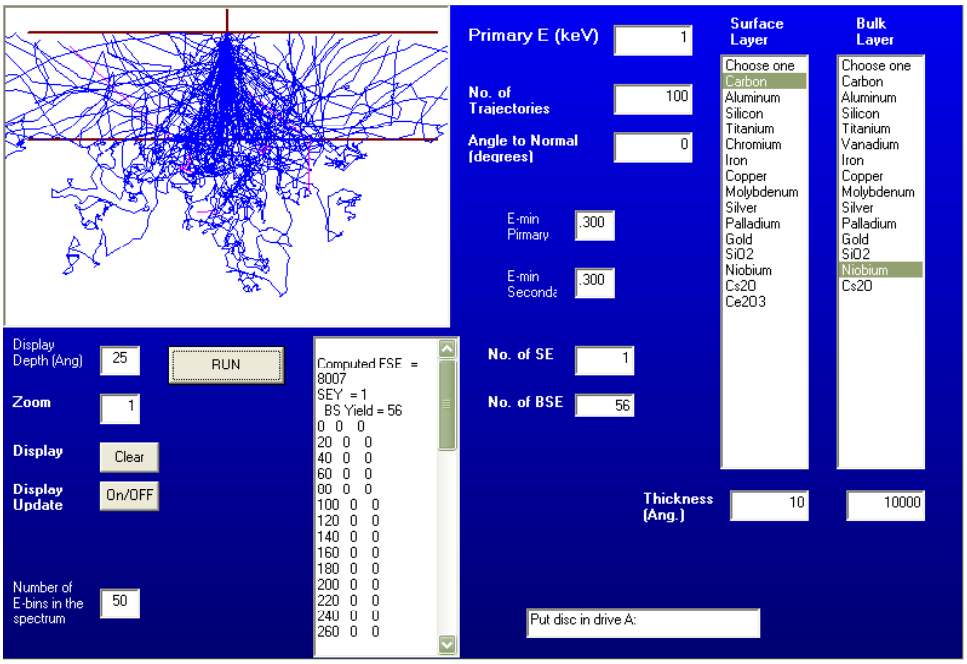

Figure 3. Typical graphical user interface output of Joy's code providing secondary electron emission and back scattering emission yields.

Project Overview

The proposed work would allow the current research effort to further complement superconducting cavity design environment. At first blush, a few degrees Kelvin may not seem to be significant. In effect, the significance lies in the change in state of the material from its normal state to its superconducting state. It is believed that secondary electron emission from a superconducting material may be different than from a cold material in a normal state. Further, what is adsorbed on the superconducting surface through natural pumping of a cold surface may influence the superconducting properties of the material. Therefore, the addition of a thermal shield may allow for new physics. To delineate this physics, enhancing the secondary electron emission Monte Carlo code is required.

Broader Impact

Particle accelerators have been used for various science including those using X-rays, free electron lasers, neutrons. The accelerators that use superconducting RF cavities made of niobium have increased significantly in the past few decades due to its higher efficiency and for other reasons.

Successful characterization of the secondary electron emission from the actual Nb surfaces after various conditions will allow cavity designers for better prediction of field emission and multipacting phenomena in the cavity. This in turn will lead to a more reliable cavity and accelerator design.

The students to be involved will learn the RF fields distribution in the cavity and various surface science that can be useful for other areas such as nuclear fusion.

Project Activities and Deliverables

A single year of funding is being requested. The following activities will result during the funding cycle:

1) Design and have built a suitable thermal shield or cooling mechanism to bring the niobium test sample to cryogenic temperatures.
2) Have a load lock chamber incorporated to the existing vacuum system to prevent changes in the vacuum environment when performing tests on a number of samples.
3) Modify the existing SEE Monte Carlo code to allow for a more rigorous study of multi-layer, multi-component surface contaminant. In this case, a weighted probability based on "a throw of the dice" will be the deciding factor if a electron collides with a particular type of molecule. Boundary interfaces require careful considerations in the collision process. [NOTE: Superconducting effects of materials will NOT be incorporated in the code during this funding cycle.]

Measurements from at least two samples prepared by Buffered Chemical Polishing (BCP) or Electro Polishing (EP) will be provided by way of a report. Based on findings uncovered, it is anticipated that measurements of the sample in both its superconducting state and its normal state (cold temperatures) will be compared and submitted for publication.

References:

1. Hasan Padamsee, Jens Knobloch, and Tom Hays, **RF Superconductivity for Accelerators**, Wiley Interscience Publication, John Wiley, N.Y. 1998.
2. I. Bojko and N. Hilleret, *Influence of Air Exposures and Thermal Treatments on the Secondary Electron Yield of Copper,"* **J. Vac. Sci. Technol. A 18** (3), 2000.
3. M. Grundner and J. Hilbritter, *"On Surface Coatings and Secondary Yield of NbSn and Nb,"* **J. Appl. Phys. 51** (10), 1980.
4. R. Noer *et. al*, *"Secondary Electron Yield of Nb RF Cavity Surfaces,"* Int. Conf. on High Energy Accelerators, KEK, Japan, 2001.

5. H. Padamsee and A. Joshi, *"Secondary Electron Emission Measurements on Materials used for Superconducting Microwave Cavities,"* **J. Applied Phys. 50** (2), 1979.
6. Anoop George and Robert A. Schill, Jr., *Preparation Studies for Secondary Electron Emission Experiments on Superconducting Niobium*, 2004 American Nuclear Society Student Conference, at University of Wisconsin Madison, Madison, Wisconsin, April 1-4, 2004.
7. D.C. Joy, **Monte Carlo Modeling for Electron Microscopy and Microanalysis,** Oxford University Press, New York, 1995. (ISNB 0-19-508874-3)

Budget

The activities outlined above will involve UNLV and a LANL staff member for the fiscal year of 2005.

Table 2: Budgetary estimate for the UNLV - LANL collaboration

Item	FY 2005	FY 2006	FY 2007
Faculty	$ -		
Other professionals	$ -		
Graduate Student	$ 9,000		
Total Salaries (incl. fringe benefits)	$ 10,600		
Equipment	$ 28,000		
Travel	$ 1,500		
Materials and Supplies	$ 6,000		
UNLV Consultants (Vacuum Specialist and a Material Scientist)	$ 8,000		
LANL Consultants (Dr. Tsuyoshi Tajima)	$ 10,000		
Total direct costs	$ 64,100		
Total indirect costs (47.5% of direct cost minus equip. [> $2000])	$ 17,148		
Total direct and indirect costs	**$ 81,248**		

Budget Justification

Faculty	Schill (Faculty)– ($9471/mo) – 0 mo. Electromagnetics, plasma, pulse power, and charged particle background. SEE and SED mechanics have close analogies to plasmas science mechanics.
Other Professionals	1 Engineering Research Associate (Professional) 1) Craig Nielsen - $4585/mo. for 0 mo. – Pulsed power, machine shop, and electronics expert – tasked to train students to operate machine, provide continuity in experiment, and perform necessary machining and assembling of SEE machine
Graduate Students	1 Graduate Students One $1,500/mo. for 6 mo.
Fringe Benefits & Salary	**UNLV Fringe Benefits Breakdown** Research Professionals - 14% of salary plus $6800/yr. prorated medical ins. Graduate Students – 10% of salary plus $1231/yr. prorated medical ins.
Materials, Supplies, Software and Training	***Total ($6,000)*** Vacuum equipment **($3,500)** -- conflat flanges, consumables), gloves, cleaning supplies, repairs Machining **($1,000)** – sample mounts, tools, gun mounts. Gas **($500) –**gasses for venting Materials **($1,000)** – target materials,
Permanent Equipment	***Total ($28,000)*** Load lock chamber with essentials **($23,000)** Manipulator arm with thermal cover **($5,000)**
Travel	One trip to LANL.
Consultant Services	***Total ($18,000)*** Stan Goldfarb -- $4,000 [Vacuum Science Expert. He works with students will coordinating research efforts associated with vacuum studies and sensors. He also alters and designs new vacuum geometries for modifications in the experiment.] Dr. Richard Kant -- $4,000 [Physicist. Extensive background in material science. He is enhancing an existing SEE Monte Carlo code which is a key software component needed to interpret experimental results.] Dr. Tsuyoshi Tajima – $10,000 [Consulting Engineer at LANL involved in collaborative efforts and overseeing progress of the materials research relevant to the rf superconducting cavities]
Indirect Costs	The UNLV indirect cost rate is 47.5% of all direct costs excluding equipment over $2000

ROBERT A. SCHILL, JR., P.E.

UNIVERSITY ADDRESS AND PHONE

Academic Rank:	Associate Professor Director & Founder of the Electromagnetics Laboratory Director and Part Founder of the Pulse Power Laboratory
Address:	Department of Electrical and Computer Engineering University of Nevada - Las Vegas Las Vegas, Nevada 89154-4026
Phone:	(702) 895-1526 / (702) 895-1430 / (702) 895-4403
Email:	schill@ee.unlv.edu
URL:	http://www.unlv.edu/~schill (Updated 1/95)
Lab URL:	http://EMandPPLabs.nscee.edu (Updated 9/04)

EDUCATION

Ph.D. (E.E.)	*University of Wisconsin - Madison (Aug. 1986)* Thesis: Free Electron Sources of High Frequency Radiation Major Area: Plasma and Controlled Fusion Secondary Area: Electrodynamics (Thesis Advisor: Dr. S.R. Seshadri)
M.S.E.E.	*University of Wisconsin - Madison (May 1981)*
B.S.E.E.	*Milwaukee School of Engineering (May 1979)*

POSITIONS HELD

Sept. 1986 - Aug. 1993	*Assistant Prof., University of Illinois at Chicago (UIC)*
Aug. 1993 – June 1997	*Assistant Prof., University of Nevada-Las Vegas (UNLV)*
July 1997 – Present	*Associate Prof., University of Nevada-Las Vegas (UNLV)*

SOME RECENT AND RELEVANT PUBLICATIONS (*REFEREED JOURNALS*)

1. V.A. Subramanian and R.A. Schill, Jr., "Measuring the Characterisctics of a Lossy Transmission Line System Using Only the Vector Network Analyzer Measured S_{11} Parameter," **IEE Proc. on Science, Measurement & Technology,** December 3, 2004.
2. R.A. Schill, Jr., *A Closer Look at the General Relation for the Vector Magnetic Field Generated by a Circular Current Loop,* **IEEE Trans. on Magnetics, 39** 2 (2003), pp. 961-967.
3. R.A. Schill, Jr., *A Simplistic Plasma Dust Removal Model Employing Radiation Pressure*, **Laser and Particle Beams 20**, 2 (2002) pp. 341-357.
4. R.A. Schill, Jr. and K. Hoff, *Characterizing and Calibrating a Large Helmholtz Coil at Low AC Magnetic Field Levels With Peak Magnitudes Below the Earth's Magnetic Field*, **Review of Scientific Instruments 72**, 6 (2001) pp. 2769-2776.

Some Relevant Conferences

1. Anoop George and Robert A. Schill, Jr., *Preparation Studies for Secondary Electron Emission Experiments on Superconducting Niobium*, **2004 American Nuclear Society Student Conference,** at University of Wisconsin Madison, Madison, Wisconsin, April 1-4, 2004. **[!!Awarded Outstanding Student Paper Award!!]**
2. M. Holl, M. Trabia, and R. A. Schill, Jr., *Optimization of a Five-Cell Niobium Cavity,* **Sixth International Topical Meeting on the Nuclear Applications of Accelerator Technology, (Accelerator Applications 2003: Accelerator Applications in a Nuclear Renaissance),** San Diego, California, June 1-5, 2003, pp. 202-206.
3. Q. Xue, S. Subramanian, M. Trabia, Y. T. Chen, and R. A. Schill, Jr., *Modeling and Optimization of the Chemical Etching Process in Niobium Cavities,* **International Congress on Advanced Nuclear Power Plants,** Hollywood, Florida, June 9-13, 2002.

2.52: Investigation of Plasma Etching for Superconducting RF Cavities surface Preparation

(new proposal)

Accelerator Physics

Contact person
Leposava Vuskovic
vuskovic@physics.odu.edu
(757) 683-4611

Institution(s)
Old Dominion University
TJNAF

New funds requested
FY05 request: 101,994
FY06 request: 54,670
FY07 request: 54,670

Investigation of Plasma Etching for Superconducting RF Cavities surface Preparation

Proposal for LCRD/UCLC 2005

Classification (subsystem)

RF cavity for the main linac

Personnel and Institutions requesting funding

Leposava Vuskovic, Old Dominion University

Collaborators

S. Popovic, Old Dominion University
M. Raskovic, Old Dominion University
A. -M. Valente, Thomas Jefferson National Accelerator Facility
L. Phillips, Thomas Jefferson National Accelerator Facility

Project Leader

Leposava Vuskovic
vuskovic@physics.odu.edu

Department of Physics
4600 Elkhorn Avenue, Room 306
Old Dominium University
Norfolk, VA 23529
Telephone: (757) 683-4611
FAX (757) 683-3038

Old Dominion University
Research Foundation
2033 Hughes Hall
P.O. Box 6369
Norfolk, VA 23508
Telephone: (757) 683-4293
Fax: (757) 683-5290

Introduction

Of the many recipes used to prepare SRF cavity surfaces, none presently will provide repeatable performance reasonably close to fundamental limits, and none are understood at the microscopic level in terms of their effect on variability of RF performance. In this context Thomas Jefferson National Accelerator Facility (Jefferson Lab) and the Atomic Collision and Plasma Physics Group of the Physics Department, Old Dominion University (ODU) in Norfolk, Virginia have joined forces to investigate plasma etching as an alternative technique for surface preparation of high purity bulk Nb cavities. The Atomic Collision and Plasma Physics Group at ODU has proven its expertise in the field of plasma modification of surfaces. The collaboration between Jefferson Lab and the Atomic Collision and Plasma Physics Group at ODU will strongly impact the Nb surface preparation procedures as well as advance the understanding of surface chemistry of high purity niobium for superconducting RF cavities, which will be beneficial for a future linear collider.

Motivation

The standard (commonly used) surface preparation techniques for Nb superconducting RF cavities are chemical (BCP) or electrochemical (EP) polishing. Those make use of extremely corrosive acids, which present both safety and environmental concerns. With wet chemical polishing, the formation of an Nb oxide layer is unavoidable since oxidation starts as soon as the chemical process stops. More over it has been demonstrated that these techniques, due to the baths composition, introduce hydrogen in the oxide layer and the bulk material [1]. Acid residues are usually left by phosphoric acid on the surface. These chemical residues are eliminated by High Pressure Water Rinsing (HPWR) with de-ionized water for several hours. Finally, especially in the case of EP, the cavity is baked under vacuum at moderate temperature (90ºC-140ºC) in order to outgas the water adsorbed on the surface and to reduce the surface hydroxides [2].
It has long been suspected that "weak links" formed by intergranular oxidation could be responsible for the RF performance degradation or "Q droop" [3]. It is also suspected that niobium surfaces under certain circumstances will form lossy sub-oxides in addition to Nb_20_5. Testing before and after oxidation would provide extremely valuable insight into this issue.
Plasma etching is one form of dry chemistry providing a unique opportunity to explore oxide-free surfaces by directly testing a cavity surface after processing without exposure to air. This technique allows also "control" on the final oxidation phase that cannot be avoided with SRF cavities (oxidation of the fresh Nb surface after treatment by O_2/N_2 ("dry air") gas injection in the system). The relatively scarce literature describes niobium [4] and niobium oxide [5] etching in reactive discharge plasmas. In the first case [4] etching rates of the order of 0.2-0.3 mm/min were obtained. In the second case [5], significant structural changes of niobium oxides were obtained. This limited experience can be used as a starting point for a systematic study of the inner surface modification of superconductive cavities using low-pressure discharge plasmas.

Advantages of dry etching:

- Takes place under vacuum.
- Allows "control" on the final oxidation phase
- Allows the possibility to avoid final oxidation
- Lower process cost.
- Reduces the number of steps for the final surface preparation.
- Gets rid of the hazard to humans and environment induced by the chemicals used for BCP and EP.
- No acid residues on the surface.
- No hydroxides formation on surface.

The investigation of plasma etching for Nb cavity surface preparation will improve the surface quality of the SRF cavities and therefore improve their performance for a linear collider.

Current ODU Collaboration with Jefferson Lab

The Atomic Collision and Plasma Physics Group at Old Dominion University has proven its expertise in the field of Plasma Physics. In the recent years, their research in plasma processing and related field has been focused on the use of subcritical surface microwave discharges for surface modification [6], the extraction of oxygen by dissociation of carbon dioxide [7], and for generating aerodynamic effects [8].

The proposed experiment is devoted to the use of metal-to-discharge plasma interfaces to generate adequate environment for transformation of Niobium oxides from the surface of SRF cavity into removable volatile compounds. When developed, the oxide removal process could serve as a complementary surface modification method to those currently used in preparing the SRF cavities for operation. The collaboration between the Jefferson Laboratory, with the expertise in SRF cavity material development and testing and the ODU team, with the experience in plasma processing will bring the needed synergy for developing the process.

Project Overview

ODU and Jefferson Lab have agreed to collaborate on the investigation of plasma etching, using the experimental systems developed for plasma studies at ODU. According to the agreement, Jefferson Lab will be responsible to provide Nb material and surface analyses for the plasma etching studies on Nb conducted at ODU. Both parties will share the efforts related to analysis and publication.

The following approach has been defined:

1) Microwave discharge in a cylindrical cavity at various pressures of
   a. Ar plasma with a biased sample
   b. Ar/Cl mixtures
   c. CCl_2 and CF_4 flow
   d. Other etchant gases as C_2F_6, SF_6, NF_3.

Microwave discharge
Scheme of experimental set-up

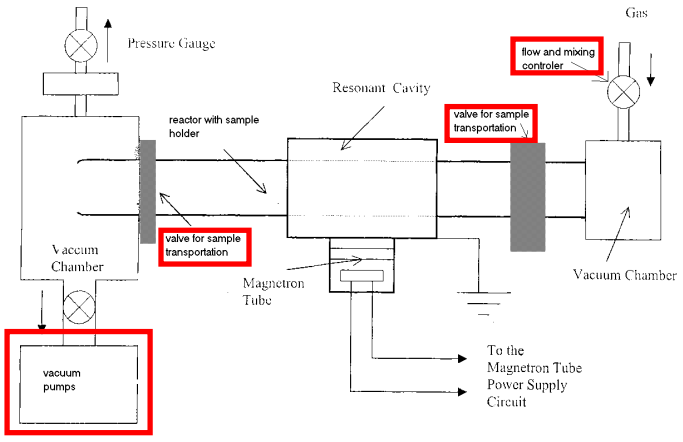

2) Capacitively-coupled RF discharge with Nb sample as one electrode, at various pressures of

a.Ar plasma with a biased sample
b.Ar/Cl mixtures

RF discharge
Scheme of experimental set-up

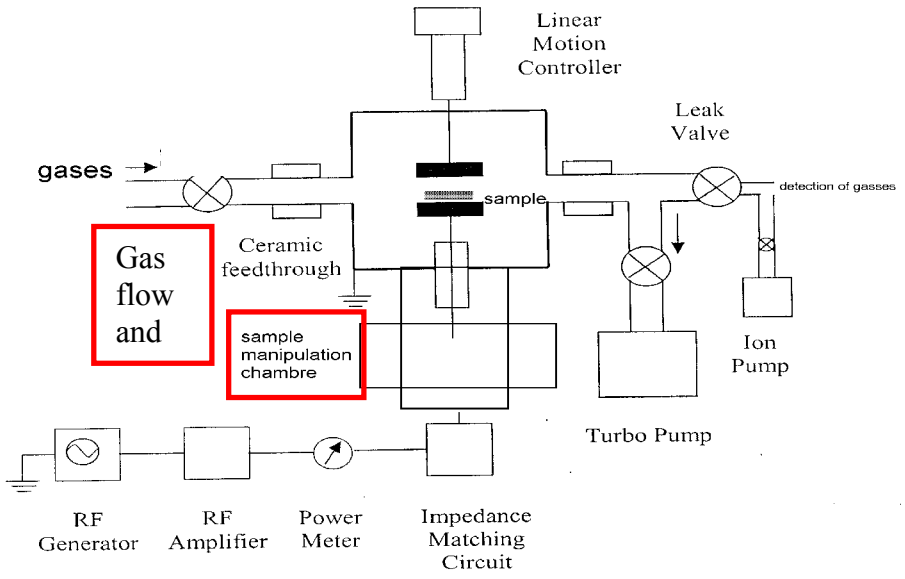

During the development of the techniques, the plasma process will be characterized with plasma diagnostics (temperature, electron density, different species density) and process controls (emission and absorption spectroscopy). The characterization of the samples produced will involve surface morphology (SEM) and composition (XPS) analyses and surface resistance measured by calorimetric method in a TE011 cavity.

3) Application of the process to Nb cavities

Once the principal of the technique will be demonstrated and the best approach being determined, the technique will be implemented in a cavity system at Jefferson Lab. The surface of elliptical RF cavities will be prepared by plasma etching and their RF performance will be tested at Jefferson Lab.

Broader Impact

Successful development and implementation of plasma etching as a surface preparation technique for high purity Nb cavities will allow a cost reduction and safer procedures in cavity surface preparation. A better control on the Nb surface composition and morphology will lead to a more reliable cavity performance. This will be beneficial for a Linear Collider as well as for any accelerator project based on Nb RF Superconductivity.

One member of the team, Marija Raskovic, is currently pursuing her doctoral thesis work at Old Dominion University, working on the characterization of the Niobium processing microwave and RF-excited plasmas. In addition, parts of these experiments will be used for training the undergraduate students as their senior summer research projects. The students involved will learn the plasma physics involved in RF and microwave discharges, various surface science methods and SRF technology.

Project Activities and Deliverables

During the first year, the two experimental systems described in the previous section will be developed. A sample study of plasma etched surfaces of high purity Nb will be conducted. Reports on the technique developments and sample surface and RF analyses will be produced.
During the second and third year, the sample study will be completed and the technique will be transposed for cavity surface preparation. Nb cavities will be prepared using plasma etching and
During these three years the technique developments and surface results obtained on samples and cavities will be published in referee journals and a PhD thesis will be presented.

References:

[1] Hasan Padamsee, Jens Knobloch, and Tom Hays, “RF Superconductivity for Accelerators”, Wiley Interscience Publication, John Wiley, N.Y. 1998
[2] Lilje, L. , Antoine, C. , **Benvenuti**, C. , Bloess, D. , Charrier, J.-P. ,Chiaveri, E. , Ferreira, L. , et. al., “Improved surface treatment of the superconducting TESLA cavities” , Nuclear Instrument and Methods A, 516, 213-227 (2004)
[3] A.M. Portis, D.W. Cooke, H. Piel, “ Microwave Surface impedance of Granular Superconductors”, Physica C. , 162-164 (part 2), 1547-1548 (1989)
[4] Jay. N. Sasserath, "Dry etching of niobium using CCl_2F_2 and CF_4: A comparison", J. Appl. Phys., 68 (1990) 5324-5328.
[5] H. Turcicova et al., "Plasma processing of $LiNbO_3$ in a hydrogen/oxygen radio-frequency discharge", J. Phys D: Appl. Phys. 31 (1998) 1052-1059.
[6] Popović, S., L. Vušković, I. I. Esakov, L. P. Gratchev, and K. V. Khodataev, “Subcritical Microwave Streamer Discharge at the Surface of a Polymer Foil,” Appl. Phys. Lett. 81**,** 1964-1965 (2002).
[7] L. Vuškovic, R. L. Ash, Z. Shi, S. Popovic, and T. Dinh, “Radio-Frequency-Discharge Reaction Cell for Oxygen Extraction from Martian Atmosphere,” Transactions of the Society of Automotive Engineers, J. of Aerospace, 107, 28 (1998).
[8] R. J. Exton, S. Popovic, G. C. Hering, and M. Cooper, “Levitation Using Microwave Induced Plasmas”, Appl. Phys. Lett., submitted.

Budget

The activities outlined above will involve ODU and Jefferson Lab staff members whose salaries are not included in the present budget request.

Table 2: Budgetary estimate for the ODU-Jefferson Lab collaboration

Item	FY 2005	FY 2006	FY 2007
Faculty	$ 24, 300	$ 24, 300	$ 24, 300
Other professionals	$ -		
Graduate Student	$ -		
Total Salaries (incl. fringe benefits)	$ 24, 300	$ 24, 300	$ 24, 300
Equipment	$ 30,000	-	-
Travel	$ -	-	-
Materials and Supplies	$ 14,000	$ 7, 000	$ 7, 000
ODU Tech. Consultants	$ 12,400	$ 7, 200	$ 7, 200
Total direct costs	$ 80,700	$ 38,500	$ 38,500
Total indirect costs (42% of direct cost minus equip.)	$ 21, 294	$ 16,170	$ 16,170
Total direct and indirect costs	**$ 101, 994**	**$ 54, 670**	**$ 54, 670**

Budget Justification for FY 2005

Faculty	Vuskovic (Faculty)– ($9,300/mo) – 0 mo. Atomic collisions and Electric discharge physics Popovic (Faculty)– ($9,000/mo) – 2 mo. Electric discharge physics
Other Professionals	-
Graduate Students	1 PhD Student ($1,800/mo) - 0 mo.
Fringe Benefits & Salary	**ODU Fringe Benefits Breakdown** Research Professionals - 35% of salary Graduate Students – 35% of salary
Materials, Supplies, Software and Training	***Total ($14,000)*** Quartz tubes **($2,000)** Gas **($5,000) –** high purity gases for discharge Materials **($2,000)** – high purity materials Test equipment fees **($3,000)** Sample manipulation supplies **($2,000)**
Permanent Equipment	***Total ($30,000)*** Corrosion-resistant vacuum components **($10,000)** Corrosion-resistant gas flow components **($10,000)** MW/RF power components **($ 10,000)**
Travel	-
Consultant Services	***Total ($12,400)*** Rey Gregory (MW/RF specialist)– ($4,000/mo) – 1.5 mo. Miroslav Cingel (Metal parts design and construction specialist) – ($3,200/mo) – 2 mo.
Indirect Costs	The ODU indirect cost rate is 42% of all direct costs excluding equipment over $2,000